CHEMICAL REVIEWS

pubs.acs.org/CR

Review

Natural and Synthetic Flavylium-Based Dyes: The Chemistry Behind the Color

Luis Cruz,[§] Nuno Basílio,[§] Nuno Mateus, Victor de Freitas,* and Fernando Pina*

Cite This: *Chem. Rev.* 2022, 122, 1416−1481

Read Online

ACCESS | Metrics & More | Article Recommendations

ABSTRACT: Flavylium compounds are a well-known family of pigments because they are prevalent in the plant kingdom, contributing to colors over a wide range from shades of yellow-red to blue in fruits, flowers, leaves, and other plant parts. Flavylium compounds include a large variety of natural compound classes, namely, anthocyanins, 3-deoxyanthocyanidins, auronidins, and their respective aglycones as well as anthocyanin-derived pigments (e.g., pyranoanthocyanins, anthocyanin-flavan-3-ol dimers). During the past few decades, there has been increasing interest among chemists in synthesizing different flavylium compounds that mimic natural structures but with different substitution patterns that present a variety of spectroscopic characteristics in view of their applications in different industrial fields. This Review provides an overview of the chemistry of flavylium-based compounds, in particular, the synthetic and enzymatic approaches and mechanisms reported in the literature for obtaining different classes of pigments, their physical-chemical properties in relation to their pH-dependent equilibria network, and their chemical and enzymatic degradation. The development of flavylium-based systems is also described throughout this Review for emergent applications to explore some of the physical-chemical properties of the multistate of species generated by these compounds.

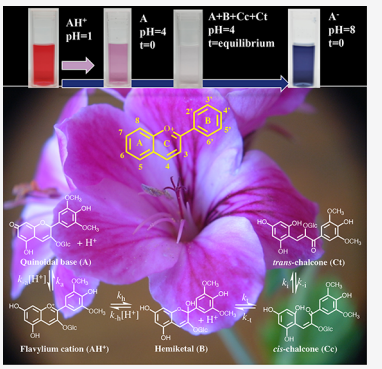

CONTENTS

Received: May 6, 2021
Published: November 29, 2021

https://doi.org/10.1021/acs.chemrev.1c00399
Chem. Rev. 2022, 122, 1416−1481

1. INTRODUCTION: OVERVIEW OF FLAVYLIUM PIGMENTS

Flavylium dyes constitute a large family of both natural and synthetic compounds that include different classes such as anthocyanins, 3-deoxyanthocyanidins, and auronidins together with their respective aglycones. Other flavylium compounds result from the reaction of these natural compounds in biological matrixes, such as the pyranoanthocyanins found in red wine. In addition, a wide variety of bioinspired synthetic flavylium compounds have been prepared and have been found to have great potential for some applications, for example, in photochromic systems.

Anthocyanins are the most frequently studied flavylium dyes because they are the largest class of water-soluble compounds present in the plant kingdom and are responsible for a range of colors in plants, from orange-red to purple-blue hues. These types of natural pigments play an important role in plant reproduction because they attract pollinators and seed dispersers by presenting attractive colors.[1,2] In addition, anthocyanins protect plants from several biotic and abiotic stresses.[3,4] Anthocyanins may act as photoprotective agents by absorbing excess visible and UV light, preventing the formation of free radicals that may affect plant tissues by compromising photosynthesis.[5,6] Because of their recognized antioxidant properties, anthocyanins may also be important in maintaining the integrity of membranes in fruits and vegetables during the postharvest period, decelerating cell senescence.[7,8] In addition, the consumption of anthocyanin-rich foods has been associated with numerous beneficial health effects owing to the multiple biological properties of these compounds (e.g., antiproliferative, anti-inflammatory, and antimicrobial properties).[9−13] Regarding the technological applications of anthocyanins, novel physicochemical properties have been discovered and multiple applications have been explored and extended to different areas, such as their use as pH-freshness indicators for food intelligent packaging and as photosensitizers for dye-sensitive solar cells (DSSCs).[14−16]

The first reported anthocyanin structure (cyanidin-3,5-diglucoside) was isolated from the flower of *Centaurea cyanus* by Willstätter and Everest in 1913[17] and was later synthesized by Robinson and Todd in 1932.[18] Scheme 1 displays the general chemical structure and substituent groups of the main 3-deoxyanthocyanidin and anthocyanin pigments.

Since the discovery of the first anthocyanin, more than 700 related chemical structures have been identified in nature.[19,20] The number of new and more complex structures with different glycosylation and acylation patterns has increased owing to the development of more advanced and sensitive analytical techniques involving fractionation chromatography and structural identification (e.g., mass spectrometry and NMR).[21]

Anthocyanins are glycosylated forms of anthocyanidins, normally occurring as 3-glycosides or 3,5-diglycosides (Scheme 1). Different types of monosaccharides (e.g., glucose, galactose, rhamnose, and arabinose) and disaccharides (e.g., rutinose, sambubiose, and sophorose) can be attached to the flavylium core, and these sugars can also be acylated with hydroxycinnamic acids (e.g., caffeic, coumaric, ferulic, and sinapic acids) or aliphatic acids (e.g., acetic, malic, oxalic, and succinic acids).[22] Auronidins are furanoflavylium dyes found in liverworts and considered the oldest class of flavylium pigments from plant evolution.[23] However, 3-deoxyanthocyanidins, which are considered the chemical ancestors of anthocyanins, are characterized by a lack of hydroxyl substituent at position C3 and can be found in mosses, ferns, and other plants such as corn and sorghum.[24] Due to their structural diversity, the existence of a multistate of species that includes purple and blue quinoidal bases, and their respective anionic forms, anthocyanins and 3-deoxyanthocyanidins are responsible for a wide array of wonderful colors found in many flowers, leaves, fruits, vegetables, roots, and stems, ranging from yellow-orange to violet-blue ($\lambda_{max} \sim 450-650$ nm). However, the colors and chemical stability of anthocyanins and 3-deoxyanthocyanidins are strongly affected by different factors such as the pH, temperature, light, oxygen, and presence of other substances, including copigments and metal ions, carbohydrates, proteins, and sulfur dioxide.[25−29] Anthocyanins are weak polyprotic acids, and depending on their predominant form in solution they may act either as electrophilic (flavylium) or nucleophilic (hemiketal) species in a variety of reactions. Altogether, anthocyanins are responsible for the rich chemistry underlying the formation of the different anthocyanin derivatives that have been described in food matrixes, from monomers to more complex structures, adducts conjugated with other polyphenols, pyranoanthocyanins, etc. (Scheme 2).[19,30−32]

In nature, many plants have anthocyanin color-stabilizing mechanisms to maintain their red and blue colors.[33−40] These mechanisms include intermolecular and intramolecular copigmentation,[41−43] self-association,[44] and metal complexation,[39] which are usually driven by several noncovalent interactions, such as hydrogen bonding, van der Waals, $\pi-\pi$ stacking, and metal−ligand interactions and hydrophobic effects. Furthermore, the ability of flavylium dyes to engage in four chemical reactions in solution (acid−base, hydration, tautomerization, and *cis*−*trans* isomerization reactions) triggered by different external stimuli (light, pH, and temperature) has attracted attention because of their many technological applications, namely, in food, textiles, cosmetics, pharmaceuticals, biomedicine, energy fields, and photochromic systems capable of functioning as models for optical memories, and even for mimicking some elementary properties of neurons.[45−48]

This Review summarizes the synthetic strategies developed in recent years to obtain different classes of flavylium-based compounds, the kinetic and thermodynamic studies of the pH-dependent multistate of species generated by flavylium cations, their photochemistry, and the awareness of the events that drive the flavylium compound degradation in solution or biological systems and provides outlooks for their potential applications. Understanding the particularity of the color of flavylium compounds is much more complex than the scientific community generally acknowledges, and this Review deals with this issue with caution. A holistic approach based on the literature that integrates all the multidisciplinary sciences behind the organic chemistry and physical chemistry of flavylium compounds is needed to fulfill the knowledge on this matter.

https://doi.org/10.1021/acs.chemrev.1c00399
Chem. Rev. 2022, 122, 1416−1481

Scheme 1. Chemical Structures of the Primary Natural 3-Deoxyanthocyanidins and Anthocyanins

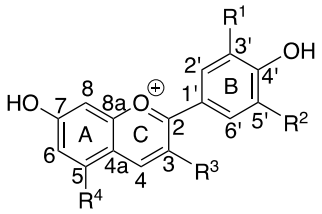

3-deoxyanthocyanidins (R^3=H, R^4=OH)	λ_{max} (nm) [a]	anthocyanins (R^3=OGly, R^4=OH or OGly)	λ_{max} (nm) [a]
apigeninidin (R^1=R^2=H)	480	pelargonidin (R^1=H; R^2=H; R^4=OH)	516
luteolinidin (R^1=OH, R^2=H)	498	peonidin (R^1=OMe; R^2=H; R^4=OH)	528
tricetinidin (R^1=R^2=OH)	530	cyanidin (R^1=OH; R^2=H; R^4=OH)	530
		malvidin (R^1=OMe; R^2=OMe; R^4=OH)	538
		petunidin (R^1=OMe; R^2=OH; R^4=OH)	540
		delphinidin (R^1=OH; R^2=OH; R^4=OH)	541

[a]In MeOH 0.01% HCl, Gly = glycoside.

Scheme 2. General Chemical Reactivity Sites of Anthocyanins

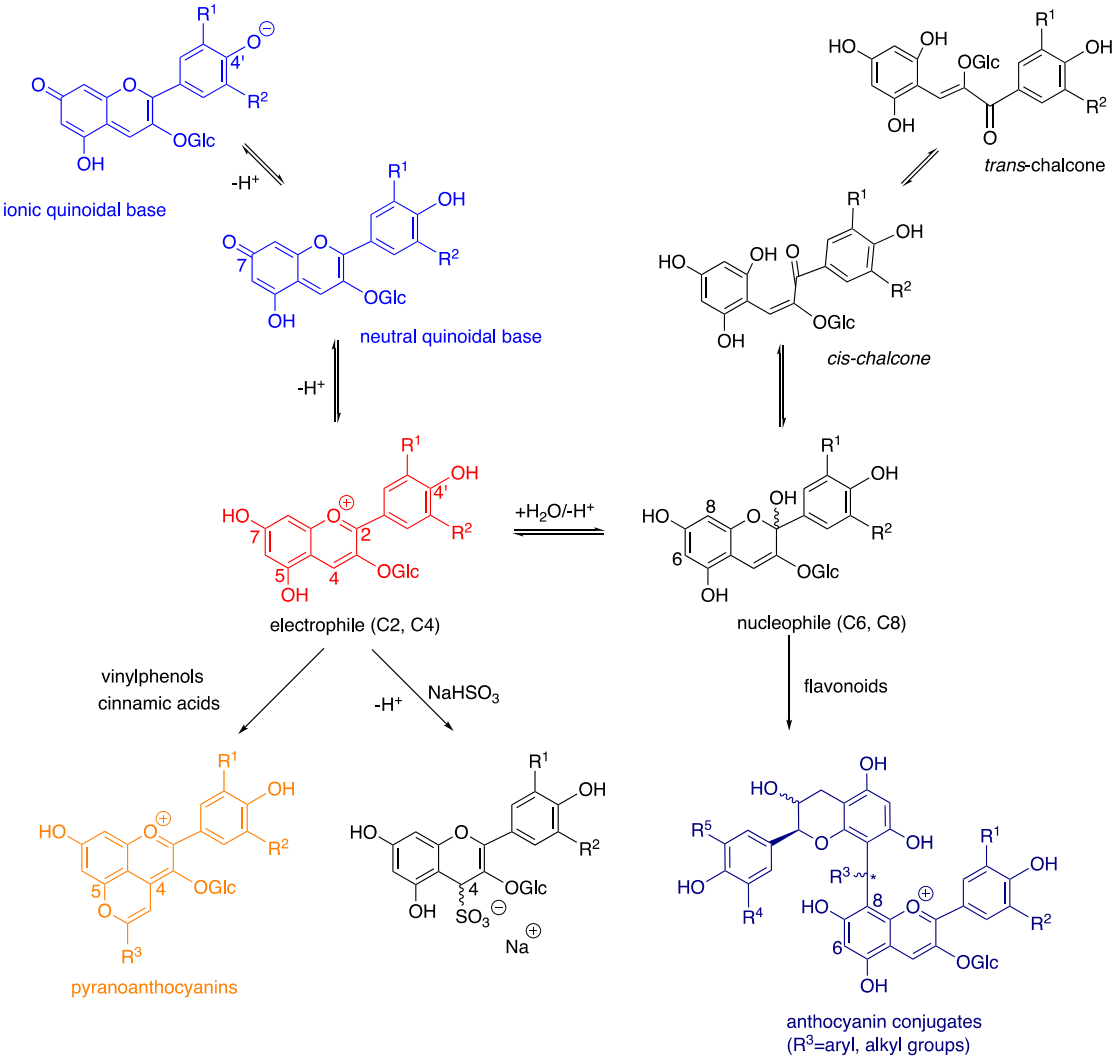

https://doi.org/10.1021/acs.chemrev.1c00399
Chem. Rev. 2022, 122, 1416−1481

Scheme 3. Flavylium Synthesis Routes through Type A and type B Acidic Aldol Condensations

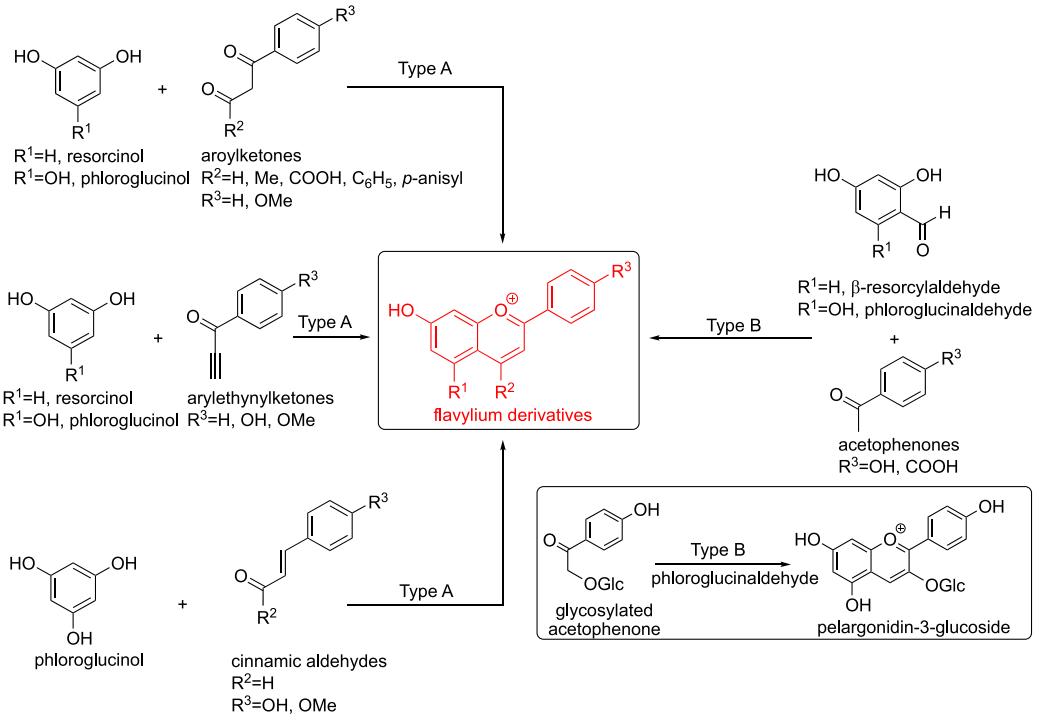

2. METHODS USED TO OBTAIN ANTHOCYANINS AND RELATED FLAVYLIUM COMPOUNDS

In this section, the current synthetic and hemisynthetic approaches to anthocyanins and their related flavylium salts and the developments that have occurred since the first synthesis described by Bülow and Wagner,[49] which is still widely used today, are carefully reviewed. Furthermore, recent findings on the genetic engineering of genes encoding biosynthetic enzymes in plant cells and microorganisms to produce anthocyanins are addressed.

Over the last century, interest in flavylium and similar compounds has increased within the scientific community, which aims to explore their magnificent chromatic and physicochemical properties. Several diverse classes of flavylium-type compounds have been synthesized using different approaches and have been discovered in many plants and plant-based foods. In the case of anthocyanins, some biotechnological approaches have been reported and are still currently being developed as alternatives to their extraction from natural sources or chemical synthesis methods, as anthocyanins can also be obtained from plant cell cultures or through microbial production.[50−52] Considering the different biotechnological approaches for producing anthocyanins on an industrial scale, the production rate will necessarily define their future economic viability.

This section is intended to give an overview of the primary synthetic methods and the flavylium-related molecules that have been reported to date. Over the years, many other important achievements have been made regarding the chemical and physicochemical properties of flavylium compounds and derivatives, highlighting the extraordinary and fascinating nature of these compounds. Subjects such as the molecular and supramolecular structures of natural anthocyanin derivative pigments (e.g., blue flower pigments) and the copigmentation effect of these compounds have been covered by some reviews, including one by Yoshida et al.[39] and another more recently by Trouillas et al.[40] in this journal.

2.1. Chemical Synthesis

2.1.1. C-Ring Cyclization. Before the discovery of natural anthocyanins in plants by Willstätter and Everest in 1913, the first flavylium-type pigment was obtained by synthesis through the reaction between aroylketones (*β*-diketones) and resorcinol (type A condensation).[49] Another route for synthesizing flavylium salts through C-ring cyclization was later discovered by Robinson and co-workers,[53−56] which resulted from the aldol condensation between 2-hydroxybenzaldehydes (e.g., phloroglucinaldehyde) and substituted acetophenones (type B condensation). Type A and type B condensations normally employ strong mineral acids, such as HCl (g), aqueous HPF_6, H_2SO_4, and HBF_4, in solvents, such as acetic acid, acetic anhydride, diethyl ether, and ethyl acetate (Scheme 3).[57−62]

The type B reaction (Robinson's method) became the most widely method for obtaining flavylium salts because of the practical convenience of obtaining acetophenone and 2-hydroxybenzaldehyde derivatives with different substituent patterns, including glycoside residues, to synthesize anthocyanins and, more recently, anthocyanin metabolites with in vivo occurrence[63−69] (Scheme 3). However, when a phloroglucinol-type derivative is used, the Robinson conditions give rise to a complex mixture of products that are difficult to purify, such as yellow-orange xanthylium pigments, and therefore, flavylium salts are isolated in low yields (5−20%). For that reason, this reaction has been tentatively improved over the years, and some authors have reported that, by using $BF_3{\cdot}Et_2O$-mediated catalysts, OH-protected starting materials, and the in situ generation of gaseous HCl (through reactions between TMSCl and MeOH), yields were increased up to 90%.[70−72] The Robinson method was further developed to synthesize a multi-^{13}C-labeled anthocyanin on the gram scale using modern organic techniques with a satisfactory yield of 40−50%.[65]

https://doi.org/10.1021/acs.chemrev.1c00399
Chem. Rev. 2022, 122, 1416−1481

Scheme 4. Synthesis Strategies for Obtaining Flavylium Pigments Using Chalcones as Intermediates

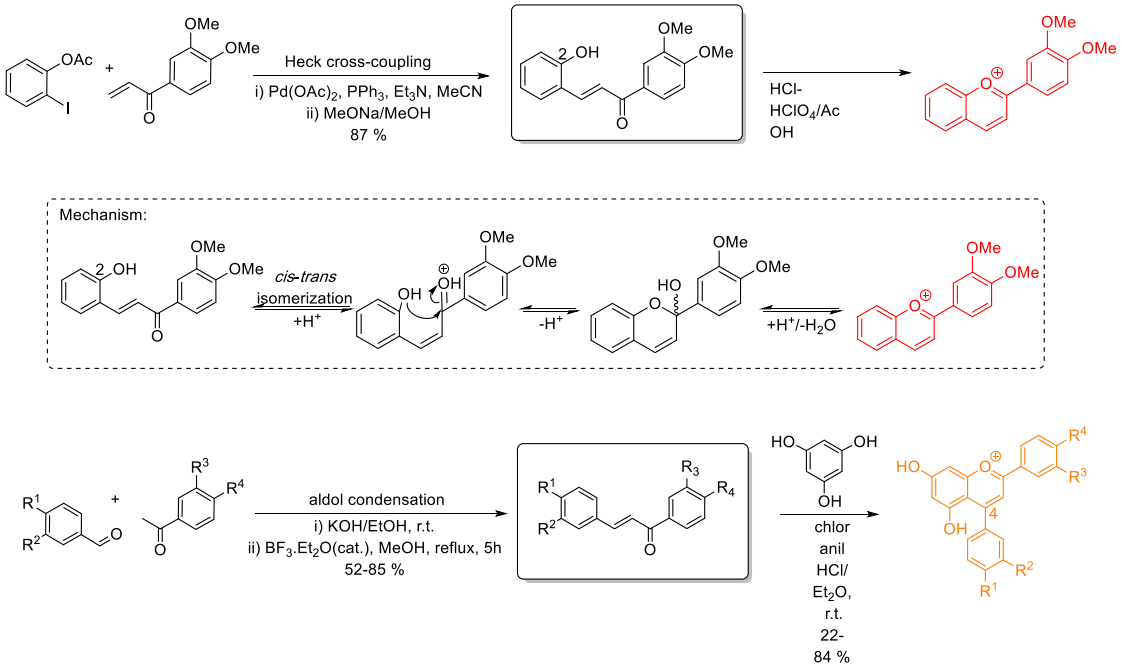

The type A condensation was also described by Johnson and Melhuish in 1947 to occur between phloroglucinol and arylethynylketones in H_2SO_4/acetic acid and was later explored by Kueny-Stotz et al. using a HPF_6 aqueous solution in acetic acid to yield highly methoxylated and hydroxylated 3-deoxyanthocyanidins in greater yields (82−99%).[73,74] Furthermore, De Freitas and co-workers also discovered that phloroglucinol-type structures could react with cinnamic aldehydes under hydroalcoholic acidic conditions, yielding 3-deoxyanthocyanidins; however, this reaction gave poor yields (∼10%).[75−77]

Other procedures reported to obtain flavylium pigments first involved the synthesis and isolation of chalcones (Scheme 4). Bianco and co-workers demonstrated that the Heck cross-coupling approach between α,β-unsaturated ketone and an aryl-iodide could be used to obtain 2-hydroxychalcones in high yields (87%). Because of the presence of a hydroxyl group at carbon 2, the corresponding flavylium cation could be obtained easily, just by acidifying the solution through a mechanism described in Scheme 4.[78,79] Chalcones could also be obtained through the base-catalyzed aldol condensation between aldehydes and acetophenones. In the absence of the hydroxyl group at carbon 2 of the benzaldehyde derivative, chalcones need to react with phloroglucinol under acidic conditions and in the presence of an oxidizing agent, such as chloranil, yielding 4-substituted 3-deoxyanthocyanidins (Scheme 4).[80]

2.1.2. Grignard Reaction. The first studies reporting on the synthesis of a 3-deoxyanthocyanidin or an anthocyanidin through this method consisted of the addition of phenyl Grignard reagent to 3-methoxy-coumarin or coumarin itself, respectively.[81,82] In 2001, Roehri-Stoeckel et al. described the synthesis of 4-substituted flavylium dyes with 64 to 99% yields from the reaction of flavones with Grignard reagents in THF followed by neutralization with HCl or NH_4Cl (Scheme 5).[83]

2.1.3. Reductive Transformations of 4-Oxo-flavonoids. Interestingly, since the early 20th century, it has been possible to obtain anthocyanins and 3-deoxyanthocyanidins

Scheme 5. Reaction of Coumarins and Flavones with Grignard Reagents to Obtain 3-Deoxyanthocyanidins and 4-Substituted Flavylium Dyes

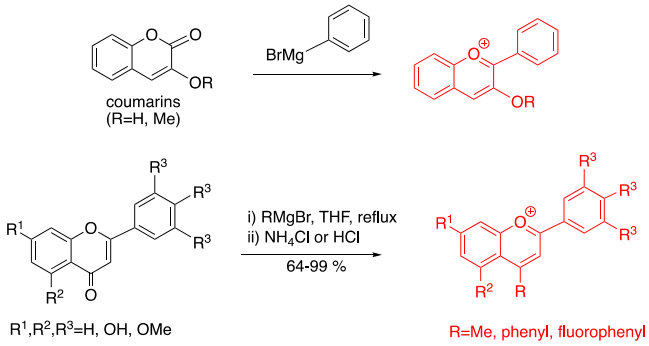

through reductive transformations of 4-oxo-flavonoids with different degrees of C-ring oxidation, namely, flavones, flavanones and 2-hydroxychalcones (Scheme 6).[84] Depending on the substituent groups of the flavone or flavonol (3-hydroxyflavone) precursor and the selected conditions, the synthesis yield of anthocyanins and 3-deoxyanthocyanidins ranges from 10 to 95%.

These reductive transformations involve the following:

(A) Clemmensen-type reduction under metal/acid conditions was investigated by a few groups in the early 20th century[85,86] and later by King and White;[87] however, the yields were low (less than 20%). The conversion of flavonol glycosides into anthocyanins was reported by Elhabiri et al., using Zn−Hg in 3% absolute methanolic hydrochloric acid with yields of 52−60%.[88] Nevertheless, Yoshida et al.[89] re-examined the rutin reduction under the Elhabiri conditions with zinc amalgam, zinc powder, or magnesium powder and always obtained cyanidin 3-*O*-rutinoside in less than 30% yield under the optimized conditions[89]. The difference in yield could be due to the value of the molar absorption coefficients for cyanidin 3-*O*-rutinoside reported by Elhabiri et al. (7000 M^{-1} cm^{-1} at 510 nm) being too

https://doi.org/10.1021/acs.chemrev.1c00399
Chem. Rev. 2022, 122, 1416−1481

Scheme 6. Reductive Transformations of Flavones, 2-Hydroxychalcones, and Flavanones into 3-Deoxyanthocyanidin and Anthocyanin Pigments

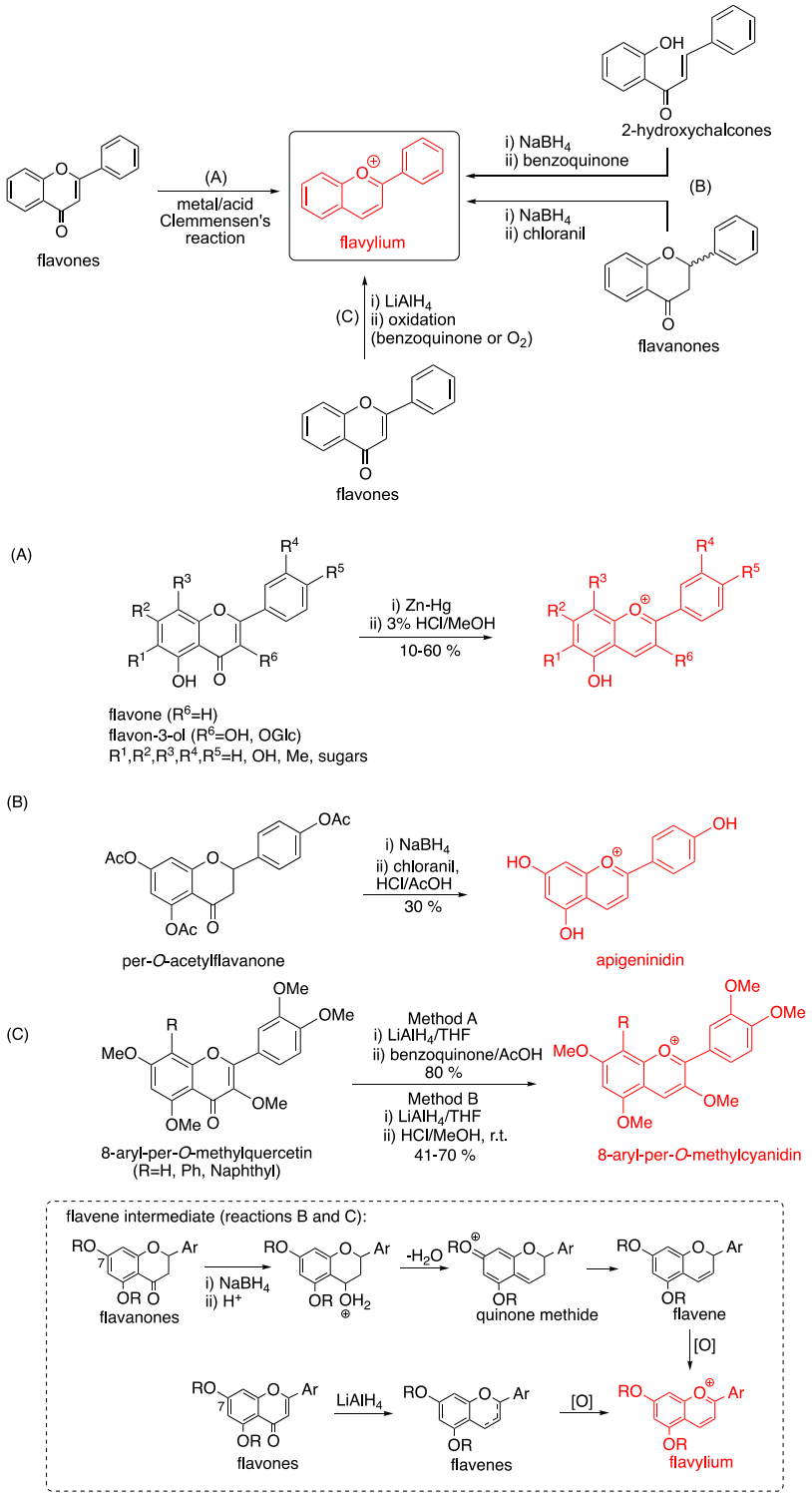

low compared with the theoretical value (around 20 000 M^{-1} cm^{-1} in Yoshida et al.'s results). Recently, Oyama et al. described a new method for the conversion of rutin into cyanidin 3-*O*-rutinoside using Zn in dried HCl−MeOH under argon atmosphere with improved reproducibility and 50% yield.[89] Other groups applied this reaction to obtain anthocyanins and 3-deoxyanthocyanidins from different starting flavone and flavonol glycosides, but the yields varied between 10 and 32%.[90,91]

(B) $NaBH_4$ reduction and a subsequent oxidation using chloranil for flavanones and benzoquinone for 2-hydroxychalcones. Clark-Lewis and Skingle introduced reductive cyclization of 2-hydroxychalcones using $NaBH_4$, giving flavenes in 60−80% yields, and then the dehydrogenation step proceeded with benzoquinone in acidic conditions to form flavylium com-

https://doi.org/10.1021/acs.chemrev.1c00399
Chem. Rev. 2022, 122, 1416−1481

Scheme 7. Chemical Synthesis of Cyanidin-3-Glucoside via Air Oxidation of a Flavene Intermediate

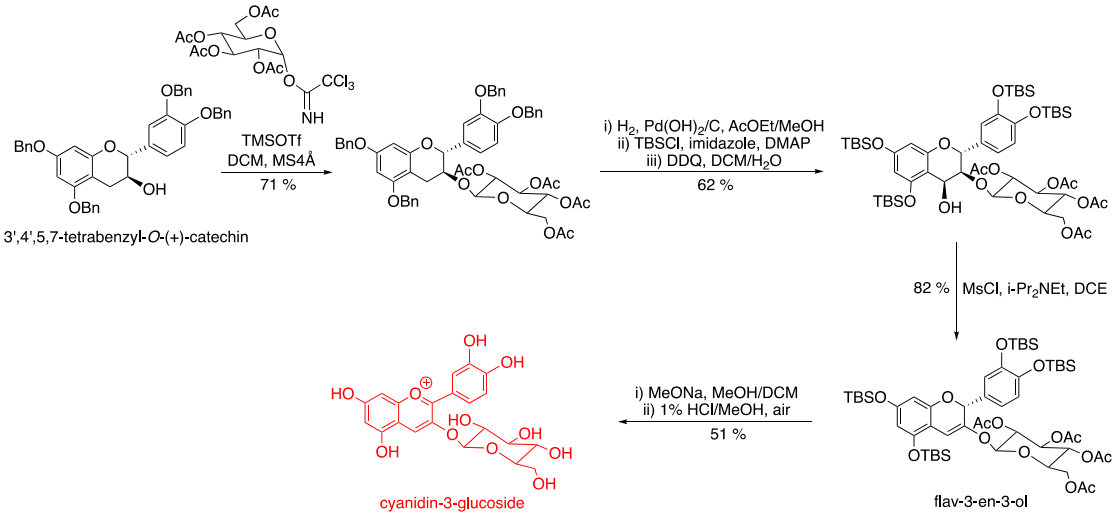

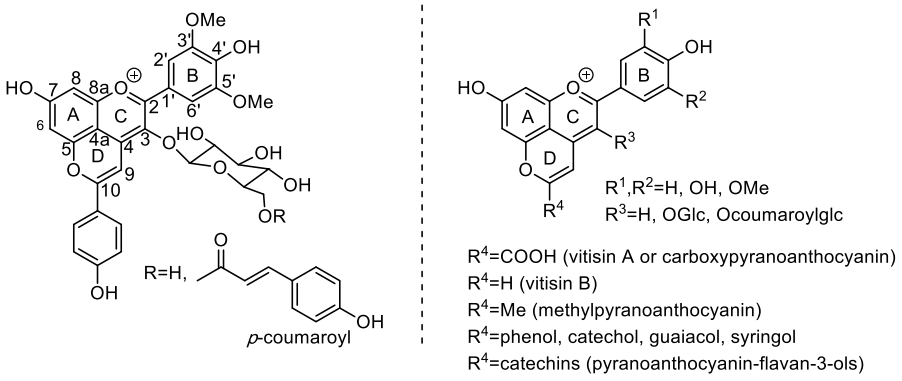

Figure 1. Structures of pyranoanthocyanins: (a) the first two pyranomalvidin-3-glucoside-derived pigments reported in wines; (b) general structure of pyranoanthocyanins.

pounds.[92] Sweeny and Iacobucci reported the formation of flavene intermediates from flavanone reduction using $NaBH_4$. The dehydration step requires an oxygen substituent at C7, suggesting the involvement of a quinone methide in flavene formation. The oxidation of flavenes with a chloranil reagent under acidic conditions then gives rise to the formation of the flavylium.[93,94]

(C) $LiAlH_4$ in the presence or absence of oxidizing agents. In 1950, Mirza and Robinson reported the use of $LiAlH_4$ reagent for the conversion of flavonols into anthocyanidins.[95] Afterward, Waiss and Jurd reported the synthesis of methylated cyanidin by a two-step reaction by using $LiAlH_4$ to reduce methylated quercetin to flavene intermediates and then introducing benzoquinone in acetic acid for flavene oxidation, giving yields of up to 80%.[96,97] In 2017, Kimura and co-workers reported using the same method to transform 8-aryl-methylated quercetins into the corresponding methylated cyanidins with 41−70% yields and without the need for any oxidizing agent.[98,99]

2.1.4. From Flavanol to Flavylium. In 2006, Oyama, Kondo, and co-workers reported a new and interesting synthesis protocol for obtaining anthocyanins from flavan-3-ols as a starting material. The first step consisted of the glucosylation of the C3 hydroxyl group in 3′,4′,5,7-tetrabenzyl-*O*-(+)-catechin with tetraacetylglucosyl imidate, yielding 3-*β*-tetracetylglucosyl-*O*-(+)-catechin tetrabenzylate. Following debenzylation and silylation, the molecule was oxidized with 2,3-dichloro-5,6-dicyano-*p*-benzoquinone (DDQ) and dehydrated to give a flav-3-en-3-ol. Further deprotection of the acetyl groups and oxidation under air in HCl−MeOH solution yielded cyanidin-3-glucoside, with a 51% yield (Scheme 7).[100] The mild air oxidative conversion of a flavene to flavylium revealed good yields and overcame the need to use oxidizing agents such as chloranil and benzoquinone reported for metal-reductive transformations.

2.1.5. Synthesis of Anthocyanin Derivatives. In the 20th century, the scientific community became aware of the high reactivity and instability of flavylium compounds, especially natural anthocyanins, which can easily be transformed into novel derivatives in food matrixes. In 1996, Cameira dos Santos et al.[101] detected a new family of anthocyanin derivatives in red wine filtrate samples. These pigments revealed a hypsochromic shift of their λ_{max} compared to anthocyanins (λ_{max} 507 nm), which have a more brick-orange color at acidic pH values. The structures of these pigments were further elucidated by Fulcrand et al.,[102] who revealed a new pyranic ring D between C4 and the hydroxyl group at C5 of anthocyanin and a hydroxylphenyl group that was connected at position 10 (Figure 1a). In 1997, Bakker and Timberlake[103] described the formation of a new pyranoanthocyanin (vitisin A); however, only one year later, the correct structure was elucidated by Fulcrand et al.[104] Since then, several classes of this type of anthocyanin derivative have been

https://doi.org/10.1021/acs.chemrev.1c00399
Chem. Rev. 2022, 122, 1416−1481

Scheme 8. General Mechanism for the Formation of Pyranoanthocyanin-Type Pigments

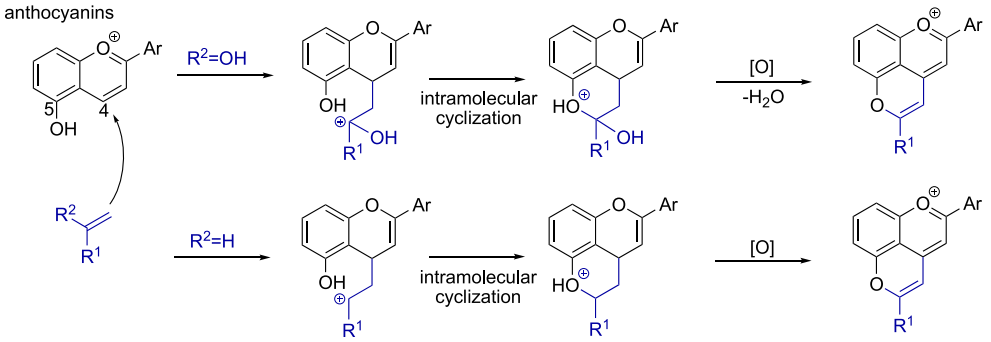

Scheme 9. Formation Pathways for the Second Generation of Pyranoanthocyanins

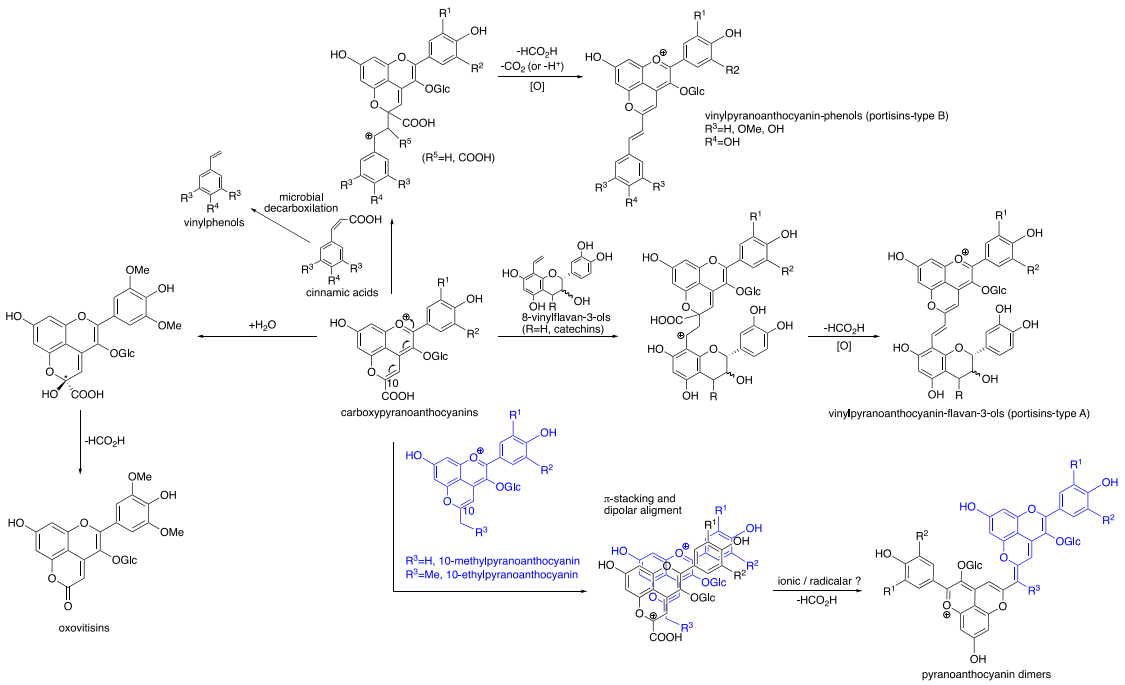

identified in different food matrixes and chemically synthesized in model solutions, and their respective formation mechanisms have been described. Although pyranoflavylium-type structures were first isolated from the resin of dragon's blood trees[105] and were also identified in other plants, such as in petals from *Rosa hybrida* and blackcurrant seeds,[106−108] the primary occurrence of pyranoanthocyanins has been described in beverages such as fruit and vegetable juices and red wines.[109] In red wines, the presence of this type of anthocyanin derivative contributes to changes in their organoleptic properties, namely, in the appearance of orange hues observed in aged red wines. The primary pyranoanthocyanins present in red wine are formed from the reactions of anthocyanins with yeast metabolites, which are released into the must during the fermentation process, for example, pyruvic acid,[103,104] acetoacetic acid,[110] acetone,[111] and acetaldehyde.[103] More complex classes of pyranoanthocyanins arise from the reaction between anthocyanins and cinnamic acids or vinylphenols (pinotins)[112−114] and between anthocyanins and flavan-3-ols (catechins and procyanidins) in the presence of acetaldehyde[115−119] (Figure 1b).

The formation pathway results from an annelation in which a nucleophilic enol derived from a carbonyl compound (R^2 = OH, Scheme 8) or a vinyl group (R^2 = H, Scheme 8) attacks the electrophilic C4 of the starting flavylium C-ring and then the phenolic OH at C5 adds to the carbonyl group, giving a hemiketal. Following H_2O elimination and some oxidation steps, a new pyrano D-ring is yielded, and for that reason these compounds were named pyranoanthocyanins (Scheme 8).

The formation mechanism of more complex pyranoanthocyanins such as pyranoanthocyanin-flavan-3-ol pigments involves the participation of 8-vinylflavan-3-ols as intermediates.[120−122] It has been postulated that these intermediates result from the preferential nucleophilic attack of the carbon 8 of the phloroglucinol A-ring of the acetaldehyde carbocation, which is formed after the protonation of the carbonyl group and further water elimination.[123] The vinyl bond of 8-vinylflavan-3-ol will attack the electrophilic C4 position of the anthocyanin, yielding a stabilized quinone methide. After some oxidation steps, the pyranoanthocyanin-flavan-3-ol pigments are obtained (Scheme 9).

Once 8-vinylflavan-3-ol was found to be an important intermediate in the formation mechanism of pyranoanthocyanin-flavan-3-ols, the synthesis of vitisin B was reported from the reaction between anthocyanins and commercially available vinyloxytrimethylsilane under hydroalcoholic conditions at acidic pH values.[124] Vitisin B-type pigments are very difficult

https://doi.org/10.1021/acs.chemrev.1c00399
Chem. Rev. 2022, 122, 1416−1481

Scheme 10. Synthesis Strategies to Obtain Synthetic 4-Substituted Flavylium Salts and Pyrano-3-deoxyanthocyanidin Salts

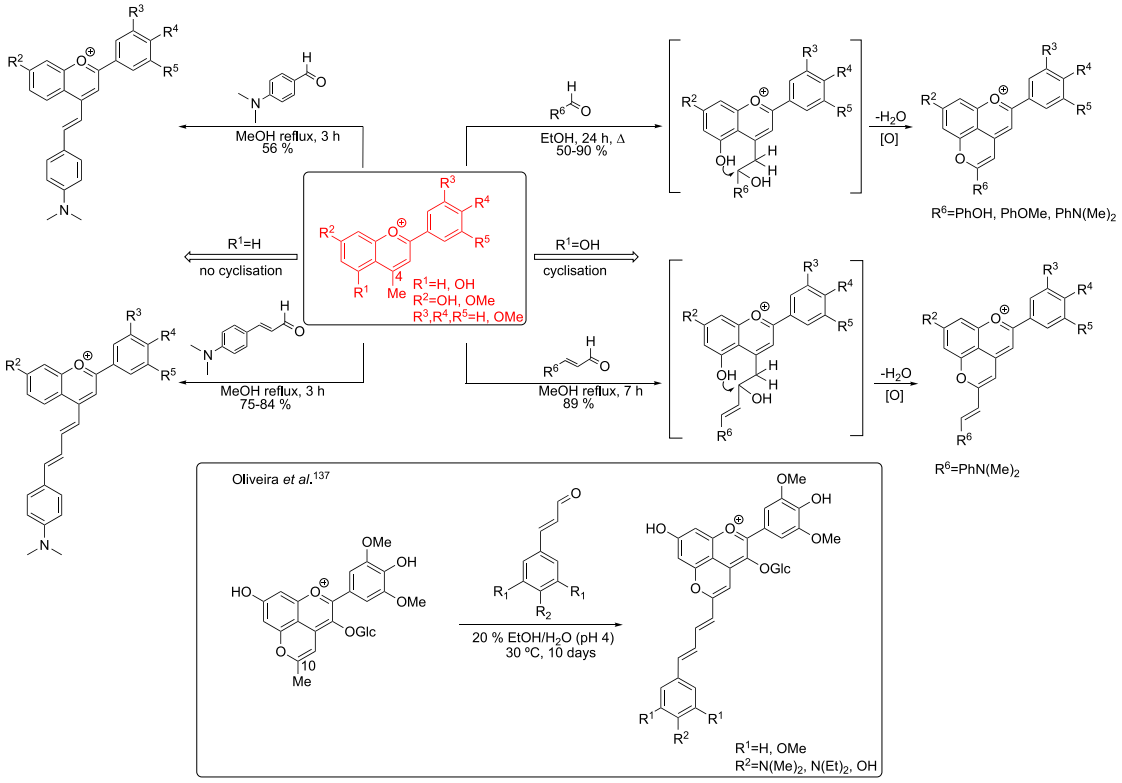

to isolate directly from food matrixes because of their very low concentrations. Thus, from this reaction, it was possible to obtain this type of pyranoanthocyanin with a yield up to 30%, which allowed for the study of some of the physical-chemical properties of this type of pigments. A few years later, a second generation of more complex pyranoanthocyanins started to emerge as a result of the chemical transformations of carboxypyranoanthocyanins into new derivatives (Scheme 9). Carboxypyranoanthocyanins (vitisin A) can react with water, yielding pyranone anthocyanin derivatives (oxovitisins) that possess a yellowish color (λ_{max} 373 nm) at pH 2. The suggested formation mechanism involves a nucleophilic attack on water at the electropositive C10 of carboxypyranoanthocyanins, yielding a hemiketal that further undergoes decarboxylation, giving a new neutral pyranone structure (Scheme 9).[125]

Carboxypyranoanthocyanins also demonstrated the ability to react with flavan-3-ols in the presence of acetaldehyde, giving rise to a new family of anthocyanin-derived pigments, vinylpyranoanthocyanin-flavan-3-ols, known as portisin-type A, because the first identified pigment was isolated from a young Port wine (Scheme 9).[126−128] These pigments have a purple-bluish color at acidic pH values (λ_{max} 570 nm), which is due to the extended conjugation of π electrons. Later, other portisin-type B pigments were detected in aged Port wines that resulted from the reaction between carboxypyranoanthocyanins and cinnamic acids (or vinylphenols resulting from microbial decarboxylation); however, these pigments have a λ_{max} hypsochromically shifted (between 533 and 540 nm in aqueous solution at pH 1 when compared to the portisin-type A pigments.[129] The formation of portisin-type pigments results from a nucleophilic attack on the vinyl group of the 8-vinylflavan-3-ol intermediate or through an attack of the double bond of cinnamic acids on the electropositive C10 of the pyranic ring. The last steps normally involve the loss of a formic acid, decarboxylation, and oxidation, giving rise to the final pyranoflavylium structure and then to the final vinylpyranoflavylium structure.[130] Moreover, new families of pigments with outstanding chromatic features were found to occur in aged Port red wines and in their respective sediments (lees). The reaction between carboxypyranoanthocyanins and 10-methylpyranoanthocyanins (or 10-ethylpyranoanthocyanins) resulted in the formation of pyranoanthocyanin dimers, which present an unusual and attractive turquoise blue color under acidic conditions (λ_{max} 680−730 nm).[131] The high delocalization of the π electrons across the two pyranoanthocyanin moieties promotes a large red shift in its maximum wavelength. Two synthetic pathways were initially proposed for the formation of dimeric pigments. The first suggested the deprotonation of the methyl group on the methylpyranoanthocyanin with the formation of a methylene group at carbon C10, followed by the double bond attack to the electrophilic carbon C10 of the carboxypyranoanthocyanin molecule. The deprotonation of the methyl group is more favorable to occur at a basic pH (pH ∼ 11); however, at the typical pH of food matrixes, the proton loss could occur to yield trace amounts of a very efficient nucleophile.[132] In the second hypothesis, it seems that charge transfer might be responsible for initiating the condensation between these two entities. This complex is stabilized by the $\pi-\pi$ interactions of the aromatic rings, and dipole−dipole interactions would place both partners in the right orientation for reaction. This formation pathway was initially proposed by Chassaing et al.;[133] however, the way this charge-transfer complex evolves remains unknown. It is proposed that further condensation between both precursors might occur through an ionic or radical reaction. The last step involves the loss of a formic acid molecule, leading to the formation of a structure with two pyranoanthocyanin moieties linked through a methine group.

https://doi.org/10.1021/acs.chemrev.1c00399
Chem. Rev. 2022, 122, 1416−1481

Scheme 11. Synthesis of Symmetrical Pyrano-3-deoxyanthocyanidin Dyes Obtained through Annelation Reactions

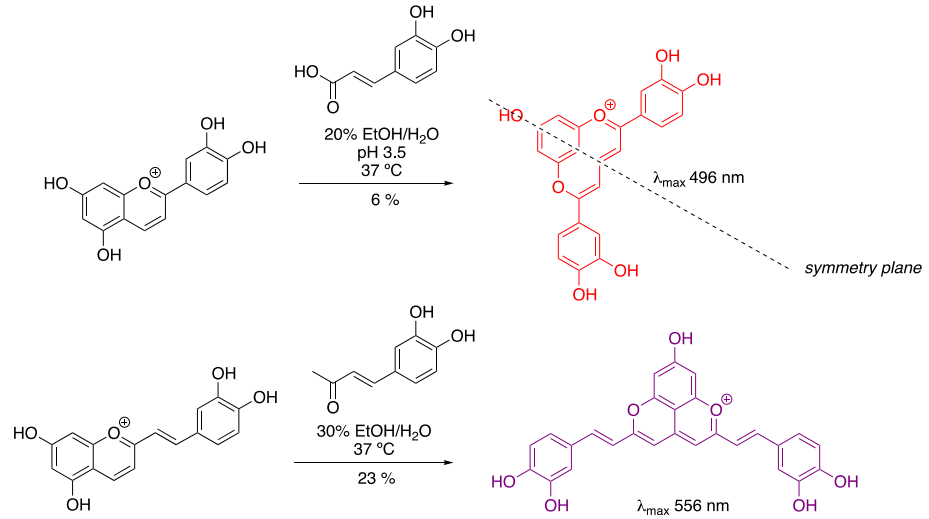

Scheme 12. Representation of the Most Stable (Based on Computational Studies) Anthocyanin A-Type Structures and B-Type Dimers (Flavene-Flavylium)

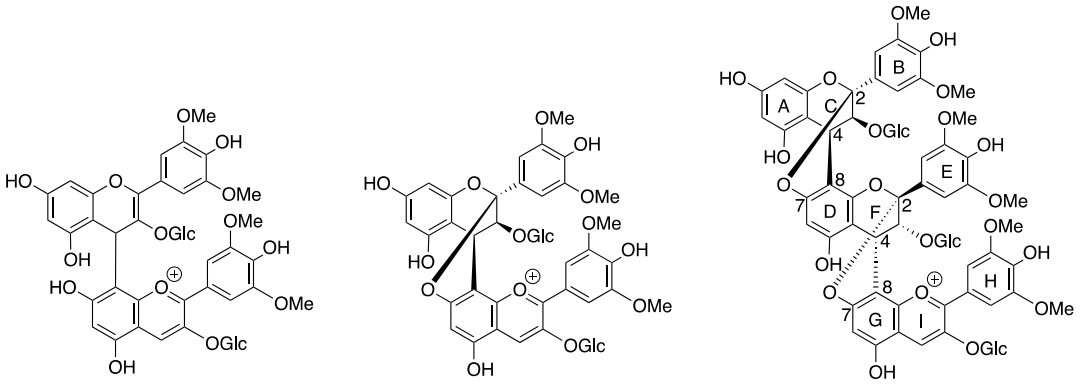

In 2001, Roehri-Stoeckel et al. reported that the synthesis of new 4-substituted flavylium salts could result from reactions between 4-methylflavylium pigments and 4-*N*,*N*-dimethylaminobenzaldehyde and 4-*N*,*N*-dimethylaminocinnamaldehyde reagents in methanol under reflux. The resulting pigments showed a large bathochromic shift, providing intense blue-violet to green colors (λ_{max} 548−730 nm, in methanol with 5% 0.1 M HCl) (Scheme 10).[83] Interestingly, the same authors also verified that, for 4-methylflavylium salts with R_1 = OH (4-methyl-5-hydroxy-3-deoxyanthocyanidins), a pyrano-3-deoxyanthocyanidin structure formed as a result of the intramolecular cyclization promoted by a hydroxyl nucleophilic attack, as described previously in the pyranoanthocyanin formation mechanism (Scheme 8). Based on those conclusions, Chassaing and co-workers later reported the synthesis of pyranoflavylium pigments through the reaction of 4-methyl-5,7-dihydroxyflavylium hexafluorophosphate salts and electron-rich aromatic aldehydes in refluxing ethanol. These authors indicated that this reaction was unlikely to occur when using aromatic aldehydes with electron-withdrawing substituents, such as fluor, cyano and nitro groups. The formation of a charge-transfer complex seems to be the responsible for initiating the condensation between aromatic aldehydes with electron-donating groups and 4-methylflavylium salts.[133,134] Later, da Silva et al. extended the scope of this reaction to aromatic aldehydes, including those with electron-withdrawing substituents or an attached heterocyclic or polycyclic aromatic ring. Three modifications were employed in the procedure by Chassaing and co-workers, namely, by using excess aromatic aldehydes under an inert atmosphere during the first hours and the presence of trifluoroacetic acid as an acid catalyst to support the formation of the corresponding products at good yields (64−89%).[135] Oliveira and co-workers also noted that 10-methylpyranoanthocyanins had the capacity to react with cinnamic aldehydes (e.g., sinapaldehyde, 4-(diethylamino)-cinnamaldehyde, and 4-(dimethylamino)cinnamaldehyde), resulting in a family of pyranoanthocyanin-based bluish pigments with two conjugated vinyl groups (butadienylidene group) presenting a λ_{max} value from 538 to 568 nm under acidic conditions, and the proposed mechanism involves a charge-transfer reaction pathway proposed by Chassing et al.,[133] and similar to the formation of pyranoanthocyanin dimers described before.[136,137] However, the pigments that were expected to present a higher maximum absorption wavelength because of the higher π delocalization unexpectedly showed a marked hypsochromic shift compared to their amino-based portisin counterparts (638 nm).[138]

https://doi.org/10.1021/acs.chemrev.1c00399
Chem. Rev. 2022, 122, 1416−1481

Scheme 13. Postulated Mechanisms for the Formation of Anthocyanin-Flavan-3-ol Dimer Adducts

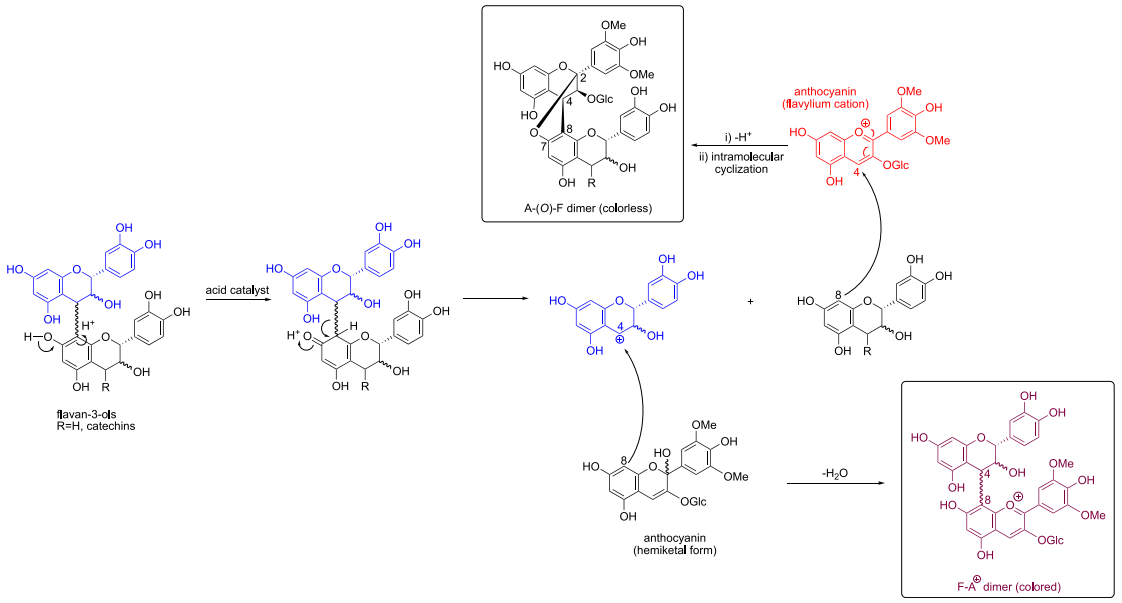

Scheme 14. Formation mechanism of Aldehyde-Mediated Aromatic Electrophilic Substitutions

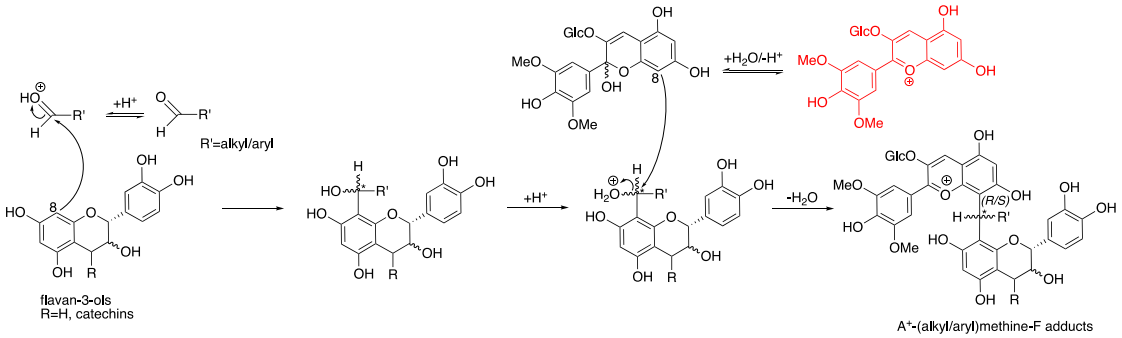

With inspiration from the formation of natural pyranoanthocyanins through annelation reactions, other synthetic pyrano-3-deoxyanthocyanidin pigments have recently been synthesized through the reaction of 3-deoxyanthocyanidins and different molecules (e.g., pyruvic acid, acetone, cinnamic acids, and styrylmethylketones), yielding a portfolio of colored compounds (λ_{max} 439−556 nm, under aqueous acidic conditions). Due to the extra pyranic ring, some pyrano-3-deoxyanthocyanidin derivatives could have interesting symmetries resulting from the positive charged distribution between the two pyranic rings and depending on the substituents in their structures (Scheme 11).[24,60,139,140]

The chemistry of other families of anthocyanin derivatives that primarily occurs in grapes and their relevance in red wines have been frequently reviewed.[141] They can be divided in two groups when considering their formation pathways: nucleophilic addition of a C-centered nucleophile (anthocyanin hemiketal form) to the C4 position of the flavylium cation and aldehyde-mediated electrophilic substitutions.

Some of them have also been synthesized under model winelike conditions. The presence of oligomeric anthocyanins (dimers and trimers) was first detected in grape skins using mass spectrometry techniques, and their structures present a flavylium cation as a terminal unit linked to a flavan or flavene form as extension units through A-type (C4-C6 and C2-*O*-C7 or C4-C8 and C2-*O*-C5) or B-type (C4-C6 or C4-C8) linkages, respectively[142−145] (Scheme 12).

A few years later, Oliveira et al. detected the occurrence of A-type anthocyanin (malvidin-3-glucoside derivative) dimers and trimers in grape skins and in a young Port wine using liquid chromatography coupled to mass spectrometry and NMR spectroscopy.[146]

These authors suggested that the presence of a flavene structure is not likely to occur because of the nucleophilic attack of the OH group in the C7 position to the unsaturated C2 of the flavene moiety. A-type anthocyanin trimers can present four isomers, (α,α), (α,β), (β,α), and (β,β), because the pyranic rings composed by C7-*O*-C2 (formed between D- and C-rings and between G- and F-rings) may be above (α) or below (β) the plane of the structure. Theoretical and computational studies suggest that the A-type malvidin-3-glucoside trimer isomer (α,β) is the most stable.

Another example of direct condensations is the reaction between anthocyanins and flavan-3-ols that can yield colorless bicyclic A-(*O*)-F[147,148] and colored F-A$^+$[149] dimeric pigments (Scheme 13). The formation of F-A$^+$ in wines is well established in the literature and is described in two steps: first, a cleavage of the interflavanolic linkage of flavan-3-ols occurs, yielding a carbocation in C4, which then undergoes a nucleophilic attack of anthocyanins in their hemiketal form. Then, the formation of an A-(*O*)-F dimer results from the nucleophilic attack of the C6 or

https://doi.org/10.1021/acs.chemrev.1c00399
Chem. Rev. 2022, 122, 1416−1481

Scheme 15. Formation Mechanism of Anthocyanin-Ellagitannin Adducts in Red Wines

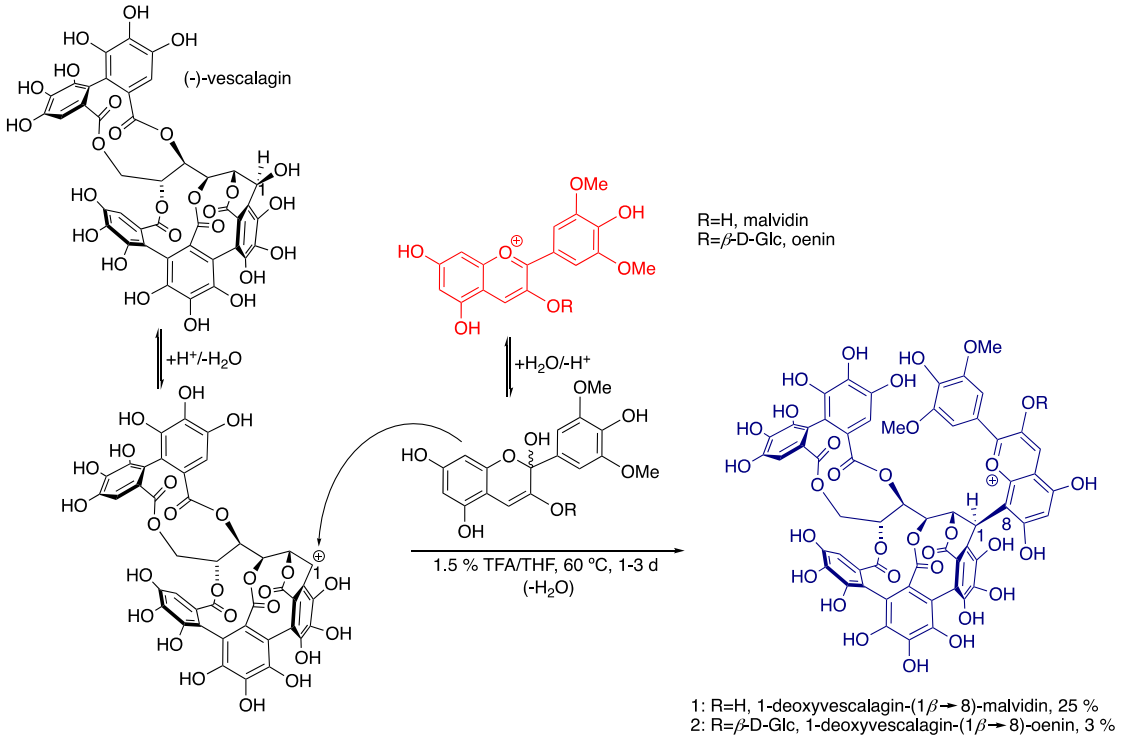

C8 of flavan-3-ols to the electropositive C4 of the flavylium cation. The flavene intermediate further evolves toward a colorless bicyclic adduct (C2-*O*-C7 and C4-C8 linkages) rather than undergoing oxidation, which gives the cationic flavylium form in the upper unit (Scheme 13).[150]

One of the first families of anthocyanin derivatives detected in red wines arose from the reaction of anthocyanins with flavan-3-ols induced by acetaldehyde.[122,151−155] Since the first adduct were described, the scientific community has identified and synthesized several new A^+-(alkyl/aryl)methine-F-type adducts[145,156−159] (Scheme 14). In accordance with their formation pathway, the aldehydes in acidic media are protonated and then undergo a nucleophilic attack from the C8/C6 of flavan-3-ols. A dehydration then occurs, yielding another carbocation, which undergoes an attack from the C6/C8 of the hemiketal of the anthocyanin. After a final dehydration, the new adduct is formed.[151]

More recently, a group of anthocyanin-ellagitannin adducts were proposed by Quideau and co-workers to occur during red wine maturation due to the reaction of anthocyanins and *C*-glucosidic ellagitannins present in oak wood. Their mechanistic pathway is described by the nucleophilic attack of the anthocyanin hemiketal species on the C1 carbocation of (−)-vescalagin formed after the protonation/dehydration steps (Scheme 15).[160−162] They present a modest bathochromic shift in the visible band compared with that of anthocyanin (**1**, λ_{max} 545 nm; **2**, λ_{max} 542 nm in HCl 0.1 M, pH 1), which can arise either from stronger intramolecular interactions between their flavylium and (−)-vescalagin aromatic moieties or from a charge-transfer contribution.[163,164] These pigments can make a significant contribution to the color change from red to more purple hues during the early stages of wine aging in oak barrels.

2.2. Biotechnological Production of Anthocyanins

Traditionally, anthocyanins are obtained directly from flowers, vegetables, and fruits. However, anthocyanins from plants are present as heterogeneous chemical structures, and plant extracts are rich in many other chemical compounds that could be a bottleneck for industrial purposes. In fact, the presence of other compounds affects the color performance of anthocyanins and their stability. However, purification of anthocyanins from complex plant extracts is often a very difficult, time-consuming, and expensive task. In addition, the anthocyanin contents of plants vary depending on the source and also on seasonal and environmental conditions.

The limited commercial availability and the diversity of anthocyanins have led to searches for alternative sources. Chemical synthesis could be an option, as described in section 2.1. Another alternative is genetic engineering of genes encoding biosynthetic enzymes in plant cells and microorganisms such as bacteria (*Escherichia coli*) and yeast (*Saccharomyces cerevisiae*) for their use as cell factories for anthocyanin synthesis.[50,52,165] In plants, the high-level production of secondary metabolites can be achieved by engineering regulatory genes as well as genes encoding specific biosynthetic enzymes. The biosynthesis of anthocyanins in plants is well established.[166,167] These compounds are synthesized via the general flavonoid pathway, and they involve the condensation of malonyl-CoA and 4-coumaroyl-CoA derived from phenylalanine or tyrosine as mediated by two key enzymes, chalcone synthase (CHS) and chalcone isomerase (CHI), to form naringenin chalcone and its isomer naringenin (a flavanone), respectively (Scheme 16). The latter compound is the primary intermediary in the biosynthesis of anthocyanins with many different decorations. Naringenin is modified through hydroxylation by enzymes such as flavanone 3β-hydroxylase (FHT *syn*. F3H), flavonoid 3′-hydroxylase (F3′H) and flavonoid 3′,5′-hydroxylase (F3′5′H), giving rise to different dihydroflavonols (dihydrokaempferol, dihydroquercetin, and dihydromyricetin). Then, dihydroflavonol 4-reductase (DFR) promotes the formation of leucoanthocyanidins (leucopelargonidin, leucocyanidin, and leucodelphinidin), and

https://doi.org/10.1021/acs.chemrev.1c00399
Chem. Rev. 2022, 122, 1416−1481

Scheme 16. Pathway of Anthocyanin Biosynthesis in Plants[a]

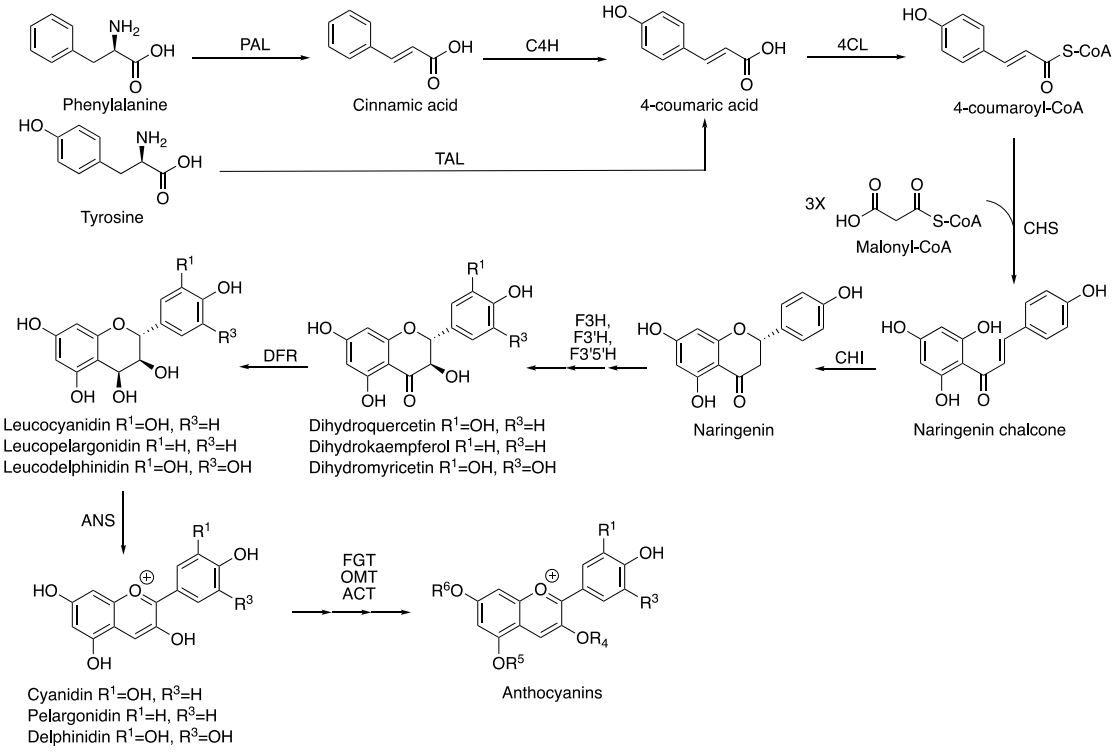

[a]Adapted with permission from ref 51. Copyright 2018, Springer Nature [Creative Commons CC BY license]. Abbreviations: PAL, phenylalanine ammonia lyase; C4H, cinnamate 4-hydroxylase; TAL, tyrosine ammonia lyase; 4CL, 4-coumaroyl-CoA ligase; CHS, chalcone synthase; CHI, chalcone isomerase; F3H, flavanone 3β-hydroxylase; F3′H, flavonoid 3′-hydroxylase; F3′5′H, flavonoid 3′, 5′-hydroxylase; DFR, dihydroflavonol 4-reductase; ANS, anthocyanidin synthase; FGT. flavonoid *O*-glycosyltransferase; OMT, *O*-methyltransferase; and ACT, anthocyanin acyltransferase.

anthocyanidin synthase (ANS *syn*. LDOX) generates the flavylium cations (anthocyanidin; pelargonidin, cyanidin, and delphinidin) by oxidation. The latter compound is then linked to a monosaccharide residue at C3 in ring C or other positions through flavonoid glucosyltransferase (FGT)-catalyzed glycosylation.

There are some clear examples in the literature of the production of anthocyanins from mutant plant cell lines that showed not only increased concentrations of anthocyanins but also changes in their decoration level and structural complexity. In a very interesting and inspiring study, Appelhagen et al. described the development of suspension cultures from tobacco plants that constitutively expressed the MYB Rosea1 (AmRos1) and bHLH Delila (AmDel) transcription factors (TF) from *Antirrhinum majus* to produce a higher level of anthocyanins.[50] These cultures produce exceptionally high amounts of anthocyanins (20−25 mg cyanidin-3-*O*-rutinoside equivalents/dry weight), 2−10 times higher than those that could be obtained from fruits, depending on the variety. Furthermore, the authors expanded the variety of anthocyanins produced using the same cell line through the coexpression of additional genes encoding F3′5′H from *Petunia hybrida* to obtain delphinidin-3-*O*-rutinoside or a gene encoding an anthocyanin 3-*O*-rutinoside-4‴-hydroxycinnamoyl transferase from *Solanum lycopersicum* (Sl3AT) to obtain the respective coumaroyl or feruloyl derivatives. That engineering strategy could be transferred to other plants with higher levels of decoration to obtain more complex anthocyanin structures. In fact, in the same study, Appelhagen et al. generated cell cultures from *Arabidopsis thaliana* expressing the same TF AmRos1 and AmDel, and their aim was to produce anthocyanins with multiple acyl groups (cyanidin 3-*O*-[2″-*O*-(2‴-*O*-(sinapoyl) xylosyl) 6″-*O*-(*p*-*O*-(glucosyl) *p*-coumaroyl) glucoside] 5-*O*-[6⁗-*O*-(malonyl) glucoside]).[50]

Other groups reported the production of ^{13}C and ^{14}C-labeled flavonoid compounds (including anthocyanins) from plant cell suspension cultures to follow their bioavailability in humans.[168,169] ^{13}C-Labeled anthocyanins were obtained by [1-^{13}C]-L-phenylalanine feeding experiments where it will enter in plant secondary metabolism resulting into incorporation into anthocyanins through the shikimate pathway. In the case of ^{14}C-labeled anthocyanins, these were obtained by using uniformly labeled [^{14}C] sucrose as the source of label delivered to the metabolizing cell cultures.

Another alternative way to produce anthocyanins is the genetic transformation of microorganisms, such as yeast and bacteria. The microbial biosynthesis approach to producing natural flavonoids dates back to 2003.[52,170] This technique starts at the selection of the proper enzymes involved in the anthocyanin biosynthesis pathways from different plant sources. Then, further modifications are required to obtain the desired functional expression. Microbes require the expression of at least 11 transgenes to introduce the complete anthocyanin biosynthetic pathway for de novo production of metabolites starting from glucose, which complicates the process. This approach can be simplified if natural precursors of anthocyanins (eriodictyol and naringenin) are supplied in the medium. However, since these precursors are too expensive, these strategies are not economically viable and it is advisible to use 4-coumaric acid as a starting point.

However, the bacterial expression of genes encoding F3′H and F3′5′H is a bottleneck. In 2005, Yan et al., cloned and

https://doi.org/10.1021/acs.chemrev.1c00399
Chem. Rev. 2022, 122, 1416−1481

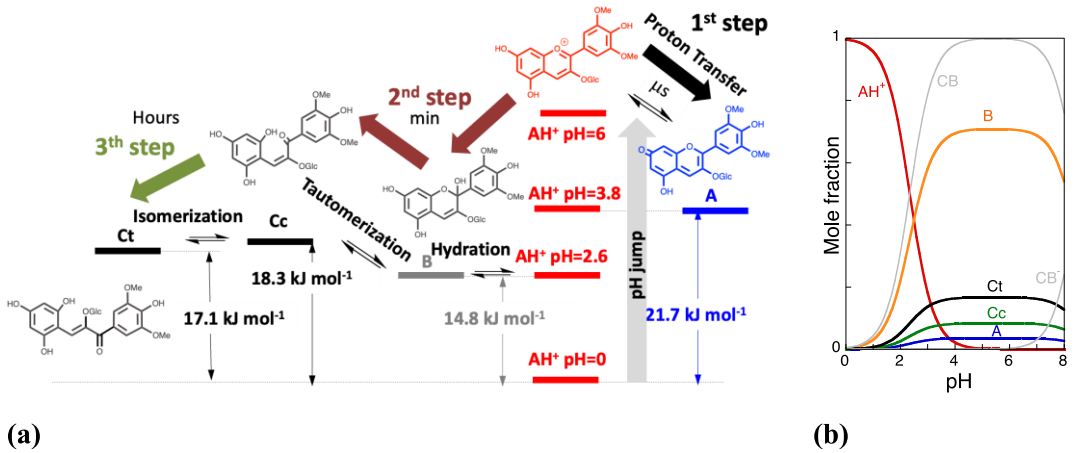

Figure 2. (a) Thermodynamic energy level of malvidin-3-glucoside (oenin), 2×10^{-5} M, in acidic medium, showing the three kinetic steps upon direct pH jump; (b) mole fraction distribution of the species AH^+ and the neutral forms A, B, Cc, and Ct at equilibrium. Anionic species are formed at higher pH values, but the oenin multistate cannot be fully characterized due to its decomposition in basic medium; CB = [A] + [B] + [Cc] + [Ct] and CB^- = $[A^-]$ + $[B^-]$ + $[Cc^-]$ + $[Ct^-]$, respectively, defined in eqs 8 and 9. Adapted with permission from ref 183. Copyright 2020, Elsevier.

expressed the genes F3H and ANS from *Malus domestica*, DFR from *Anthurium andraeanum*, and flavonoid 3-*O*-glucosyltransferase (F3GT) from *Petunia hybrida* in *E. coli*, and after optimization of the supplied UDP-glucose the bacterium produced 350 mgL^{-1} cyanidin 3-*O*-glucoside and 113 mgL^{-1} pelargonidin 3-*O*-glucoside by using eriodictyol and naringenin as precursors, respectively.[171]

Unlike in plant cells, in which anthocyanins are moved from the cytoplasm to the vacuole and stored, microbial hosts lack the machinery for anthocyanin transport and stabilization. The intracellular pH of bacteria commonly used for metabolic engineering is approximately pH 7, and at this pH anthocyanins begin to suffer degradation. To stabilize anthocyanins, a two-step biocatalysis has been proposed, and after a specific growth stage during the metabolic process at pH 7 the cells should be transferred to fresh medium in which the pH is adjusted to 5 to minimize anthocyanin degradation.[172]

More recently, specific anthocyanin biosynthetic genes recruited from *A. thaliana* and *Gerbera hybrida* were introduced into a *S. cerevisiae* strain expressing PAL, TAL, C4H, CPR, 4CL, CHS, CHI, F3H, DFR, ANS and 3GT.[51] In this microbial model, pelargonidin 3-*O*-glucoside was formed directly from glucose and located inside yeast cells, albeit at low concentrations. During the same year, Eichenberger et al. reported the reconstruction of the complete machinery for biosynthesizing P3G-, C3G-, and D3G-expressing enzymes from different plant sources within *S. cerevisiae*.[173] However, the resulting concentrations are low (P3G, 0.85 mg/L; C3G, 1.55 mg/L; and D3G 1.85 mg/L), and one of the limiting steps seems to be the activity of ANS, which has shown a strong ability to convert leucoanthocyanins into flavonol, bypassing the synthesis of anthocyanins. Interestingly, Zhang et al. reported that ANS extracted from *Vitis vinifera* (*Vv*ANS) catalyzes the in vitro transformation of natural leucocyanidin into flavan-3,3,4-triols and quercetin, suggesting that anthocyanidin synthase requires other substrates for the in vivo formation of anthocyanidins.[174]

From another perspective, other biotechnological tools can be used toward the modulation of the acylation pattern of anthocyanins. A recent example is the production of a specific and highly selective catalytic diacylation enzyme by genetic engineering using *E. coli* codon-optimized gene encoding enzymes. This enzyme was shown to selectively remove acyl groups bound to Glc-1 of the 3-sophorose moiety of a cyanidin derivative from red cabbage while leaving the acyl group on Glc-2 intact, converting polyacylated anthocyanins into a monoacylated anthocyanin having a blue color at pH 7 (λ_{max} of 640 nm).[175]

In conclusion, replicating the plant anthocyanin biosynthesis pathway in microorganisms such as *E. coli* or *S. cerevisiae* is a challenging task that is intended to respond to the growing industrial need for these natural pigments. Considering the different biotechnological approaches to produce anthocyanins at the industrial scale, the production rate will necessarily define their future economic viability.

However, industrial applications of plant cell cultures for secondary metabolite production, including anthocyanins, are still rare, mostly as a result of the limited stability of long-term cultures, variable product yields, and high costs.

From other perspectives, engineered anthocyanin biosynthesis has also been used to enrich these pigments in fruits, legumes, and cereals to improve their sensorial and nutritional quality. In the literature, some studies have described the production of anthocyanin-enriched fruits and cereals, such as purple tomatoes and purple endosperm rice.[176,177]

3. MULTISTATE OF CHEMICAL SPECIES GENERATED BY FLAVYLIUM CATIONS: THERMODYNAMIC AND KINETIC ASPECTS

Anthocyanins are generally identified in the literature by their respective flavylium cations.[19] The systematic attribution of the identity of anthocyanins to their flavylium form without considering the pH conditions at which the experiments are performed could lead to misinterpretations of experimental results. In fact, the flavylium cation is a molecule (generally observed in very acidic solutions) of a complex system that includes other species that are reversibly interconnected by external stimuli such as pH, light and temperature.

The history of anthocyanins and related compounds evolution up to the present perception of this system was previously described.[178] Under acidic to moderately acidic pH values, five chemical species, namely, flavylium cation (AH^+), quinoidal base (A), hemiketal (B), and *cis* and *trans* chalcones (Cc and Ct), are connected through four chemical reversible reactions, proton transfer, hydration, tautomerization, and *cis*–

https://doi.org/10.1021/acs.chemrev.1c00399
Chem. Rev. 2022, 122, 1416−1481

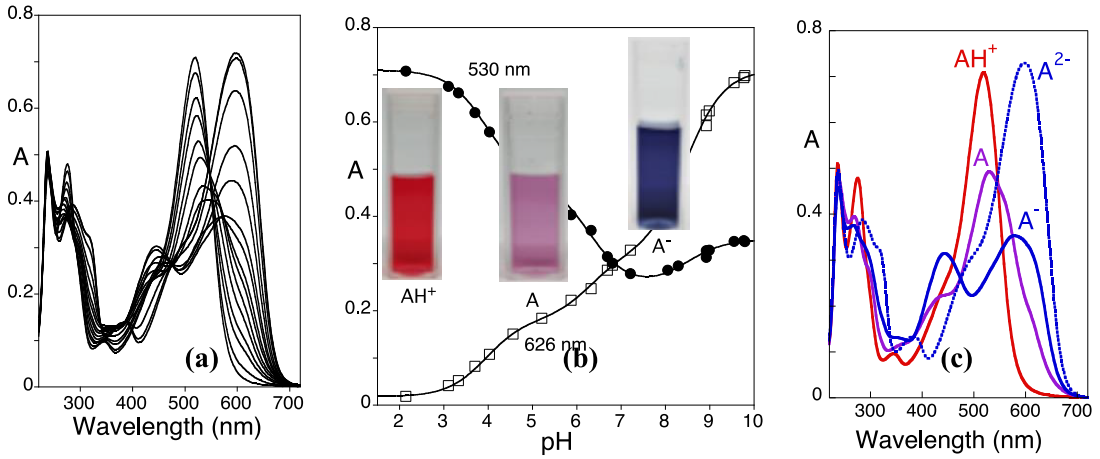

Figure 3. (a) Spectral variations in malvidin-3-glucoside (oenin) 10 ms after a set of direct pH jumps monitored by stopped flow; (b) fitting of the absorbance of (a) at two representative wavelengths versus the pH permits us to calculate two acid−base constants regarding the first deprotonation, pK_a = 3.95 (to give quinoidal base) and the second deprotonation, pK_{a2} = 6.3 (to give anionic quinoidal base), and pK_{a3} = 8.5 (to give dianionic quinoidal base); and (c) deconvolution of the spectra in (a) to individuate the absorption spectra of each species.

Scheme 17. Acid−Base Polyprotic Equilibria for Cyanidin-3-glucoside Showing Some Relevant Tautomers[a]

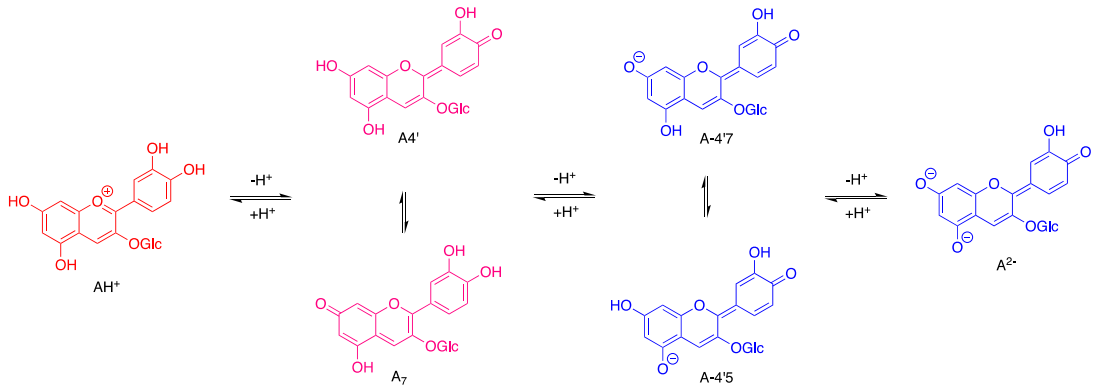

[a]Adapted with permission from ref 189. Copyright 2019, PCCP Owner Societies.

trans isomerization, as shown in Figure 2a for malvidin-3-glucoside (oenin). Going forward, this system is labeled as the "flavylium multistate". The flavylium multistate is characterized by its thermodynamics and kinetics. The thermodynamics of this system can be described by its respective energy level diagram[179,180] (Figure 2a) or by a representation of the mole fraction distribution of the flavylium multistate species as a function of pH (Figure 2b).[181,182] Both representations can be extended to the anionic forms obtained through deprotonation of the hydroxyl substituents in neutral and basic solutions.

Conveniently, the kinetics of the flavylium multistate are studied by adding a base to equilibrated solutions of the flavylium cations at pH ≤ 1 (direct pH jumps)[182,184] or by adding acid to equilibrated solutions at higher pH values back to pH ≤ 1 (reverse pH jumps).[185] Stopped-flow equipment is necessary to account for the kinetic steps over a time domain from milliseconds to several seconds.

3.1. Direct pH Jumps

The sequence of events after a direct pH jump was reported for oenin,[186] but mutatis mutandis is the behavior of any multistate in which the *cis*−*trans* isomerization is much slower than other kinetic processes. After a direct pH jump, three distinct kinetic steps take place. The first step is a proton transfer, which occurs in submicroseconds, as shown in eqs 1 and eq 2.[184,187] This rate is faster than the mixing time of the stopped-flow and requires other techniques, such as temperature jumps[184] or flash photolysis[187] (see section 5 of this Review). Although the kinetic information of the proton transfer step cannot be obtained from the pH-jump experiments, the thermodynamic parameters (i.e., pK_a) can be found in a straightforward manner from the absorption spectra registered approximately 10 ms after a direct pH jump to several pH values (Figure 3a). During this short time interval, the other species are not yet present (B, Cc, and Ct), and therefore, using the spectroscopic data as a function of pH allows us to obtain the corresponding pK_a's, as reported in Figure 3b for oenin, which indicates the existence of three inflection points, resulting from the equilibrium between $AH^+ \rightleftharpoons A \rightleftharpoons A^- \rightleftharpoons A^{2-}$ with pK_a's of 3.95, 6.3 and 8.5.

For polyprotic systems, deconvolution techniques may be employed to estimate the individual spectra, and consequently, the color expressed by the pure species, as shown in Figure 3c for oenin. Based on experimental data supporting the higher acidity of OH groups in position 7 comparatively with 4'-OH, the neutral quinoidal base (A) is usually represented with the former deprotonated as in Figure 2a. For example, the pK_a of 7-β-D-glucopyranosyloxy-4′-hydroxyflavylium was reported to be 5.4 while for 4′-β-D-glucopyranosyloxy-7-hydroxyflavylium it is 3.7.[188] Nevertheless, compounds comprising several OH groups can be considered to exist in tautomeric equilibria, with the

https://doi.org/10.1021/acs.chemrev.1c00399
Chem. Rev. 2022, 122, 1416−1481

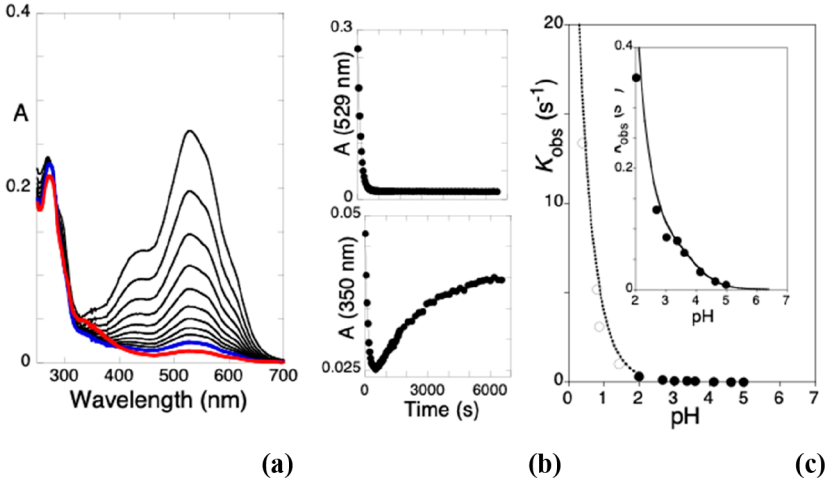

Figure 4. (a) Spectral variations in oenin (1.0×10^{-5} M) upon a direct pH jump from pH = 1.0 to pH = 5.0; blue curve corresponds to the absorption spectrum after the end of the hydration reaction (pseudoequilibrium), and red curve the absorption spectrum at the equilibrium; (b) traces of the kinetic steps at 529 and 350 nm; and (c) pH-dependent rate constant of the hydration reaction (●) with direct pH jumps fitted with eq 5 and (○) reverse pH jumps followed by stopped-flow fitting with eq 22, see below. Adapted with permission from ref 186. Copyright 2012, Elsevier.

different tautomers contributing to the observed absorption spectra of these species, as exemplified in Scheme 17 for cyanidin-3-glucoside. Recent molecular dynamics and TDDFT studies suggested the quinoidal species shown in Scheme 17 as major species with other possible tautomers excluded on the basis of their computed DFT energies.[189] Although the computed absorption UV−vis spectra showed excellent agreement with the experimentally measured spectra, the authors acknowledged that entropic contributions, not taken into account in this study, may affect the relative energies computed for each species. The authors also highlighted the excellent agreement between the experimental spectrum measured at pH ≥ 7 and the one computed for $A^-_{4'5}$ which comprises a distinctive shoulder-maximum two peak shape that is absent in the computed spectrum of $A^-_{4'7}$. This led the authors to suggest the $A^-_{4'5}$ protomer to be the dominant colored species at neutral/slightly basic pHs, despite its higher computed energy, pointing out the negative effect of the higher energy shoulder at $\lambda \approx 440$ nm to blue color expression and the glycosylation of position 5 to hinder this effect. It is worth mentioning that recent experimental studies with 3,5-diglucosides support this last observation.[190]

Considering that the successive kinetic steps are much slower, the species AH^+ (red color) and A (purple color) as well as A^- and A^{2-} (blue color) observed in neutral to moderately basic solutions can be considered to be at equilibrium during the subsequent kinetic events.

In a moderately acidic medium, eqs 1 and 2 account for the proton transfer.

$$AH^+ + H_2O \underset{k_{-a}}{\overset{k_a}{\rightleftharpoons}} A + H_3O^+ \quad K_a \text{ proton transfer} \tag{1}$$

[Equation 1 can be generalized to anionic species. Here, for the sake of simplicity, the first equilibrium is presented.]

$$k_{1st(direct)} = k_a + k_{-a}[H^+] \tag{2}$$

The second step presented in Figure 4a corresponds to the disappearance of AH^+/A to form species B through the hydration reaction, followed by a faster tautomerization to give Cc. Since the hydration at the pH values used in direct pH jumps is generally much slower than tautomerization, the second step is kinetically controlled by the hydration. A particular feature of the hydration reaction is that it takes place from AH^+ and not from A (which does not hydrate in acidic to moderately acidic solutions). This achievement was a breakthrough discovery by Brouillard and Dubois[184] and is fundamental for the comprehension of the flavylium multistate kinetics. Equations 3 and 4 together with eq 5 account for this kinetic step.

$$AH^+ + 2H_2O \underset{k_{-h}}{\overset{k_h}{\rightleftharpoons}} B + H_3O^+ \quad K_h \text{ hydration} \tag{3}$$

$$B \underset{k_{-t}}{\overset{k_t}{\rightleftharpoons}} Cc \quad K_t \text{ tautomerization} \tag{4}$$

The expression that accounts for the second step was achieved in a straightforward manner considering that the species AH^+ and A on one side and B and Cc on the other are in fast equilibrium during the hydration step, in eq 5.[191]

$$k_{2nd(direct)} = \chi_{AH^+} k_h + \chi_B k_{-h}[H^+] = \frac{[H^+]}{[H^+] + K_a} k_h + \frac{1}{1 + K_t} k_{-h}[H^+] \tag{5}$$

Here, χ_{AH^+} and χ_B are the mole fraction of AH^+ in its equilibrium with A and the mole fraction of B in its equilibrium with Cc, respectively. An example of the spectral variations that occur during the second step was again reported for oenin.[186] After a direct pH jump to pH = 5.0, the resulting quinoidal base disappears according to a biexponential process. The faster process occurs over a time scale of minutes, while the slower process, from the blue spectrum to the red spectrum shown in Figure 4a and b, takes a few hours. The faster kinetic process corresponds to the second step, controlled by the hydration reaction (Figure 2a), while the slower process corresponds to the third one (*cis*−*trans* isomerization). This large difference in rates between the second and third steps allows for the definition of a pseudoequilibrium to be reached before the significant formation of *trans*-chalcone. In fact, during *cis*−*trans* isomerization, the species AH^+, A, B, and Cc have enough time to equilibrate. Usually, the observed rate constants are taken for a series of pH values to fit the data to eq 5 and to determine the

https://doi.org/10.1021/acs.chemrev.1c00399
Chem. Rev. 2022, 122, 1416−1481

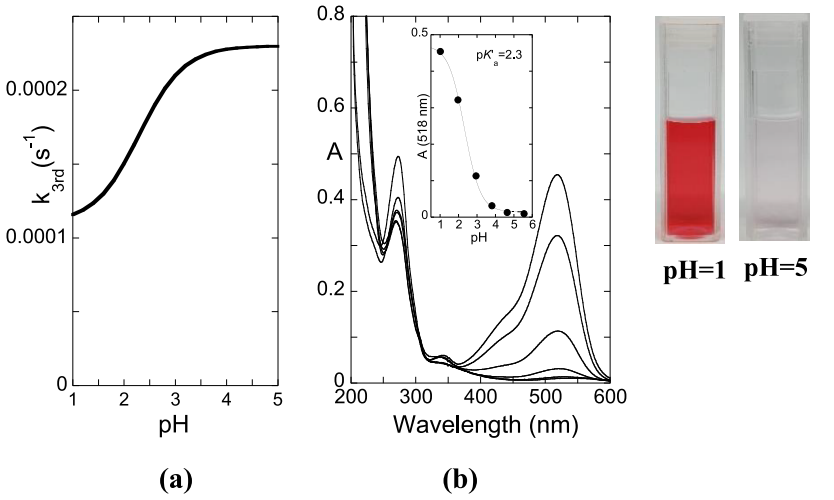

Figure 5. (a) Rate constants of the isomerization process of oenin at 1.4×10^{-5} M obtained upon direct pH jumps and reverse pH jumps (see below). Fitting was performed with eq 7 and (b) the absorption spectra of oenin at equilibrium. The system behaves as a single acid−base equilibrium in acidic medium.

respective rate and equilibrium constants (Figure 4c). This kinetic approach is not exclusive of anthocyanins and has been observed in many other flavylium-based multistates exhibiting very slow *cis*−*trans* isomerization kinetics. [The very slow isomerization rate may result from the very small mole fraction of Cc at the pseudoequilibrium or from the high *cis*−*trans* isomerization barrier, which is the case for anthocyanins.]

The third step, leading to the formation of Ct, is given by eqs 6 and 7.

$$\mathrm{Cc} \underset{k_{-i}}{\overset{K_i}{\rightleftharpoons}} \mathrm{Ct} \quad K_i \text{ isomerization} \tag{6}$$

$$k_{3rd(direct)} = \chi_{Cc} k_i + k_{-i} = \frac{K_h K_t}{[H^+] + K_a + K_h + K_h K_t} k_i + k_{-i} \tag{7}$$

where χ_{Cc} is the mole fraction of Cc at pseudoequilibrium. Despite the small spectral variations from the pseudoequilibrium to equilibrium shown in Figure 4a (as observed in common anthocyanins), the respective rate constants can be calculated and represented as a function of the pH (Figure 5a). The absorption spectra at equilibrium in acidic medium versus the pH are shown in Figure 5b.

The spectral variations of oenin in Figure 5b are fitted according to a single acid−base equilibrium with an acidity constant $pK'_a = 2.3$. This is a relevant result, which was already clearly intuited by Brouillard et al. in 1978, that allows for a dramatic simplification of the system.[182] In fact, the four equilibria represented by eqs 1, 3, 4, and 6 can be simplified as a single acid−base equilibrium involving AH^+ and the apparent conjugated base CB, in eq 8, defined as the sum of the concentrations of all the species in equilibrium with AH^+, [CB] = [A] + [B] + [Cc] + [Ct]

$$AH^+ + H_2O \rightleftharpoons CB + H_3O^+$$

$$K'_a = K_a + K_h + K_h K_t + K_h K_t K_i \tag{8}$$

The constant K'_a was deduced from the definition of a single acid−base equilibrium through a mass balance and the definition of the equilibrium constants that allow the expression of all species in terms of the AH^+ concentration.

The mathematical treatment is extended to the anionic forms.[192] This extension is particularly necessary when acylated anthocyanins, such as those found in heavenly blue anthocyanin (*Ipomoea tricolor*),[29,193] red cabbage,[194] Japanese morning glory (*Pharbitis Ipomoea nil*),[195] or sweet potato,[196] are studied as well as those in many synthetic flavylium compounds, which are stable in basic medium. The extension to the monoanionic species is presented here for the sake of simplicity, but it can be generalized to higher deprotonated forms.[192]

$$CB + H_2O \rightleftharpoons CB^- + H_3O^+ \quad K''_a$$

$$[CB^-] = [A^-] + [B^-] + [Cc^-] + [Ct^-] \tag{9}$$

$$K''_a = \frac{K_{A/A^-} K_a + K_{B/B^-} K_h + K_{Cc/Cc^-} K_h K_t + K_{Ct/Ct^-} K_h K_t K_i}{K'_a} \tag{10}$$

and K_{X/X^-} (X = A, B, Cc, and Ct) are the respective acid−base constants to give the anionic forms defined by eq 11.

$$X + H_2O \rightleftharpoons X^- + H_3O^+ \quad K_{X/X^-} \tag{11}$$

The equilibrium constants K'_a and K''_a are obtained experimentally by fitting the absorption spectra at the equilibrium, as shown in Figure 5b, upon its extension to the basic region. [In Figure 4b, this extension was not possible due to the decomposition of oenin in basic medium, which prevents a clear definition of the equilibrium for higher pH values.]

Regarding pseudoequilibrium, the experimental constants $K^{\wedge}_a$ and $K^{\wedge\wedge}_a$ are accounted for in eqs 8 and 10, respectively, by removing the term corresponding to Ct.

To summarize, despite the complexity of the flavylium multistate, in particular, when it is extended to the anionic forms, AH^+ behaves as a simple diprotic acid, giving the respective conjugate bases CB and CB^-. The mole fractions of AH^+, CB, and CB^- are obtained according to eq 12. It is worth noting that the mole fractions in eq 12 are obtained from the two experimental constants K'_a and K''_a.

$$\chi_{AH^+} = \frac{[H^+]^2}{D}; \quad \chi_{CB} = \frac{K'_a [H^+]}{D}; \quad \chi_{CB^-} = \frac{K'_a K''_a}{D} \tag{12}$$

https://doi.org/10.1021/acs.chemrev.1c00399
Chem. Rev. 2022, 122, 1416−1481

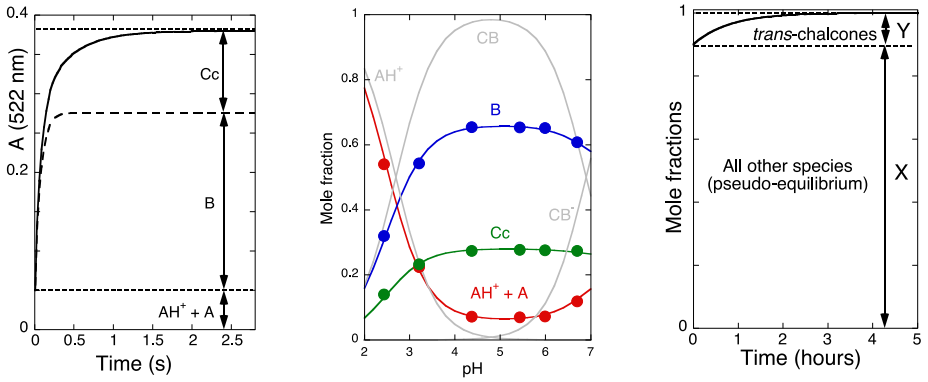

Figure 6. (a) Reverse pH jump of oenin, at 1.25×10^{-5} M, from a pseudoequilibrated solution at pH = 4.5; (b) mole fraction distribution of the pseudoequilibrium species: in gray, the mole fraction distribution according to eq 13, $pK_a^{\wedge} = 2.7$, and $pK_a^{\wedge\wedge} = 6.9$; and (c) mole fraction of Ct formed after a reverse pH jump from pH = 5 followed by a common spectrophotometer. Adapted with permission from ref 186. Copyright 2012, Elsevier.

with $D = [H^+]^2 + K'_a[H^+] + K'_aK''_a$. The mole fraction distribution of all the species of diprotic acid were calculated in a straightforward fashion from a mass balance and the definition of the equilibrium constants, eqs 1, 3, 4, and 6 as well as the acid−base constants K_{X/X^-}, as defined above in eq 11 (C_0 = total concentration of the anthocyanins). This substitution leads directly to the mole fraction distribution of the flavylium cation, from which all the others were directly obtained, eq 13.

$$\chi_{AH^+} = \frac{[AH^+]}{C_0} = \frac{[H^+]^2}{D}; \quad \chi_A = \frac{K_a[H^+]}{D}; \quad \chi_B = \frac{K_h[H^+]}{D};$$
$$\chi_{Cc} = \frac{K_hK_t[H^+]}{D}; \quad \chi_{Ct} = \frac{K_hK_tK_i[H^+]}{D};$$
$$\chi_{A^-} = \frac{K_{A/A^-}K_a}{D}; \quad \chi_{B^-} = \frac{K_{B/B^-}K_h}{D};$$
$$\chi_{Cc^-} = \frac{K_{Cc/Cc^-}K_hK_t}{D}; \quad \chi_{Ct^-} = \frac{K_{Ct/Ct^-}K_hK_tK_i}{D} \tag{13}$$

C_0 = total concentration of the flavylium-derived species and D defined in eq 12.

The mole fractions presented in eq 13 can also be applied to the pseudoequilibrium with $D^{\wedge}$ defined by eq 14, substituting D.

$$D^{\wedge} = [H^+]^2 + K_a^{\wedge}[H^+] + K_a^{\wedge}K_a^{\wedge\wedge} \tag{14}$$

For more details regarding the mole fraction equations, please see the previously published work on this topic.[192]

3.2. Reverse pH jumps

Additional and complementary information from reverse pH jumps has been reported (Figure 6).[185,192]

In Figure 6a, the kinetic trace after a reverse pH jump from pseudoequilibrated oenin solutions at pH = 4.5 is shown. The trace can be fitted to a biexponential equation, with rate constants of 90 s^{-1} and 12 s^{-1}. The initial absorption is due to the fast conversion of the quinoidal base in the flavylium cation during the mixing time of the stopped flow, together with the flavylium cation present at the initial pH of the pseudoequilibrium. [At this initial pH the fraction of flavylium cation is very small, but it is significant when the reverse pH jumps take place from lower pH values.] The faster observable kinetic trace was attributed to the conversion of the hemiketal into a flavylium cation. This conversion occurs because, at pH = 1, the hydration (at this pH essentially the dehydration contribution) becomes faster than the tautomerization (change of regime).[197,198] The slowest trace corresponds to the formation of more flavylium cations from *cis*-chalcone via the hemiketal. The normalization of the amplitudes of the traces, Figure 6a, to give ($AH^+ + A + B + Cc + Ct$) equal to unity, leads directly to the mole factions of the pseudoequilibrium species at pH = 4.5. The extension of the reverse pH jumps to higher pH values permits the evaluation of the composition of the multistate under more basic conditions (Figure 6b). As shown in Figure 6b, the mole fraction of CB, eq 15, can be decomposed in the contributions of A, B and Cc, eq 16. Mutatis mutandis, the identical conclusion is true for CB^-, eq 17.[192]

$$\chi_{AH^{+\wedge}} = \frac{[H^+]^2}{D^{\wedge}}; \quad \chi_{CB^{\wedge}} = \frac{K_a^{\wedge}[H^+]}{D^{\wedge}}; \quad \chi_{CB^{\wedge-}} = \frac{K_a^{\wedge}K_a^{\wedge\wedge}}{D^{\wedge}} \tag{15}$$

$$\chi_{CB^{\wedge}} = \chi_A + \chi_B + \chi_{Cc} = \frac{a_0K_a^{\wedge}[H^+] + b_0K_a^{\wedge}[H^+] + c_0K_a^{\wedge}[H^+]}{D^{\wedge}} \tag{16}$$

$$\chi_{CB^{\wedge-}} = \chi_{A^-} + \chi_{B^-} + \chi_{Cc^-} = \frac{a_1K_a^{\wedge}K_a^{\wedge\wedge} + b_1K_a^{\wedge}K_a^{\wedge\wedge} + c_1K_a^{\wedge}K_a^{\wedge\wedge}}{D^{\wedge}} \tag{17}$$

Considering the mole fraction distribution of quinoidal base (A), $\chi_A = \frac{K_a[H^+]}{D^{\wedge}}$, from eq 13 at pseudoequilibrium and that given by eq 16, it can be concluded that $K_a = a_0K_a^{\wedge}$. In extending this comparison to all the species, the following set of equations is obtained,

$$K_a = a_0K_a^{\wedge}; \quad K_h = b_0K_a^{\wedge}; \quad K_hK_t = c_0K_a^{\wedge} \tag{18}$$

which gives the equilibrium constants K_a, K_h, and K_t from experimental values with good precision because they are based on a fitting with many points.

Regarding the anionic species, the relations in eq 19 were deduced by using an identical comparison, allowing for the calculation of the acid−base constants X/X^-, as introduced in eq 11.

$$K_{A/A^-}K_a = a_1K_a^{\wedge}K_a^{\wedge\wedge}; \quad K_{B/B^-}K_h = b_1K_a^{\wedge}K_a^{\wedge\wedge};$$
$$K_{Cc/Cc^-}K_hK_t = c_1K_a^{\wedge}K_a^{\wedge\wedge} \tag{19}$$

https://doi.org/10.1021/acs.chemrev.1c00399
Chem. Rev. 2022, 122, 1416−1481

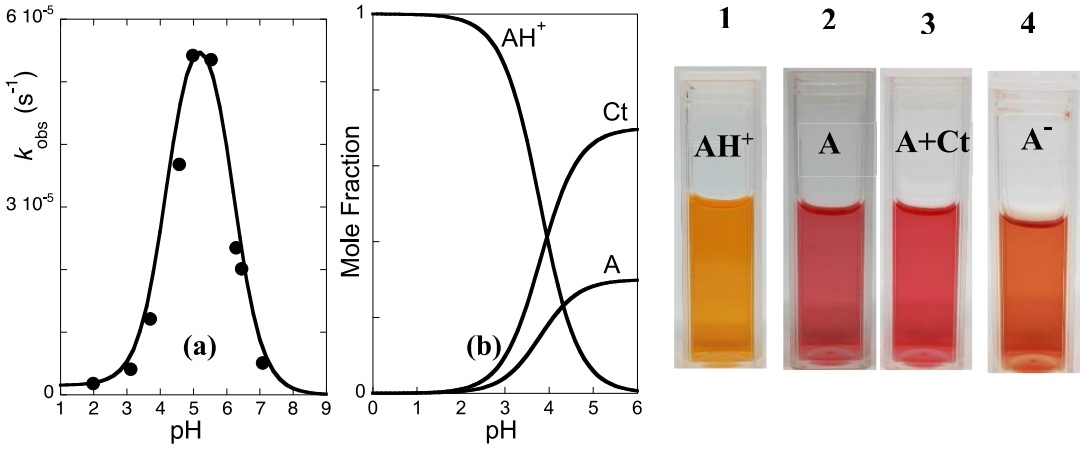

Figure 7. (a) Bell-shaped curve of the reaction toward equilibrium versus the pH of luteolinidin at 2.5×10^{-5} M in ethanol/water (1:1). Fitting was performed using eq 10 for $K_hK_tK_i = 4 \times 10^{-9}$ M^{-1} s^{-1}; $K_t/k_i/k_{-h} = 6.5 \times 10^{-7}$ M^{-1} s^{-1}; $k_{-I} = 1.5 \times 10^{-6}$ s^{-1}; and $pK_a = 3.8$; (b) mole fraction distribution of the species at equilibrium, which basically consists in a quinoidal base in equilibrium with *trans*-chalcone; and (c) (1) flavylium cation at pH = 1.0; (2) quinoidal base immediately after a pH jump to pH = 5; (3) at the equilibrium, pH = 5; and (4) immediately after a pH jump to pH = 8.0. Immediately after a direct pH jump to pH = 12, the color is dark orange (not shown). Adapted with permission from ref 183. Copyright 2020, Elsevier.

In eq 19, the coefficients a_1, b_1, and c_1 are the equivalents of a_0, b_0, and c_0, respectively, for the anionic species.[192]

The mole fraction of *trans*-chalcone at equilibrium was calculated from reverse pH jumps, as in that reported in Figure 6c, using a common spectrophotometer. The initial absorption corresponds to the total concentration of the species AH^+, A, B, and Cc at equilibrium, and they have been converted in flavylium cations through a fast reaction (for the time resolution of this experiment) at very low pH values. The amplitude of the kinetic trace corresponds to the formation of more flavylium cations from Ct. The ratio between the amplitude of the trace divided by the total absorbance gives the mole fraction of *trans*-chalcone, χ_{Ct}. The mole fraction distribution of Ct versus pH (including basic medium) was obtained by a series of reverse pH jumps, as shown in Figure 6c, to an extended series of pH values. The fitting of these values can be achieved from the representation of the mole fractions of the *trans*-chalcones versus pH.

$$\chi_{Ct} = \frac{d_0K'_a}{D}; \quad \chi_{Ct^-} = \frac{d_1K'_aK''_a}{D} \tag{20}$$

where d_0 and d_1 are defined by the fitting with eq 20.

The mole fraction of the Ct species can be written as given above in eq 13 or in eq 20. A comparison between these two sets gives the constant K_i and the acid−base K_{Ct/Ct^-}

$$K_hK_tK_i = d_0K'_a; \quad K_{Ct/Ct^-}K_hK_tK_i = d_1K'_aK''_a \tag{21}$$

At this point, all equilibrium constants of the flavylium multistate are obtained and the mole fraction of the species AH^+, A, B, Cc, and Ct can be calculated, eq 13.

In conclusion, the reverse pH jumps from the equilibrium and pseudoequilibrium are powerful experimental procedures that allow for complete characterization of the thermodynamic parameters for the flavylium multistate. More details on this mathematical procedure can be found in a previously published work.[192]

The rate constants were evaluated using eq 5 (k_h and k_{-h}) and eq 7 (k_i and k_{-i}). However, reverse pH jumps, such as that shown in Figure 6c, to very acidic medium give k_{-i}, which is the value of the plateau in very acidic medium, as shown in Figure 5a, the limit of eq 7 at very high proton concentration. The rate constant k_i is equal to the product K_ik_{-i}. The rate constants k_i and k_{-i} were also obtained from the *cis*−*trans* isomerization rates by fitting with eq 7.[191] Determination of the tautomerization rate constants can be done from the data of the reverse pH jumps (in the pH range where change of regime is observed) monitored by stopped flow: k_{-t} is the rate of the slower kinetic step, and k_t is calculated from the equilibrium constant K_t. A global fitting of all the experimental data is convenient to ensure the coherence of the calculations. As mentioned above, in the case of k_a and k_{-a}, specific techniques are required, such as temperature jumps,[184] or when an excited state proton transfer for the flavylium cation is observed by nanosecond flash photolysis.[187]

It is important to stress that the observed rate constants for the hydration step were obtained under very acidic conditions (for example, the experimental open circle points reported in Figure 4c), which were usually obtained through reverse pH jumps, in which a change of regime (hydration was faster than tautomerization) is observed, as described by eq 22 (and not eq 5). Equation 22 is similar to eq 5, but in this case there is no reversibility from B to Cc since the former, as soon as it appears, gives AH^+.

$$k_{1r} = \frac{[H^+]}{[H^+] + K_a}k_h + k_{-h}[H^+] \tag{22}$$

3.3. Lack of Pseudoequilibrium. The Case of 3-Deoxyanthocyanidins

When the pseudoequilibrium is not achieved, because there is not a high energy barrier for the *cis*−*trans* isomerization, B and Cc behave as steady state species. Once formed, they are consumed to give Ct in direct pH jumps or AH^+/A in reverse pH jumps. Consequently, at lower pH values, the process is controlled by the *cis*−*trans* isomerization that increases with the pH increasing, while at higher pH values the control is made by the hydration reaction which decreases by pH increasing. The result is a bell-shaped curve as in Figure 7a. The situation is summarized in Scheme 18.[191]

This kinetic behavior can be promptly identified because the direct conversion of AH^+/A into Ct occurs via a single step of pseudo-first-order kinetics. Considering AH^+ in fast equilibrium

https://doi.org/10.1021/acs.chemrev.1c00399
Chem. Rev. 2022, 122, 1416−1481

Scheme 18. Kinetic Scheme of a Flavylium Multistate Lacking Pseudoequilibrium

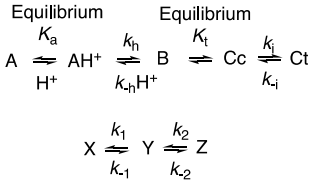

with A (X) on one side and B in fast equilibrium with Cc (Y) on the other to produce Ct (Z), a mechanism equivalent to a reversible kinetic scheme involving three species is required. When the steady state approach is applied to Y, eq 23 can be deduced.[191]

$$k_{bell} = \frac{\frac{[H^+]}{[H^+]+K_a} K_h K_t k_i + k_{-i}[H^+]}{[H^+] + \frac{k_i K_t}{k_{-h}}} \quad (23)$$

Equation 23 gives a bell-shaped curve when represented as a function of pH. In Figure 7a, the bell-shaped curve of luteolinidin is shown.

For luteolinidin and related compounds, the rate constants of the reverse pH jumps are equal to the direct ones for the same final pH. Moreover, B and Cc are elusive species appearing at unmeasurable concentrations in the stationary state. However, the mole fractions of A and Ct can be calculated from the data of the bell-shaped curve to obtain the respective mole fraction distribution from the ratios $K_a/([H^+] + K'_a)$ and $K_h K_t K_i/([H^+] + K'_a)$ Figure 7b).

Once the equilibrium constants are calculated, the energy level diagram reported in Figure 2a is constructed from the thermodynamic relation $\Delta G^0 = -RT \ln K$, where ΔG^0 is the Gibbs free energy, R is the perfect gases constant, T is the temperature (Kelvin), and K is the equilibrium constant. A detailed description of how to construct this diagram can be found elsewhere.[180]

Despite of the fact that UV−vis absorption spectroscopy (including stopped-flow) is the most common technique employed to monitor this system, other techniques, such as ^{1}H NMR, have also been used to investigate both the equilibrium and kinetics.[199,200] However, regardless of the physical-chemical spectroscopy used to monitored the system, it is presupposed that the anthocyanin concentration is fixed and the pH is variable. This procedure does not account for the considerable variations in these constants with the anthocyanin concentrations due to self-aggregation.[186] A systematic study on the effects of self-aggregation on the kinetic and thermodynamic properties of the network of chemical reactions in 3-glucoside anthocyanins clearly demonstrated that these parameters are, in fact, apparent constants that depend on the concentration of the dye (see Figure 8) and they can be extrapolated to infinite dilutions to account for the properties of the monomeric species.[186] Alternatively, the aggregation can be minimized by performing measurements at low anthocyanin concentrations, which is easily achieved by UV−vis spectrometry but not by ^{1}H NMR. In some plants, anthocyanins are sequestered in anthocyanic vacuolar inclusions (AVIs) promoting intramolecular copigmentation or self-association involving quinoidal bases, which explains the purple/blue color observed.[201] Thus, a challenge for the future is the development of new

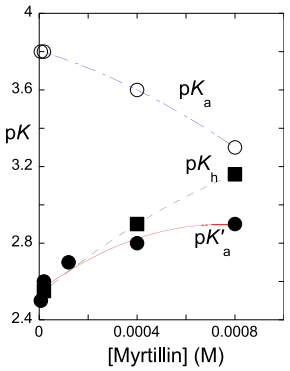

Figure 8. Effect of concentration on the apparent equilibrium constants of myrtillin. With permission from ref 186. Copyright 2012, Elsevier.

experimental tools and mathematical expressions that would consider the self-aggregation of anthocyanins.

Although it is important to highlight that, in subclasses of flavylium compounds, such as 3-glucoside anthocyanins, the kinetic and thermodynamic properties are not substantially different among their homologues,[186] which are distinguished by the different substitution patterns in the B-ring, and these parameters can be dramatically affected by the introduction/modification of substituents in critical positions of the flavylium skeleton. For this reason, there is growing interest in the search for new structures using innovative synthetic approaches to obtain different flavylium compounds with different hydroxylation/methoxylation patterns and also with different sugar moieties in simple systems (anthocyanin only) or by using a host−guest approach; see section 6. In section 4, the effects of the nature and position of the substituents decorating the flavylium structure on the reactivity/stability of these compounds is analyzed in more detail.

4. EFFECTS OF THE NATURE AND POSITION OF THE SUBSTITUENTS ON THE THERMODYNAMICS AND KINETICS OF FLAVYLIUM DERIVATIVES

The thermodynamic and kinetic behaviors of the flavylium multistate are very dependent on the nature and position of the 2-phenylbenzopyrylium (flavylium) substituents. Regarding thermodynamics, they define the pH domain of the flavylium cation; the relative mole fraction distributions among the quinoidal base, hemiketal, *cis*- and *trans*-chalcones; and the respective anionic forms. In other words, the nature and position of the flavylium substituents define the position of each species in the energy level diagram of the flavylium multistate (see Figure 2a). Concerning the kinetics, the substituents also have a substantial influence on their profile. As an example, while 4′-hydroxyflavylium and anthocyanins exhibit three distinct kinetic steps, 3-deoxyanthocyanidins and 7-hydroxyflavylium display two kinetic steps that follow a bell-shaped kinetic curve, as defined in section 2. The reactivity is also dramatically influenced by the substituents, in particular, in position 3. The paradigmatic example is the much higher stability of anthocyanins compared with anthocyanidins.[202] Alkyl substituents in position 4 prevent the hydration reaction in water.[203,204] A catechin substituent in position 8 of malvidin-3-glucoside (8,8-methylmethine catechin-malvidin 3-glucoside) hinders the hydration reaction and bisulfite discoloration.[205] The kinetics, thermodynamics and reactivity are also very dependent on the acylation of the sugars and are reviewed in section 4.4 of this work. Nature uses these different substitution

https://doi.org/10.1021/acs.chemrev.1c00399
Chem. Rev. 2022, 122, 1416−1481

Scheme 19. Representative Compounds Possessing Flavylium Multistates Similar to Those of Anthocyanins

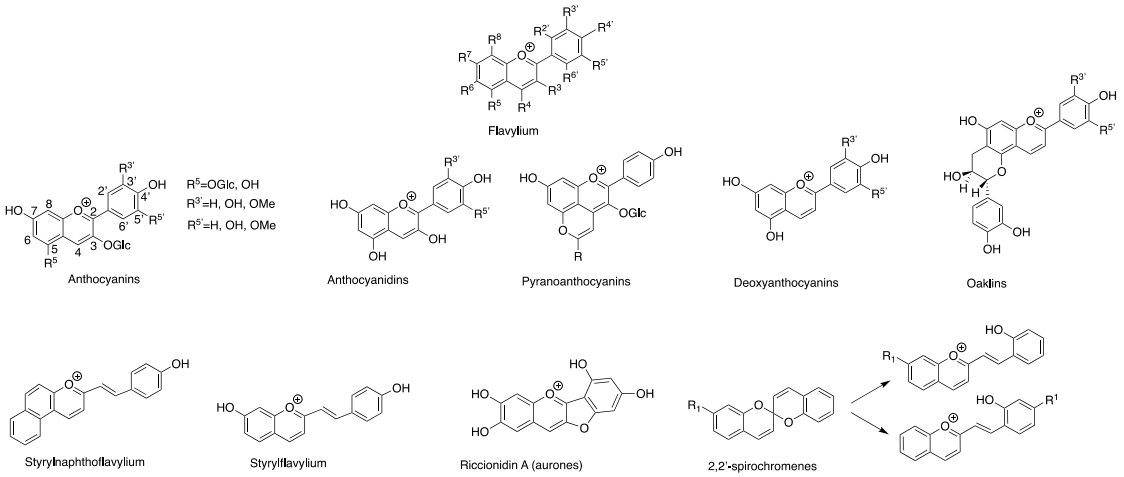

Scheme 20. Early Pyranoanthocyanins Isolated from Red Wine[103,209−211]

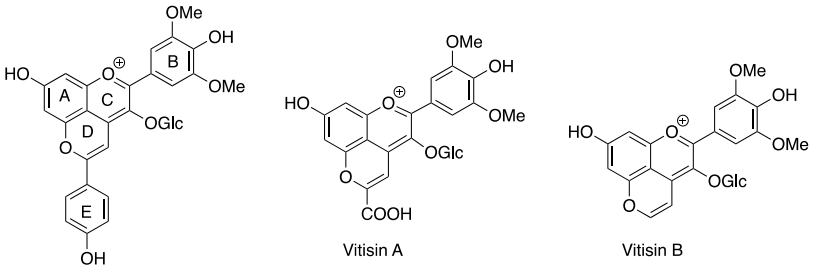

Scheme 21. Representation of the Typical Chemical Equilibria for a Pyrano-3-deoxyanthocyanidin-Catechol Dye with pH Variation

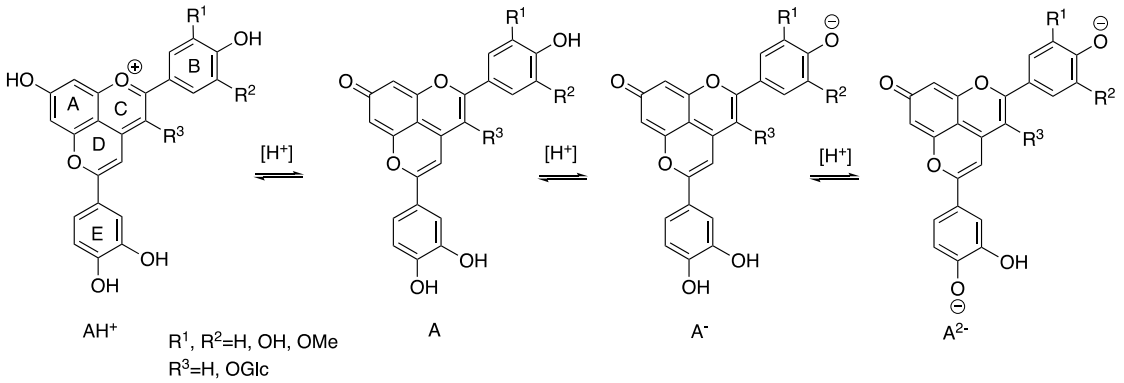

patterns to adapt the multistate to the function they have in plants, leading chemists to design bioinspired systems for different applications. In this section and throughout this review, several examples of this endless versatility are presented.

Scheme 19 displays examples of flavylium cations that generate multistates possessing the equivalent chemical species, which are interconnected by the same chemical reactions as those described in section 2.

4.1. Pyranoanthocyanins

Dracorubin is one of the molecules (in the quinoidal base form) that give the deep red color to dragoon's blood, a natural resin obtained from various trees, specifically *Dracaena draco* and *Dracaena cinnabari* belonging to the *Liliaceae* family or the palm tree *Calamus draco* (*Dæmonorops draco*).[206] The structure of dracorubin was fully revealed in 1950 by Robertson, Whalley, and co-workers,[105,207] but it was not synthesized until 1976.[208] Dracorubin, while not claimed to be, is most likely the first pyranoflavylium structure (reported in the quinoidal base form) to appear in the literature. However, to our knowledge, no other similar structure was assigned before the 1990s, when the isolation of the first pyranoflavylium compounds extracted from wine, as shown in Scheme 20,[103,209−211] triggered an increasing number of publications regarding the extraction, synthesis, and physical chemistry of pyranoflavylium compounds, as described in section 2.[30,135,212−215]

The chromatic features of natural and synthetic pyranoflavylium-type compounds are very different from their respective flavylium precursor pigments.[216,217] Particular attention has been paid to pyranoflavylium cations, which normally experience a hypsochromic shift in λ_{max} (478−510 nm) compared to their flavylium precursors (λ_{max} 516−541 nm),

https://doi.org/10.1021/acs.chemrev.1c00399
Chem. Rev. 2022, 122, 1416−1481

displaying a more orange color, except for portisins and pyranoanthocyanin dimers, which have revealed a bathochromic shift to more bluish to green hues (λ_{max} 570−730 nm).[109,218] Unlike anthocyanins, pyranoanthocyanins are much less prone to water addition at C2 as a result of the presence of the pyranic ring D.[219] Consequently, the species from the flavylium cation to the quinoidal bases (neutral and anionic) practically do not experience a color fade, extending the appearance of the visible color toward much higher pH values, as shown in Scheme 21.[140,219,220] The formation of the colorless hemiketal was observed in 10-acetylpyranomalvidin-3-*O*-*β*-glucoside and 10-acetyl-pyranopeonidin-3-*O*-*β*-glucoside, but its mole fraction is much lower than that in common anthocyanins and the color of the quinoidal bases is still dominant in the absorption spectra for higher pH values.[221] Pyranoflavylium compounds, together with 4-methyl-7-hydroxyflavylium (in water) and similar compounds with substituents in position 4,[222] are thus an exception to the general flavylium multistate because the hydration and the subsequent chemical reactions are not observed at all or only to a very small extent.[223]

The acid−base chemical equilibria of several pyranoanthocyanins and pyrano-3-deoxyanthocyanidins with different substituents have been characterized by UV−vis and NMR spectroscopic techniques, and they are summarized in Scheme 22 and Table 1.

For pigments **17** and **20**, the amine substituent in position 10 is protonated only at very acidic pH values with the first pK_{a0} corresponding to the deprotonation of AH_2^{2+}. Regarding pigments **16**, **21**, and **22**, they have a carboxylic substituent, and the first deprotonation (pK_{a1}) gives rise to a zwitterionic

Scheme 22. Pyranoanthocyanins Reported in Table 1

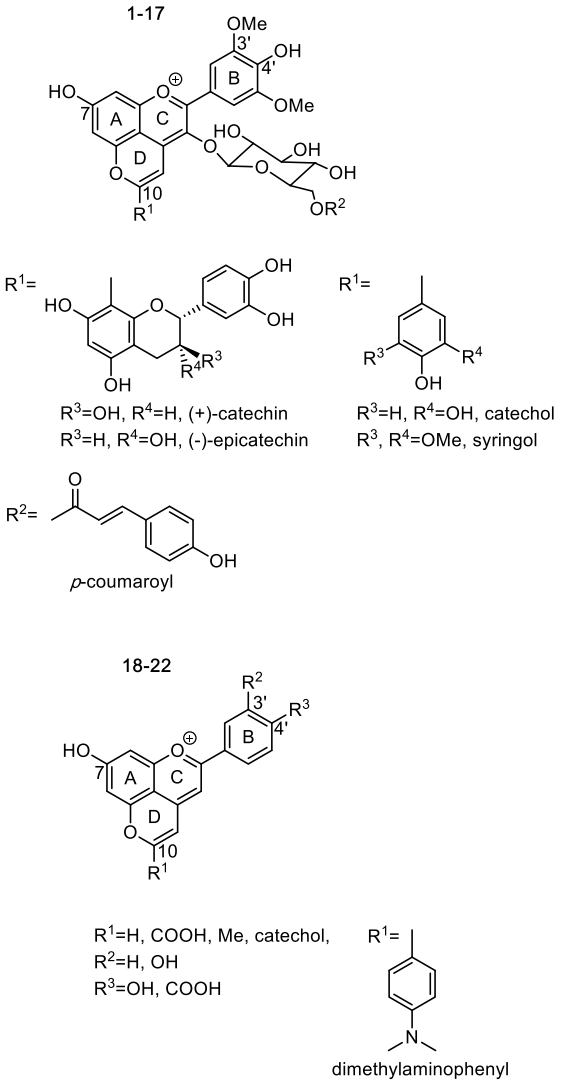

Table 1. pK_a Values of Pyranoanthocyanins 1−17 and Pyrano-3-deoxyanthocyanidins 18−22 (Scheme 22) as Obtained by UV−Vis Spectroscopy[a]

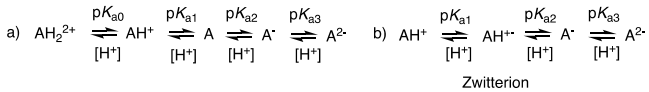

pigments **1**−**17**	pK_{a1}	pK_{a2}	pK_{a3}
1 (R^1 = Me, R^2 = H)[223]	4.57 ± 0.07	8.23 ± 0.04	
2 (R^1 = (+)-catechin, R^2 = H),[219b]	5.05 ± 0.05	7.90 ± 0.07	9.77 ± 0.06
3 (R^1 = (+)-catechin, R^2 = *p*-coumaroyl),[219b]	5.35 ± 0.08	8.06 ± 0.09	9.76 ± 0.07
4 (R^1 = (−)-epicatechin, R^2 = H)[219b]	4.80 ± 0.09	7.82 ± 0.09	9.5 ± 0.1
5 (R^1 = (−)-epicatechin, R^2 = *p*-coumaroyl),[219b]	5.2 ± 0.1	8.0 ± 0.1	9.60 ± 0.08
6 (R^1 = catechol, R^2 = H),[219b]	4.20 ± 0.06	7.84 ± 0.05	10.28 ± 0.07
6 (R^1 = catechol, R^2 = H),[224c]	4.3 ± 0.009		
7 (R^1 = 2-methoxyphenol, R^2 = H),[224c]	4.35 ± 0.11		
8 (R^1 = catechol, R^2 = *p*-coumaroyl),[219b]	4.31 ± 0.07	8.34 ± 0.06	10.20 ± 0.06
9 (R^1 = vinyl-(+)-catechin, R^2 = H)[220]	4.61 ± 0.03	8.36 ± 0.03	10.11 ± 0.06
10 (R^1 = vinyl-catechol, R^2 = H)[220]	4.09 ± 0.03	7.98 ± 0.05	10.18 ± 0.05
11 (R^1 = vinyl-syringol, R^2 = H)[220]	3.60 ± 0.02	8.66 ± 0.05	12.16 ± 0.05
12 (R^1 = butadienylidene-syringol, R^2 = H)[136]	3.64 ± 0.01	8.02 ± 0.01	11.19 ± 0.01
13 (R^1 = methine-pyranomalvidin-3-glc, R^2 = H)[220]	4.93 ± 0.04	8.33 ± 0.04	9.10 ± 0.04
14 (R^1 = H, R^2 = H)[225]	4.34 ± 0.02	7.34 ± 0.03	
15 (R^1 = H, R^2 = *p*-coumaroyl[225]	4.8 ± 0.1	6.8 ± 0.1	
16 (R^1 = COOH, R^2 = H),[226e]	1.18 ± 0.07	4.42 ± 0.01	7.78 ± 0.02
17 (R^1 = dimethylaminophenyl, R^2 = H)[214]	5.4 ± 0.1	9.5 ± 0.1	
pigments **18**−**22**	pK_{a1}	pK_{a2}	pK_{a3}
18 (R^1 = catechol, R^2, R^3 = OH)[140]	4.7 ± 0.1	7.9 ± 0.1	
19 (R^1 = Me, R^2, R^3 = OH)[140]	5.0 ± 0.1	6.5 ± 0.1	
20 (R^1 = dimethylaminophenyl, R^2, R^3 = OH)[140]	3.6 ± 0.1	8.4 ± 0.1	
21 (R^1 = COOH, R^2, R^3 = OH),[140d,e]	1.6 ± 0.3	4.9 ± 0.1	
22 (R^1, R^3 = COOH, R^2 = H),[140d,e]	1.2 ± 0.3	4.9 ± 0.1	8.1 ± 0.1
23, malvidin-3-*O*-glucoside (oenin)[f]	3.95 ± 0.05	6.3 ± 0.1	8.5 ± 0.1

[a]The formation of AH_2^{2+} species in compounds comprising amino substituents usually occurs at very acidic pH values (pK_{a0} < 1). [b]Universal buffer 10% ethanol. [c]Acetate buffer 12% ethanol. [d]Universal buffer, 25% ethanol. [e]Zwitterion formation, scheme b in the graphic at the top of the table. [f]Malvidin-3-glucoside for comparative purposes.

https://doi.org/10.1021/acs.chemrev.1c00399
Chem. Rev. 2022, 122, 1416−1481

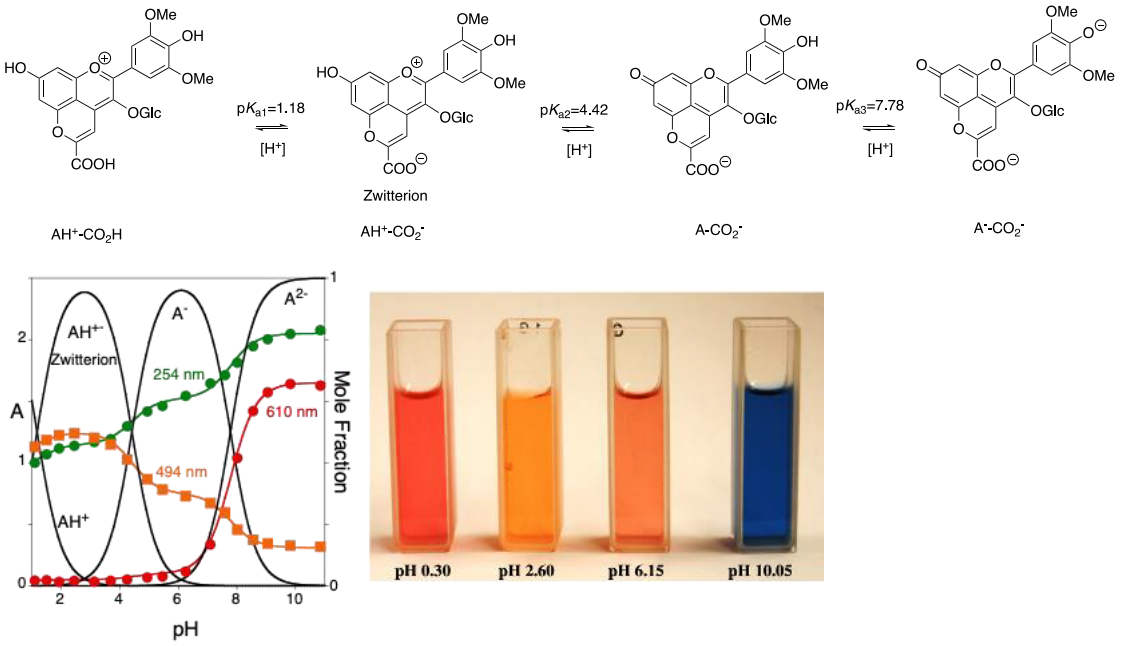

Figure 9. Deprotonation sequence in pigment **16**. The color palette is extended over a large pH range.[226] Adapted with permission from ref 226. Copyright 2013, Elsevier.

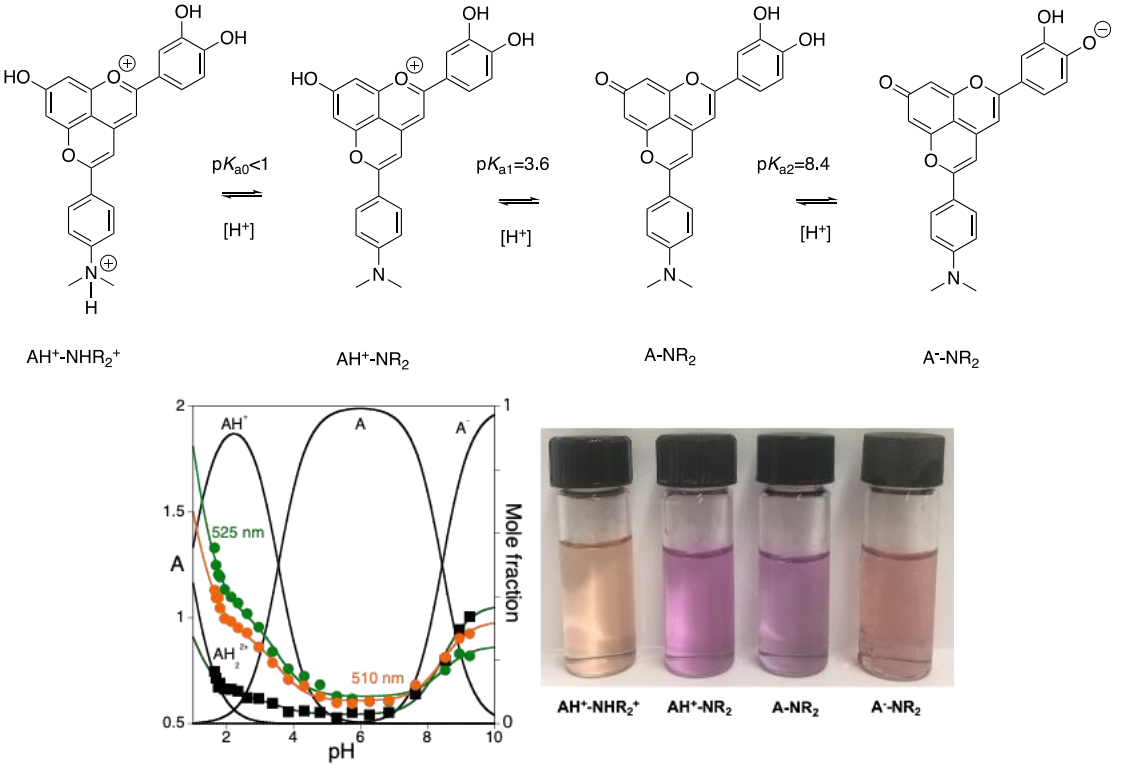

Figure 10. Chemical equilibria of compound **20** in aqueous solutions. Adapted with permission from ref 140. Copyright 2017, Elsevier.

species, as defined in (b) in the top of Table 1.[226] The pyranoflavylium compound capacity for tuning the color pallet over an extended range of pH values is shown in Figures 9 and 10 for two representative patterns of substitution in position 10: a carboxylic, pigment **16** (Vitisin A), and dimethylaminophenyl, pigment **20**.[226]

From these examples, it can be concluded that natural pyranoflavylium pigments as well as their bioinspired synthetic parents are very promising for applications as colorants, for example, in foodstuffs, but they still require full toxicity clearance.

4.2. Furanoflavylium Derivatives

Natural and synthetic furanoflavylium compounds, a term coined by Seshadri and Chakravarty,[227] have been reported in the literature.[228] Recently, Davies, Andersen, and co-workers[229] characterized the compound auronidin-2′-neohesperidoside

https://doi.org/10.1021/acs.chemrev.1c00399
Chem. Rev. 2022, 122, 1416−1481

isolated from the liverwort *Marchantia polymorpha* (marchantia), and they proposed the name auronidins for this family of compounds, as in Scheme 23. [In the original paper, the first compound is named auronidin-4-neohesperidoside. In the present Review, we use auronidin-2′-neohesperidoside to be consistent with flavylium compound numeration.]

Scheme 23. Natural and Synthetic Furanoflavylium Compounds[229a]

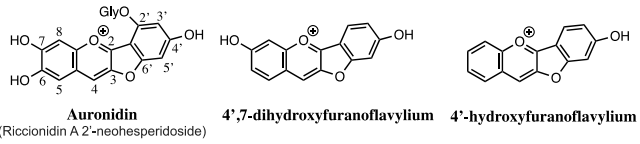

[a]Nhp = neohesperidoside.

The thermodynamics and kinetics of riccionidin A, the aglycone of the auronidin shown in Scheme 23, were described.[183] Riccionidin A was identified in several liverworts, such as, for example, in the Antarctic *Cephaloziella varians*, in response to an abrupt increase in UVB radiation,[230] and in the cell walls of *Ricciocarpos natans*[231] as well as in adventitious root cultures of Anacardiaceae member *Rhus javanica*.[232]

Riccionidin A follows the same multistate as anthocyanins, as shown in Scheme 24.[183] The most dramatic difference when compared with other flavylium multistates is however the extremely slow interconversion rate between flavylium cation and *trans*-chalcone. This was observed during the riccionidin A synthesis carried out according to the paper of Dyker and Bauer.[233] The suitable aldehyde and ketone were dissolved in acetic acid saturated with HCl gas at 100 °C, to give initially the *trans*-chalcone. The evolution of the synthesis was monitored by UV−vis spectrophotometry, as shown in Figure 11. Despite the extreme temperature and acidity, the *trans*-chalcone was only converted into flavylium cation after 11 days.[183]

A sequence of direct pH jumps (from flavylium cation) give spectral variations that are compatible with the existence of four acid−base constants, $pK_{a1} = 4.2$, $pK_{a2} = 6.5$, $pK_{a3} = 7.7$, and $pK_{a4} = 10.7$, as shown in Figure 12a. The colors at the representative pH values are shown in Figure 12b. It is notable that, similar to dracorubin and the other colorants of dragoon's blood resin,[206] as well as the auronidin reported by Davies, Andersen, and coworkers[229] and its aglycone, riccionidin A,[183] the flavylium cation is yellow and only the quinoidal bases range from red to purple. In riccionidin A, no significant spectral modifications were observed after 500 h at pH < 4, indicating that the flavylium cation is stable in that pH region.

At higher pH values, however, spectral variations corresponding to the disappearance of the quinoidal bases take place. The kinetics are multiexponential, with the slowest processes ($t_{1/2}$ > 100 h at room temperature for pH values between 5.4 and 9.1)

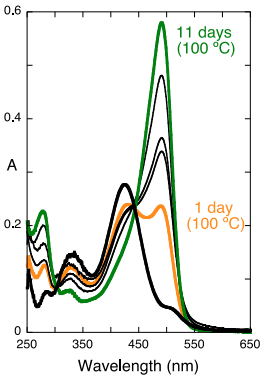

Figure 11. Spectral variations during the synthesis of riccionidin A in water. Adapted with permission from ref 183. Copyright 2020, Elsevier.

being attributed to the formation of decomposition products. Identically, *trans*-chalcone at pH = 5.0 in methanol/water (1:1) at 45 °C reacts according to a multiexponential process and the spectral variations are also compatible with the formation of decomposition products. HPLC-MS experiments performed after direct and reverse pH jumps allowed for the identification of the chromatographic peaks of the multistate as well as those of the decomposition products. The results are summarized in Scheme 25.[183]

An inspection of Scheme 25 shows that experimental evidence was obtained for the five species of the multistate in acidic medium (red structures). The decomposition products were also identified by their respective mass spectra. Possible mechanisms to account for the decomposition products are also included.

The flavylium multistates of the riccionidin model compounds 4′-hydroxyfuranoflavylium[234] and 4′,7-dihydroxyfuranoflavylium[228,234] were also described. For 4′-hydroxyfuranoflavylium,[234] a similar order of magnitude in the rate constants for hydration and tautomerization leads to peculiar kinetics from the flavylium cation (pH = 1) to the *cis*-chalcone. The hemiketal appears from the flavylium cation and disappears to give *cis*-chalcone, the observed species at pseudoequilibrium, as in Figure 13a. The kinetics followed by UV−vis absorption can be fitted with two consecutive reactions of the type A → B → C. This kinetic behavior was also corroborated by ^{1}H NMR. The equilibrium is reached from the isomerization of the *cis*-chalcone toward *trans*-chalcone, as exemplified by the trace after a pH jump to pH = 5.5, as shown in Figure 13b.

The other riccionidin A model compound, 4′,7-dihydroxyfuranoflavylium, presents a kinetic pattern that is similar to that of the parent 4′,7-dihydroxyflavylium and 3-deoxyanthocyanidins; its kinetics toward equilibrium is a single monoexponential following a bell-shaped curve, but it is much slower than that of

Scheme 24. Multistates of Riccionidin A in Acidic Medium[a]

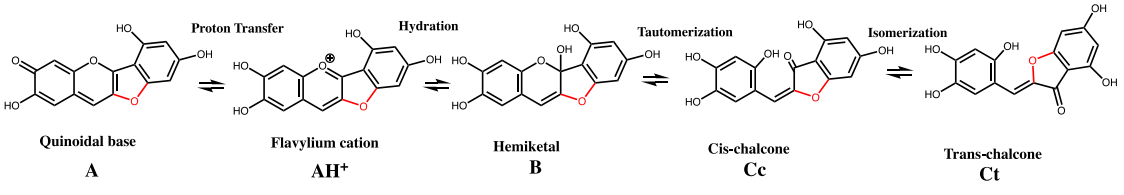

[a]Adapted with permission from ref 183. Copyright 2020, Elsevier.

https://doi.org/10.1021/acs.chemrev.1c00399
Chem. Rev. 2022, 122, 1416−1481

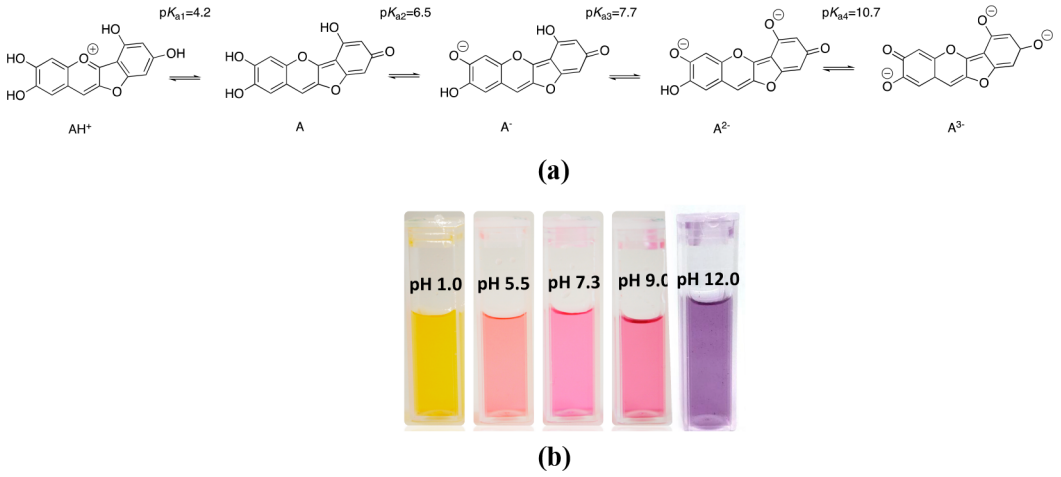

Figure 12. (a) Proposed deprotonation sequence for the flavylium cation of riccionidin A and (b) the colors of the flavylium cation and quinoidal bases of riccionidin A at representative pH values immediately after preparation. Adapted with permission from ref 183. Copyright 2020, Elsevier.

Scheme 25. Proposed Chemical Structures of the Degradation Products (Peaks 1, 2, 5, and 6) Detected by HPLC-MS and the Possible Mechanistic Pathways Leading to Their Formation[a]

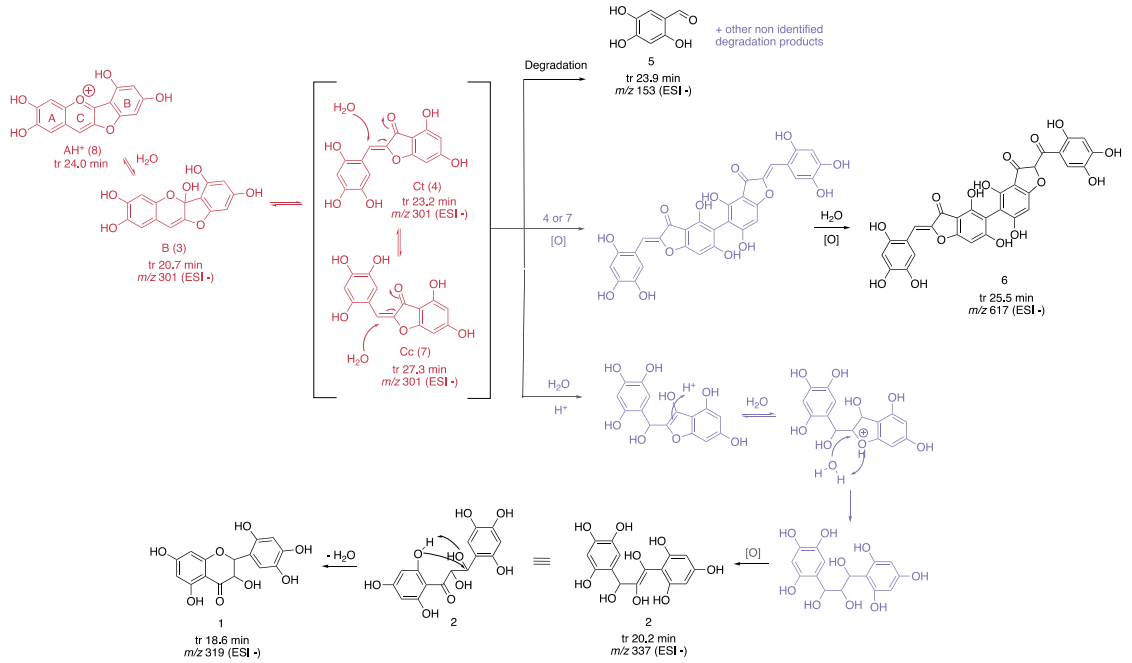

[a]The position of the methyl group was randomly assigned in the structure from peak 6. The proposed intermediate structures are shown in purple. Adapted with permission from ref 183. Copyright 2020, Elsevier.

its parent compound without the bridge, as shown in Figure 13c.[234]

The aglycone riccionidin A is very stable up to pH = 4, but its color is limited to the yellow flavylium cation and the reddish quinoidal base. According to Scheme 25, the hydroxyl in position 2′ seems to participate in the degradation processes in this compound. Further studies extended to the neutral and basic pH values with auronidins bearing a sugar in position 2′, like that reported by Davies, Andersen, and co-workers,[23] would be very interesting to assess the effect of the glucosylation.

4.3. Styrylflavylium Derivatives

The synthesis of styrylflavylium compounds was patented by Jurd in 1967, Scheme 26.[203] His patent was based on two considerations: (i) "*my researches have shown that the instability of natural pigments is primary due to the substituents on the 3-position*"; (ii) "*in the compounds of the invention, the 3-position is unsubstituted or is provided particular substituents such as hydrogen, lower alkyl, phenyl, lower alkoxy and phenoxy.*" Moreover, he mentioned that "*the compounds of the invention contain a styrene nucleous attached to the benzopyrylium at position 2. This styryl group has the advantage that the compounds exhibit deeper hues than is possible with the flavylium type structure wherein a phenyl nucleous is attached at position 2.*"

The multistates of styrylflavylium compounds have the theoretical ability to duplicate the number of their species through the addition of the *cis* isomers obtained during the rotation around the double bond of the styryl unit, as shown in Scheme 27.

https://doi.org/10.1021/acs.chemrev.1c00399
Chem. Rev. 2022, 122, 1416−1481

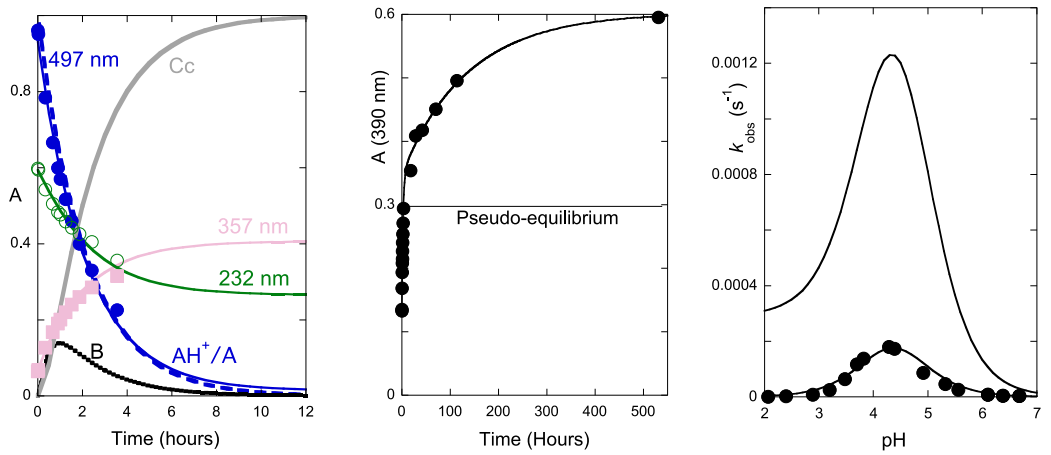

Figure 13. (a) Absorbance of 4′-hydroxyfuranoflavylium as a function of time after a direct pH jump to pH = 5.5, toward pseudoequilibrium. The kinetic traces can be fitted by two consecutive reactions with the observed rate constants 1.3×10^{-4} and 6.0×10^{-4} s^{-1}. (b) A third and much slower step leads to *trans*-chalcone with an observed rate constant of 2.8×10^{-6} s^{-1}; (c) observed rate constants of the kinetic processes of 4′,7-dihydroxyfuranoflavylium toward equilibrium. Fitting was performed in a bell-shaped curve for the following parameters: $pK_{a1} = 4.2$; $K_hK_tk_i = 3.1 \times 10^{-7}$ M s^{-1}; $k_{-i} \approx 0$; $k_iK_t/k_{-h} = 3.0 \times 10^{-5}$ M; and full line, the same curve for 4′,7-dihydroxyflavylium. Adapted with permission from ref 234, Copyright 2019, American Chemical Society; and ref 228, Copyright 2019, the PCCP Owner Societies.

Scheme 26. Styrylflavylium Compounds Patented by Jurd[203]

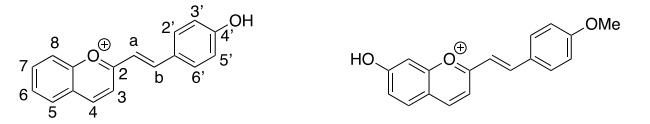

2-(4-hydroxystyryl)-benzopyrylium

7-hydroxy-2-(4-methoxystyryl)-benzopyrylium

The thermodynamics and kinetics of the styrylflavylium compounds with a hydroxyl substituent in position 7, 7-hydroxy-2-(styryl)-benzopyrylium and 7-hydroxy-2-(4-hydroxystyryl)-benzopyrylium, were compared with their flavylium analogues.[58,235] They behave similarly in following kinetics, exhibiting a bell-shaped profile, as shown in Figure 14 for 7-hydroxy-2-(styryl)-benzopyrylium, but with kinetic constants that are substantially lower than that of 7-hydroxyflavylium. The same finding was observed for 7-hydroxy-2-(4-hydroxystyryl)-benzopyrylium, but in this case the rates of the kinetic constants compared with those of the flavylium parent are similar.[235,236] No experimental evidence was found for the formation of the *cis*-isomers from the styryl unit.

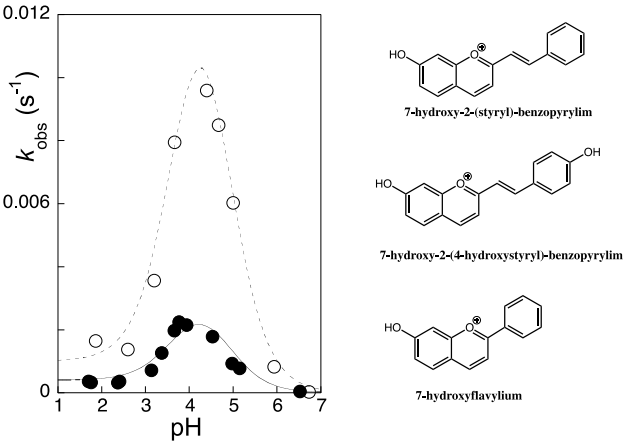

Figure 14. pH-Dependent rate constants of the interconversion between the 7-hydroxy-2-(4-hydroxystyryl)-benzopyrylium cation and the respective *trans*-chalcone follows a bell-shaped curve (●); the same for 7-dihydroxyflavylium for comparison purposes (○). Adapted with permission from refs 235 and ref 236. Copyright 2009, Elsevier and Copyright 1988, European Chemical Societies Publishing, respectively.

Scheme 27. Number of Possible Species in Styrylflavylium Multistates That Can Theoretically Be Duplicated When Compared with the Flavylium Compounds

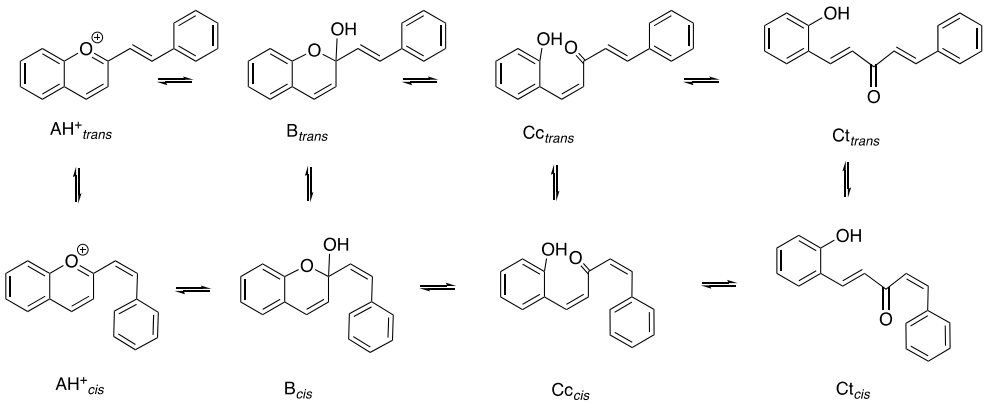

https://doi.org/10.1021/acs.chemrev.1c00399
Chem. Rev. 2022, 122, 1416−1481

Scheme 28. Sketch of the Metalloanthocyanin Responsible for the Color of *Commelina communis*[a]

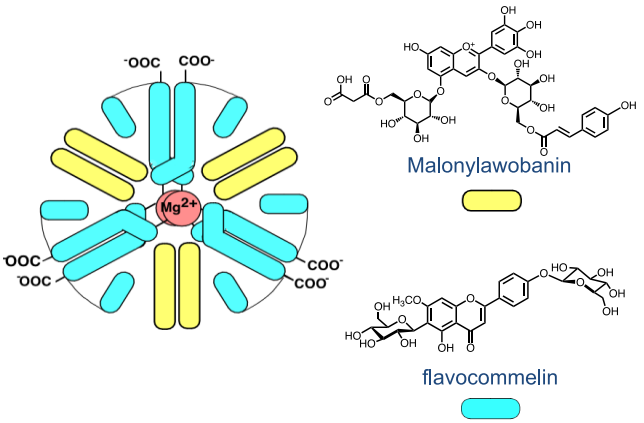

[a]The sketch was provided by Prof. Kumi Yoshida. The building blocks self-associate to produce the supramolecule in a bottom-up approach.

4.4. Acylated Anthocyanins

The most common anthocyanins possess simple structures that are not able, by themselves, to confer the red color of the flavylium cation in vivo, except at a relatively acidic pH. With respect to the purple and blue colors, the situation is even more dramatic since the quinoidal base is a minor component of the anthocyanin's equilibrium at a moderately acidic pH, while to a lesser extent the same is true for the anionic quinoidal base. The vacuolar pH, at which anthocyanins exist in flowers and fruits, may vary considerably, but a pH of approximately 5 is often observed.[237] However, the pH of the vacuoles could be as low as 2.0 in citrus fruits[238] and 7.7 in some flowers.[29] A beautiful example of the strategies used by nature to overcome this limitation is the supramolecular structure of the molecular entity that confers the blue color to *Commelina communis*, as shown in Scheme 28.[28,39]

An anthocyanin, a flavone, and a metal ion in a 6:6:2 ratio are organized into two parallel planes, each containing three anthocyanins, three flavones, and a metal ion that organizes the space. Other strategies have been adopted by nature for identical purposes. Copigmentation is the most frequently studied phenomenon and has been extensively reviewed.[1,2,40]

Scheme 29. Structures of an Anthocyanin Bearing Acylated Residues in Positions 7 and 3′

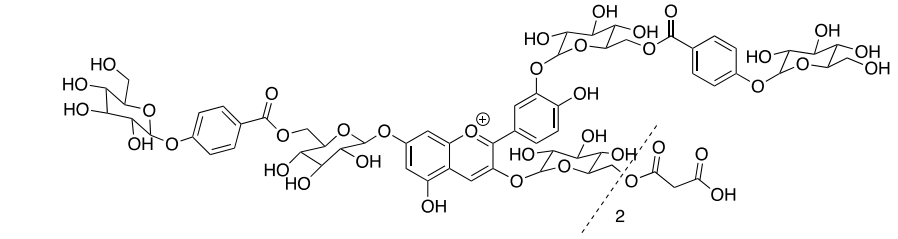

1

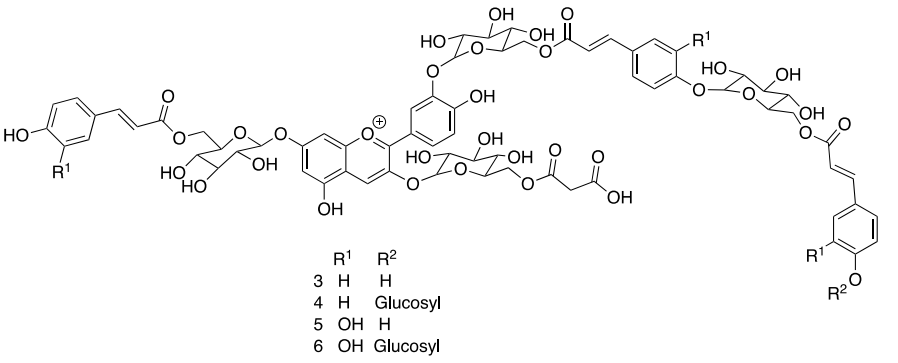

	R^1	R^2
3	H	H
4	H	Glucosyl
5	OH	H
6	OH	Glucosyl

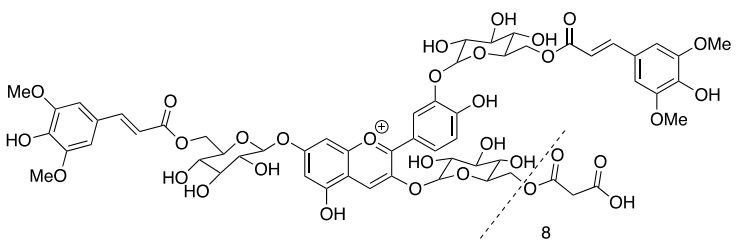

7 8

https://doi.org/10.1021/acs.chemrev.1c00399
Chem. Rev. 2022, 122, 1416−1481

Scheme 30. Pigment 3 and the Respective Deacylated Derivatives, Pigment 2 (Bis-deacyl) and Pigment 1 (Tris-deacyl)[193]

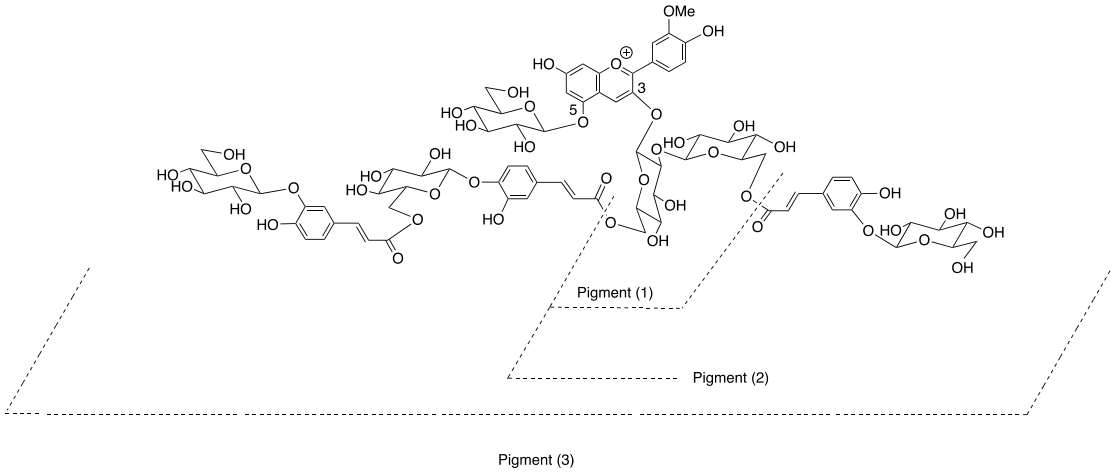

The focus of this section is the intramolecular copigmentation observed in anthocyanins bearing acylated residues.

The fact that acylated anthocyanins exhibit higher resistance to color loss when compared with common anthocyanins could be viewed from two different perspectives: (i) the extension of the pH domain of the flavylium cation and the stabilization of the purple and blue colors at higher pH values and (ii) higher resistance to degradation. The term "stability" will be used in the sense of item (i), and "storage stability" will be used for item (ii). In this section, more recent examples will be provided with a few cases that have been revisited to frame recent achievements.

The intramolecular copigmentation of a series of interesting acylated anthocyanin derivatives (Scheme 29) was investigated by UV−vis absorption spectroscopy.[239] The authors reported that these anthocyanins did not undergo hydration over the acidic to moderately acidic pH range (up to pH = 6), which implies that both flavylium cations and quinoidal bases are the primary species. It was proposed that the presence of acylated residues in positions 3′ and 7 optimizes the overlap of the acylated substituents, leading to enhanced interactions between the aromatic residues with the dye core, which results in improved dye stability.

The peculiar behavior of heavenly blue anthocyanin, a peonidin derivative extracted from the flowers of morning glory (*Ipomoea tricolor*) that confers a purple color to buds and a blue color to petals, was associated early with the $\pi-\pi$ stacking interaction of the acylated residues with the flavylium core, as indicated in Scheme 30.[29,37]

The first quantitative study of the thermodynamics and kinetics of acylated anthocyanins was reported by Dangles et al.,[195] as shown in Scheme 31, for anthocyanins extracted from another morning glory variety, the flower of *Pharbitis Ipomoea nil* (a pelargonidin derivative).

Similarly to common anthocyanins, two kinetic processes that were well differentiated over time were observed by UV−vis spectrophotometry. The faster process is controlled by the hydration reaction, and the slower reaction is controlled by *cis*−*trans* isomerization. The rate constants of the faster step from pigment **1** (0.38 s^{-1}) to pigment **4** (6.7×10^{-2} s^{-1}) decrease continuously. This result constitutes the first reported quantitative argument for the existence of a protective effect of the hydration of the flavylium cation caused by the $\pi-\pi$ stacking of the acylated residues with the flavylium core. The higher number of acylated residues results in more efficient protection

Scheme 31. Polyacylated Anthocyanins Reported by Dangles et al.[195]

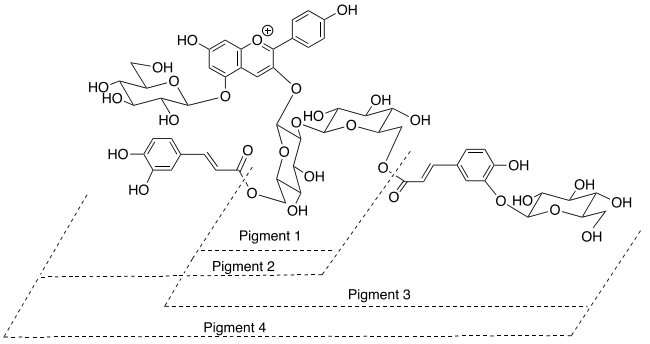

toward hydration. Similar to the heavenly blue anthocyanin reported by Goto and Kondo,[37] the presence of the acylated residues not only confer stability to the color of the pigment but also allows for color diversification.[195]

Recently, heavenly blue anthocyanin (from *Ipomoea tricolor*) was revisited, and its thermodynamics and kinetics were explained.[193] In addition to their flavylium core, what distinguishes the two acylated anthocyanins shown in Schemes 30 and 31 is the fact that in the first example pigment **3** possesses three acylated residues while in last pigment **4** only possesses two. In Scheme 32, the energy level diagrams of the quinoidal base and the hemiketal in relation to the respective flavylium cations are shown for both systems.

Scheme 32 visualizes a common behavior. The increase in acylated residues has a weak effect on the stability of the quinoidal bases but has a dramatic effect on the instability of the hemiketal (in equilibrium with *cis*-chalcone), which becomes much more unstable when increasing the number of acylated residues. This effect is also dependent on the position and nature of the acylated units, as in pigments **2** and **3** in Scheme 31. It is noteworthy that three acylated residues invert the relative stability of the quinoidal base and the hemiketal in Scheme 32b.

The mole fraction distribution of heavenly blue anthocyanin (from *Ipomoea tricolor*) pigment **3** is shown in Scheme 33a. At approximately pH = 7, relatively small changes in pH could lead to large color changes from purple to blue. Vacuolar pH measurements of morning glory petals in the abaxial epidermis have shown that the purplish red buds, purple flowers, and blue open flowers were at pH = 6.6, 6.9, and 7.7, respectively.[29]

https://doi.org/10.1021/acs.chemrev.1c00399
Chem. Rev. 2022, 122, 1416−1481

Scheme 32[a]

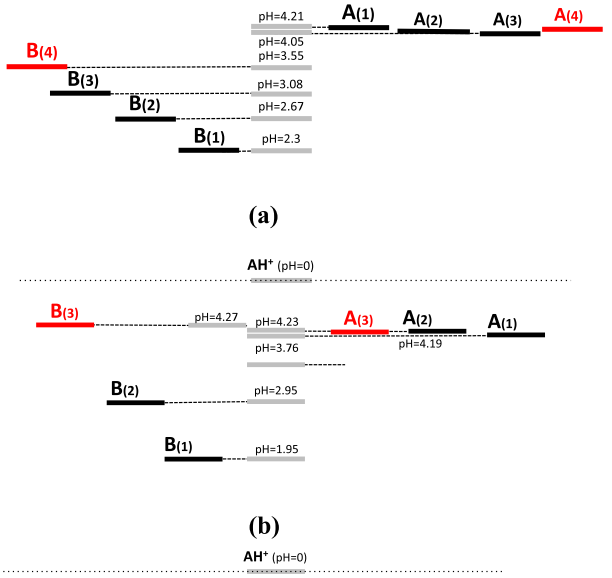

[a](a) Quinoidal base and hemiketal energy level diagram constructed with the equilibrium constants reported by Dangles et al.[195] (b) The same parameters for those reported by Mendoza et al.[193] This scheme is slightly different from the original because it was calculated taking by the value of $K_h(1 + K_t)$ to maintain the same conditions used to draw (a).

Moreover, the spectra of pigment **3** in aqueous solutions at pH values of 7.68 and 6.37 corresponded to the reflective spectra of the open petal and bud, respectively.[29]

By means of a series of direct and reverse pH jumps monitored by stopped flow, it was possible to calculate the hydration rate constants with great accuracy (Scheme 33b). According to these results, the increasing acyl residues from pigment **1** to pigment **3** led to a very significant decrease in the hydration constant (k_h) and an increase in the dehydration constant (k_{-h}), both of which increased the relative instability of the hemiketal species.

Significant information regarding the effect of the acylation on the thermodynamics and kinetics of the flavylium multistate was obtained from an extensive study of red cabbage anthocyanins, as shown in Scheme 34.[240]

In this study, three monoacylated anthocyanins were compared to three diacylated ones. Compared to the monoacylated anthocyanins, the hydration rate constants (k_h) of the diacylated anthocyanins are almost 1 order of magnitude lower. In addition, the dehydration rates (k_{-h}) are weakly affected. The equilibrium pK'_a changes from 2.65 to 2.69 (nonacylated) to 3.57−3.80 (diacylated), extending the pH range of the flavylium cation. In diacylated anthocyanins, the pK'_a is generally closer to the pK_a than the monoacylated anthocyanins, which provides mathematical evidence that the mole fraction of the quinoidal base is higher in these compounds. Considering the case of the quinoidal base at pH values at which the anionic form can be neglected, its mole fraction is given by eq 24.

$$\chi_A = \frac{K_a}{[H^+] + K'_a} \tag{24}$$

The limit of eq 24 when $[H^+]$ decreases is the K_a/K'_a ratio. Although the equilibrium and rate constants were not fully calculated in neutral to weakly basic solutions, the authors stressed the appearance of the blue quinoidal bases. Degradation studies performed at room temperature and pH = 8 in the dark indicated that the diacylated anthocyanins exhibit substantially higher storage stability than the monoacylated anthocyanins.[240]

Unlike for polyacylated anthocyanins, few examples of the effect of a single acylated unit on the anthocyanin color stability involving intramolecular interactions are reported in the literature.[39,40,175] In acylated anthocyanins, two different types of interactions coexist, intermolecular (self-association), as in common anthocyanins, and intramolecular interactions involving the acylated residue and the flavylium core, as described above.[33] Moreover, the type of the sugar spacer and acylation site are critical.

One example of the effect of a single acylated residue was reported for malvidin 3-*O*-(6-*O*-*p*-coumaroyl)-glucoside (oenincoum) and malvidin 3-*O*-glucoside (oenin).[43]

The results of a circular dichroism (CD) analysis of both compounds are presented in Figure 15. Interestingly, the CD signal corresponding to the intermolecular interaction disappears in both compounds at high temperatures (70−80 °C), but the CD signals of the intramolecular interaction of oenincoum in the visible spectrum remain (Figure 15). This

Scheme 33[a]

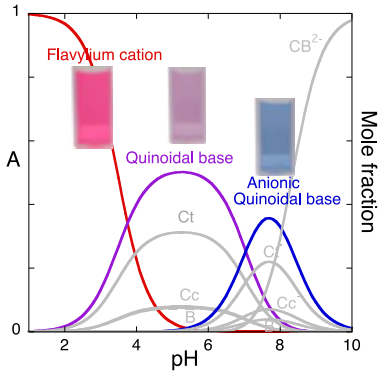

(a)

Rate constants of hydration		
	k_h/s^{-1}	$k_{-h}/M^{-1}\ s^{-1}$
Pigment 1	0.01	377
Pigment 2	0.12	145
Pigment 3	0.35	43

(b)

[a](a) Mole fraction distribution of the blue anthocyanin (*Ipomoea tricolor*) including the anionic forms and (b) rate constants of hydration (k_h) and dehydration (k_{-h}). Pigments defined in Scheme 30.

https://doi.org/10.1021/acs.chemrev.1c00399
Chem. Rev. 2022, 122, 1416−1481

Scheme 34. Structure of Red Cabbage Anthocyanins[a]

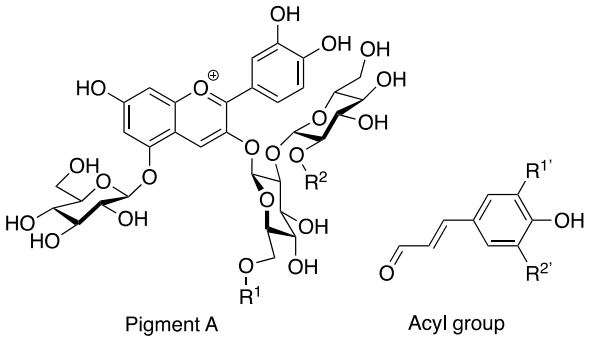

Pigment	R^1	R^2
Pigment A	H	H
P1	pC	H
P2	Fl	H
P3	Sp	H
P4	pC	Sp
P5	Fl	Sp
P6	Sp	Sp
Acyl group	**$R^{1'}$**	**$R^{2'}$**
pC	H	H
FI	OMe	H
SP	OMe	OMe

[a]pC, *p*-coumaric acid residue; Sp, sinapic acid residue, Fl, ferulic acid residue[240].

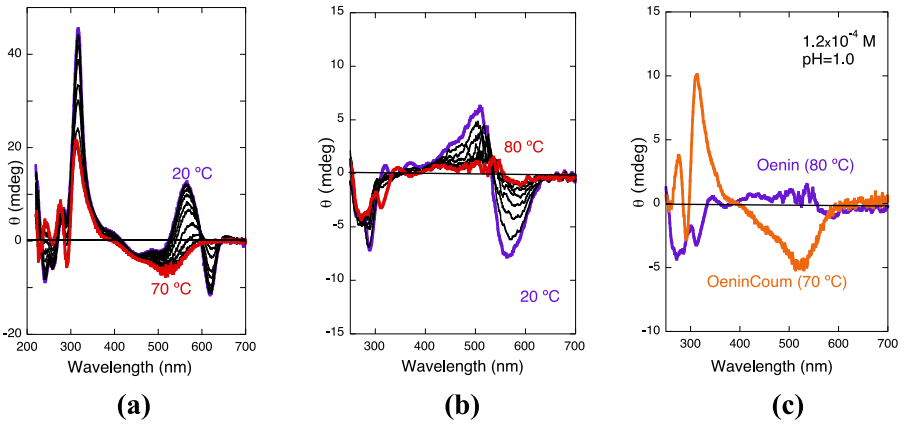

Figure 15. (a) Circular dichroism spectra of oenincoum in water at 2.5×10^{-4} M, pH 1.0, (20−70 °C); (b) the same parameters for oenin in water at 1.2×10^{-4} M, pH 1.0 as a function of temperature (20−80 °C); and (c) comparison of the CD spectra of oenincoum and oenin under the same conditions. Adapted with permission from ref 43. Copyright 2020, Elsevier.

phenomenon was corroborated by variable temperature NMR experiments. The signals for the H6 and H8 of the A-ring are shielded in oenincoum compared to oenin and move upfield in the NMR spectra suggesting a folded structure such as the one showed in Figure 16.

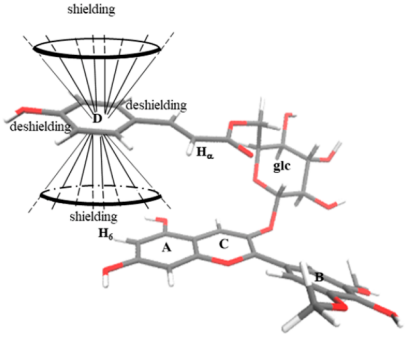

Figure 16. Proposed oenincoum model representing the effect of the coumaroyl moiety on the ^{1}H NMR chemical shifts on the flavylium backbone. Adapted with permission from ref 43. Copyright 2020, Elsevier.

Acylation of the sugars in anthocyanins is another strategy used in nature to display purple and blue colors, not only in flowers but also in vegetables, such as red cabbage, black carrots, sweet potatoes, and pigmented potatoes.[196,241−247] Despite the higher storage stability of acylated anthocyanins, compared with nonacylated anthocyanins, their industrial applications, in particular, blue colors, are still limited by their storage instability. Encapsulation in biocompatible matrixes of these and other anthocyanins could be a research challenge for the future.[248,249] For example, calcium-alginate microparticles have been optimized to encapsulate an anthocyanin-rich extract from haskap berries (*Lonicera caerulea*),[250] and the degradation due to ascorbic acid of anthocyanins extracted from black carrots in beverages was reduced through encapsulation in various lecithin liposomal systems.[251]

In recent years, a new series of acylated anthocyanins with aromatic/aliphatic acids have been synthesized to improve their liposolubility, and their stability in hydrophobic environments makes their application in lipid-based foods and cosmetics possible. Chemical approaches to obtain anthocyanin-fatty acid conjugates have been employed by using fatty acid chlorides in acetonitrile/dimethylformamide and triethylamine or via EDC-

https://doi.org/10.1021/acs.chemrev.1c00399
Chem. Rev. 2022, 122, 1416−1481

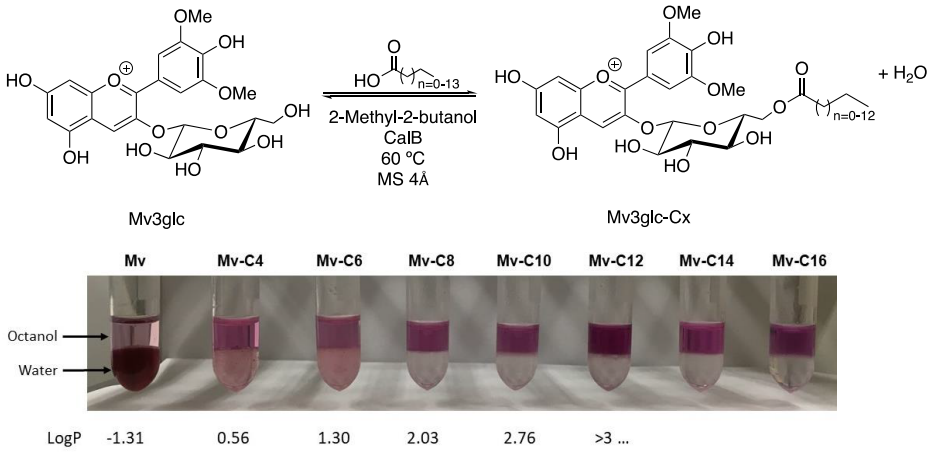

Figure 17. Enzymatic lipophilization of anthocyanins using CalB as a biocatalyst and partition coefficient determination (log *P*) of native malvidin-3-glucoside (Mv3glc) and its lipophilic derivatives (Mv3glc-Cx) in an octanol−water biphasic mixture. The red color increases in the octanol phase as long as the fatty acid chain length increases.

activated fatty acids (lauric acid), but the reactions revealed low regioselectivity, and complex mixtures of ester isomers were obtained.[252−254] Enzymatic reactions of pure anthocyanins and anthocyanin-rich extracts with fatty acids or fatty acid methyl esters in tertiary alcohols (*tert*-amyl alcohol, *tert*-butanol) or in aprotic solvents such as acetone, acetonitrile ,and pyridine using *Candida antarctica* lipase B as a biocatalyst have emerged as a novel approach to enabling higher regioselectivity and higher yields.[255−259] Anthocyanin-fatty acid adducts showed preferential organic miscibility in an octanol−water biphasic mixture and increased lipophilicity with chain length (Figure 17). Lipophilic anthocyanins up to the C8 chain length were also shown to have improved the antioxidant activity of their precursors, exerting a greater protective effect.[260]

Table 2 shows the effect of the environment (micelles vs aqueous solution) and the fatty acid acyl residue on the thermodynamic properties of anthocyanins. Micellar systems largely increase the color stability of anthocyanins by increasing their pK'_a and pK_h to high pH mainly due to the formation of ion-pair interactions between the flavylium cation and the negatively charged sulfate and phosphate groups and also due to the lower local pH at the negatively charged micellar surface.

Furthermore, acylated anthocyanin with fatty acids was shown to extend even more the domain of red flavylium cation to higher pH values. The mole fraction of the purple quinoidal base was also stabilized at neutral pH compared with its respective precursors when dissolved in micellar systems (SDS and PEGylated phospholipids) (Figure 18).[257,261−263] Comparatively with their precursors in the same media, anthocyanins grafted with aliphatic alkyl chains showed slightly higher flavylium cation stability (higher pK'_a) in SDS micellar system while in the presence of mPEG-DSPE micelles the relative stabilization of lipophilic anthocyanins is more pronounced (i.e., the synergy between anthocyanin lipophilization and encapsulation is more clear). Overall, both SDS and mPEG-DSPE can be combined with these anthocyanin derivatives to achieve formulations with improved color stability being the absolute effects higher for SDS. However, further systematic studies are required to generalize the behavior observed in these particular systems.

Table 2. Equilibrium Constants Obtained by UV−Vis Spectroscopy for cy3glc, Mv3glc, and Their Respective Lipophilic Derivatives in Water and in Micellar Systems of SDS (0.1 M) and mPEG-DSPE (1.3 mM)[a]

compd	pK_a	$pK_a^{\wedge}$	pK'_a	pK_h	K_t	K_i
Mv3glc (water)	3.7	2.4	2.3	2.6	0.12	
Mv3glc (SDS)[264]	6.0		5.4	6.2		
Mv3glc-C6 (SDS)	6.1	5.9	5.7	6.48	0.6	4
Mv3glc-C12 (SDS)	6.0	5.75	5.65	6.30	0.5	2
Cy3glc (water)	3.89	2.88	2.83	3.01	0.21	0.78
Cy3glc (mPEG-DSPE)	4.13	3.47	3.36	3.66	0.22	2.0
Cy3glc-C12 (mPEG-DSPE)	5.09	4.85	4.69	5.34	0.30	4.6

[a]Estimated error ≈10%. K_a, acidity constant; $K_a^{\wedge}$, pseudoequilibrium constant; K'_a, equilibrium constant; K_t, tautomerization constant; K_h, hydration constant; and K_i, isomerization constant.

5. PHOTOCHROMIC PROPERTIES

5.1. Photochromism

The photochemistry history of flavylium multistates and related work through 2012 were previously reviewed.[178] Nevertheless, this section will provide a short overview to frame more recent studies on this unique photochromic system.

The photochemical/photochromic properties based on the flavylium multistate arise most often from photoinduced *cis*−*trans* isomerizations as well as from photoinduced ring opening of the hemiketal (vide infra).

In contrast with other popular photochromic systems, such as azobenzenes and diarylethenes,[265,266] the direct photochemical product (i.e., the *cis*-chalcone) is often subject to further transformations to yield other species, such as the flavylium cation or, to a lesser extent, the quinoidal base, as the final outputs of the photochemical reaction. In this respect, flavylium photochromic systems have some resemblances to spiropyrans, for which *trans*−*cis* photoisomerization of the merocyanine leads to the formation of the *cis*-species, which further evolves to the spiro form through a thermal ring-closing reaction, as indicated in Scheme 35.[267,268]

Figure 19 summarizes how the *trans*-chalcone of flavylium multistates possessing a high *cis*−*trans* isomerization barrier responds to the light impulse.

https://doi.org/10.1021/acs.chemrev.1c00399
Chem. Rev. 2022, 122, 1416−1481

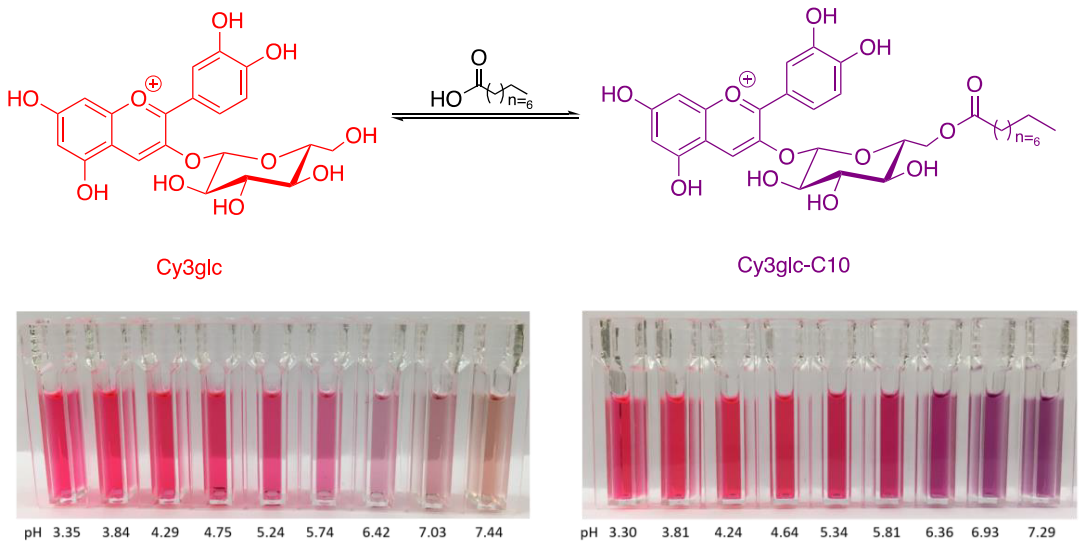

Figure 18. Aqueous solutions of 5×10^{-5} M Cy3glc and Cy3glcC10 (SDS 0.1 M) at different pH values.

Scheme 35. Ring-Closing Reactions Induced by *trans*–*cis* Photoisomerization in (a) Spiropyran- and (b) Flavylium-Based Photoswitches

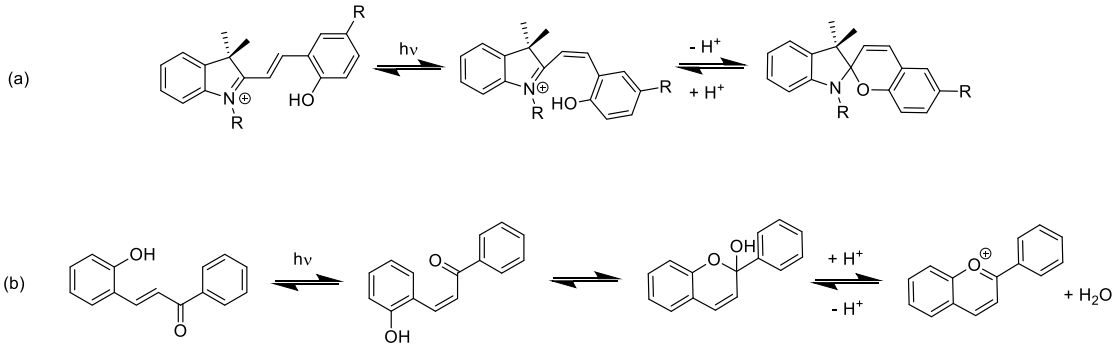

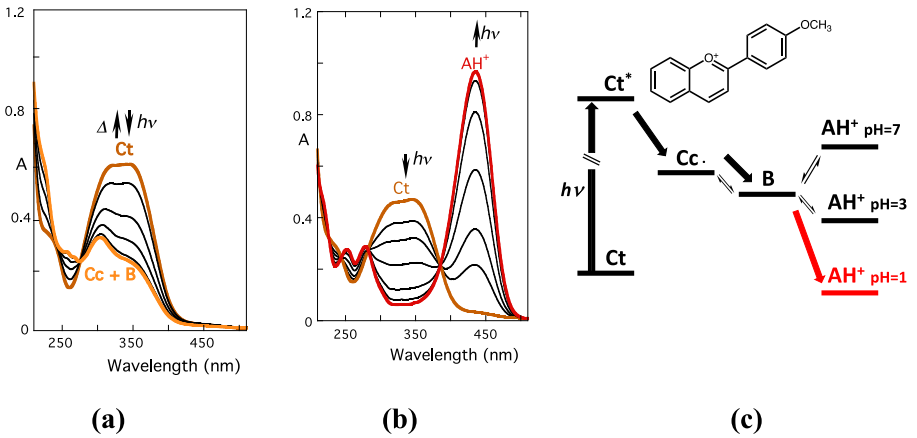

Figure 19. Photochemistry of 4′-methoxyflavylium: (a) spectral variations of 4′-methoxyflavylium at pH = 7.0, [Ct] = 3.2×10^{-5} M; the curves correspond to irradiation times 0, 0.25, 1.5, 3, 6, and 10 min; λ_{exc} = 365 nm; (b) pH 1.0, [Ct] = 2.5×10^{-5} M; the curves correspond to irradiation times 0. 0.5, 1, 2, 4, 7, and 12 min; λ_{exc} = 365 nm; and (c) energy level diagram of 4′-methoxyflavylium. Adapted with permission from ref 179. Copyright 1997, American Chemical Society.

The *trans*-chalcone of 4′-methoxyflavylium is stable at pH = 7.0, as shown in Figure 19c. Light absorption by this species gives the *cis*-chalcone (in a domain of nanoseconds[178]), which equilibrates in subseconds with hemiketal,[179] Figure 19a. At this pH, the flavylium cation is not thermodynamically accessible and the photoproducts are *cis*-chalcone in equilibrium with hemiketal. Although it reacts very slowly at room temperature, due to its high *cis*–*trans* isomerization barrier, a back reaction to the stable *trans*-chalcone occurs. At pH = 1.0, the *trans*-chalcone is metastable and the photoproduct *cis*-chalcone in fast equilibrium with hemiketal evolves spontaneously and irreversibly to the stable flavylium cation, as shown in Figure 19b.

https://doi.org/10.1021/acs.chemrev.1c00399
Chem. Rev. 2022, 122, 1416−1481

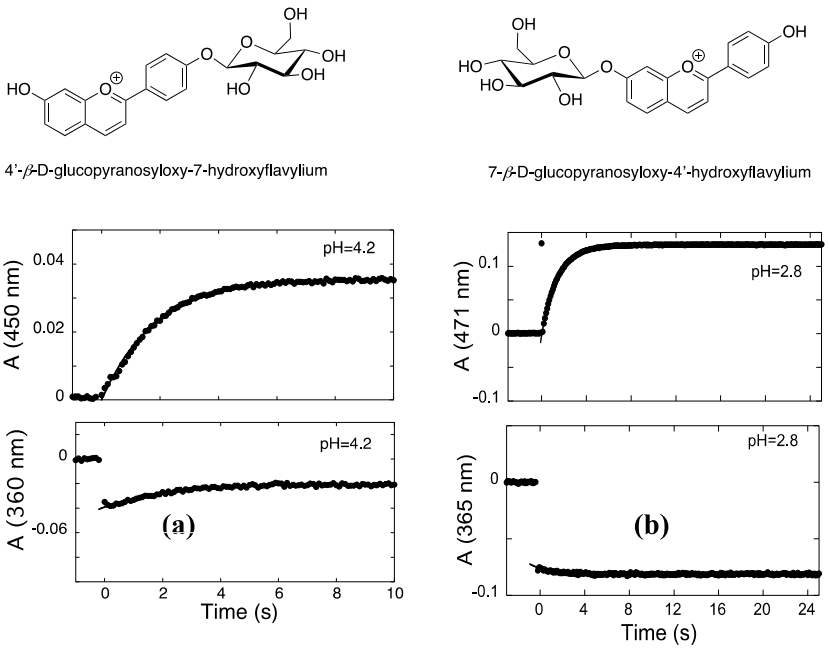

Figure 20. (a) Flash photolysis traces of 4′-β-D-glucopyranosyloxy-7-hydroxyflavylium of the absorption of the flavylium cation (top) and *trans*-chalcone (bottom) and (b) the same experiment for 7-β-D-glucopyranosyloxy-4′-hydroxyflavylium. Adapted with permission from ref 188. Copyright 2016, MDPI.

Reversible photochromism at a constant pH can be optimized by setting the pH at a value at which the flavylium cation can be effectively formed by light irradiation of the *trans*-chalcone but then reverts to the initial thermodynamically stable state when kept in the dark (also defined as the autolock pH; approximately pH = 3 for 4′-methoxyflavylium).

In general, anthocyanins are poor photochromic compounds due to the small mole fraction of *trans*-chalcone at equilibrium.[180,269] From this point of view, 3-deoxyanthocyanidins are much better photochromic compounds because *trans*-chalcone (major) together with a quinoidal base (minor) are the species present at moderately acidic pH values at equilibrium. The photochromism of 3-deoxyanthocyanidins was recently reviewed.[270]

Models of 3-deoxyanthocyanidins were synthesized,[72] and their respective photochromism was investigated.[188] Flash photolysis over a time scale of seconds/subseconds is a very powerful tool for determining the kinetics of the flavylium multistate.[271] This technique was performed in two representative compounds, 4′-β-D-glucopyranosyloxy-7-hydroxyflavylium and 7-β-D-glucopyranosyloxy-4′-hydroxyflavylium ions, without and with a *cis*−*trans* isomerization barrier, respectively, as shown in Figure 20. The *cis*-chalcone is formed during the lifetime of the flash (milliseconds) and corresponds to the initial bleaching at 360 nm (the maximum absorption of the *trans*-chalcone) because the *trans* isomer has a higher mole absorption coefficient than the *cis* isomer. Regarding 4′-β-D-glucopyranosyloxy-7-hydroxyflavylium, the increase of the flavylium cation absorption is accompanied by a partial recovery of the *trans*-chalcone absorption. Both traces have the same rate constant. This finding is explained by the lack of a *cis*−*trans* isomerization barrier. Once formed, *cis*-chalcone disappears through two competitive pathways, (i) forward to form a flavylium cation and (ii) backward to recover part of the *trans*-chalcone (Scheme 36).

The fraction of *trans*-chalcone that was not completely recovered corresponds to the fraction of the flavylium cation

Scheme 36. Flash Photolysis: When There is a *cis*−*trans* Isomerization Barrier, No Backward Kinetics Are Observed

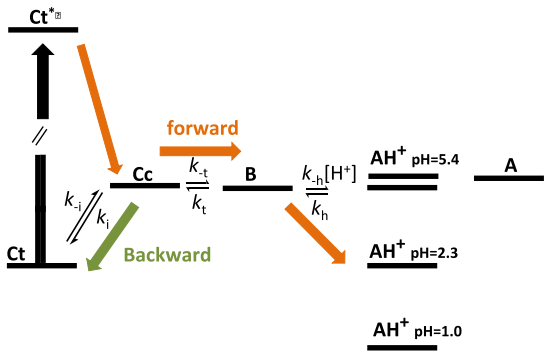

that formed. In a slower kinetic step (not shown in Figure 20), the absorption of the flavylium cation starts to disappear at the same time that *trans*-chalcone is recovered. For 7-β-D-glucopyranosyloxy-4′-hydroxyflavylium, there is a *cis*−*trans* isomerization barrier and no recovery of the *trans*-chalcone takes place, as shown in Figure 20b.

Photochromic systems, such as that shown in Figure 19, were explored as models for optical memories capable of write-lock-read-unlock-erase actions.

The *trans*-chalcone as a stable species at pH = 7.0 or a metastable species at pH = 1.0 is the photoactive species, Scheme 37. At pH = 7.0, irradiating the Ct leads to the formation of a Cc that equilibrates with B in subseconds. Despite the high *cis*−*trans* isomerization barrier, these two species tend to revert back to the stable Ct slowly. Moreover, using light to read the system at this point is not convenient because irradiating *cis*-chalcone gives *trans*-chalcone and erases the signal. The lock step consists of a pH jump to pH = 1. At this pH, the Cc in equilibrium with B moves spontaneously to the flavylium cation, constituting a stable signal, which can be read at will. To erase the memory model, it is necessary to unlock the system through

https://doi.org/10.1021/acs.chemrev.1c00399
Chem. Rev. 2022, 122, 1416−1481

Scheme 37. Illustrating the Concept of a Flavylium Multistate System Behaving as a Model for an Optical Memory

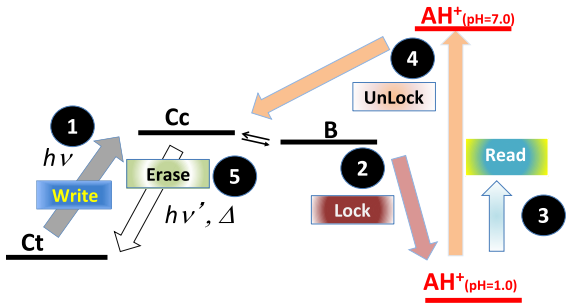

a pH jump back to pH = 7, allowing it to reach the initial state spontaneously, eventually using high temperature and/or light.

Numerous flavylium multistates with similar behaviors have been reported and previously reviewed.[178] Based on the same concept, a system using hyper-Rayleigh scattering experiments and quantum chemical calculations demonstrated that nonlinear optics can be used to probe unequivocally, within a non-destructive process, the multiple electronic states that are activated upon pH and light-triggered transformations of the 4′-hydroxyflavylium ion, as shown in Scheme 38.[272]

Scheme 38. Write−Lock−Read−Unlock−Erase Cycle Starting From the AH^+ form[a]

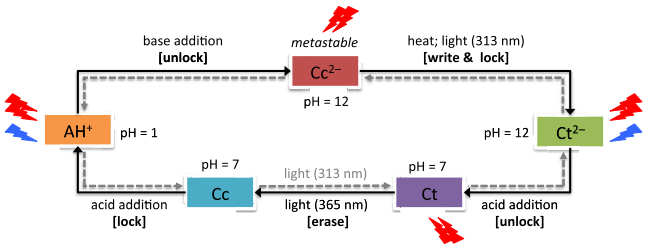

[a]Blue (double red) flashes symbolize the possibility of reading without altering the information by means of linear (nonlinear) optical spectroscopy. Reprinted with permission from ref 273. Copyright 2015, Royal Society of Chemistry.

In addition to *cis*−*trans* isomerization, the flavylium multistate has another potential source of photochromism: the ring-opening closure (tautomerism), as shown in Scheme 39.

The photoinduced ring opening of hemiketal was considered as a possible pathway in flavylium-based photochromic systems by Matsushima et al.[274] and Wünscher et al.[275] Unequivocal

Scheme 39. Two Photochromic Systems Arising from a Flavylium-Based Multistate[a]

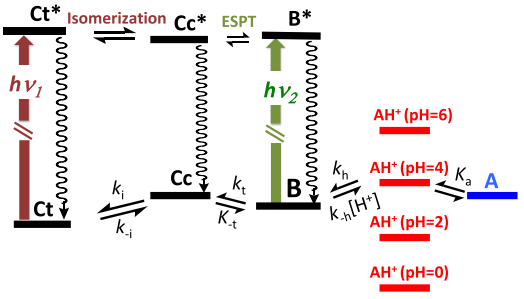

[a]The arrows representing the excitation energy are not to scale.

experimental evidence of this phenomenon was reported by Maçanita et al., who observed that, in three common anthocyanins (pelargonin, cyanin, and malvin), phototautomerization yields *cis*-chalcone in the ground state within a few picoseconds, Figure 21.[276]

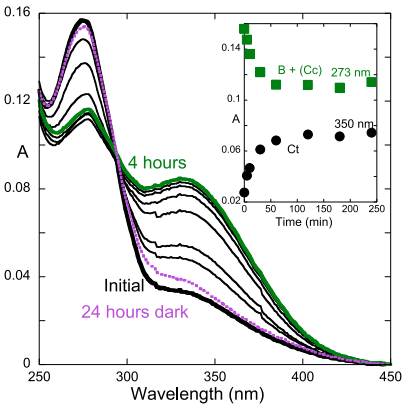

Figure 21. Photochromism of hemiketal. Absorption spectra of malvin (malvidin 3,5-diglucoside) in water at pH 4.5 and 20 °C as a function of time at an irradiation wavelength of 275 nm. Courtesy of Prof. Maçanita.[276]

According to Maçanita et al., the formation of *trans*-chalcone from the steady state irradiation of hemiketal takes place in two steps: (i) the hemiketal excited state leads to the ground state *cis*-chalcone via a conical intersection and (ii) the irradiation of *cis*-chalcone leads to *trans*-chalcone to reach a photostationary state. An alternative mechanism is the existence of excited state energy transfer that gives Cc* from B*, the Ct (and Cc) in the ground state obtained from the further decay of Cc*.

In contrast to the case of anthocyanins, in which the *trans*-chalcone is a minor species, 4′,7-dihydroxy-3-methoxyflavylium possesses a high mole fraction distribution of *trans*-chalcone together with the major hemiketal species.[273] This property allows for both photochromic systems to be explored, as addressed by two different light inputs, which is shown in Figure 22.

Irradiation of hemiketal at 275 nm leads to a photostationary state in which trans-chalcone is formed (green spectrum). In the opposite direction, the irradiation of chalcone at 365 nm results in another photostationary state in which hemiketal is the dominant form (brown spectrum). Equilibrium is thermally reached from each photostationary state.

5.2. Fluorescence: Excited State Proton Transfer

Studying flavylium multistate fluorescence is difficult due to the high number of species that are emitting together. The exceptions are flavylium cations at sufficiently low pH values (to be the sole species in solution) and systems in which hydration is prevented, as in flavylium cations with alkyl substituents in position 4 or pyranoanthocyanins. Similar to other phenols like β-naphthol, flavylium cations exhibit excited state proton transfer (ESPT).[277] This phenomenon is illustrated in Scheme 40.[278]

Light absorption from the flavylium cation leads to its excited state. Since the rate constants k^*_a and k^*_{-a} are much faster (picoseconds) than the rate of the decay processes from both excited states to the ground states, a steady state equilibrium under continuous irradiation is quantified by $K^*_{ap} = (k^*_a/k^*_{-a})(\tau_{AH+}/\tau_A)(1/\eta_a^*)$, with $\eta_A^* = k^*_a/(k_c+k_f+k^*_a)$.[279] As

https://doi.org/10.1021/acs.chemrev.1c00399
Chem. Rev. 2022, 122, 1416−1481

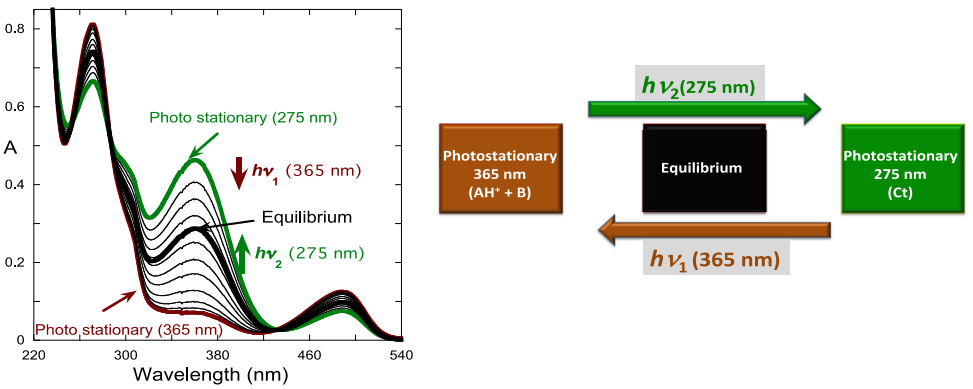

Figure 22. Dual photochromic system based on 4′,7-dihydroxy-3-methoxyflavylium, 9.2×10^{-5} M, pH = 3.5. Adapted with permission from ref 273. Copyright 2015, Royal Society of Chemistry.

Scheme 40[a]

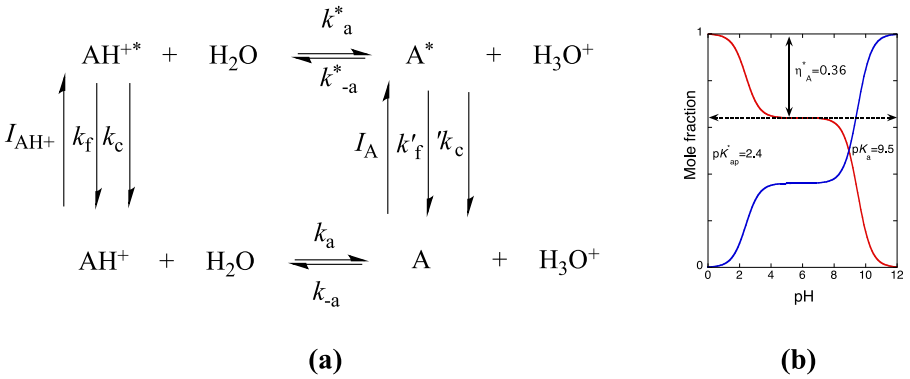

[a](a) General scheme for excited state proton transfer; (b) simulation of the fluorescence titration of β-naphthol: parameters $pK_a = 9.5$, $pK^*_{ap} = 2.4$ and $\eta_{A^*} = 0.36$, and emissions from the acid (red) and from the base (blue). For more details, see ref 278. AH^+ stands for the phenol in its acid form or the flavylium cation.

exemplified for β-naphthol in Scheme 40b, the excitation of the acidic form at pH = 5, for example, leads to emission of the acid plus that of the base. The parameter n_{A^*} measures the efficiency of the ESPT from the excited acidic form. The anthocyanins malvidin-3,5-diglucoside (malvin), cyanidin-3,5-diglucoside (cyanin), and pelargonidin-3,5-diglucoside (pelargonin) are among the flavylium compounds exhibiting ESPT.[280] 4-Methyl-7-hydroxyflavylium is one of the flavylium cations that was studied in more detail, as shown in Figure 23.[281−283]

The emission of 4-methyl-7-hydroxyflavylium is shown in Figure 23. The blue-shifted fluorescence emission of the flavylium cation evolves toward a red-shifted emission of the quinoidal base by increasing pH. The excitation of the flavylium cation at pH = 1 or pH = 2, ($pK_a = 4.4$) gives essentially the emission of the quinoidal base, as shown in Figure 23b. In fact, the efficiency of this process is 0.93, and for that reason, these types of compounds are known as superphotoacids.[280] It is worth noting that even in extremely acid solutions, such as $[H^+] = 1$ M, there is still significant emission from the quinoidal base ($pK^*_{ap} = -1 \pm 0.3$).

ESPT could also give information regarding the rate constant of the ground state through nanosecond laser flash photolysis experiments as a function of pH. After the flash at a wavelength at which the flavylium cation absorbs, high amounts of the quinoidal base in its excited state are formed in pico-seconds, and it later decay to its ground state. This change leads to an excess of quinoidal base in the ground state, and the observed rate back to the equilibrium is given by $k_{obs} = k_a + k_{-a}[H^+]$. The

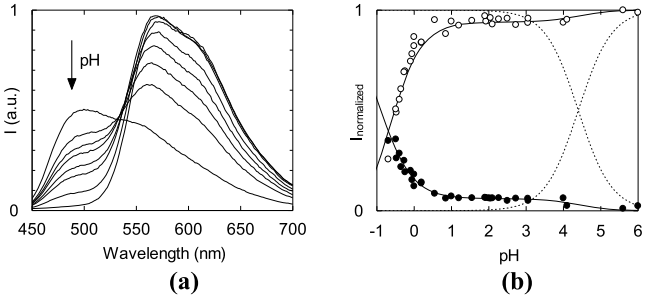

Figure 23. (a) Fluorescence emission spectra of the compound 4-methyl-7-hydroxyflavylium at an excitation wavelength of 438 nm (isosbestic point of the absorption). pH was varied between 6 and −0.69. For pH values lower than 1, the negative logarithm of the analytical concentration of the added acid was used to calculate the apparent pH. (b) Normalized fluorescence emission curves: (●) emission from the acidic species ($\lambda_{em} = 493$ nm); (○) emission from the basic species ($\lambda_{em} = 603$ nm); fitting achieved for $pK_a = 4.4$, $pK^*_{ap} = -1 \pm 0.3$ and $\eta_{A^*} = 0.93 \pm 0.02$, full lines; and traced lines show the mole fraction distribution of the ground state. Reprinted with permission from ref 283. Copyright 1998, Royal Society of Chemistry.

fitting of the observed rate constant as a function of $[H^+]$ gives k_a and k_{-a}, which should coincide with the pK_a ($K_a = k_a/k_{-a}$ is calculated independently, as shown in section 2).[187,280] In Table 3, some examples of these rates are presented. In particular, the constant k_{-a} seems to be controlled by diffusion. Recent studies on the photophysics of synthetic pyranoflavyliums (Scheme 41)

https://doi.org/10.1021/acs.chemrev.1c00399
Chem. Rev. 2022, 122, 1416−1481

Table 3. Rate Constants of the Equilibrium Flavylium Cation-Quinoidal Base[187,280a]

compd	k_a (s^{-1})	k_{-a} (M^{-1} s^{-1})	pK_a
pelargonidin	1.3×10^6	3.6×10^{10}	4.44
cyanin	1.8×10^6	2.2×10^{10}	4.09
malvin	3.8×10^6	2.9×10^{10}	3.88
HMF	1.4×10^6	3.5×10^{10}	4.4
DHF	3.1×10^6	3.1×10^{10}	4.0

[a]HMF, 7-hydroxy-4-methylflavylium chloride; DHF; 4′,7-dihydroxyflavylium chloride. In the case of pelargonidin there is a substantial difference between the pK_a reported in refs 187 and 281 (pK_a = 4.4, Table 3), in comparison with ref 186, pK_a = 3.9. The authors of the present Review repeated this calculation by means of reverse pH jumps monitored by stopped flow and obtained pK_a = 4.3, in good agreement with the data of Table 3.

Scheme 41. Structure of the Synthetic Pyranoflavylium Compounds Employed for Photophysical Investigations of Their Photoacidity and Triplet Formation

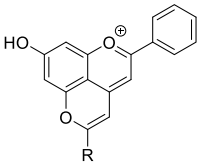

		pK^*_a	pK_a
1	R = *p*-Methoxyphenyl	0.66	3.8
2	R = *p*-Methylphenyl	0.61	3.7
3	R = 2-Naphthyl	0.58	3.6
4	R = Phenyl	0.52	4.2
5	R = *p*-Fluorophenyl	0.51	3.7
6	R = *m*-Pyridyl	0.47	4.4
7	R = *p*-Cyanophenyl	0.37	3.7
8	R = *p*-Nitrophenyl	0.22	3.4

showed that these compounds also display photoacid properties, with pK^*_a values in the 0.2−0.7 range, depending on the substituents that decorate the pyranoflavylium core.[284,285] However, compared with their flavylium analogues, the rate of excited-state proton transfer was found to be approximately 2 orders of magnitude slower for pyranoflavylium salts, resulting in less efficient photoacidity and much longer excited state lifetimes.

Interestingly, although the formation of triplet states at room temperature has not been clearly demonstrated for other flavylium cations, the pyranoflavylium salts of Scheme 41 were observed to readily form triplet states in acidic acetonitrile solutions at room temperature.[286] The triplets where shown to have microsecond lifetimes and are quenched by oxygen forming singlet oxygen detected by its emission in the near-infrared spectral region.

One of the most frequently reported practical uses of fluorescent probes is in optical imaging and sensing.[287] These analytical techniques are among the most powerful tools for targeting tissues and organs, and they are therefore very useful in clinical diagnoses and surgical procedures. Flavylium-type dyes have been explored as fluorophores for use in optical imaging. Among other important features, as previously mentioned, these dyes must comprise substituents that block the hydration of the flavylium cation, leading to improved stability in biorelevant media. Earlier work performed in the 1990s already indicated the potential of these chromophores for use as fluorescent lasers and near-infrared dyes.[288−290] More recently, flavylium-based fluorescent probes have reemerged in different studies focused in the development of dyes with imaging applications, although they are not always identified as flavylium compounds.[291,292] In the following paragraphs, two representative examples are described to illustrate the potential of these compounds in the field.

Locked-flavylium dyes (Scheme 42a) were shown to display unique fluorescence ratiometric responses in three channels by

Scheme 42. Novel Classes of Flavylium Dyes for Fluorescence Imaging[293,295]

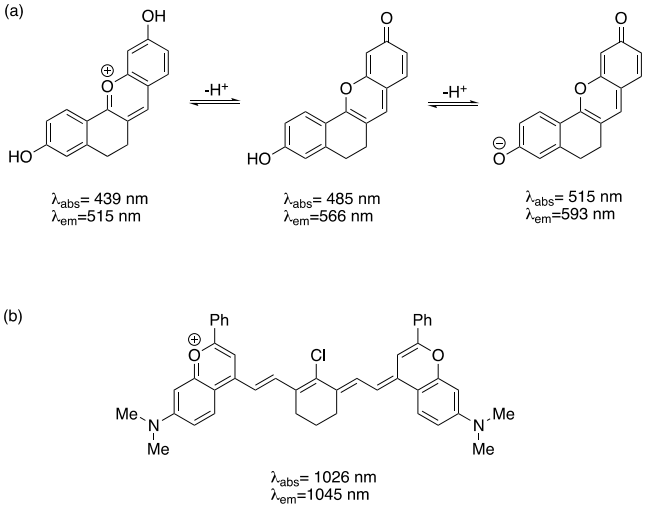

tuning the intramolecular charge transfer efficiencies suitable for three-color ratiometric imaging of pH in living cells.[293] A subsequent study of these compounds confirmed the thermodynamic stability of the locked flavylium dyes against hydration under neutral and acidic pH conditions but also showed that in the presence of CTAB micelles, equilibrium is driven to the *trans*-chalcone, raising a question about whether the similar fading of the fluorescent flavylium and quinoidal base species may occur in complex biological media.[294]

More recently,[295] a new class of polymethine dyes with dimethylamino flavylium heterocycles emitting in the near-infrared (NIR, λ = 700−1000 nm) and in the shortwave infrared (SWIR, λ = 1000−2000 nm) ranges was developed (Scheme 42b). The synthesized dyes revealed high brightness, good biocompatibility, and strong photophysical properties (enhanced photostability, high absorption coefficients, and high fluorescence quantum efficiency). The in vivo performance of the dye in phospholipid micelle formulation suggests that this polymethine flavylium is a promising SWIR imaging agent that could be translated from diagnostics to the clinic.[296]

The photosensitizing property of the flavylium-based dyes has been explored for applications in dye-sensitive solar cells (DSSCs). Cherepy et al. elucidated the photoelectrochemical behavior of anthocyanin dyes extracted from blackberries, and the first DSSC using an anthocyanin, cyanidin-3-glucoside, displayed a conversion yield of 0.56%.[297] Anthocyanins such as delphinidin-3-glucoside and cyanidin-3-glucoside can anchor efficiently to TiO_2 through the catechol unit, but the donor−acceptor pattern is not optimized for electron transfer. Considering that many other natural and synthetic flavylium compounds have the same chemical equilibria network as those observed in anthocyanins, a series of flavylium derivatives were synthesized and tested in DSSCs. The best yield conversion of 3.05% was obtained for the compound 7-diethylamino-3′,4′-dihydroxyflavylium.[298] More recently, the impact of the catechol versus carboxyl linkage on the DSSC performance of synthetic pyranoflavylium salts was reported. The presence of the catechol unit was shown to be essential for the efficient electron injection of the dye into TiO_2 semiconductors since carboxylic units

https://doi.org/10.1021/acs.chemrev.1c00399
Chem. Rev. 2022, 122, 1416−1481

Scheme 43. Structures of Small Synthetic Receptors for Flavylium Compounds

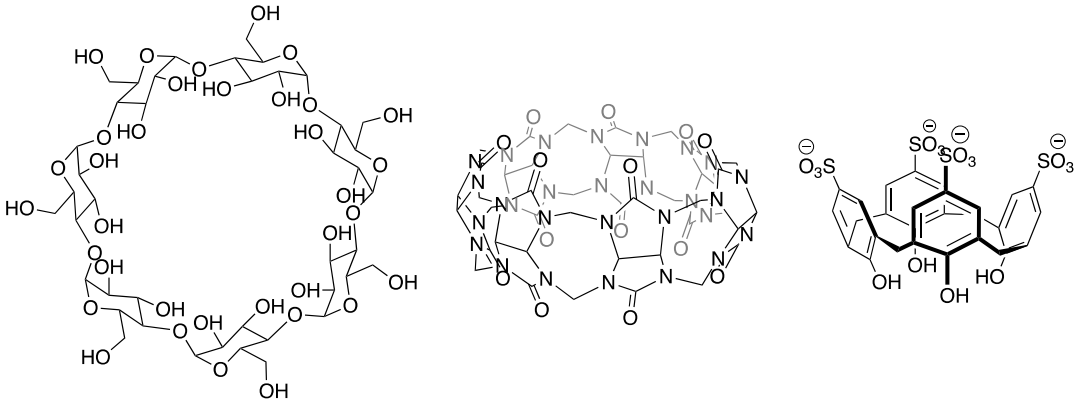

showed a deleterious effect during electron injection due to their electron withdrawing character.[299] Recently, the orbital energies obtained from vertical excitations in TD-DFT calculations of a series of anthocyanins were claimed to be a screening method to provide complementary information to experimental data in DSSCs.[300]

6. STIMULI-RESPONSIVE HOST–GUEST SYSTEMS

Both natural and synthetic flavylium compounds have a rich history in supramolecular chemistry, primarily motivated by the quest to rationalize the color stabilization phenomenon in natural systems. This exploration led to several important studies regarding self-association, copigmentation, and interactions with metal cations, which have been reviewed previously.[39,40] Furthermore, the pH-dependent photochemical properties observed in synthetic flavylium salts, in particular, the reversible interconversion between neutral and cationic species, offer highly attractive features for applications in supramolecular chemistry, nanotechnology, or biological systems.[301−305] However, this family of photochromic compounds has been overlooked, and its potential is now beginning to emerge. Host−guest systems involving the flavylium multistate and different classes of hosts ranging from simple macrocycles to polymeric materials can be explored. The first consist of monodisperse oligomeric receptors with well-defined binding sites that allow for a detailed molecular-level characterization of their complexes using routine spectroscopic techniques. The second involves large macromolecules consisting of more or less polydisperse mixtures comprising several binding sites (or sets of binding sites) that often yield elusive detailed molecular-level pictures of their complexes. Given the differences between these two class systems, which make direct rational comparisons between binding properties unfeasible, they will be reviewed in separate sections.

Host−guest chemistry is a subfield of supramolecular chemistry focused on molecular recognition (noncovalent binding) of small molecules or ions (guests) by larger receptors (hosts) to form a host−guest complex.[306] Examples of host−guest complexes span from enzymes and their substrates to simple complexes formed by a cation bound to a synthetic macrocycle, such as a crown ether. Low molecular weight synthetic molecules, such as macrocycles, molecular clips and tweezers, which have well-defined and structurally preorganized binding sites, can be highly effective supramolecular receptors for binding small guest molecules or ions. Among the different low molecular weight host molecules for flavylium cations, molecular clips were previously reviewed,[178] and thus, this section focuses on cyclodextrins, cucurbiturils, and *p*-sulfonatocalixarenes (Scheme 43).

6.1. Cyclodextrins

Cyclodextrins (CD) are macrocyclic oligosaccharides, with the most common ones being those with six (α-CD), seven (β-CD), and eight (γ-CD) D-glucose units linked by α-1,4-glucose bonds.[307,308] The primary complexation properties of these water-soluble host molecules arise from their conical structure with a defined hydrophobic cavity that can accommodate different molecules and ions of the appropriate shape, size and polarity within their interior. Generally, the affinity of CD toward target guest molecules increases for more hydrophobic species.

Due to their unique structural features, cyclodextrins have been used in several industrial sectors, with applications in food, pharmacy, cosmetics, agriculture, and others with relevance to anthocyanin research. In the food industry, these natural host molecules are primarily used to control flavor release, to mask odors and tastes, to stabilize emulsions, to control ingredient degradation (thermal and oxidative) and to control or mask colors.[309,310]

Earlier studies on the impact of CDs on the stability of anthocyanins indicated the absence of interactions among γ-, β- and α-CD and sterically hindered 3,5-diglycosylated anthocyanin species.[199,311,312] However, the complexation of anthocyanin 3-monoglycosides has been reported by different groups.[311−315] Cyclodextrins lead to significant decreases in the absorption bands of flavylium cations under acidic conditions, suggesting that their equilibrium is shifted toward colorless species due to their selective inclusion in the host's cavity. Due to its bleaching effect, this behavior was called anticopigmentation by Dangles et al.[313] β-CD shows stronger anticopigmentation effects than for α-CD, which are attributed to the higher affinity of the flavylium multistate species toward the former.

Quantitative studies demonstrated that the binding constants of β-CD for the colorless species of two model anthocyanins, cyanidin-3-*O*-glucoside and pelargonidin-3-O-glucoside, are approximately 30 fold higher than the ones observed for the respective flavylium cations, in line with the so-called anticopigmentation effect.[311]

https://doi.org/10.1021/acs.chemrev.1c00399
Chem. Rev. 2022, 122, 1416−1481

Scheme 44. Proposed Structure of the Complex Formed between the β-Cyclodextrin and the Hemiketal forms of Cyanidin-3-*O*-glucoside[a]

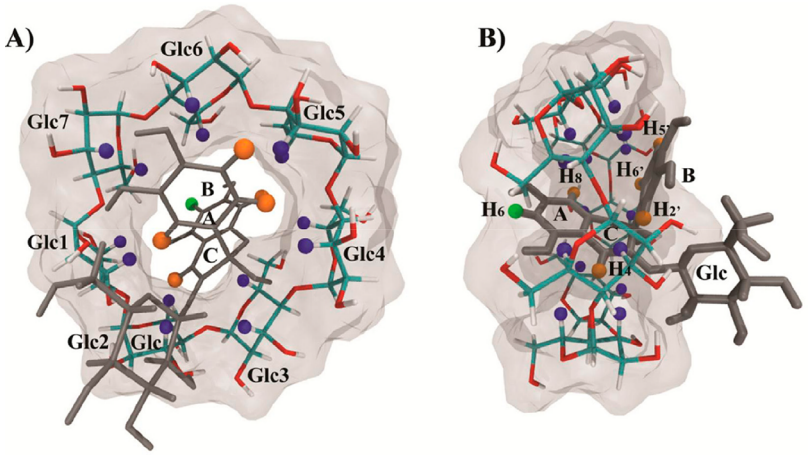

[a](A) Top view and (B) side view. Reprinted with permission from ref 315. Copyright 2014, Elsevier.

The effects of β-CD and α-CD on the kinetics and thermodynamics of the reaction network of cyanidin-3-*O*-glucoside were investigated by de Freitas and co-workers.[314] These authors found that both pK'_a and pK_a decrease in the presence of β-CD, consistent with the selective binding of the neutral species. This host was also observed to decrease the hydration rate constants slightly and accelerate the apparent *cis*-*trans* isomerization. This last kinetic effect was also observed for a synthetic flavylium compound in an earlier study.[316] As in previous studies, α-CD was found to have only moderate effects on the kinetic and thermodynamic properties of the cyanidin-3-*O*-glucoside reaction network. Detailed investigations through NMR and molecular dynamic simulations suggested the preferential binding of the hemiketal and the *cis*-chalcone of cyanidin-3-*O*-glucoside through the inclusion of the A and C ring in the cavity of the β-CD (Scheme 44) while, somewhat surprisingly, the *trans*-chalcone seems to establish weaker interactions.[315]

The selectivity of CD toward more hydrophobic species has been widely explored to devise many different stimuli responsive systems using guest molecules that change their polarity or ionization state upon application of stimuli such as light, redox potential, temperature, or added chemicals.[303,317−321] In this context, synthetic flavylium compounds were found to be excellent candidates for photoresponsive host−guest cyclodextrin-based systems owing to their potential to interconvert between neutral and charged species using light inputs.[322−328]

The influence of β-CD complexation on the kinetics and thermodynamics of the network of reactions involving different synthetic flavylium derivatives was investigated in great detail using different techniques, including NMR, ITC, circular dichroism, UV−vis, and stopped-flow.[322−328] All these studies revealed that, among the flavylium multistate species, the neutral uncolored species (B, Cc, and Ct) bind with higher affinity (K usually in the 10^3 M^{-1} range) to the hydrophobic cavity of β-CD while the respective flavylium cations do not bind or show much weaker affinities.

Ct is the most stable species of many synthetic flavylium multistates under slightly acidic conditions. The fact that Ct shows a much higher affinity toward β-CD than AH^+ and A (often the ultimate species formed after photoirradiation of Ct) provides the required conditions to devise robust photo-responsive host−guest complexes. As shown in Figure 24, the irradiation of Ct in the presence of 8 mM β-CD ($K = 9 \times 10^3$ M^{-1}, 88% of complex) leads to the formation of AH^+, which binds very weakly to cyclodextrin (K < 10 M^{-1}, < 8% of complex) and is therefore (photo)ejected from the cavity of the host upon irradiation.[326]

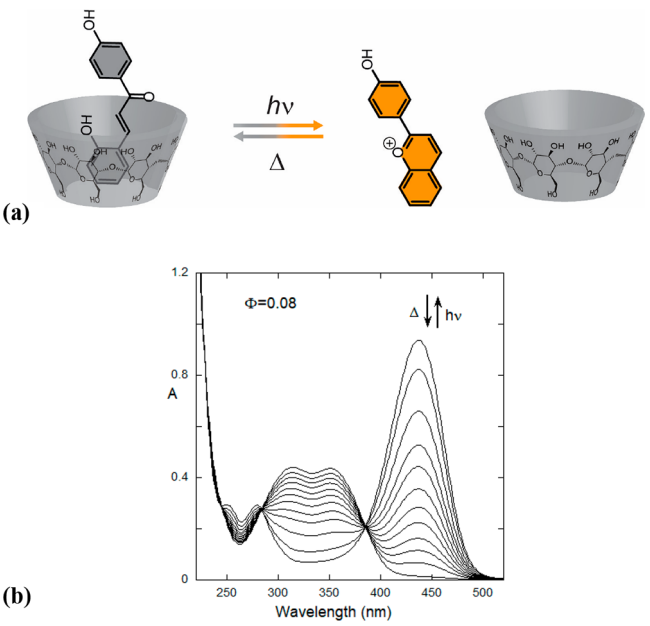

Figure 24. (a) Illustration showing the photoejection of the flavylium guest from the cavity of β-cyclodextrin upon irradiation of the *trans*-chalcone species. (b) Spectral modifications observed upon irradiation of *trans*-chalcone from flavylium **4** in the presence of 8 mM β-cyclodextrin at pH = 2. Reprinted with permission from ref 326. Copyright 2015, American Chemical Society.

6.2. Cucurbiturils

Similar to cyclodextrins, cucurbit[*n*]urils (CB[*n*]) constitute another important class of neutral water-soluble host molecules that were explored as synthetic receptors for flavylium compounds.[329−339] These highly symmetric and rigid pumpkin-shaped macrocycles containing *n* glycoluril units linked by

https://doi.org/10.1021/acs.chemrev.1c00399
Chem. Rev. 2022, 122, 1416−1481

2*n* methylene bridges result from the acid condensation of glycoluril with formaldehyde. Depending on the reaction conditions, different homologues that differ only in the number of glycoluril units present in their structure can be obtained. This feature dictates the cavity sizes, which are crucial for the binding affinity and stoichiometry toward different guest molecules and also for solubility; odd-numbered CB[*n*]s are more soluble in pure water. CB6, CB7, and CB8 are by far the most frequently investigated homologues, owing to their appropriate cavity size for the binding of small organic and inorganic compounds, including drugs, biomolecules, dyes, and other functional molecules with potential application in drug delivery, catalysis, sensors, etc.[340−343] Compared with other water-soluble synthetic receptors, CB[*n*] host molecules show unpaired binding properties that reach attomolar affinities for highly complementary guest molecules.[344]

The combination of a hydrophobic cavity with the highly electronegative character of the two carbonyl rimmed portals of CB[*n*]s makes these receptors particularly suitable for binding positively charged organic guests.[345] However, it should be stressed that the hydrophobic effects (i.e., the release of high-energy water from the CB[*n*] cavity) make a major contribution to the complexation driving energy and, in exceptional cases, neutral guests may bind with similar or higher affinities than their positively counterparts.[346−348]

Based on the previously mentioned recognition properties of CB[*n*]s, it was not surprising to verify that synthetic flavylium cations are efficiently complexed by CB7 (which has the appropriate cavity volume to include one flavylium guest) with binding constants varying between 10^5 and 10^7 M^{-1}. The stability of the complexes was found to depend on the position and nature of the substituents decorating the flavylium skeleton being more tightly bound to those comprising amino groups and the nonfunctionalized, more hydrophobic, B-ring.[331]

The effect of CB7 complexation on the pH-dependent stability of the flavylium cations was investigated for 7-hydroxyflavylium, 3′,4′,7-trihydroxyflavylium, and 3′,4′,7-trimethoxyflavylium.[329,330,337] In all cases, CB7 increased the stability of the colored flavylium at less acidic pH values, with the quite remarkable effect of 3′,4′,7-trimethoxyflavylium presumably due to the formation of a 2:1 host:guest complex. Interestingly, for compound 7-hydroxyflavylium, complexation with CB7 was demonstrated to not only stabilize the flavylium cation but also the quinoidal base at a neutral pH, which implies selectivity for this colored form over the colorless hemiketal and chalcones.

The possibility of using *trans*-chalcone-flavylium photoswitches to prepare light-responsive CB[*n*] complexes as initially proposed for compound 3′,4′,7-trihydroxyflavylium[329] was further explored to control the complexation of photochemically silent functional molecules (such as drugs) via competitive binding.[334] Memantine, a drug prescribed to Alzheimer's patients, was selected to demonstrate the proof of concept. With a binding constant of 2.5×10^4 M^{-1}, this value is high enough to preclude the competitive dissociation of the complex in the presence of *trans*-chalcone (3.0×10^2 M^{-1}) but is lower than that determined for flavylium cation **14** (9.0×10^5 M^{-1}), thus fulfilling the required conditions to observe competitive displacement of the drug upon irradiation (Scheme 45). Under the selected conditions (pD = 4.4), the memantine/CB7 complex cannot be dissociated by the *trans*-chalcone, but upon irradiation, the high affinity flavylium cation is efficiently generated, displacing the drug from the CB7 cavity by competitive binding.

Scheme 45. *trans*-Chalcone/Flavylium Photoswitch Was Used to Trigger the Release of a Photochemically Silent Drug from the CB7 Nanocontainer via Competitive Binding[a]

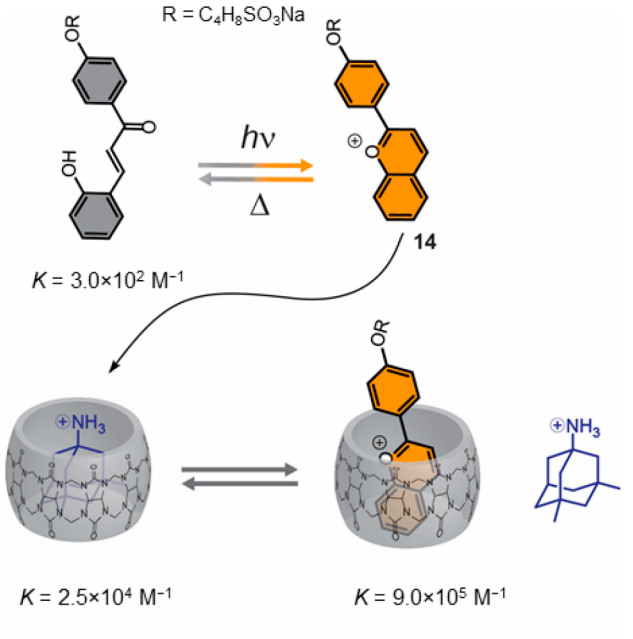

[a]Adapted with permission from ref 334. Copyright 2016, John Wiley & Sons.

Flavylium-based photoswitches behave as photobases (the formation of the cation consumes H^+) and require slightly acidic conditions to have thermodynamic access to the flavylium cation. Quantitatively, this property can be evaluated by determining the apparent pK_a of the photostationary state. Compounds such as **14**, which have high isomerization barriers, display a very slow thermal recovery by the *trans*-chalcone from the photostationary state. When the system is irradiated at a neutral pH, B and Cc are the major products and they can be converted into the flavylium cation by acidifying the solution after irradiation. Conversely, the system behaves as an AND molecular logic gate with H^+ (i.e., the output signal/function is only verified when both stimuli are simultaneously applied) and light serving as inputs.[349−351] While the output (i.e., the formation of the flavylium and consequent release of the drug molecule) of the two-input system described above does not depend on the order by which the stimuli are applied, systems that depend on the sequence of the applied stimuli are less common and more difficult to obtain. With this context in mind, a photoresponsive flavylium-based host−guest system that shows sequential logic was developed.[336]

This was achieved by using a chalcone-flavylium photoswitch with a lower thermal *cis*−*trans* isomerization barrier that upon photochemical excitation at neutral pH relaxes back quantitatively to the *trans*-chalcone, preventing the accumulation of hemiketal and *cis*-chalcone at the photostationary state. At lower pH values, however, the rate of the dehydration, which is accelerated by the $[H^+]$, becomes faster than that of the isomerization and the flavylium cation is efficiently formed. Due to these kinetic features, the positively charged product is only formed if the two inputs are applied in the correct order, first H^+ and then light.

The system was then coupled with a host−guest system. CB8 was selected due to its ability to simultaneously include two

https://doi.org/10.1021/acs.chemrev.1c00399
Chem. Rev. 2022, 122, 1416−1481

Scheme 46. pH and Light Sequence Dependent Generation of a Flavylium Cation and Its Induced Release of a Phe-Gly-Gly Tripeptide from its CB8 Complex by Competitive Binding[a]

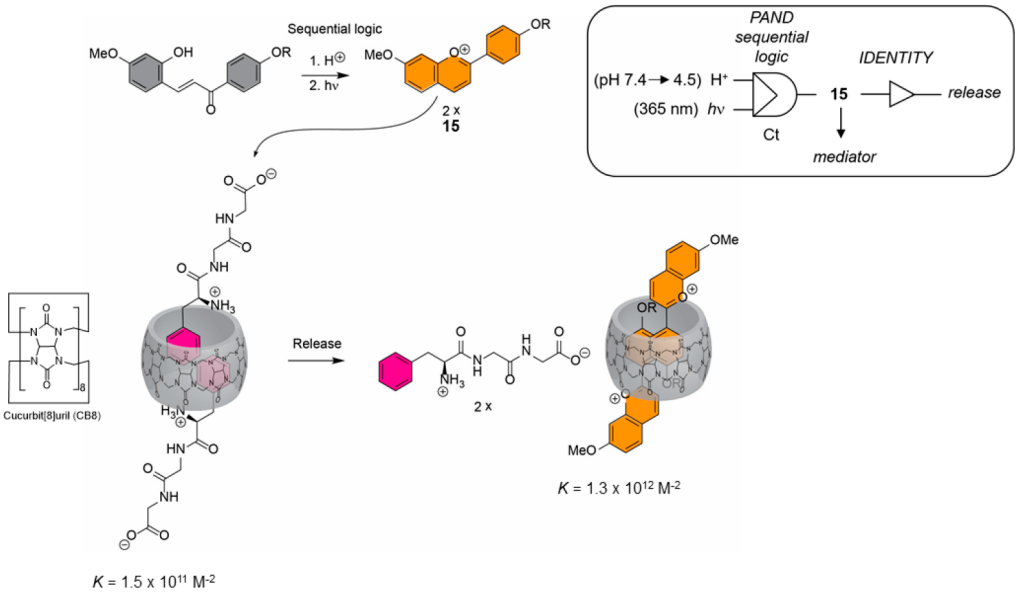

[a]Adapted with permission from ref 336. Copyright 2018, Royal Society of Chemistry.

Scheme 47. Application of Photoresponsive Host-Guest Complexes Based on *p*-Sulfonatocalix[4]arene and Flavylium Compounds to Release Photochemically Inactive Biological Guests from the Host by Competitive Binding[a]

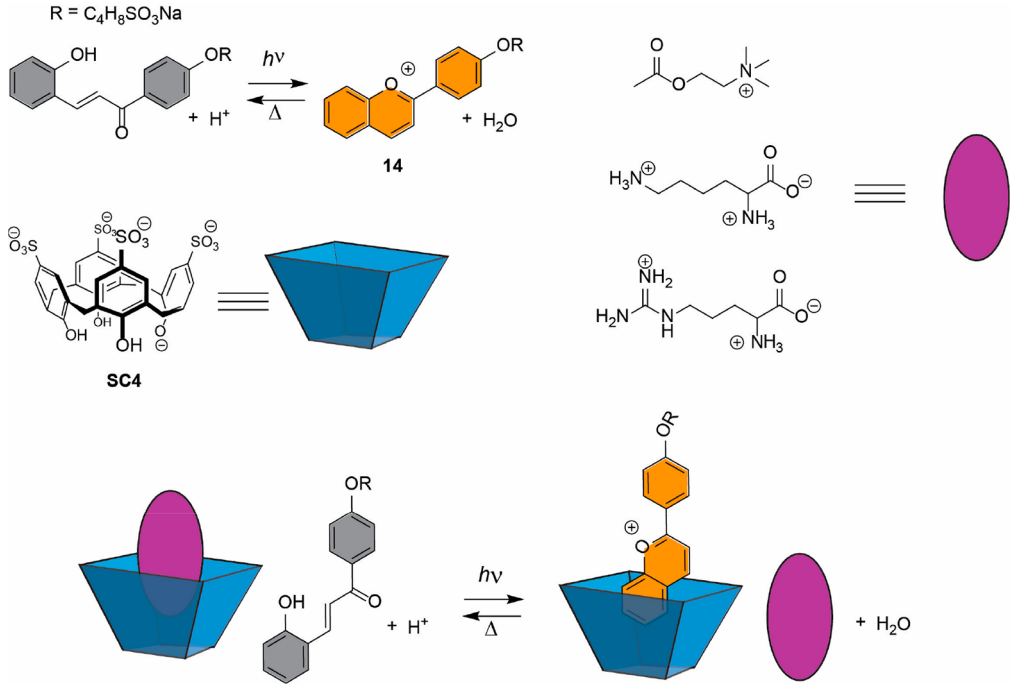

[a]Adapted with permission from ref 365. Copyright 2019, American Chemical Society.

guest molecules in its cavity. This feature has been explored in a variety of contexts, including supramolecular polymers, hydrogels, microcapsules, surface patterning and protein dimerization.[352−358] A Phe-Gly-Gly tripeptide was selected as a guest molecule owing to its cooperative 1:2 host:guest binding with CB8 (overall $K = 1.5 \times 10^{11}$ M^{-2}) and its relevance for protein recognition and dimerization.[358−360]

UV−vis absorption and fluorescence host−guest titrations of flavylium cation **15** with CB8 showed the cooperative encapsulation of two guests with $K = 1.3 \times 10^{12}$ M^{-2}. However, the *trans*-chalcone is only weakly complexed by CB8, satisfying the required conditions for the stimuli-responsive activation of an effective competitor under biologically relevant conditions. The operation of this system is summarized in Scheme 46, and, as in the case of the CB7:memantine complex, the release of the peptide after the correct sequence of the pH (7.4 → 4.5) and light (365 nm) was unequivocally demonstrated by simple ^{1}H NMR experiments.

https://doi.org/10.1021/acs.chemrev.1c00399
Chem. Rev. 2022, 122, 1416−1481

Scheme 48. pH-Gated Photoresponsive Pseudorotaxane[a]

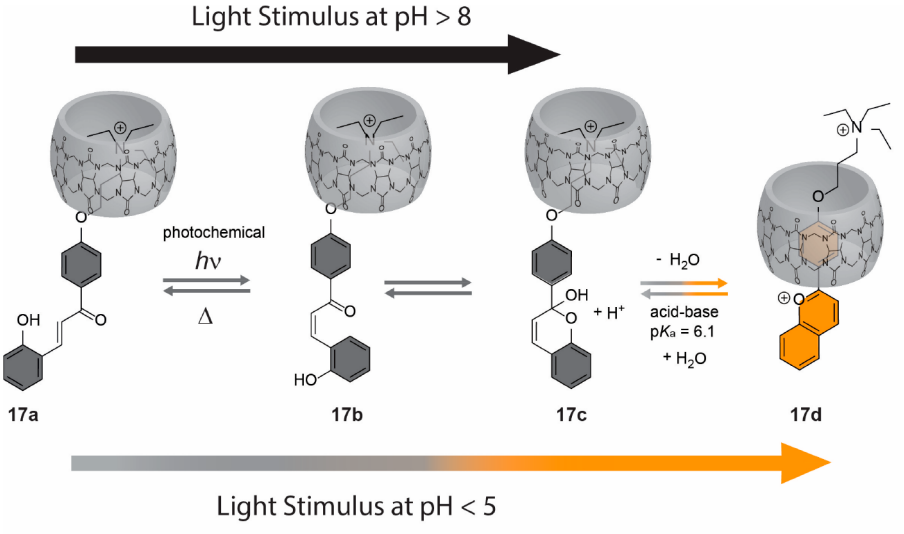

[a]Reprinted with permission from ref 338. Copyright 2018, Royal Society of Chemistry.

6.3. *p*-Sulfonatocalixarenes

p-Sulfonatocalix[*n*]arenes (SC[*n*]s) comprise a class of negatively charged macrocyclic host molecules that show high affinity and selectivity for cationic guests.[361] Due to their exceptional binding properties, water solubility, and low toxicity, these macrocyclic receptors have become important building blocks for developing host–guest systems with potential applications of biological and pharmaceutical intertest.[362−364] Similar to CB[*n*]s, SC[*n*]s have suitable properties for the selective binding of flavylium cations. This behavior was confirmed by Basílio and co-workers, who investigated the formation of host–guest complexes between a series of synthetic flavylium cations and SC4.[365] Using a combination of UV–vis absorption, fluorescence, and ^{1}H NMR techniques, the authors determined 1:1 association constants in the range of 6×10^3–1×10^5 M^{-1} for the binding of selected flavylium cations to the SC4 system at pH = 2. Compound **14** was investigated in more detail to demonstrate the potential of the system to devise photoresponsive host–guest complexes. The binding constant of the flavylium cation ($K = 3.5 \times 10^4$ M^{-1}) was found to be approximately 3 orders of magnitude higher than that found for the respective *trans*-chalcone species ($K = 40$ M^{-1}), which provided the required conditions for robust photoinduced complexation. The optimal conditions for operating the photoresponsive host–guest system required slightly acidic pH values (4.0), which allow for >95% conversion of the flavylium cation upon irradiation and the recovery of approximately 95% of the *trans*-chalcone in the dark at 70 °C. The photoresponsive host–guest system was also applied to regulate the complexation of photoinactive biologically relevant guests (acetylcholine, lysine, and arginine) by competitive binding using a similar strategy to that described above for CB7 (Scheme 47).

6.4. Flavylium-Based Rotaxanes

Rotaxanes and pseudorotaxanes, along with catenanes, are probably the most widely studied prototypes of molecular machines with great potential for advanced applications in nanotechnological devices.[366−368] Among the various structures that have been reported to date, stimuli-responsive bistable (pseudo)rotaxanes made from an axle molecule containing two recognition sites for macrocyclic wheel are particularly attractive owing to the possible controlling location of the wheel with external stimuli. These apparently simple molecular devices have found numerous potential applications in information processing, molecular muscles, catalysis, drug-delivery and sensing, to name a few.[369−374]

Flavylium compounds and CB[*n*], in particular, CB7, were demonstrated to be a successful combination for the development of stimuli-responsive bistable pseudorotaxanes.

The axle molecule **17** was designed to explore the photoresponsive properties of flavylium-based pseudorotaxanes (Scheme 48).[338] The triethylalkylammonium headgroup was carefully selected owing to the ability of CB7 to include this residue deep inside its cavity with high affinity. ^{1}H NMR experiments readily confirmed this binding mode for *trans*-chalcone **17a**. However, for flavylium cation **17d**, the phenyl group is included inside the cavity, exposing the tetraalkylammonium group to the bulk solution. This differential binding fulfilled the required conditions for stimulated shuttling movements upon irradiation.

As demonstrated by pH-dependent photochemical experiments, photoinduced CB7 shuttling from the tetralkylammonium binding site in **17a** to the phenyl site in **17d** is gated by the pH of the solution (Scheme 48). Conversely, at pH > 8, irradiation of the *trans*-species **17a** leads to the efficient formation of a *cis*-chalcone **17b**/hemiketal **19c** mixture that does not evolve to cation **17d**, and therefore, the CB7 wheel is not translocated. Notably, at pH < 5, flavylium cation **17d** is efficiently formed (through **17b** and **17c**), resulting in the translocation of the CB7 macrocycle. An apparent $pK_a = 6.1$ was determined for the pH-gated photoinduced translocation (i.e., **17d** formation), which matches the requirements for improved performance in slightly acidic yet biologically relevant conditions. These properties together with the strong fluorescence emission ($\Phi = 0.24$) of the flavylium pseudorotaxane offer appealing conditions for potential advanced biomedical applications.

In an attempt to devise multiresponsive pseudorotaxanes, another viologen-flavylium axle derivative was synthesized and was shown to form inclusion complexes with CB7.[335] Upon

https://doi.org/10.1021/acs.chemrev.1c00399
Chem. Rev. 2022, 122, 1416−1481

chalcone to flavylium interconversion, the CB7 molecule was again shown to translocate CB7 from the viologen to the flavylium unit. However, despite its redox and pH-responsive properties, the system showed poor photoinduced chalcone-to-flavylium interconversion in the reversible pH range.

7. INTERACTIONS WITH POLYMERS

The interactions between polymeric materials including biological and synthetic polymers and also inorganic matrixes, such as zeolites, clays, and mesoporous materials, and anthocyanins have been thoroughly investigated, primarily as a strategy to develop formulations that improve color by selective interactions with colored species of the flavylium multistate and that promote the thermal stability of this class of natural dyes against irreversible degradation.[375−385]

Among the different macromolecules, negatively charged polyelectrolytes have been shown to establish stronger interactions with the flavylium species, providing a potential approach to address color stabilization by increasing the pH domain of the colored cationic species.

The recognition of flavylium multistate compounds by proteins has also attracted considerable attention due to the potential of these biomacromolecules to impact their transport, stabilization, and sensory properties. Despite the considerable amounts of data published on this topic, detailed investigations at the molecular level are still scarce, and thus, the binding of flavylium multistate species and their effects on the flavylium network of reversible reactions are not well documented.[31] Moreover, the complexity of both flavylium multistate systems and biomacromolecules is helping to increase the challenge of in-depth characterizations on these systems. Unlike the copigmentation phenomena with small molecules, established characterization protocols for the interaction of biomacromolecules with flavylium compounds have not been implemented. This lack of information makes the comparison of reported data, which were obtained under a variety of conditions and using different techniques, less feasible and thus hampers a more generalized understanding of these systems.

7.1. Polysaccharides

Plant cell wall polysaccharides such as pectin have received considerable attention due to their potential to bind anthocyanins.[386] Studies on the interactions of two anthocyanins (cyanidin-3-*O*-glucoside and delphinidin-3-*O*-glucoside) with pectin from citrus fruits using NMR, UV−vis, and molecular dynamics simulation have suggested a moderate interaction between the hemiketal species at pH = 4 ($K = 4.0 \times 10^3$ and 5.5×10^3 M^{-1} for delphinidin-3-*O*-glucoside and cyanidin-3-*O*-glucoside, respectively) and the stronger binding of the flavylium cation under acidic conditions ($K = 5 \times 10^5$ M^{-1}).[387] Interestingly, for the latter species, and based on molecular dynamic simulations, it was suggested that the binding of multiple dye molecules to pectin promoted their alignment along the polymer backbone. These adducts can be stabilized by ion pairs, hydrogen bonds and dispersive dye-pectin interactions and by $\pi-\pi$ interactions between adjacent dye molecules.[387]

However, despite the higher affinity of the macromolecule for the flavylium cation, no changes were observed in the equilibrium constants of the flavylium reaction network in the presence of pectin. As suggested by Fernandes et al. and Dangles and Fenger, this unexpected behavior may eventually be assigned to the concentration effects used in the different experiments.[31,387] In order to fully clarify the (non)effect of pectin in the anthocyanin equilibrium constants, further systematic studies are probably required.

Four citrus pectic fractions were investigated to evaluate the effect of the type and degree of pectin esterification on its interactions with cyanidin-3-*O*-glucoside, using isothermal titration calorimetry (ITC) and nuclear magnetic resonance (NMR).[388] The ITC data obtained at pH 3.4 showed that the binding affinity is higher for the polysaccharides with a low degree of methyl esterification (K varies from 4.2×10^3 to 2.5×10^4 M^{-1}), while for polymers with a higher degree of methyl esterification values from $K = 6.2 \times 10^2$ to $K = 1.3 \times 10^3$ M^{-1} were reported. The results suggest that polymers with higher contents of free carboxyl groups display higher affinity as a result of possible ionic interactions with the positively charged flavylium. In all cases, both the entropy and enthalpy changes were favorable, given that the association process was mostly controlled by entropy, probably due to the desolvation phenomena associated with the hydrophobic effect and ionic interactions. ^{1}H NMR titrations retrieved binding constants comparable with those obtained by ITC and, importantly, provided further evidence that the flavylium cation is the primary species interacting with the pectin polymers. In a recent study, grape skin pectic polysaccharides were found to improve the thermal stability of malvidin-3-glucoside in model solutions at slightly acidic pH values. The authors concluded that the establishment of ion-pair complexes between cationic flavylium species and negatively charged galacturonic acid residues of pectin fractions is the primary driving force responsible for the interaction and consequent increased thermostability from 60 to 80 °C.[389]

Pectin polymers can also be explored to stabilize blue anthocyanin metal complexes. Kammerer et al. showed that anthocyanins carrying a catechol or pyrogallol moiety in the B-ring form complexes with metal ions present in pectins enriched with aluminum and ferric cations.[390] These blue-colored complexes are stabilized by pectic structures that prevent precipitation.

Other ionic polysaccharides such as chondroitin sulfate and dextran sulfate were also found to interact with the anthocyanins' flavylium cations, leading to hyperchromic effects under moderately acidic conditions.[391−393] The interaction of chondroitin sulfate with cyanidin-3-glucoside was shown to induce the formation of nanocomplexes (200−300 nm), which were suggested to contain stacks of cyanidin-3-glucoside within the aggregates (Scheme 49).[391] The formation of these nanostructured aggregates stabilized the anthocyanin flavylium and quinoidal species against degradation at pH values ranging from 3 to 12. Studies on ternary systems made from polyelectrolytes (chondroitin sulfate and chitosan), copigments, and anthocyanins showed synergistic effects for dye encapsulation, stabilization, and color quality, especially at pH values below 4.[394,395] The effects were attributed to the coencapsulation of anthocyanin and copigments within hydrophobic microenvironments provided by the polyelectrolyte capsules.

7.2. Lignin Derivatives

Lignosulfonates are polyelectrolytes obtained from natural polymers (lignins) after the sulfite pulping method and during the manufacture of paper, and they are primarily used in the food industry and in cosmetics as encapsulating agents. The formation of complexes between malvidin-3-*O*-glucoside and lignosulfonate polymers was studied by UV−vis and stopped

https://doi.org/10.1021/acs.chemrev.1c00399
Chem. Rev. 2022, 122, 1416−1481

Scheme 49. Chondroitin Sulfate-Induced Stacking of Cyanidin-3-glucoside and Its Hierarchical Aggregation into Nanocomplexes[a]

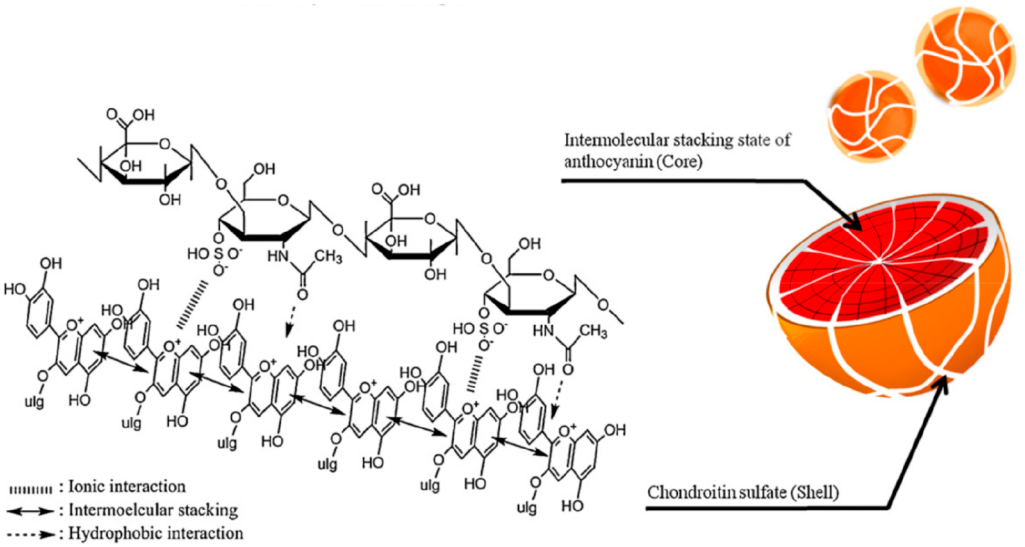

[a]Reprinted with permission from ref 391. Copyright 2012, Elsevier.

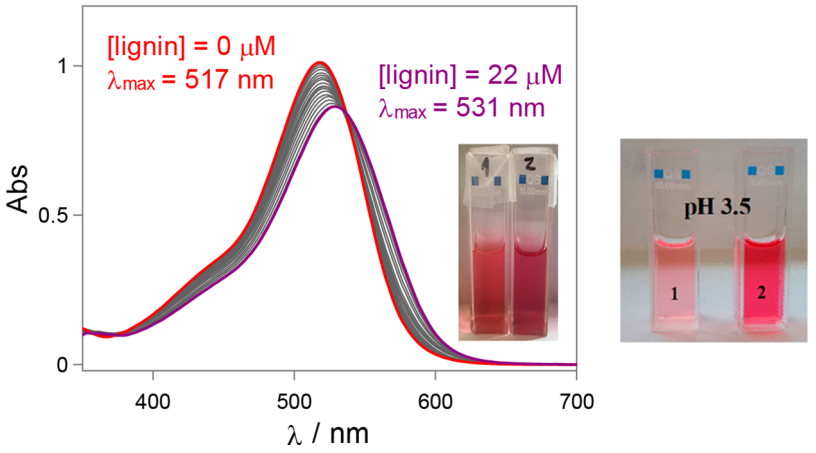

Figure 25. Absorption spectra of malvidin-3-*O*-glucoside with different concentrations of lignosulfonate at pH 1. Colors of the malvidin-3-*O*-glucoside solutions in the absence and presence of lignosulfonate at pH 1. Effect of lignin on the color of malvidin-3-*O*-glucoside at pH 3.5: (**1**) malvidin-3-*O*-glucoside (160 μM) and (**2**) malvidin-3-*O*-glucoside (160 μM) and lignin (58 μM). Adapted with permission from ref 396. Copyright 2018, American Chemical Society.

flow techniques. The addition of a lignosulfonate polymer to a solution of malvidin-3-*O*-glucoside at pH 1 produced spectral changes (red shift from 517 to 531 nm) that were used to obtain an apparent binding constant of $K = 1.6 \times 10^5\ M^{-1}$, indicating a strong interaction of the lignosulfonate macromolecule with the red flavylium cation. The thermodynamic and kinetic properties of the malvidin-3-*O*-glucoside network of chemical reactions was investigated in detail, showing that the pK_a, $pK^{\wedge}_a$, and pK'_a increased, leading to an extension of the pH domain of the red flavylium cation to higher pH values in the presence of this macromolecule and confirming the higher affinity of the negatively charged lignin to the cationic flavylium species (Figure 25).[396]

The interaction of pyranoanthocyanins, such as bluish portisins and pyranoanthocyanin dimers, with lignosulfonates was also investigated.[397] This study demonstrated that the lignosulfonates induce the cooperative stacking of the dye at lower macromolecule concentrations due to the binding of several dyes to adjacent binding sites. It should be stressed that the polyelectrolyte-induced dye stacking is cooperative given that the observed binding constant for the association of the second and third dyes molecules to the same binding site occurs with higher affinity than the first.

At higher polymer concentrations (and higher numbers of binding sites), this process becomes less likely to occur due to the reduced probability of binding two or more guest molecules to adjacent sites, leading to their redistribution over distant binding sites (Scheme 50). This process allows for color modulation and can significantly improve the water solubility and stability of the pigments over time (Figure 26).

7.3. Proteins

Peptides and proteins may also interact with anthocyanins. When studying the effect of aromatic amino acids (tryptophan, phenylalanine and tyrosine) and a polylysine, McClements and co-workers reported that the color of purple carrot anthocyanins is stabilized by these additives in model beverages containing citric acid and ascorbic acid at pH 3, with the higher effect

https://doi.org/10.1021/acs.chemrev.1c00399
Chem. Rev. 2022, 122, 1416−1481

Scheme 50. Proposed Mechanism for the Binding of a Portisin and Pyranoanthocyanin Dimer to Lignosulfonates[a]

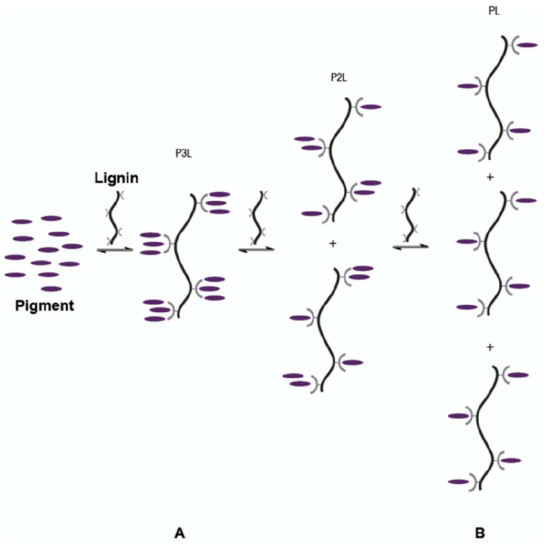

[a]Reprinted with permission from ref397. Copyright 2018, Elsevier.

observed in the case of tryptophan.[398] Dangles and Brouillard have determined an apparent binding constant of $K = 65\ M^{-1}$ for the interaction of this amino acid with malvin at pH = 3.5 which is both enthalpically and entropically favorable.[399] It should be also mentioned that in these studies no copigmentation interactions for phenylalanine and tyrosine with anthocyanin were observed.

Carrier proteins such as human serum albumin (HSA), which is the most abundant protein in the plasma, may affect the transport of endogenous and exogenous ligands to tissues and their distribution into cells.[400] HSA is a 585-residue single polypeptide chain protein consisting of three α-helical domains numbered I–III, each of which contains two subdomains, A and B. Based on crystal structure analysis, it has been proposed that the primary HSA binding sites are in the hydrophobic cavities in subdomains IIA and IIIA.[401] The important role of this polypeptide as a ligand carrier in plasma has attracted the attention of different research groups that are investigating the binding of anthocyanins and other polyphenols with HSA.[402−406] Using fluorescence techniques, Gordon and Cahyana investigated the effect of the pH and the anthocyanin structure on the binding affinity toward HSA.[403] Four anthocyanidins (pelargonidin, cyanidin, delphinidin, and malvidin) and pelargonidin-3-glucoside were selected to investigate the associated phenomena by fluorescence spectroscopy over a pH range of 4–7.4. The authors reported a moderate variation in the association constants from $K = 1.1 \times 10^5$ to $K = 1.3 \times 10^6\ M^{-1}$ depending on the anthocyanin structure, pH, and temperature, which suggests that HSA binds all the ligands with comparable affinity levels. The binding affinities were observed to be generally higher at pH = 4 and were almost constant from 5 to 7.4. This trend can be attributed, on the one hand, to the appearance of higher fractions of quinoidal and ionized quinoidal bases at higher pH values and, on the other hand, to the increased hydrophobic character of HSA at pH = 4 (which is below the isoelectric point). This interpretation is supported by the fact that, at pH = 4, the binding affinity of the different ligands was observed to increase as their polarity decreases. By contrast, at pH = 7.4, the electrostatic interactions became more important and the aglycones tended to bind strongly to the HSA as the number of hydroxyl groups in the B ring increased. The same results were observed for the pelargonidin-3-glucoside, which also has a higher affinity for HSA than its aglycone counterpart at this pH. These results are consistent with those reported by Tang et al., who also observed an increase in the binding affinity with the number of hydroxyl groups in the B-ring at pH 7.4 for anthocyanin-3-glucosides.[406] These authors also performed site-specific competitive experiments to demonstrate that these anthocyanins primarily bind to subdomain IIA (site 1).

The binding of synthetic 3-deoxyflavylium compounds with HSA has also been addressed. Dangles and co-workers observed that the *trans*-chalcones bind with slightly higher affinities to HSA than their respective quinoidal bases. Fluorescence titrations suggested that these compounds bind to or near subdomain IIA with association constants in the $K = 1.8 \times 10^4$–$3.4 \times 10^5\ M^{-1}$ range.[407]

Cyanidin-3-*O*-glucoside was used as a representative anthocyanin to investigate the binding properties of this class of compounds with three proteins, bovine serum albumin (BSA), hemoglobin (Hb), and myoglobin (Mb).[408] The binding constants were obtained by fluorescence titrations, with values ranging from $K = 8 \times 10^3$ to $7 \times 10^4\ M^{-1}$ at 298 K and pH = 7.4. BSA and Mb displayed similar affinities for the anthocyanin, while Hb had approximately 1 order of magnitude weaker affinity. The authors also used different spectroscopic techniques to observe evidence of alteration in the secondary structure of the proteins upon binding.

Milk proteins, such as β-lactoglobulin (β-Lg), the most abundant protein in whey protein, have also attracted attention as potential targets that bind anthocyanins. Cyanidin-3-*O*-glucoside binds to β-Lg with $K = 3.1 \times 10^4\ M^{-1}$ by an entropy-driven process mediated by hydrophobic effect. The apparent structure-dependent binding affinity of β-Lg toward anthocya-

Figure 26. Colors of portisin solutions at different concentrations in the absence (a) and presence (b) of lignin 19 μM; colors of pyranoanthocyanin dimer solutions at different concentrations in the absence (c) and presence (d) of lignin 19 μM in citrate buffer at pH 3.5 after 30 days in the dark. Reprinted with permission from ref 397. Copyright 2018, Elsevier.

https://doi.org/10.1021/acs.chemrev.1c00399
Chem. Rev. 2022, 122, 1416–1481

nin 3-*O*-glucosides seems to suggest that, unlike HSA, this protein is highly selective.[409] This binding causes structural alterations in the protein, increasing β-sheets while reducing α-helixes. Malvidin-3-*O*-glucoside also binds to β-Lg but with a much weaker affinity of $K = 6.7 \times 10^2$ M^{-1}. Nevertheless, it would be desirable to confirm and further explore this surprising binding selective by more accurate techniques such as ITC.[410] Despite its low affinity, the complexation of β-Lg was shown to improve the thermal- and photostability of the dye. A more recent study reported endothermic, entropy-driven interactions of β-Lg with delphinidin-3-*O*-glucoside with a $K = 2.2 \times 10^6$ M^{-1}, which also imposed variations on the secondary structure of the protein. The structure-dependent binding affinity of β-Lg toward anthocyanin 3-*O*-glucosides suggests that, unlike HSA, this protein is highly selective.[411]

Caseins are the primary proteins found in bovine milk, and they are important food sources of amino acids, carbohydrates, calcium, and phosphorus. The binding properties of α- and β-casein toward malvidin-3-*O*-glucoside were investigated at pH 6.3 by Chen and co-workers, who showed that anthocyanin binds with a similar affinity to both proteins ($K = 5 \times 10^2$ M^{-1} at 297 K).[412] Nevertheless, although the binding affinity was similar for the two proteins, the association of malvidin-3-*O*-glucoside with α-casein was enthalpy-driven, while in the case of β-casein the binding was endothermic and therefore entropy-driven. The presence of casein was also found to improve the stability of the dye. Bouhallab and co-workers analyzed the effects of ionic strength and pH on the interaction of cyanidin-3-*O*-glucoside with sodium caseinate.[413] This class of proteins is present as soluble, self-assembled loose micelle-like aggregates of different unfolded caseins (α-, β-, and κ-casein variants in a 5:4:1 proportion) stabilized by weak noncovalent interactions and the hydrophobic effect.".[414] The formation of complexes between cyanidin-3-*O*-glucoside and sodium caseinate was evidenced by fluorescence and dynamic light scattering experiments at pH 2 and 7. For both pH values, two sets of binding sites were observed, with the first binding constant being 5-fold higher at pH 7 ($K_1 = 5 \times 10^6$ M^{-1} vs $K_1 = 1 \times 10^6$ M^{-1} at pH = 2) and the second binding constant being independent of the pH ($K_2 = 3 \times 10^5$ M^{-1}). The association process was found to be enthalpy-driven at a neutral pH, while at an acidic pH it is entropy-driven. It was also observed that, at pH = 7, the binding interactions were weakened by adding NaCl, while under acidic conditions the affinity remained practically unaffected by the ionic strength. The authors suggested that hydrophobic effects may be dominant at lower pH values, while at a neutral pH electrostatic interactions are more important. However, considering the complexity of the system, the authors acknowledged that an accurate interpretation of the binding parameters would require further studies. Unfortunately, most of these works largely ignore the structural transformations of anthocyanins as a function of pH (or even the chemical degradation of their aglycones under the conditions used) and do not specify the impact of the proteins on the color.

In addition to color, anthocyanins and their derivatives are thought to influence other sensory properties in foods, such as bitterness and astringency sensations. Astringency is said to be due to the interaction of polyphenols with salivary proteins in the oral cavity, particularly in proline-rich proteins (PRPs).[415] These sensory phenomena have motivated investigations on the recognition properties of PRPs toward anthocyanins at a molecular level through different techniques, such as saturation transfer difference NMR, fluorescence quenching, mass spectrometry, and HPLC.[416−418] Acid PRP (aPRP), for which the N-terminal domain is dominated by negatively charged amino acids, was found to recognize both the hemiketal ($K = 5.2 \times 10^2$ M^{-1}) and the flavylium ($K = 5.5 \times 10^2$ M^{-1}) forms of malvidin-3-glucoside with similar affinity levels.[416] Moreover, the simultaneous presence of malvidin-3-glucoside and epicatechin was observed to display synergism in their interactions with salivary proteins, in particular, with aPRPs.[417] Pyranoanthocyanins were also observed to interact with aPRP.[419] Unlike common anthocyanins, these dyes are primarily present in their colored flavylium and quinoidal base forms. At pH = 3, pyranomalvidin-3-glucoside showed a moderate binding constant for aPRP ($K = 5.74 \times 10^2$ M^{-1}) that increased for the pyranomalvidin-3-glucoside-epicatechin ($K = 1.15 \times 10^3$ M^{-1}) due to the presence of the flavanol unit. Regarding bitterness, using a model based on taste receptors expressed individually in HEK293T cells, Soares and co-workers have shown that malvidin-3-glucoside interacts specifically with the receptor TAS2R7 (from 25 existing human receptors), showing an EC_{50} = 12.6 mM. Because these experiments were performed at pH 7.4, the predominant species were the hemiketal and quinoidal base. However, the available data regarding the interactions of anthocyanin compounds with salivary proteins is still very scarce, and further research is still needed.

7.4. Dendrimers

Dendrimers are synthetic treelike macromolecules composed of repetitive layers of branching units that emerge from a central core. Their large functional surface, globular architecture at the nanometer scale, and inherent multivalency make them ideal candidates for a wide range of applications, from bio- and nanotechnology to catalysis and materials science.[420,421]

Despite the great potential of dendrimer applications for the color and chemical stability of anthocyanins, these studies are scarce in the literature. Only a recent study reported the use of silica-PAMAM dendrimer nanoparticles to encapsulate anthocyanins and to evaluate their antiproliferative activity against neuroblastoma (Neuro 2A).[422]

The interaction between a gallic acid triethylene glycol based polyanionic dendrimer decorated with 162 sulfate groups with cyanidin-3-glucoside and malvidin-3-glucoside was investigated by UV−vis, stopped-flow, and NMR techniques. The study concluded that the dendrimer established stronger interactions with cyanidin-3-glucoside and exerted a strong stabilization effect on its color, increasing the pH domain of the flavylium cation by approximately one pH unit.[423] It was verified that the red flavylium cation is strongly shielded by the host due to the formation of ionic pairs, indicating the binding of approximately two anthocyanin molecules by each sulfate group ($n \sim 295$) and with an association constant of $K \sim 700$ M^{-1} per binding site, which implies an effective binding constant of $nK = 2.1 \times 10^5$ M^{-1} (Figure 27).[423] It is worth noting that the apparent binding constant is comparable with the one obtained for the lignosulfonate polymer consisting of approximately 200 sulfonate groups per molecule. This is a value that underlines the efficiency of multivalent ionic interactions in the stabilization of cationic dyes.

The studies reported in the literature on the interactions between anthocyanins and related compounds with polymers have assisted in the development of pH-responsive materials (films, membranes, and nanoparticles) for food packaging applications. In recent years, several studies have reported the

https://doi.org/10.1021/acs.chemrev.1c00399
Chem. Rev. 2022, 122, 1416−1481

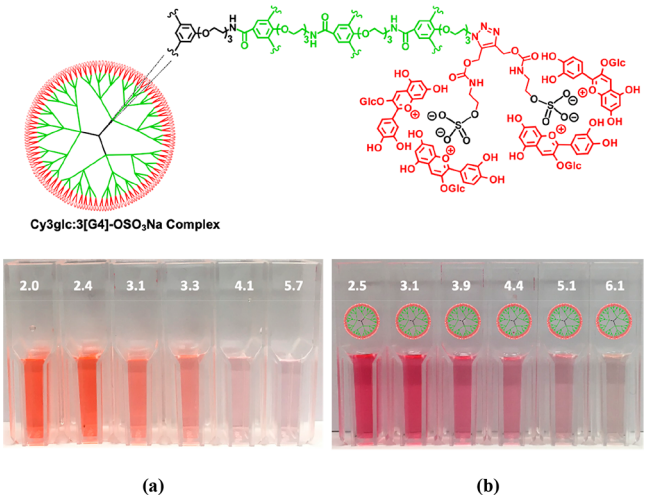

Figure 27. Effects of dendrimers on the color of cyanidin-3-glucoside at different pH values: (a) cyanidin-3-glucoside (19.8 μM) and (b) cyanidin-3-glucoside (19.8 μM) and dendrimer (26 μM). Adapted with permission from ref 423. Copyright 2019, John Wiley & Sons.

use of anthocyanin-rich plant extracts for developing colorimetric smart films for food-packaging applications such as pH and temperature indicators (sensors) for monitoring food freshness and spoilage at early stages. These approaches include the immobilization/encapsulation of anthocyanin-rich plant extracts (e.g., red cabbage, purple sweet potatoes, tomato) in biocompatible polymers (chitosan, pectin, starch, cellulose, and agar) to monitor color variations in food products, especially milk, fish, seafood, and meat.[424−435]

8. DEGRADATION OF ANTHOCYANINS AND RELATED COMPOUNDS

In anthocyanins and related multistate compounds, it is necessary to distinguish between (i) reversible reactions that take place upon exposure to external stimuli such as pH and light; (ii) irreversible reactivity with other compounds, for example, those present in food matrixes such as wine, which in most cases lead to the production of other compounds in which the benzopyrylium group is still present; and (iii) irreversible decomposition reactions (related to storage stability) that break the molecule into fragments. Item (i) was discussed in sections 3 and 4 of this Review, item (ii) was discussed in section 2, and some of this information was recently reviewed.[31] In this section, we focus on item (iii). The clear distinction between reversible (water addition) and irreversible (autoxidation) components of color loss, especially around neutrality when both processes contribute to fading, was recently reported for red cabbage anthocyanins.[436]

The mechanisms involved in the anthocyanin degradation that occurs in biological systems "in vivo" or in solution "in vitro" are different, because in plants active enzyme-driven breakdown processes are involved, as also reviewed in this section. In both cases, oxygen and its reduced species play a crucial role and will be reviewed in this section.

8.1. Factors that Affect Anthocyanin Degradation in Solution

The term "stabilization" as used in anthocyanin's literature can have two different meanings, leading to possible misunderstandings: (i) resistance to hydration, which means the extension of the pH domain of the flavylium cation and quinoidal base (and its anionic form) when the bases are accompanied by an increase in their color expression; (ii) decrease of degradation in relation to their storage stability.[202] There is a large number of studies in the literature that highlight the influence of structural factors on the radical scavenging activity of anthocyanins but only a few that relate their chemical stability and degradation with structural features. Scheme 51 summarizes the mains products identified resulting from the oxidative breakage of the anthocyanin structure.

The nature of the substituents in position 3 of the flavylium cation has long been associated with degradation.[203] In fact, the decomposition rate decreases dramatically from anthocyanidins to anthocyanins and 3-deoxyanthocyanidins.[202] Moreover, early studies concluded that anthocyanins with a higher hydroxylation degree are less stable while those with a higher methoxylation degree increase the storage stability.[202]

Scheme 51. Summary of the Degradation Products of Anthocyanins[437−439a]

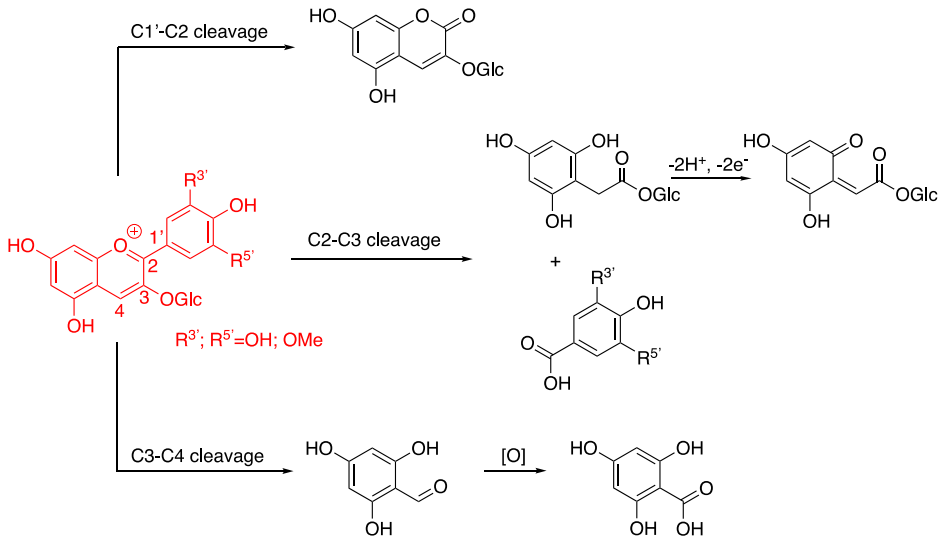

[a]Adapted with permission from ref 31 Copyright 2018, MDPI.

https://doi.org/10.1021/acs.chemrev.1c00399
Chem. Rev. 2022, 122, 1416−1481

The stability of 3-deoxyanthocyanidins has been less studied. Some of the studies on this subject associate the stability of 3-deoxyanthocyanidins with the extended pH domain of the flavylium cation and not to its degradation processes. A study on the effect of storage time and temperature on phenolic compounds of sorghum grain and flour (including the 3-deoxyanthocyanidins luteolinidin and apigeninidin) showed that the color of the samples remained stable for 120 days.[440]

The thermodynamics and kinetics of cyanidin (aglycone) were studied by direct and reverse pH jumps.[441] The pH dependence of the flavylium cation decomposition follows a bell-shaped curve, without reversibility, as shown in Figure 28a

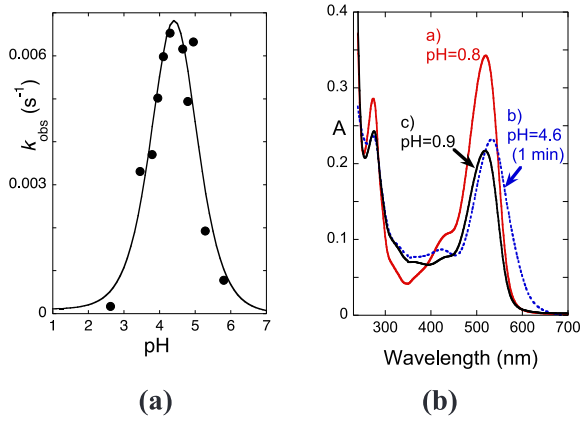

Figure 28. (a) pH dependence of the cyanidin flavylium rate constants decomposition after a direct pH jump and (b) sequence of pH jumps: initial solution of cyanidin at pH 0.8 (a) red, followed by a direct pH jump to pH 4.6 (b) blue; after a delay of 1 min at this pH, a reverse jump back to pH = 0.9 (c) black. Only 63% of the flavylium absorption was recovered. In the case of a delay of 20 min at pH = 4.6 before the reverse pH jump, only a small fraction of flavylium absorption was recovered. Adapted with permission from ref 441. Copyright 2014, Royal Society of Chemistry.

and Scheme 52. In the ascending branch of the bell-shaped curve, the increase in the decomposition rate can be explained by the increase in the chalcone availability to decompose. The decreasing branch of this curve results from the fact that the rate of the hydration reaction decreases with increasing pH. This branch of the curve is controlled by the hydration reaction that retards the formation of Cc and Ct. Even if the degradation of the chalcones is very fast, it is not faster than the rate of the hydration reaction. In kinetic terms, it is similar to the bell-shaped curve already described in section 3 but, instead of the pH-reversible isomerization, is a nonreversible kinetics leading to the fragmentation of the chalcone, as shown in Scheme 52.

The confirmation of the fast degradation rate is given in Figure 28b. The following sequence of direct and reverse pH jumps was performed: (i) a direct pH jump from a solution of cyanidin at pH = 0.8 to pH = 4.6, (ii) remaining at this pH for 1 min (delay), (iii) followed by a reverse pH jump back to the same (or very close) pH. In the experiment shown in Figure 28b, only 63% of the flavylium cation was recovered. In an identical experiment with a 20 min delay at pH = 4.6, practically no flavylium recovery was observed.

The degradation of cyanidin at pH = 2.8 is much slower and the respective kinetics can be followed by HPLC, as shown in Figure 29a. The flavylium cation disappears, giving rise to the

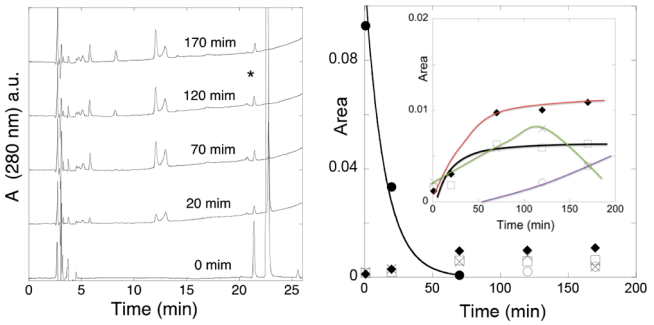

Figure 29. (a) HPLC chromatograms extracted at 280 nm showing peaks separated from cyanidin solutions at pH = 2.25 as a function of time: 3,4-dihydroxybenzoic acid (5.8 min); 2,4,6-trihydroxybenzoic acid (8.2 min); 2,4,6-trihydroxybenzaldehyde (12.1 min); hemiketal/*cis*-chalcone (13.0 min); cyanidin (22.7 min). (b) Representation of peak areas of network and degradation products of cyanidin as a function of time at pH 2.25: (●) cyanidin; (◆) 2,4,6-trihydroxybenzaldehyde (red curve); (×) chalcone (green curve); (□) 3,4-dihydroxybenzoic acid (black curve); and (○) 2,4,6-trihydroxybenzoic acid (black curve). Asterisk (*) indicates impurity. Reprinted with permission from ref 441. Copyright 2014, Royal Society of Chemistry.

chalcone and some degradation products. Indeed it was observed the formation of 3,4-dihydroxybenzoic acid from

Scheme 52. Kinetic Scheme to Explain the Decomposition of Cyanidin (Aglycone) after Direct pH Jumps[441]

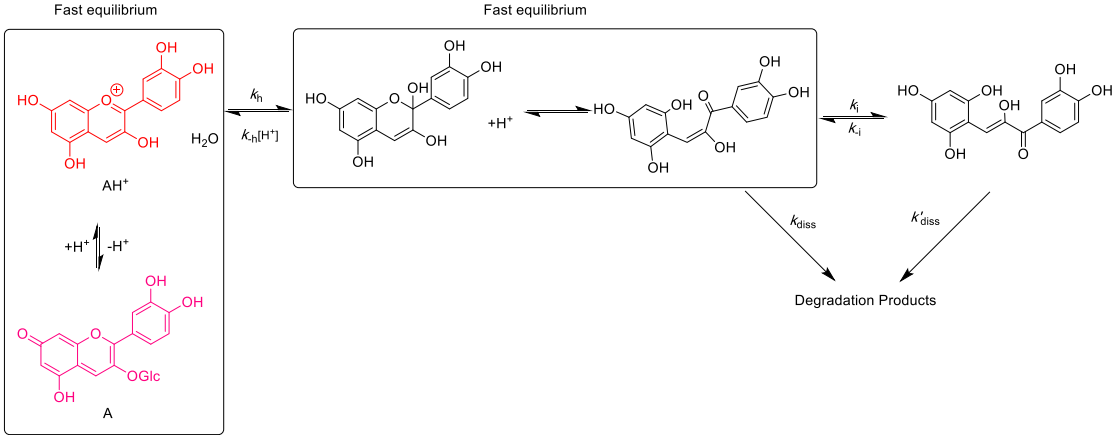

https://doi.org/10.1021/acs.chemrev.1c00399
Chem. Rev. 2022, 122, 1416−1481

Scheme 53. Mechanism Proposed to Account for the Degradation of Anthocyanins

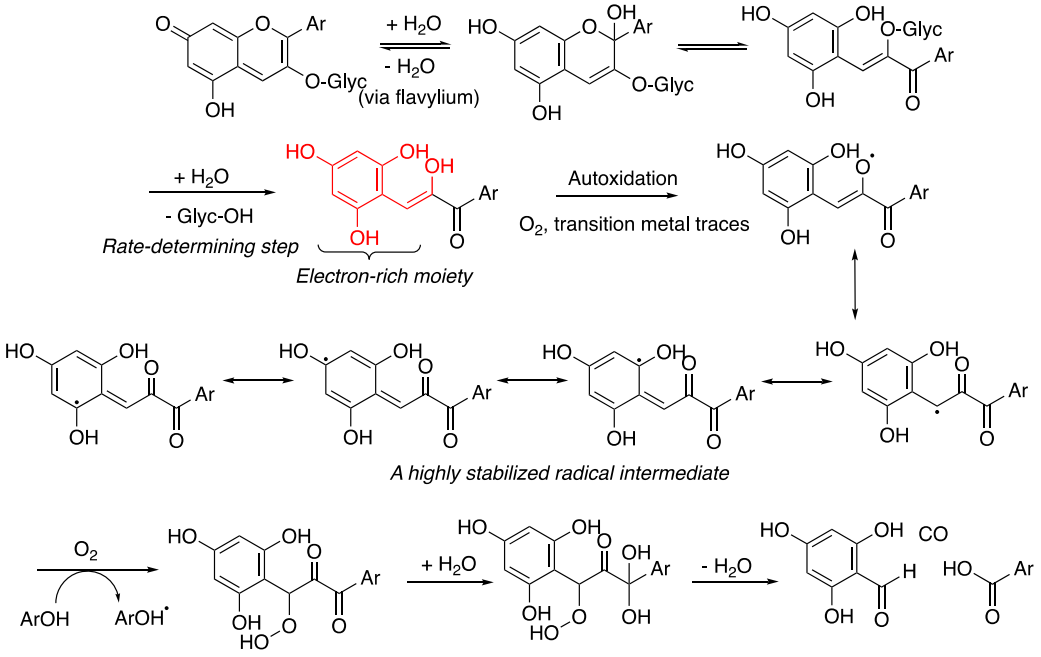

Scheme 54. Acylated Anthocyanins Extracted from Red Cabbage[444a]

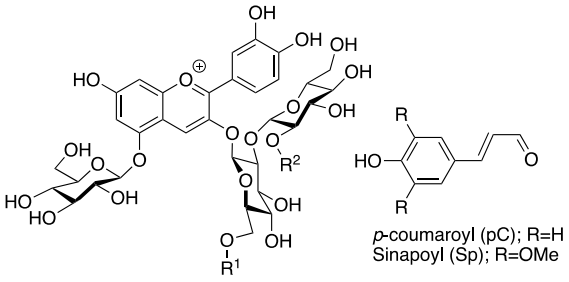

Pigment	R^1	R^2
PA	H	H
PB	H	Sp
P1	pC	H
P4	pC	Sp

[a]pC, *p*-Coumaric acid residue; Sp, sinapic acid residue, Fl, ferulic acid residue.

ring B and 2,4,6-trihydroxybenzaldehyde from ring A, together with 2,4,6-trihydroxybenzoic acid from the oxidation of the respective benzaldehyde during a second stage, consistent with previous results and shown in Figure 29b.[442] Noteworthy, the thermal degradation pattern (the products, not the respective rate) of other anthocyanidins (aglycone) pelargonidin, cyanidin, delphinidin, and malvidin at room temperature and under acidic to moderately acidic conditions is similar.[442]

As previously mentioned, under physiological conditions (pH = 7.4, 37 °C), anthocyanidins degrade to phenolic acids and aldehydes at much higher rates than their glucoside counterparts, especially those with a higher level of B-ring hydroxylation.[443] That mechanisms involved are probably different especially if the glucose moiety is still linked to the structure. A possible explanation for the degradation of anthocyanins at acidic pH is shown in Scheme 53 involving two main steps: (i) hydrolysis promoting deglycosylation of position 3 (rate-determing step) and (ii) autoxidation and degradation (breakage) of the electron-rich chalcone aglycone form.

Regarding acylated anthocyanins, acylation extends the pH domain of the colored species, stabilizing the color, (see section 4.4 of this Review) but some studies stressed that acylation also increases the thermal degradation rate, in particular, at higher pH values.[240,436] This apparent paradox was highlighted by Dangles and co-workers in an extensive study about the color stability and degradation of acylated anthocyanins of red cabbage (Scheme 54).[444]

These authors have followed the kinetics of color loss of these pigments at pH = 7 (50 °C) for 8 h and have observed that the color stability increases with acylation. However, by measuring the red flavylium ion resulting from the fast conversion of all reversible forms (except *trans*-chalcones) by reverse pH jump back to pH = 1.0−1.5, they observed a higher irreversible degradation of the acylated anthocyanins compared to anthocyanins nonacylated (PA). After 24 h, the percentage of residual flavylium cation lies within a range from 40 to 60% and is mostly independent of the acylation pattern. The degradation products consisted of new pigments (isomers, deacylation, and intramolecular acyl transfer) and products from the oxidative degradation. At intermediate and advanced thermal degradation, oxidative mechanisms led to degradation products; some of them shown in Schemes 51 and 53.

It should be mentioned that acylated anthocyanins around the neutral pH have a high molar fraction of quinoidal base and its anionic quinoidal base at the equilibrium, which are probably more prone to degradation. While it is well-known after the work of Brouillard and Dubois[184] that the quinoidal base does not hydrate in moderately acidic medium, it has also reported that in

https://doi.org/10.1021/acs.chemrev.1c00399
Chem. Rev. 2022, 122, 1416−1481

basic medium the anionic bases react very rapidly with OH^- to give *trans*-chalcone and other final products.[445] As far as we know, this has never been proved for anthocyanins due to their high instability at basic conditions, but it was reported for other flavylium compounds such as 4′-aminoflavylium and 7-(*N*,*N*-diethylamino)-4′-hydroxyflavylium after direct pH jumps to the basic region followed by stopped-flow (Figure 30).[446,447]

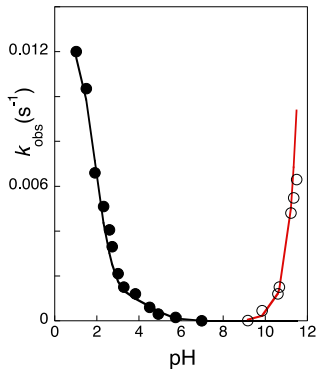

Figure 30. Apparent rate constant of color loss after a pH jump for the 7-(*N*,*N*-diethylamino)-4′-hydroxyflavylium ion followed by stopped-flow: Reverse pH jumps (●); direct pH jumps (○). The degradation in basic medium is expected to occur for the chalcones. Adapted with permission from ref 179. Copyright 1997, American Chemical Society.

Representation of the observed rate constant as a function of pH shows at lower pHs a decrease of the rate as expected from eq 5 (section 3), followed at higher pH by a monoexponential rise directly proportional to $[OH^-]$. In basic medium, the pseudoequilibrium and equilibrium species were identified as *cis*- and *trans*-chalcones or their deprotonated forms, depending on the final pH. In consequence, degradation in basic medium is expected to occur for the chalcones.[179]

Also, the stability of the flavylium multistate species increases dramatically upon *O*-glycosylation or *O*-methylation of anthocyanidins at position 3. The former strategy (with glucose or other sugars) is used by nature to confer stability to anthocyanins at slightly acidic or neutral pH values. It is noteworthy that the isolation and characterization of two 3-*O*-methylated anthocyanins from mauve flowers of *Erlangea tomentosa* (*Bothriocline longipes*) was achieved by Andersen and co-workers,[448] as shown in Scheme 55. No detailed

Scheme 55. Two Erlangidin Derivatives Reported by Andersen and Co-workers[448]

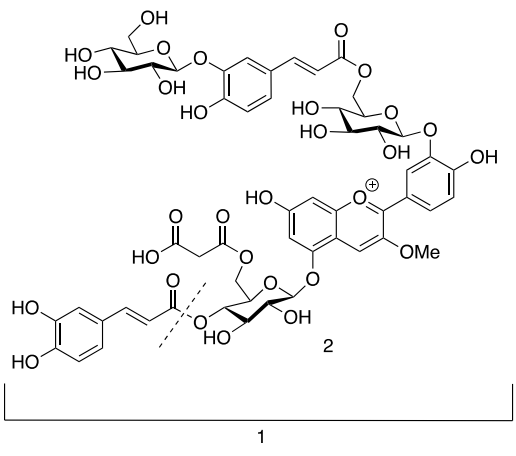

information is given regarding the stability of this anthocyanin, but during extraction, isolation and storage in acidified methanolic solvents both anthocyanins were partly converted to their demalonylated and methylmalonyl esterified forms.

The stability of cyanidin, its 3-*O*-glucoside derivative, and the model compound 3-*O*-methylcyanidin was studied by Yoshida and co-workers.[438] In aqueous solution at pH = 1.0, the percentages of flavylium cation of these three species after 20 days in the dark were 5%, 90%, and 97%, respectively.

Thermogravimetric analysis of cyanidin-3-glucoside has shown that the first step toward the decomposition of the anthocyanin, which occurred from 30 to 200 °C, corresponds to the cleavage of the glucose yielding the aglycone.[449]

The results reported above have been corroborated by other studies regarding the degradation of anthocyanins at high temperatures (from 60 to 95 °C).[450,451,451−453] In summary, the rates of these degradations are monoexponential, with lifetimes ranging from approximately 1 to 5 h. The degradation rate increases with the increase of temperature and pH (up to pH = 6).

In general, liquid-phase reactions of organic substances with molecular oxygen have been reported to usually proceed by a free radical chain mechanism.[454] These oxidations are of autocatalytic nature and are known as autoxidations.[455]

In argon atmosphere, the degradation rate of anthocyanins is reduced, showing that O_2 contributes to this process.[436] In spite of the experimental difficulties to calculate the standard redox potentials of anthocyanins, the data available in the literature[456] strongly suggests that the one electron oxidation to form superoxide is unlikely to occur with anthocyanins.

These kinetic limitations are overcome when catalysts, for example, iron and copper ions or enzymes, are present.[31,457] While the preliminary formation of H_2O_2 in the absence of catalysts remains unclear,[31] the oxidation by H_2O_2 and the role of O_2 and Fe^{2+} in the degradation mechanisms have been discussed.[31,457]

It is common to find iron and copper ions in substantial concentrations in biological material such as plants and foods, free or bound to proteins. Thus, it is worth mentioning the role of these transition metal ions in the oxidative processes involving micronutrients such as phenols. In the case of substituted catechols, Nkhili and co-workers found experimental quantitative evidence for the formation of a metal complex involving catechol, Fe^{2+}, or Cu^+ and dioxygen at pH = 7.4.[458] It was shown that plant phenols are more easily oxidized with the concomitant formation of H_2O_2 when bound to copper than to iron. Two different electron transfer mechanisms are proposed: In the case of Fe^{2+}, the electron transfer takes place from the metal to the O_2 leading to hydrogen peroxide and the catechol complex with Fe^{3+}; for Cu^+-induced autoxidation, the electron transfer occurs from the organic compound to O_2 mediated by Cu^+ leading to hydrogen peroxide and a complex mixture of oligomers.

Alongside the direct oxidation of phenolics in metal-catalyzed oxidation, hydrogen peroxide has been described to have an important role in the direct chemical degradation of polyphenols.

The oxidation of cyanidin-3-*O*-glucoside by hydrogen peroxide was investigated in a range of solvents. A plausible oxidation mechanism was proposed based on the resulting reaction products, and this mechanism was confirmed by HPLC-MS experiments using ^{18}O-labeled reagents, as shown in Scheme 56.[457]

https://doi.org/10.1021/acs.chemrev.1c00399
Chem. Rev. 2022, 122, 1416−1481

Scheme 56. Proposed Oxidation Mechanism of Cyanidin-3-glucoside by H_2O_2[a]

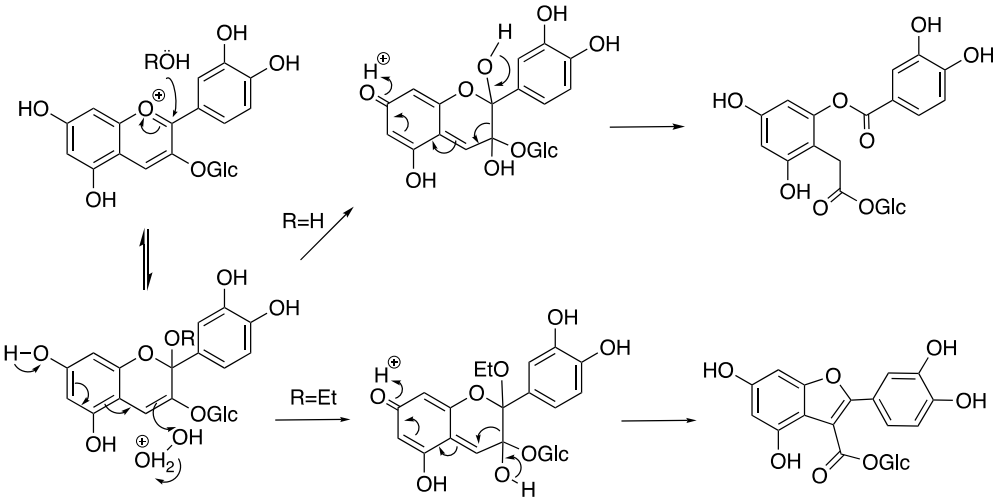

[a]Adapted with permission from ref 457. Copyright 2018, Elsevier.

It is noteworthy that, in water, the reactive species is the hemiketal, which could explain the experimentally observed increase of the degradation rate as the pH increases in the pH range of the pK'_a. The mono-oxygenation of the hemiketal (electrophilic addition of H_2O_2) occurs at the 3-position owing to an electron donation from the phenolic hydroxyl group at the 7-position of the A-ring.

The putative role of H_2O_2 in the formation of a quinone methide derivative resulting from the oxidative degradation of maldivin-3-*O*-glucoside under acidic conditions was also observed in a wine model solution stored at 90 and 25 °C (see in Scheme 51, C2−C3 cleavage).[439]

In conclusion, strong experimental evidence was obtained for at least two degradation steps for anthocyanins: (i) deglycosylation of position 3 of the anthocyanin, leading to unstable anthocyanidins, and (ii) oxidation by O_2 (autoxidation), probably involving radical intermediates. In this last process, the presence of traces of metal cations such as iron or copper leads to catalytic processes (e.g., Fenton reaction traces) that overcome the thermodynamic barriers and facilitate degradation.[444] Deglycosylation of position 3 was detected with flavylium cations (under acidic conditions) from thermogravimetry experiments. The resulting aglycone is very unstable (Figure 28) involving the fast autoxidation and degradation (breakage) of the chalcone form as proposed in Scheme 53. At pH values close to neutrality or higher, autoxidation of the electron-rich anionic base must occur first, followed by the hydrolysis of labile ester bonds (arylesters, glycosylesters) thus formed. This process may involve the concomitant production of H_2O_2 and its fast subsequent reaction as an electrophile (Scheme 56).

During autoxidation, H_2O_2 is formed, which could react as an electrophile with the most nucleophilic anthocyanin forms (hemiketal, anionic base) or via the Fenton reaction (due to inevitable iron and/or copper traces). The formation of H_2O_2 in complex biological media may involve many other substrates than anthocyanins. For instance, catechol moieties from other phenolics (e.g., catechins and caffeic acid derivatives) can undergo autoxidation (in the presence of metal traces), yielding *O*-semiquinones that, in turn and depending on their structure, can transfer one electron to molecular oxygen, yielding superoxide radical that in turn by dismutation give rise to the formation of H_2O_2.[459,460]

8.2. Anthocyanin Degradation in Biological Systems

A transient accumulation of anthocyanins occur in some plants and fruits, appearing and disappearing during plant development, and also depending on the environmental conditions.[461] For instance, UV light and low temperatures promotes anthocyanin biosynthesis while high temperature induces its degradation.[462−465] It was postulated that since anthocyanins absorb visible and UV light, their accumulation in young leaves may serve as a "sunscreen", protecting the photosynthetic apparatus of the plants. On the other hand, their antioxidant properties may also confer protection to plant cells against oxidative damage.[466,467] There are some examples of anthocyanin degradation in flowers such as *Brunfelsia calycina* (Solanaceae) and petunia mutants whose petal color faded after flower opening.[468,469]

In fruits such as eggplants, peppers, tomatoes, blood oranges, and litchis, the concentration of anthocyanins increases during ripening, reaching a maximum and declining at later stages of maturity.[470−472] In general, the type of color hue and intensity are important sensorial quality parameters that attract consumers. Despite the economic interests of the food industry, there are very few studies in the literature addressing the mechanisms behind this transient accumulation of anthocyanins. In some plants, there is evidence of simultaneous anthocyanin accumulation and degradation (turnover effect). In other cases, these compounds are synthesized and remain stable in the plant vacuole, at least until cell degradation.

Anthocyanin degradation and its consequent discoloration may occur in vivo as a result of active enzyme-driven breakdown processes such as by anthocyanase (anthocyanin-glucosidase), polyphenoloxidases (PPO), and peroxidases (POD). These enzymes hydrolyze and oxidize anthocyanins and are primarily active during fruit senescence and later in processed food. During food processing and storage, cell-wall degradation occurs, leading to an intracellular decompartmentalization and setting the conditions for anthocyanin exposure to enzymes that, at least originally in plant cells, are located in different compartments.

Oren-Shamir has clearly summarized three alternative pathways for the enzymatic degradation of anthocyanins and tissue browning:[461] (1) anthocyanase ($\alpha\,\beta$-glucosidase enzyme)

https://doi.org/10.1021/acs.chemrev.1c00399
Chem. Rev. 2022, 122, 1416−1481

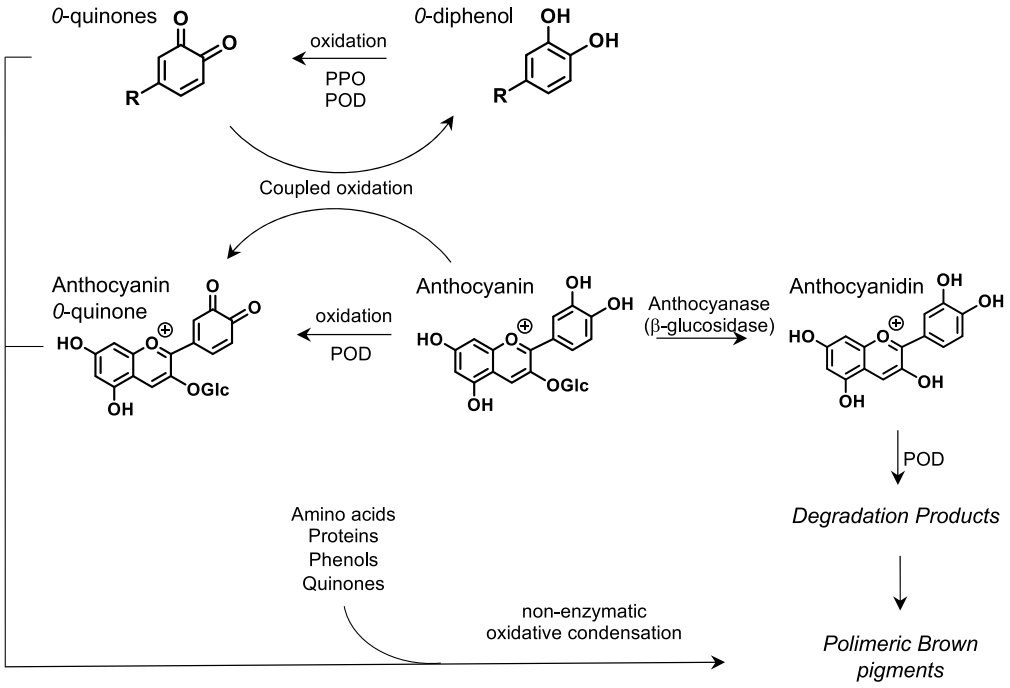

Figure 31. Proposed scheme describing three alternative pathways for enzymatic anthocyanin degradation in plants. Nonenzymatic oxidative degradation involved in the browning process. POD, peroxidase; PPO, polyphenol oxidase. The class of anthocyanins was represented as usually by the flavylium form, but oxidation is more likely to occur from other anthocyanin forms. Adapted with permission from ref 461. Copyright 2009, Elsevier.

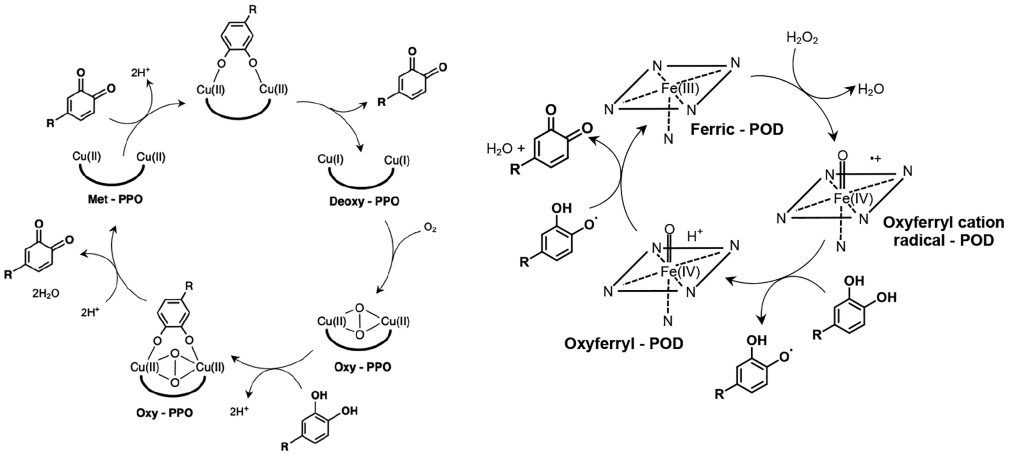

Figure 32. Catalytic cycles of peroxidases (POD) and phenol oxidase (PPO). Adapted with permission from ref 473 under the terms of the Creative Commons Attribution License and from ref 474. Copyright 1998, Elsevier.

may promote deglycosylation, forming the aglycone (anthocyanidin), which is extremely unstable with consequent chemical and/or enzymatic oxidation; (2) a coupled (indirect) oxidation, i.e., a reduction of the quinones of phenolic compounds (formed previously through the action of PPO) to the original phenolic compounds (major PPO substrates such as caffeic acid derivatives) in parallel to the oxidation of anthocyanin to anthocyanin quinone, which might be thermodynamically feasible, depending on the kinetic constrains. Direct enzymatic oxidation of anthocyanins promoted by PPO is not expected to occur since anthocyanins are poor substrates for that enzyme; and (3) anthocyanin may also be directly oxidized by peroxidase in the presence of H_2O_2 (Figure 31).

In processed food, this complex enzymatic system leading to the formation of quinones involved in coupled oxidation and direct chemical reactions (e.g., Michael addition) could be responsible for a faster anthocyanin degradation (essentially present in their hemiketal, chalcone, and base forms) and also in browning processes involving the reaction of quinones with other substrates (proteins, carbohydrates, polyphenols, etc.). The catalytic cycle of peroxidases[473] and phenol oxidase[474] showing the events (oxidation−reduction) is described in Figure 32.

Polyphenol oxidase is a copper(II)-containing oxidoreductase. This enzyme could be inhibited by using copper chelating agents such as organic acids (citric acid, oxalic acid, and ethylenediaminetetraacetic acid), sodium pyrophosphate, sodium hexametaphosphate, and ascorbate, and also by decreasing the pH to below 4.0. As an example, oxalic and citric acids have been used in fruit juice to delay anthocyanin degradation probably by inhibiting of the formation of quinones involved in

https://doi.org/10.1021/acs.chemrev.1c00399
Chem. Rev. 2022, 122, 1416−1481

the coupled oxidation of anthocyanins as described in Figure 31.[475]

Hydrogen peroxide (H_2O_2) play a major role in these catalytic processes and its presence in tissues may have different origins. H_2O_2 and other reactive oxygen species (ROS) are produced during a number of cellular events through enzymatic and nonenzymatic reactions.[476−478] On the other hand, during cellular respiration, a complex series of mitochondrial electron-transfer reactions occurs, promoting the one- to three-electron reduction of oxygen to form different ROS species, namely, $O_2^{\bullet-}$, H_2O_2, and the hydroxyl radical ($HO^{\bullet}$).

Some of these reduced species of oxygen are highly reactive and capable of directly oxidizing various cellular components and different compounds. These species can react with some forms of anthocyanins, initiating their irreversible degradation and yielding the final products from the C1′−C2, C2−C3, and C3−C4 cleavage from Scheme 51, as described by Dangles and Fenger.[31,457]

9. CONCLUSIONS AND OUTLOOK

The flavylium multistate is intrinsically complex due to the large number of species that are reversibly interconnected by external stimuli, such as pH, light, and heat. However, the system is dramatically simplified when the flavylium cation is considered as a polyprotic acid in equilibrium with its conjugated base, CB, which is the sum of the quinoidal base, hemiketal, *cis*- and *trans*-chalcone, and their respective anionic species, including CB^-, CB^{2-}, etc. This perspective is the starting point for developing the mathematical expressions reported throughout this review.

The study of the thermodynamic and kinetics of flavylium-based dyes is indispensable not only to rationalize their degradation mechanisms and the in vitro and in vivo color expression problem but also to rationalize their application as food colorants, functional ingredients, and dietary supplements[479−482] as well as in more emergent areas, such as in the design of new photochromic systems, stimuli-responsive smart materials, and supramolecular devices.[178] The use of anthocyanins as food/beverage additives is allowed within Europe (E163), Japan, and the United States, among other countries.[483] Nevertheless, the application of anthocyanins as colorants is limited by the pH of the food and the possibility of their chemical reaction with other molecules or ions.[31] A top priority of the food industry regarding food colorants is to search for natural blue pigments that are stable over a wide pH range. This stability would allow these pigments to be used in foods to replace synthetic blue dyes that are no longer allowed in the food industry. The only natural source of blue pigments used in foods is phycocyanin from the blue alga *Spirulina*, but its production is somewhat expensive, increasing the cost of the final product. Thus, one of the biggest challenges in the food industry is the stabilization of blue quinoidal bases of anthocyanins at neutral and slightly acidic pH values. The colors of anthocyanins, particularly the more acylated ones, can be modulated according to the pH during food processing. A recent example was described by Appelhagen et al. in an experiment to produce cupcakes decorated with icing sugar with different colors. These authors supplemented icing sugar with anthocyanin extracts produced from mutant *Arabidopsis* cell cultures.[50]

More recently, an anthocyanin-based cyan blue previously discovered as a minor component in red cabbage was characterized.[175] Interestingly, this minor monoacylated anthocyanin bearing a sinapoyl group on Glc-2 of the sophorose moiety (3-*O*-(2-*O*-(2-*O*-(*E*)-sinapoyl-*β*-D-glucopyranosyl)-*β*-D-glucopyranosyl)-5-*O*-*β*-D-glucopyranosyl-cyanidin) was found to have a particularly high λ_{max} of 640 nm at pH 7. This compound in the presence of Al^{3+} is described to form a blue colored trimeric complex $Al^{3+}(P2-)_3$ with a large bathochromic shift of >40 nm. These chromatic properties make this blue pigment P2 a strong candidate for food applications free or complexed with metals. In order to increase the production of this pigment, an *E. coli* codon-optimized gene encoding hydrolytic enzymes was developed by synthetic biology to produce a specific and highly selective catalytic diacylation enzyme. The enzyme was shown to selectively remove any acyl group bound to Glc-1 of the sophorose moiety while leaving the sinapoyl group on Glc-2 intact, thus converting polyacylated anthocyanins into the pigment of interest.

Another use of both the coloring and antioxidant properties of anthocyanins and their derivatives concerns hair coloring and cosmetic dermatological products.[484−487] Toxicological studies have revealed that anthocyanins are not harmful to human health[488] and have shown beneficial effects,[489−491] thus making them a sustainable, advantageous alternative to many current synthetic and toxic hair dyes. Blackburn, Rayner, and co-workers have developed a natural hair dye made from anthocyanins extracted from waste blackcurrant (*Ribes nigrum* L.) fruit skins. Intense blue-colored dye on hair could be achieved with a λ_{max} at 580 nm, typical of the anionic quinoidal base. Hair has been suggested as being able to provide an environment that enables the stabilization of the anionic quinoidal base upon adsorption through association with cations in hair and copigmentation effects.[492] In addition, the use of anthocyanins as viable alternatives to synthetic lipstick colorants was studied by Westfall and co-workers.[493,494] The incorporation of anthocyanin extracts into the matrix of lipstick formulations proved to be stable, even under the accelerated environmental testing used to predict a shelf life of at least 2 years. Sources containing both nonacylated cyanidin-based and acylated cyanidin-based anthocyanins, such as those from elderberries, purple corn, and purple sweet potatoes, were shown to have the greatest stability compared with purple carrot, red grape, and red radish formulas. More recently, Giusti et al.,[494] confirmed that anthocyanins incorporated into lipstick formulations maintain their biological activity as antioxidants through the scavenging of free radicals and function as filters for UV light, especially anthocyanins with cinnamic acid acylation.

The ubiquity of the anthocyanin multistate of species in other families of compounds is in some way surprising. Plants in different positions of the evolutionary tree, from liverworts, mosses, and ferns to angiosperm, use different flavylium cations, auronidins (furanoflavylium), 3-deoxyanthocyanidins, and anthocyanins to confer color. While the colors and the interconversion rates are different, the reactions of the multistate are the same: proton transfer, hydration, tautomerization, and isomerization.

A great deal of progress has been made regarding the reactivity of different multistate species in recent years. Knowledge of the degradation of anthocyanins, while not yet completely understood, in particular, the way in which autoxidation processes are triggered, has advanced. There is, however, one intrinsic contradiction regarding anthocyanin stability. The antioxidant properties of anthocyanins are related to their ability to easily oxidize by donating electrons to ROS species. This action is not compatible with a strong storage stability toward the autoxidation processes needed for their applications as food colorants, for example. In these cases, mixtures of anthocyanins

https://doi.org/10.1021/acs.chemrev.1c00399
Chem. Rev. 2022, 122, 1416−1481

with or without the presence of copigments would be worthwhile. Despite the fact that acylated anthocyanins possess higher chemical stability than nonacylated ones, they are still not sufficiently stable for industrial applications. Encapsulation in biocompatible matrixes of these and other anthocyanins could be a challenge for future studies, and some studies in this direction have already appeared in the literature.

The strategies developed by nature to fix the colors of anthocyanins, namely, supramolecular structures involving metals, intra- and intermolecular interactions, and the role of acylated anthocyanins, have been rationalized and used to design bioinspired systems. The photodegradation of anthocyanins is another field that requires further investigation. The information collected on the in vitro anthocyanin properties is the basis for further technological studies and human trials. It is expected that these types of studies will increase in the future. Understanding anthocyanin behavior in plant vacuoles will pose many interesting theoretical and instrumental challenges.

AUTHOR INFORMATION

Corresponding Authors

Fernando Pina − *LAQV-REQUIMTE, Department of Chemistry, Faculty of Sciences and Technology, New University of Lisbon, 2829-516 Caparica, Portugal;* orcid.org/0000-0001-8529-6848; Email: fp@fct.unl.pt

Victor de Freitas − *LAQV-REQUIMTE, Department of Chemistry and Biochemistry, Faculty of Sciences, University of Porto, 4169-007 Porto, Portugal;* orcid.org/0000-0003-0586-2278; Email: vfreitas@fc.up.pt

Authors

Luis Cruz − *LAQV-REQUIMTE, Department of Chemistry and Biochemistry, Faculty of Sciences, University of Porto, 4169-007 Porto, Portugal;* orcid.org/0000-0003-2226-0404

Nuno Basílio − *LAQV-REQUIMTE, Department of Chemistry, Faculty of Sciences and Technology, New University of Lisbon, 2829-516 Caparica, Portugal;* orcid.org/0000-0002-0121-3695

Nuno Mateus − *LAQV-REQUIMTE, Department of Chemistry and Biochemistry, Faculty of Sciences, University of Porto, 4169-007 Porto, Portugal*

Complete contact information is available at: https://pubs.acs.org/10.1021/acs.chemrev.1c00399

Author Contributions

§L.C. and N.B. contributed equally to the paper.

Notes

The authors declare no competing financial interest.

Biographies

Luis Cruz graduated with a Chemistry degree in 2004, received a MSc in Chemistry in 2006, and obtained his PhD in Chemistry in 2010 from the University of Porto (Portugal). He is currently an Independent Researcher in the Food Quality and Technology Group of the Associate Laboratory of Green Chemistry (LAQV-REQUIMTE). His research interests are related to the chemistry of natural anthocyanins and related flavylium dyes, which include chemical/enzymatic synthesis, physical-chemical characterization, and the development of flavylium-based smart materials toward novel applications in cosmetics, food packaging, energy and biomedical fields.

Nuno Basílio studied Chemistry at the University of the Algarve (Portugal) and obtained his PhD in 2011 from the University of Santiago de Compostela with Prof. Luis García Rio and Prof. José Ramón Leis. He then moved to the NOVA University of Lisbon to work as a Postdoctoral Fellow with Prof. Fernando Pina. He is currently an assistant researcher at the same university. His research interests focus on stimuli-responsive self-assembled systems, supramolecular catalysis, and the molecular recognition of biologically relevant compounds using synthetic receptors.

Nuno Mateus received his undergraduate degree in Biochemistry in 1997 and obtained his PhD in Chemistry in 2002, both from the University of Porto (Portugal). He is currently a member of the LAQV-REQUIMTE Research Center and is an Associate Professor and Director of the Department of Chemistry and Biochemistry of the Faculty of Sciences at the University of Porto. His field of research concerns food chemistry and biochemistry, essentially food polyphenols and, in particular, red wine chemistry. Presently, his primary area of research addresses the biological properties of food phenolics and recycling them from industrial wastes for novel technological applications.

Victor de Freitas is a Full Professor at the Department of Chemistry and Biochemistry at the University of Porto. He obtained his PhD in Biological and Medical Sciences at the University of Bordeaux II (France) in 1995. He is a member of the LAQV-REQUIMTE Research Center and is the leader of a research group focusing on the study of the physicochemical properties of polyphenols, and he explores their applications in different fields. He has been President of the "Groupe Polyphénols" society between 2016 and 2020 (http://www.groupepolyphenols.com).

Fernando Pina received his PhD in Chemical Engineering in 1983 from the Technical University of Lisbon, IST, was a postdoctoral fellow with Vincenzo Balzani, University of Bologna, Italy, and is Full Professor of Chemistry at the New University of Lisbon. He has been working for more than 20 years on the physical chemistry of anthocyanins and related compounds. He has focused his interests on the pH-dependent kinetics and thermodynamics of flavylium-based multistate systems, particularly their photochromic properties (https://publons.com/researcher/2799656/fernando-pina/).

ACKNOWLEDGMENTS

This research was supported by project grants (PTDC/OCE-ETA/31250/2017; PTDC/QUI-COL/32351/2017), with financial support from FCT/MEC through national funds and cofinancing from FEDER, in Partnership Agreement PT2020 (UIDB/50006/2020 - POCI-01-0247-FEDER-017687); and AgriFoodXXI I&D&I (Norte-01-0145 FEDER-000041) cofinanced by European Regional Development FUND (ERDF), through the NORTE 2020 (Programa Operacional Regional do Norte 2014/2020). L.C. and N.B. acknowledge financial support from FCT/MEC, respectively contract (DL 57/2016/CP1334/CT0008) and (CEECIND/00466/2017).

REFERENCES

(1) Harborne, J. B.; Williams, C. A. Advances in Flavonoid Research since 1992. *Phytochemistry* **2000**, *55*, 481−504.

(2) Hoballah, M. E.; Gübitz, T.; Stuurman, J.; Broger, L.; Barone, M.; Mandel, T.; Dell'Olivo, A.; Arnold, M.; Kuhlemeier, C. Single Gene-Mediated Shift in Pollinator Attraction in Petunia. *Plant Cell* **2007**, *19*, 779−790.

(3) Ahmed, N. U.; Park, J. I.; Jung, H. J.; Yang, T. J.; Hur, Y.; Nou, I. S. Characterization of Dihydroflavonol 4-Reductase (Dfr) Genes and

Their Association with Cold and Freezing Stress in Brassica Rapa. *Gene* **2014**, *550*, 46−55.
(4) Chalker-Scott, L. Environmental Significance of Anthocyanins in Plant Stress Responses. *Photochem. Photobiol.* **1999**, *70*, 1−9.
(5) Guo, J.; Wang, M. Ultraviolet a-Specific Induction of Anthocyanin Biosynthesis and Pal Expression in Tomato (Solanum Lycopersicum L.). *Plant Growth Regul.* **2010**, *62*, 1−8.
(6) Zhu, H.; Zhang, T. J.; Zheng, J.; Huang, X. D.; Yu, Z. C.; Peng, C. L.; Chow, W. S. Anthocyanins Function as a Light Attenuator to Compensate for Insufficient Photoprotection Mediated by Non-photochemical Quenching in Young Leaves of Acmena Acuminatissima in Winter. *Photosynthetica* **2018**, *56*, 445−454.
(7) Tilbrook, J.; Tyerman, S. D. Cell Death in Grape Berries: Varietal Differences Linked to Xylem Pressure and Berry Weight Loss. *Funct. Plant Biol.* **2008**, *35*, 173−184.
(8) Xiao, Z.; Liao, S.; Rogiers, S. Y.; Sadras, V. O.; Tyerman, S. D. Effect of Water Stress and Elevated Temperature on Hypoxia and Cell Death in the Mesocarp of Shiraz Berries. *Aust. J. Grape Wine Res.* **2018**, *24*, 487−497.
(9) Fernandes, I.; Pérez-Gregorio, R.; Soares, S.; Mateus, N.; De Freitas, V. Wine Flavonoids in Health and Disease Prevention. *Molecules* **2017**, *22*, 292.
(10) Quideau, S.; Deffieux, D.; Douat-Casassus, C.; Pouységu, L. Plant Polyphenols: Chemical Properties, Biological Activities, and Synthesis. *Angew. Chem., Int. Ed.* **2011**, *50*, 586−621.
(11) Bars-Cortina, D.; Sakhawat, A.; Piñol-Felis, C.; Motilva, M.-J. Chemopreventive Effects of Anthocyanins on Colorectal and Breast Cancer: A Review. *Semin. Cancer Biol.* **2021**, DOI: 10.1016/j.semcancer.2020.12.013.
(12) Ma, Y.; Ding, S.; Fei, Y.; Liu, G.; Jang, H.; Fang, J. Antimicrobial Activity of Anthocyanins and Catechins against Foodborne Pathogens Escherichia Coli and Salmonella. *Food Control* **2019**, *106*, 106712.
(13) Oliveira, H.; Fernandes, I.; de Freitas, V.; Mateus, N. Ageing Impact on the Antioxidant and Antiproliferative Properties of Port Wines. *Food Res. Int.* **2015**, *67*, 199−205.
(14) Oliveira, H.; Correia, P.; Pereira, A. R.; Araújo, P.; Mateus, N.; de Freitas, V.; Oliveira, J.; Fernandes, I. Exploring the Applications of the Photoprotective Properties of Anthocyanins in Biological Systems. *Int. J. Mol. Sci.* **2020**, *21*, 7464.
(15) Amogne, N. Y.; Ayele, D. W.; Tsigie, Y. A. Recent Advances in Anthocyanin Dyes Extracted from Plants for Dye Sensitized Solar Cell. *Mater. Renew. Sustain. Energy* **2020**, *9*, 23.
(16) Roy, S.; Rhim, J.-W. Anthocyanin Food Colorant and Its Application in Ph-Responsive Color Change Indicator Films. *Crit. Rev. Food Sci. Nutr.* **2021**, *61*, 2297−2235.
(17) Willstätter, R.; Everest, A. E. Untersuchungen Über Die Anthocyane. I. Über Den Farbstoff Der Kornblume. *Justus Liebigs Ann. Chem.* **1913**, *401*, 189−232.
(18) Robinson, R.; Todd, A. R. Experiments on the Synthesis of Anthocyanins Part Xvii the Syntheses of Pelargonin, Peonin, and Cyanin Chlorides. *J. Chem. Soc.* **1932**, 2488−2496.
(19) Andersen, O. M.; Markham, K. R. The Anthocyanins. *Flavonoids: Chemistry, Biochemistry, and Applications*; CRC Press: Boca Raton, FL, 2006; Chapter 10, pp 471−551.
(20) Wallace, T. C.; Giusti, M. M. Anthocyanins—Nature's Bold, Beautiful, and Health-Promoting Colors. *Foods* **2019**, *8*, 550.
(21) Oliveira, J.; Alhinho da Silva, M.; Teixeira, N.; De Freitas, V.; Salas, E. Screening of Anthocyanins and Anthocyanin-Derived Pigments in Red Wine Grape Pomace Using Lc-Dad/Ms and Maldi-Tof Techniques. *J. Agric. Food Chem.* **2015**, *63*, 7636−7644.
(22) Clifford, M. N. Anthocyanins - Nature, Occurrence and Dietary Burden. *J. Sci. Food Agric.* **2000**, *80*, 1063−1072.
(23) Berland, H.; Albert, N. W.; Stavland, A.; Jordheim, M.; McGhie, T. K.; Zhou, Y.; Zhang, H.; Deroles, S. C.; Schwinn, K. E.; Jordan, B. R.; et al. Auronidins Are a Previously Unreported Class of Flavonoid Pigments That Challenges When Anthocyanin Biosynthesis Evolved in Plants. *Proc. Natl. Acad. Sci. U. S. A.* **2019**, *116*, 20232−20239.
(24) Khalil, A.; Baltenweck-Guyot, R.; Ocampo-Torres, R.; Albrecht, P. A Novel Symmetrical Pyrano-3-Deoxyanthocyanidin from a Sorghum Species. *Phytochem. Lett.* **2010**, *3*, 93−95.
(25) Berké, B.; Chèze, C.; Vercauteren, J.; Deffieux, G. Bisulfite Addition to Anthocyanins: Revisited Structures of Colorless Adducts. *Tetrahedron Lett.* **1998**, *39*, 5771−5774.
(26) Berké, B.; De Freitas, V. A. P. Influence of Procyanidin Structures on Their Ability to Complex with Oenin. *Food Chem.* **2005**, *90*, 453−460.
(27) Fernandes, A.; Bras, N. F.; Oliveira, J.; Mateus, N.; de Freitas, V. Impact of a Pectic Polysaccharide on Oenin Copigmentation Mechanism. *Food Chem.* **2016**, *209*, 17−26.
(28) Hondo, T.; Yoshida, K.; Nakagawa, A.; Kawai, T.; Tamura, H.; Goto, T. Structural Basis of Blue-Color Development in Flower Petals from Commelina-Communis. *Nature* **1992**, *358*, 515−518.
(29) Yoshida, K.; Kondo, T.; Okazaki, Y.; Katou, K. Cause of Blue Petal Color. *Nature* **1995**, *373*, 291−291.
(30) Oliveira, J.; Mateus, N.; De Freitas, V. Wine-Inspired Chemistry: Anthocyanin Transformations for a Portfolio of Natural Colors. *Synlett* **2017**, *28*, 898−906.
(31) Dangles, O.; Fenger, J.-A. The Chemical Reactivity of Anthocyanins and Its Consequences in Food Science and Nutrition. *Molecules* **2018**, *23*, 1970.
(32) Rentzsch, M.; Schwarz, M.; Winterhalter, P. Pyranoanthocyanins - an Overview on Structures, Occurrence, and Pathways of Formation. *Trends Food Sci. Technol.* **2007**, *18*, 526−534.
(33) Fernandes, A.; Bras, N. F.; Mateus, N.; de Freitas, V. A Study of Anthocyanin Self-Association by Nmr Spectroscopy. *New J. Chem.* **2015**, *39*, 2602−2611.
(34) Di Meo, F.; Garcia, J. C. S.; Dangles, O.; Trouillas, P. Highlights on Anthocyanin Pigmentation and Copigmentation: A Matter of Flavonoid Pi-Stacking Complexation to Be Described by Dft-D. *J. Chem. Theory Comput.* **2012**, *8*, 2034−2043.
(35) Escribano-Bailon, M. T.; Santos-Buelga, C. Anthocyanin Copigmentation - Evaluation, Mechanisms and Implications for the Colour of Red Wines. *Curr. Org. Chem.* **2012**, *16*, 715−723.
(36) He, F.; Liang, N. N.; Mu, L.; Pan, Q. H.; Wang, J.; Reeves, M. J.; Duan, C. Q. Anthocyanins and Their Variation in Red Wines I. Monomeric Anthocyanins and Their Color Expression. *Molecules* **2012**, *17*, 1571−1601.
(37) Goto, T.; Kondo, T. Structure and Molecular Stacking of Anthocyanins - Flower Color Variation. *Angew. Chem., Int. Ed. Engl.* **1991**, *30*, 17−33.
(38) Mendoza, J.; Basílio, N.; Pina, F.; Kondo, T.; Yoshida, K. Rationalizing the Color in Heavenly Blue Anthocyanin: A Complete Kinetic and Thermodynamic Study. *J. Phys. Chem. B* **2018**, *122*, 4982−4992.
(39) Yoshida, K.; Mori, M.; Kondo, T. Blue Flower Color Development by Anthocyanins: From Chemical Structure to Cell Physiology. *Nat. Prod. Rep.* **2009**, *26*, 884−915.
(40) Trouillas, P.; Sancho-García, J. C.; De Freitas, V.; Gierschner, J.; Otyepka, M.; Dangles, O. Stabilizing and Modulating Color by Copigmentation: Insights from Theory and Experiment. *Chem. Rev.* **2016**, *116*, 4937−4982.
(41) Muller-Maatsch, J.; Bechtold, L.; Schweiggert, R. M.; Carle, R. Co-Pigmentation of Pelargonidin Derivatives in Strawberry and Red Radish Model Solutions by the Addition of Phenolic Fractions from Mango Peels. *Food Chem.* **2016**, *213*, 625−634.
(42) Iwashina, T. Contribution to Flower Colors of Flavonoids Including Anthocyanins: A Review. *Nat. Prod. Commun.* **2015**, *10*, 529−544.
(43) Mendoza, J.; Oliveira, J.; Araújo, P.; Basílio, N.; Teixeira, N.; Brás, N. F.; Pina, F.; Yoshida, K.; de Freitas, V. The Peculiarity of Malvidin 3-O-(6-O-P-Coumaroyl) Glucoside Aggregation. Intra and Intermolecular Interactions. *Dyes Pigm.* **2020**, *180*, 108382.
(44) Qian, B. J.; Liu, J. H.; Zhao, S. J.; Cai, J. X.; Jing, P. The Effects of Gallic/Ferulic/Caffeic Acids on Colour Intensification and Anthocyanin Stability. *Food Chem.* **2017**, *228*, 526−532.

https://doi.org/10.1021/acs.chemrev.1c00399
Chem. Rev. 2022, 122, 1416−1481

(45) Pina, F.; Melo, M. J.; Maestri, M.; Passaniti, P.; Balzani, V. Artificial Chemical Systems Capable of Mimicking Some Elementary Properties of Neurons. *J. Am. Chem. Soc.* **2000**, *122*, 4496−4498.
(46) Melo, M. J.; Moura, S.; Maestri, M.; Pina, F. Micelle Effects on Multistate/Multifunctional Systems Based on Photochromic Flavylium Compounds. The Case of Luteolinidin. *J. Mol. Struct.* **2002**, *612*, 245−253.
(47) Pina, F.; Maestri, M.; Balzani, V. Photochromic Flavylium Compounds as Multistate/Multifunction Molecular-Level Systems. *Chem. Commun.* **1999**, 107−114.
(48) Melo, M. J.; Moura, S.; Roque, A.; Maestri, M.; Pina, F. Photochemistry of Luteolinidin: "Write-Lock-Read-Unlock-Erase" with a Natural Compound. *J. Photochem. Photobiol., A* **2000**, *135*, 33−39.
(49) Bülow, C.; Wagner, B. H. *Ber. Dtsch. Chem. Ges.* **1901**, *34*, 1782−1806.
(50) Appelhagen, I.; Wulff-Vester, A. K.; Wendell, M.; Hvoslef-Eide, A.-K.; Russell, J.; Oertel, A.; Martens, S.; Mock, H.-P.; Martin, C.; Matros, A. Colour Bio-Factories: Towards Scale-up Production of Anthocyanins in Plant Cell Cultures. *Metab. Eng.* **2018**, *48*, 218−232.
(51) Levisson, M.; Patinios, C.; Hein, S.; de Groot, P. A.; Daran, J.-M.; Hall, R. D.; Martens, S.; Beekwilder, J. Engineering De Novo Anthocyanin Production in Saccharomyces Cerevisiae. *Microb. Cell Fact.* **2018**, *17*, 103.
(52) Zha, J.; Koffas, M. A. G. Production of Anthocyanins in Metabolically Engineered Microorganisms: Current Status and Perspectives. *Synth. Syst. Biotechnol.* **2017**, *2*, 259−266.
(53) Perkin, W. H.; Robinson, R.; Turner, M. R. Cx.—the Synthesis and Constitution of Certain Pyranol Salts Related to Brazilein and Haematein. *J. Chem. Soc., Trans.* **1908**, *93*, 1085−1115.
(54) Pratt, D. D.; Robinson, R. Clxxxviii.-a Synthesis of Pyrylium Salts of Anthocyanidin Type. *J. Chem. Soc., Trans.* **1922**, *121*, 1577−1585.
(55) Pratt, D. D.; Robinson, R. A Synthesis of Pyrylium Salts of Anthocyanidin Type. Part V. The Synthesis of Cyanidin Chloride and of Delphinidin Chloride. *J. Chem. Soc., Trans.* **1925**, *127*, 166−175.
(56) Robertson, A.; Robinson, R. Ccxxv.—Experiments on the Synthesis of Anthocyanins. Part I. *J. Chem. Soc.* **1926**, *129*, 1713−1720.
(57) Kueny-Stotz, M.; Chassaing, S.; Brouillard, R.; Nielsen, M.; Goeldner, M. Flavylium Salts as in Vitro Precursors of Potent Ligands to Brain Gaba-a Receptors. *Bioorg. Med. Chem. Lett.* **2008**, *18*, 4864−4867.
(58) Diniz, A. M.; Gomes, R.; Parola, A. J.; Laia, C. A. T.; Pina, F. Photochemistry of 7-Hydroxy-2-(4-Hydroxystyryl)-1-Benzopyrylium and Related Compounds. *J. Phys. Chem. B* **2009**, *113*, 719−727.
(59) Gomes, R.; Diniz, A. M.; Jesus, A.; Parola, A. J.; Pina, F. The Synthesis and Reaction Network of 2-Styryl-1-Benzopyrylium Salts: An Unexploited Class of Potential Colorants. *Dyes Pigm.* **2009**, *81*, 69−79.
(60) Gomes, V.; Mateus, N.; de Freitas, V.; Cruz, L. Synthesis and Structural Characterization of a Novel Symmetrical 2,10-Bis-Styryl-1-Benzopyrylium Dye. *Synlett* **2018**, *29*, 1390−1394.
(61) Mora-Soumille, N.; Al Bittar, S.; Rosa, M.; Dangles, O. Analogs of Anthocyanins with a 3′,4′-Dihydroxy Substitution: Synthesis and Investigation of Their Acid−Base, Hydration, Metal Binding and Hydrogen-Donating Properties in Aqueous Solution. *Dyes Pigm.* **2013**, *96*, 7−15.
(62) Barcena, H. S.; Chen, P.; Tuachi, A. Synthetic Anthocyanidins and Their Antioxidant Properties. *SpringerPlus* **2015**, *4*, 499.
(63) Cruz, L.; Mateus, N.; De Freitas, V. First Chemical Synthesis Report of an Anthocyanin Metabolite with in Vivo Occurrence: Cyanidin-4′-O-Methyl-3-Glucoside. *Tetrahedron Lett.* **2013**, *54*, 2865−2869.
(64) Cruz, L.; Fernandes, I.; Évora, A.; de Freitas, V.; Mateus, N. Synthesis of the Main Red Wine Anthocyanin Metabolite: Malvidin-3-O-B-Glucuronide. *Synlett* **2017**, *28*, 593−596.
(65) Zhang, Q.; Botting, N. P.; Kay, C. A Gram Scale Synthesis of a Multi-^{13}c-Labelled Anthocyanin, [6,8,10,3′,5′-$^{13}c_5$]Cyanidin-3-Glucoside, for Use in Oral Tracer Studies in Humans. *Chem. Commun.* **2011**, *47*, 10596−10598.
(66) Cruz, L.; Basílio, N.; Mateus, N.; Pina, F.; de Freitas, V. Characterization of Kinetic and Thermodynamic Parameters of Cyanidin-3-Glucoside Methyl and Glucuronyl Metabolite Conjugates. *J. Phys. Chem. B* **2015**, *119*, 2010−2018.
(67) Robertson, A.; Robinson, R. Experiments on the Synthesis of Anthocyanins. Part V. A Synthesis of 3-B-Glucosidylpelargonidin Chloride, Which Is Believed to Be Identical with Callistephin Chloride. *J. Chem. Soc.* **1928**, *0*, 1460−1472.
(68) Murakami, S.; Robertson, A.; Robinson, R. Ccclxxii.—Experiments on the Synthesis of Anthocyanins. Part Vi. A Synthesis of Chrysanthemin Chloride. *J. Chem. Soc.* **1931**, *0*, 2665−2671.
(69) Dangles, O.; Elhajji, H. Synthesis of 3-Methoxy-Flavylium and 3-(B-D-Glucopyranosyloxy)Flavylium Ions - Influence of the Flavylium Substitution Pattern on the Reactivity of Anthocyanins in Aqueous-Solution. *Helv. Chim. Acta* **1994**, *77*, 1595−1610.
(70) Kuhnert, N.; Clifford, M. N.; Radenac, A. G. Boron Trifluoride-Etherate Mediated Synthesis of 3-Desoxyanthocyanidins Including a Total Synthesis of Tricetanidin from Black Tea. *Tetrahedron Lett.* **2001**, *42*, 9261−9263.
(71) Mas, T. A New and Convenient One-Stepsynthesis of the Natural 3-DeoxyanthoCyanidins Apigeninidinand Luteolinidin Chlorides from 2,4,6-TriacetoxyBenzaldehyde. *Synthesis* **2003**, *2003*, 1878−1880.
(72) Al Bittar, S.; Mora, N.; Loonis, M.; Dangles, O. A Simple Synthesis of 3-Deoxyanthocyanidins and Their O-Glucosides. *Tetrahedron* **2016**, *72*, 4294−4302.
(73) Johnson, A. W.; Melhuish, R. R. A New Synthesis of Benzopyrylium Salts. *J. Chem. Soc.* **1947**, 346−350.
(74) Kueny-Stotz, M.; Isorez, G.; Chassaing, S.; Brouillard, R. Straightforward Synthesis of Highly Hydroxylated Phloroglucinol-Type 3-Deoxyanthocyanidins. *Synlett* **2007**, *2007*, 1067−1070.
(75) Sousa, A.; Mateus, N.; De Freitas, V. A Novel Reaction Mechanism for the Formation of Deoxyanthocyanidins. *Tetrahedron Lett.* **2012**, *53*, 1300−1303.
(76) Sousa, C.; Mateus, N.; Perez-Alonso, J.; Santos-Buelga, C.; De Freitas, V. Preliminary Study of Oaklins, a New Class of Brick-Red Catechinpyrylium Pigments Resulting from the Reaction between Catechin and Wood Aldehydes. *J. Agric. Food Chem.* **2005**, *53*, 9249−9256.
(77) De Freitas, V.; Sousa, C.; Silva, A. M. S.; Santos-Buelga, C.; Mateus, N. Synthesis of a New Catechin-Pyrylium Derived Pigment. *Tetrahedron Lett.* **2004**, *45*, 9349−9352.
(78) Bianco, A.; Cavarischia, C.; Guiso, M. Total Synthesis of Anthocyanidins Via Heck Reaction. *Nat. Prod. Res.* **2006**, *20*, 93−97.
(79) Bianco, A.; Cavarischia, C.; Farina, A.; Guiso, M.; Marra, C. A New Synthesis of Flavonoids Via Heck Reaction. *Tetrahedron Lett.* **2003**, *44*, 9107−9109.
(80) Dekić, M.; Kolašinac, R.; Radulović, N.; Šmit, B.; Amić, D.; Molčanov, K.; Milenković, D.; Marković, Z. Synthesis and Theoretical Investigation of Some New 4-Substituted Flavylium Salts. *Food Chem.* **2017**, *229*, 688−694.
(81) Willstätter, R.; Schmidt, O. T. Synthesis of New Anthocyanidins. *Ber. Dtsch. Chem. Ges. B* **1924**, *57B*, 1945−1950.
(82) Willstätter, R.; Zechmeister, L. Syntheses of Pelargonidin. *Sitzb. kgl. preuss. Akad.* **1914**, 886−893.
(83) Roehri-Stoeckel, C.; Gonzalez, E.; Fougerousse, A.; Brouillard, R. Synthetic Dyes: Simple and Original Ways to 4-Substituted Flavylium Salts and Their Corresponding Vitisin Derivatives. *Can. J. Chem.* **2001**, *79*, 1173−1178.
(84) Iacobucci, G. A.; Sweeny, J. G. The Chemistry of Anthocyanins, Anthocyanidins and Related Flavylium Salts. *Tetrahedron* **1983**, *39*, 3005−3038.
(85) Shibata, K.; Shibata, Y.; Kasiwagi, I. Studies on Anthocyanins: Color Variation in Anthocyanins. *J. Am. Chem. Soc.* **1919**, *41*, 208−220.
(86) Asahina, Y.; Nakagome, G.; Inubuse, M. Flavonoid Glycosides. V. Reduction of Flavone and Flavonone Derivatives. *Ber. Dtsch. Chem. Ges. B* **1929**, *62B*, 3016−3021.
(87) King, H. G. C.; White, T. 775. The Conversion of Flavonols into Anthocyanidins. *J. Chem. Soc.* **1957**, 3901−3903.

https://doi.org/10.1021/acs.chemrev.1c00399
Chem. Rev. 2022, 122, 1416−1481

(88) Elhabiri, M.; Figueiredo, P.; Fougerousse, A.; Brouillard, R. A Convenient Method for Conversion of Flavonols into Anthocyanins. *Tetrahedron Lett.* **1995**, *36*, 4611−4614.
(89) Oyama, K.-i.; Kimura, Y.; Iuchi, S.; Koga, N.; Yoshida, K.; Kondo, T. Conversion of Flavonol Glycoside to Anthocyanin: An Interpretation of the Oxidation−Reduction Relationship of Biosynthetic Flavonoid-Intermediates. *RSC Adv.* **2019**, *9*, 31435−31439.
(90) Bjoroy, O.; Rayyan, S.; Fossen, T.; Kalberg, K.; Andersen, O. M. C-Glycosylanthocyanidins Synthesized from C-Glycosylflavones. *Phytochemistry* **2009**, *70*, 278−287.
(91) Oyama, K. I.; Kawaguchi, S.; Yoshida, K.; Kondo, T. Synthesis of Pelargonidin 3-O-6 ″-O-Acetyl-B-D-Glucopyranoside, an Acylated Anthocyanin, Via the Corresponding Kaempferol Glucoside. *Tetrahedron Lett.* **2007**, *48*, 6005−6009.
(92) Clark-Lewis, J.; Skingle, D. Flavan Derivatives. Xviii. Synthesis of Hemiketals Containing the Peltogynol Ring System: 3(3′)-Hydroxyisochromano (4′,3′:2, 3) Chromans. Conversion of 2′-Hydroxychdcones into Flav-3-Enes and Its Biosyntheticimplications. *Aust. J. Chem.* **1967**, *20*, 2169−2190.
(93) Sweeny, J. G.; Iacobucci, G. A. Synthesis of Anthocyanidins—Ii: The Synthesis of 3-Deoxyanthocyanidins from 5-Hydroxy-Flavanones. *Tetrahedron* **1977**, *33*, 2927−2932.
(94) Sweeny, J. G.; Iacobucci, G. A. Synthesis of Anthocyanidins—I: The Oxidative Generation of Flavylium Cations Using Benzoquinones. *Tetrahedron* **1977**, *33*, 2923−2926.
(95) Mirza, R.; Robinson, R. Conversion of Flavonols into Anthocyanidins. *Nature* **1950**, *166*, 997−997.
(96) Jurd, L. Quinone Oxidation of Flavenes and Flavan-3,4-Diols. *Chem. Ind.* **1966**, *40*, 1683−1684.
(97) Waiss, A. C.; Jurd, L. Synthesis of Flav-2-Enes and Flav-3-Enes. *Chem. Ind.* **1968**, *23*, 743−744.
(98) Kimura, Y.; Oyama, K.; Murata, Y.; Wakamiya, A.; Yoshida, K. Synthesis of 8-Aryl-O-Methylcyanidins and Their Usage for Dye-Sensitized Solar Cell Devices. *Int. J. Mol. Sci.* **2017**, *18*, 427.
(99) Kimura, Y.; Oyama, K. I.; Kondo, T.; Yoshida, K. Synthesis of 8-Aryl-3,5,7,3 ′,4 ′-Penta-O-Methylcyanidins from the Corresponding Quercetin Derivatives by Reduction with Lialh4. *Tetrahedron Lett.* **2017**, *58*, 919−922.
(100) Kondo, T.; Oyama, K.; Nakamura, S.; Yamakawa, D.; Tokuno, K.; Yoshida, K. Novel and Efficient Synthesis of Cyanidin 3-O-B-D-Glucoside from (+)-Catechin Via a Flav-3-En-3-Ol as a Key Intermediate. *Org. Lett.* **2006**, *8*, 3609−3612.
(101) Cameira dos Santos, P. J.; Brillouet, J. M.; Cheynier, V.; Moutounet, M. Detection and Partial Characterisation of New Anthocyanins Derived Pigments in Wine. *J. Sci. Food Agric.* **1996**, *70*, 204−208.
(102) Fulcrand, H.; Cameira dos Santos, P.; Sarni-Manchado, P.; Cheynier, V.; Favre-Bonvin, J. Structure of New Anthocyanin-Derived Wine Pigments. *J. Chem. Soc., Perkin Trans. 1* **1996**, 735−739.
(103) Bakker, J.; Timberlake, C. F. Isolation, Identification, and Characterization of New Color-Stable Anthocyanins Occurring in Some Red Wines. *J. Agric. Food Chem.* **1997**, *45*, 35−43.
(104) Fulcrand, H.; Benabdeljalil, C.; Rigaud, J.; Cheynier, V.; Moutounet, M. A New Class of Wine Pigments Generated by Reaction between Pyruvic Acid and Grape Anthocyanins. *Phytochemistry* **1998**, *47*, 1401−1407.
(105) Robertson, A.; Whalley, W. B.; Yates, J. The Pigments of Dragons Blood Resins.3. The Constitution of Dracorubin. *J. Chem. Soc.* **1950**, *0*, 3117−3123.
(106) Fukui, Y.; Kusumi, T.; Masuda, K.; Iwashita, T.; Nomoto, K. Structure of Rosacyanin B, a Novel Pigment from the Petals of Rosa Hybrida. *Tetrahedron Lett.* **2002**, *43*, 2637−2639.
(107) Andersen, O. M.; Fossen, T.; Torskangerpoll, K.; Fossen, A.; Hauge, U. Anthocyanin from Strawberry (Fragaria Ananassa) with the Novel Aglycone, 5-Carboxypyranopelargonidin. *Phytochemistry* **2004**, *65*, 405−410.
(108) Lu, Y. R.; Sun, Y.; Foo, L. Y. Novel Pyranoanthocyanins from Black Currant Seed. *Tetrahedron Lett.* **2000**, *41*, 5975−5978.
(109) Rentzsch, W.; Schwarz, M.; Winterhalter, P. Pyranoanthocyanins - an Overview on Structures, Occurrence, and Pathways of Formation. *Trends Food Sci. Technol.* **2007**, *18*, 526−534.
(110) He, J.; Santos-Buelga, C.; Silva, A. M. S.; Mateus, N.; De Freitas, V. Isolation and Structural Characterization of New Anthocyanin-Derived Yellow Pigments in Aged Red Wines. *J. Agric. Food Chem.* **2006**, *54*, 9598−9603.
(111) Hayasaka, Y.; Asenstorfer, R. E. Screening for Potential Pigments Derived from Anthocyanins in Red Wine Using Nano-Electrospray Tandem Mass Spectrometry. *J. Agric. Food Chem.* **2002**, *50*, 756−761.
(112) Schwarz, M.; Wabnitz, T. C.; Winterhalter, P. Pathway Leading to the Formation of Anthocyanin-Vinylphenol Adducts and Related Pigments in Red Wines. *J. Agric. Food Chem.* **2003**, *51*, 3682−3687.
(113) Schwarz, M.; Winterhalter, P. A Novel Synthetic Route to Substituted Pyranoanthocyanins with Unique Colour Properties. *Tetrahedron Lett.* **2003**, *44*, 7583−7587.
(114) Schwarz, M.; Winterhalter, P. *225th National Meeting of the American Chemical Society*, New Orleans, LA, 2003; American Chemical Society, Washington, DC, 2003; p 179−197.
(115) Mateus, N.; Silva, A. M. S.; Santos-Buelga, C.; Rivas-Gonzalo, J. C.; De Freitas, V. Identification of Anthocyanin-Flavanol Pigments in Red Wines by Nmr and Mass Spectrometry. *J. Agric. Food Chem.* **2002**, *50*, 2110−2116.
(116) Francia-Aricha, E. M.; Guerra, M. T.; Rivas-Gonzalo, J. C.; Santos-Buelga, C. New Anthocyanin Pigments Formed after Condensation with Flavanols. *J. Agric. Food Chem.* **1997**, *45*, 2262−2265.
(117) Rentzsch, M.; Schwarz, M.; Winterhalter, P.; Hermosin-Gutierrez, I. Formation of Hydroxyphenyl-Pyranoanthocyanins in Grenache Wines: Precursor Levels and Evolution During Aging. *J. Agric. Food Chem.* **2007**, *55*, 4883−4888.
(118) Hakansson, A. E.; Pardon, K.; Hayasaka, Y.; de Sa, M.; Herderich, M. Structures and Colour Properties of New Red Wine Pigments. *Tetrahedron Lett.* **2003**, *44*, 4887−4891.
(119) Schwarz, M.; Jerz, G.; Winterhalter, P. Isolation and Structure of Pinotin a, a New Anthocyanin Derivative from Pinotage Wine. *Vitis* **2003**, *42*, 105−106.
(120) Cruz, L.; Teixeira, N.; Silva, A. M. S.; Mateus, N.; Borges, J.; De Freitas, V. Role of Vinylcatechin in the Formation of Pyranomalvidin-3-Glucoside-(+)-Catechin. *J. Agric. Food Chem.* **2008**, *56*, 10980−10987.
(121) Cruz, L.; Borges, E.; Silva, A. M. S.; Mateus, N.; De Freitas, V. Synthesis of a New (+)-Catechin-Derived Compound: 8-Vinylcatechin. *Lett. Org. Chem.* **2008**, *5*, 530−536.
(122) Es-Safi, N. E.; Fulcrand, H.; Cheynier, V.; Moutounet, M. Studies on the Acetaldehyde-Induced Condensation of (−)-Epicatechin and Malvidin 3-O-Glucoside in a Model Solution System. *J. Agric. Food Chem.* **1999**, *47*, 2096−2102.
(123) Bendz, G.; Martensson, O.; Nilsson, E. Studies of Flavylium Compounds. I. Some Flavylium Compounds and Their Properties. *Ark. Kemi* **1967**, *27*, 67−77.
(124) Oliveira, J.; De Freitas, V.; Mateus, N. A Novel Synthetic Pathway to Vitisin B Compounds. *Tetrahedron Lett.* **2009**, *50*, 3933−3935.
(125) He, J. R.; Oliveira, J.; Silva, A. M. S.; Mateus, N.; De Freitas, V. Oxovitisins: A New Class of Neutral Pyranone-Anthocyanin Derivatives in Red Wines. *J. Agric. Food Chem.* **2010**, *58*, 8814−8819.
(126) Mateus, N.; Oliveira, J.; Haettich-Motta, M.; De Freitas, V. New Family of Bluish Pyranoanthocyanins. *J. Biomed. Biotechnol.* **2004**, *2004*, 299−305.
(127) Mateus, N.; Carvalho, E.; Carvalho, A. R. F.; Melo, A.; Gonzalez-Paramas, A. M.; Santos-Buelga, C.; Silva, A. M. S.; De Freitas, V. Isolation and Structural Characterization of New Acylated Anthocyanin-Vinyl-Flavanol Pigments Occurring in Aging Red Wines. *J. Agric. Food Chem.* **2003**, *51*, 277−282.
(128) Mateus, N.; Oliveira, J.; Pissarra, J.; Gonzalez-Paramas, A. M.; Rivas-Gonzalo, J. C.; Santos-Buelga, C.; Silva, A. M. S.; De Freitas, V. A New Vinylpyranoanthocyanin Pigment Occurring in Aged Red Wine. *Food Chem.* **2006**, *97*, 689−695.

https://doi.org/10.1021/acs.chemrev.1c00399
Chem. Rev. 2022, 122, 1416−1481

(129) Oliveira, J.; De Freitas, V.; Silva, A. M. S.; Mateus, N. Reaction between Hydroxycinnamic Acids and Anthocyanin-Pyruvic Acid Adducts Yielding New Portisins. *J. Agric. Food Chem.* **2007**, *55*, 6349−6356.
(130) Mateus, N.; Oliveira, J.; Santos-Buelga, C.; Silva, A. M. S.; De Freitas, V. Nmr Structure Characterization of a New Vinylpyranoanthocyanin-Catechin Pigment (a Portisin). *Tetrahedron Lett.* **2004**, *45*, 3455−3457.
(131) Oliveira, J.; Azevedo, J.; Silva, A. M. S.; Teixeira, N.; Cruz, L.; Mateus, N.; De Freitas, V. Pyranoanthocyanin Dimers: A New Family of Turquoise Blue Anthocyanin-Derived Pigments Found in Port Wine. *J. Agric. Food Chem.* **2010**, *58*, 5154−5159.
(132) Oliveira, J.; Petrov, V.; Parola, A. J.; Pina, F.; Azevedo, J.; Teixeira, N.; Bras, N. F.; Fernandes, P. A.; Mateus, N.; Ramos, M. J.; et al. Chemical Behavior of Methylpyranomalvidin-3-O-Glucoside in Aqueous Solution Studied by Nmr and Uv-Visible Spectroscopy. *J. Phys. Chem. B* **2011**, *115*, 1538−1545.
(133) Chassaing, S.; Isorez, G.; Kueny-Stotz, M.; Brouillard, R. En Route to Color-Stable Pyranoflavylium Pigments—a Systematic Study of the Reaction between 5-Hydroxy-4-Methylflavylium Salts and Aldehydes. *Tetrahedron Lett.* **2008**, *49*, 6999−7004.
(134) Chassaing, S.; Isorez-Mahler, G.; Kueny-Stotz, M.; Brouillard, R. Aged Red Wine Pigments as a Source of Inspiration for Organic Synthesis—the Cases of the Color-Stable Pyranoflavylium and Flavylium-(4→8)-Flavan Chromophores. *Tetrahedron* **2015**, *71*, 3066−3078.
(135) da Silva, C. P.; Pioli, R. M.; Liu, L.; Zheng, S. S.; Zhang, M. J.; Silva, G. T. D.; Carneiro, V. M. T.; Quina, F. H. Improved Synthesis of Analogues of Red Wine Pyranoanthocyanin Pigments. *ACS Omega* **2018**, *3*, 954−960.
(136) Oliveira, J.; Mateus, N.; de Freitas, V. Synthesis of a New Bluish Pigment from the Reaction of a Methylpyranoanthocyanin with Sinapaldehyde. *Tetrahedron Lett.* **2011**, *52*, 1996−2000.
(137) Oliveira, J.; Araújo, P.; Fernandes, A.; Mateus, N.; de Freitas, V. Synthesis and Structural Characterization of Amino-Based Pyranoanthocyanins with Extended Electronic Delocalization. *Synlett* **2016**, *27*, 2459−2462.
(138) Oliveira, J.; Fernandes, A.; de Freitas, V. Synthesis and Structural Characterization by Lc−Ms and Nmr of a New Semi-Natural Blue Amino-Based Pyranoanthocyanin Compound. *Tetrahedron Lett.* **2016**, *57*, 1277−1281.
(139) Cruz, L.; Sousa, J. L. C.; Marinho, A.; Mateus, N.; de Freitas, V. Synthesis and Structural Characterization of Novel Pyranoluteolinidin Dyes. *Tetrahedron Lett.* **2017**, *58*, 159−162.
(140) Sousa, J. L. C.; Gomes, V.; Mateus, N.; Pina, F.; de Freitas, V.; Cruz, L. Synthesis and Equilibrium Multistate of New Pyrano-3-Deoxyanthocyanin-Type Pigments in Aqueous Solutions. *Tetrahedron* **2017**, *73*, 6021−6030.
(141) Vallverdú-Queralt, A.; Meudec, E.; Eder, M.; Lamuela-Raventos, R. M.; Sommerer, N.; Cheynier, V. The Hidden Face of Wine Polyphenol Polymerization Highlighted by High-Resolution Mass Spectrometry. *ChemistryOpen* **2017**, *6*, 336−339.
(142) Vidal, S.; Meudec, E.; Cheynier, V.; Skouroumounis, G.; Hayasaka, Y. Mass Spectrometric Evidence for the Existence of Oligomeric Anthocyanins in Grape Skins. *J. Agric. Food Chem.* **2004**, *52*, 7144−7151.
(143) Alcalde-Eon, C.; Escribano-Bailon, M. T.; Santos-Buelga, C.; Rivas-Gonzalo, J. C. Identification of Dimeric Anthocyanins and New Oligomeric Pigments in Red Wine by Means of Hplc-Dad-Esi/Msn. *J. Mass Spectrom.* **2007**, *42*, 735−748.
(144) Pati, S.; Liberatore, M. T.; Gambacorta, G.; Antonacci, D.; La Notte, E. Rapid Screening for Anthocyanins and Anthocyanin Dimers in Crude Grape Extracts by High Performance Liquid Chromatography Coupled with Diode Array Detection and Tandem Mass Spectrometry. *J. Chromatogr. A* **2009**, *1216*, 3864−3868.
(145) Salas, E.; Duenas, M.; Schwarz, M.; Winterhalter, P.; Cheynier, W.; Fulcrand, H. Characterization of Pigments from Different High Speed Countercurrent Chromatography Wine Fractions. *J. Agric. Food Chem.* **2005**, *53*, 4536−4546.
(146) Oliveira, J.; Bras, N. F.; da Silva, M. A.; Mateus, N.; Parola, A. J.; de Freitas, V. Grape Anthocyanin Oligomerization: A Putative Mechanism for Red Color Stabilization? *Phytochemistry* **2014**, *105*, 178−185.
(147) Remy, S.; Fulcrand, H.; Labarbe, B.; Cheynier, V.; Moutounet, M. First Confirmation in Red Wine of Products Resulting from Direct Anthocyanin-Tannin Reactions. *J. Sci. Food Agric.* **2000**, *80*, 745−751.
(148) Hayasaka, Y.; Kennedy, J. A. Mass Spectrometric Evidence for the Formation of Pigmented Polymers in Red Wine. *Aust. J. Grape Wine Res.* **2003**, *9*, 210−220.
(149) Salas, E.; Atanasova, V.; Poncet-Legrand, C.; Meudec, E.; Mazauric, J. P.; Cheynier, V. Demonstration of the Occurrence of Flavanol-Anthocyanin Adducts in Wine and in Model Solutions. *Anal. Chim. Acta* **2004**, *513*, 325−332.
(150) Cruz, L.; Mateus, N.; De Freitas, V. Identification by Mass Spectrometry of New Compounds Arising from the Reactions Involving Malvidin-3-Glucoside-(O)-Catechin, Catechin and Malvidin-3-Glucoside. *Rapid Commun. Mass Spectrom.* **2012**, *26*, 2123−2130.
(151) Timberlake, C. F.; Bridle, P. Interactions between Anthocyanins, Phenolic Compounds and Acetaldehyde and Their Significance in Red Wines. *Am. J. Enol. Vitic.* **1976**, *27*, 97−105.
(152) Rivas-Gonzalo, J. C.; Bravo-Haro, S.; Santos-Buelga, C. Detection of Compounds Formed through the Reaction of Malvidin-3-Monoglucoside and Catechin in the Presence of Acetaldehyde. *J. Agric. Food Chem.* **1995**, *43*, 1444−1449.
(153) Dallas, C.; Ricardo-da-Silva, J. M.; Laureano, O. Products Formed in Model Wine Solutions Involving Anthocyanins, Procyanidin B-2, and Acetaldehyde. *J. Agric. Food Chem.* **1996**, *44*, 2402−2407.
(154) Escribano-Bailón, T.; Dangles, O.; Brouillard, R. Coupling Reactions between Flavylium Ions and Catechin. *Phytochemistry* **1996**, *41*, 1583−1592.
(155) Lee, D. F.; Swinny, E. E.; Jones, G. P. Nmr Identification of Ethyl-Linked Anthocyanin-Flavanol Pigments Formed in Model Wine Ferments. *Tetrahedron Lett.* **2004**, *45*, 1671−1674.
(156) Sousa, C.; Mateus, N.; Silva, A. M. S.; Gonzalez-Paramas, A. M.; Santos-Buelga, C.; De Freitas, V. Structural and Chromatic Characterization of a New Malvidin 3-Glucoside-Vanillyl-Catechin Pigment. *Food Chem.* **2007**, *102*, 1344−1351.
(157) Pissarra, J.; Lourenco, S.; Gonzalez-Paramas, A. M.; Mateus, N.; Buelga, C. S.; Silva, A. M. S.; De Freitas, V. Isolation and Structural Characterization of New Anthocyanin-Alkyl-Catechin Pigments. *Food Chem.* **2005**, *90*, 81−87.
(158) Pissarra, J.; Lourenco, S.; Gonzalez-Paramas, A. M.; Mateus, N.; Santos-Buelga, C.; De Freitas, V. Formation of New Anthocyanin-Alkyl/Aryl-Flavanol Pigments in Model Solutions. *Anal. Chim. Acta* **2004**, *513*, 215−221.
(159) Atanasova, V.; Fulcrand, H.; Le Guerneve, C.; Cheynier, W.; Moutounet, M. Structure of a New Dimeric Acetaldehyde Malvidin 3-Glucoside Condensation Product. *Tetrahedron Lett.* **2002**, *43*, 6151−6153.
(160) Chassaing, S.; Lefeuvre, D.; Jacquet, R.; Jourdes, M.; Ducasse, L.; Galland, S.; Grelard, A.; Saucier, C.; Teissedre, P. L.; Dangles, O.; et al. Physicochemical Studies of New Anthocyano-Ellagitannin Hybrid Pigments: About the Origin of the Influence of Oak C-Glycosidic Ellagitannins on Wine Color. *Eur. J. Org. Chem.* **2010**, *2010*, 55−63.
(161) García-Estévez, I.; Gavara, R.; Alcalde-Eon, C.; Rivas-Gonzalo, J. C.; Quideau, S.; Escribano-Bailón, M. T.; Pina, F. Thermodynamic and Kinetic Properties of a New Myrtillin−Vescalagin Hybrid Pigment. *J. Agric. Food Chem.* **2013**, *61*, 11569−11578.
(162) Quideau, S.; Jourdes, M.; Lefeuvre, D.; Montaudon, D.; Saucier, C.; Glories, Y.; Pardon, P.; Pourquier, P. The Chemistry of Wine Polyphenolic C-Glycosidic Ellagitannins Targeting Human Topoisomerase Ii. *Chem. - Eur. J.* **2005**, *11*, 6503−6513.
(163) Ferreira da Silva, P.; Lima, J. C.; Freitas, A. A.; Shimizu, K.; Maçanita, A. L.; Quina, F. H. Charge-Transfer Complexation as a General Phenomenon in the Copigmentation of Anthocyanins. *J. Phys. Chem. A* **2005**, *109*, 7329−7338.
(164) Alluis, B.; Pérol, N.; El hajji, H.; Dangles, O. Water-Soluble Flavonol (=3-Hydroxy-2-Phenyl-4h-1-Benzopyran-4-One) Deriva-

https://doi.org/10.1021/acs.chemrev.1c00399
Chem. Rev. 2022, 122, 1416−1481

tives: Chemical Synthesis, Colouring, and Antioxidant Properties. *Helv. Chim. Acta* **2000**, *83*, 428−443.
(165) Wang, Y.; Chen, S.; Yu, O. Metabolic Engineering of Flavonoids in Plants and Microorganisms. *Appl. Microbiol. Biotechnol.* **2011**, *91*, 949−956.
(166) Holton, T. A.; Cornish, E. C. Genetics and Biochemistry of Anthocyanin Biosynthesis. *Plant Cell* **1995**, *7*, 1071−1083.
(167) Tanaka, Y.; Sasaki, N.; Ohmiya, A. Biosynthesis of Plant Pigments: Anthocyanins, Betalains and Carotenoids. *Plant J.* **2008**, *54*, 733−749.
(168) Krisa, S.; Waffo Téguo, P.; Decendit, A.; Deffieux, G.; Vercauteren, J.; Mérillon, J.-M. Production of 13c-Labelled Anthocyanins by Vitis Vinifera Cell Suspension Cultures. *Phytochemistry* **1999**, *51*, 651−656.
(169) Yousef, G. G.; Seigler, D. S.; Grusak, M. A.; Rogers, R. B.; Knight, C. T. G.; Kraft, T. F. B.; Erdman, J. W.; Lila, M. A. Biosynthesis and Characterization of 14c-Enriched Flavonoid Fractions from Plant Cell Suspension Cultures. *J. Agric. Food Chem.* **2004**, *52*, 1138−1145.
(170) Hwang, E. I.; Kaneko, M.; Ohnishi, Y.; Horinouchi, S. Production of Plant-Specific Flavanones by Escherichia Coli Containing an Artificial Gene Cluster. *Appl. Environ. Microbiol.* **2003**, *69*, 2699−2706.
(171) Yan, Y.; Chemler, J.; Huang, L.; Martens, S.; Koffas, M. A. G. Metabolic Engineering of Anthocyanin Biosynthesis in *Escherichia Coli*. *Appl. Environ. Microbiol.* **2005**, *71*, 3617−3623.
(172) Yan, Y.; Li, Z.; Koffas, M. A. G. High-Yield Anthocyanin Biosynthesis in Engineered Escherichia Coli. *Biotechnol. Bioeng.* **2008**, *100*, 126−140.
(173) Eichenberger, M.; Hansson, A.; Fischer, D.; Dürr, L.; Naesby, M. Novo Biosynthesis of Anthocyanins in Saccharomyces Cerevisiae. *FEMS Yeast Res.* **2018**, *18*, foy046.
(174) Zhang, J.-R.; Trossat-Magnin, C.; Bathany, K.; Delrot, S.; Chaudière, J. Oxidative Transformation of Leucocyanidin by Anthocyanidin Synthase from Vitis Vinifera Leads Only to Quercetin. *J. Agric. Food Chem.* **2019**, *67*, 3595−3604.
(175) Denish, P. R.; Fenger, J.-A.; Powers, R.; Sigurdson, G. T.; Grisanti, L.; Guggenheim, K. G.; Laporte, S.; Li, J.; Kondo, T.; Magistrato, A.; et al. Discovery of a Natural Cyan Blue: A Unique Food-Sourced Anthocyanin Could Replace Synthetic Brilliant Blue. *Sci. Adv.* **2021**, *7*, eabe7871.
(176) Butelli, E.; Titta, L.; Giorgio, M.; Mock, H.-P.; Matros, A.; Peterek, S.; Schijlen, E. G. W. M.; Hall, R. D.; Bovy, A. G.; Luo, J.; et al. Enrichment of Tomato Fruit with Health-Promoting Anthocyanins by Expression of Select Transcription Factors. *Nat. Biotechnol.* **2008**, *26*, 1301−1308.
(177) Zhu, Q.; Yu, S.; Zeng, D.; Liu, H.; Wang, H.; Yang, Z.; Xie, X.; Shen, R.; Tan, J.; Li, H.; et al. Development of "Purple Endosperm Rice" by Engineering Anthocyanin Biosynthesis in the Endosperm with a High-Efficiency Transgene Stacking System. *Mol. Plant* **2017**, *10*, 918−929.
(178) Pina, F.; Melo, M. J.; Laia, C. A. T.; Parola, A. J.; Lima, J. C. Chemistry and Applications of Flavylium Compounds: A Handful of Colours. *Chem. Soc. Rev.* **2012**, *41*, 869−908.
(179) Pina, F.; Melo, M. J.; Maestri, M.; Ballardini, R.; Balzani, V. Photochromism of 4'-Methoxyflavylium Perchlorate. A "Write-Lock-Read-Unlock-Erase" Molecular Switching System. *J. Am. Chem. Soc.* **1997**, *119*, 5556−5561.
(180) Basilio, N.; Pina, F. Chemistry and Photochemistry of Anthocyanins and Related Compounds: A Thermodynamic and Kinetic Approach. *Molecules* **2016**, *21*, 1502.
(181) Brouillard, R.; Iacobucci, G. A.; Sweeny, J. G. Chemistry of Anthocyanins Pigments.9. Uv Visible Spectrophotometric Deetrmination of the Acidity Constants of Apigeninidin and 3 Related 3-Deoxyflavylium Salts. *J. Am. Chem. Soc.* **1982**, *104*, 7585−7590.
(182) Brouillard, R.; Delaporte, B.; Dubois, J. E. Chemistry of Anthocyanins Pigments.3. Relaxation Amplitudes in Ph-Jump Experiments. *J. Am. Chem. Soc.* **1978**, *100*, 6202−6205.
(183) Alejo-Armijo, A.; Mendoza, J.; Parola, A. J.; Pina, F. The Chemical Evolution of the Colour Systems Generated by Riccionidin a, 3-Deoxyanthocyanidins and Anthocyanins. *Phytochemistry* **2020**, *174*, 112339.
(184) Brouillard, R.; Dubois, J. E. Mechanism of Structural Transformations of Anthocyanins in Acidic Media. *J. Am. Chem. Soc.* **1977**, *99*, 1359−1364.
(185) McClelland, R. A.; Gedge, S. Hydration of the Flavylium Ion. *J. Am. Chem. Soc.* **1980**, *102*, 5838−5848.
(186) Leydet, Y.; Gavara, R.; Petrov, V.; Diniz, A. M.; Parola, A. J.; Lima, J. C.; Pina, F. The Effect of Self-Aggregation on the Determination of the Kinetic and Thermodynamic Constants of the Network of Chemical Reactions in 3-Glucoside Anthocyanins. *Phytochemistry* **2012**, *83*, 125−135.
(187) Macanita, A. L.; Moreira, P. F.; Lima, J. C.; Quina, F. H.; Yihwa, C.; Vautier-Giongo, C. Proton Transfer in Anthocyanins and Related Flavylium Salts. Determination of Ground-State Rate Constants with Nanosecond Laser Flash Photolysis. *J. Phys. Chem. A* **2002**, *106*, 1248−1255.
(188) Basilio, N.; Al Bittar, S.; Mora, N.; Dangles, O.; Pina, F. Analogs of Natural 3-Deoxyanthocyanins: O-Glucosides of the 4 ',7-Dihydroxyflavylium Ion and the Deep Influence of Glycosidation on Color. *Int. J. Mol. Sci.* **2016**, *17*, 1751.
(189) Rusishvili, M.; Grisanti, L.; Laporte, S.; Micciarelli, M.; Rosa, M.; Robbins, R. J.; Collins, T.; Magistrato, A.; Baroni, S. Unraveling the Molecular Mechanisms of Color Expression in Anthocyanins. *Phys. Chem. Chem. Phys.* **2019**, *21*, 8757−8766.
(190) Fenger, J.-A.; Roux, H.; Robbins, R. J.; Collins, T. M.; Dangles, O. The Influence of Phenolic Acyl Groups on the Color of Purple Sweet Potato Anthocyanins and Their Metal Complexes. *Dyes Pigm.* **2021**, *185*, 108792.
(191) Pina, F. Chemical Applications of Anthocyanins and Related Compounds. A Source of Bioinspiration. *J. Agric. Food Chem.* **2014**, *62*, 6885−6897.
(192) Mendoza, J.; Basilio, N.; de Freitas, V.; Pina, F. New Procedure to Calculate All Equilibrium Constants in Flavylium Compounds: Application to the Copigmentation of Anthocyanins. *ACS Omega* **2019**, *4*, 12058−12070.
(193) Mendoza, J.; Basilio, N.; Pina, F.; Kondo, T.; Yoshida, K. Rationalizing the Color in Heavenly Blue Anthocyanin: A Complete Kinetic and Thermodynamic Study. *J. Phys. Chem. B* **2018**, *122*, 4982−4992.
(194) Moloney, M.; Robbins, R. J.; Collins, T. M.; Kondo, T.; Yoshida, K.; Dangles, O. Red Cabbage Anthocyanins: The Influence of D-Glucose Acylation by Hydroxycinnamic Acids on Their Structural Transformations in Acidic to Mildly Alkaline Conditions and on the Resulting Color. *Dyes Pigm.* **2018**, *158*, 342−352.
(195) Dangles, O.; Saito, N.; Brouillard, R. Kinetic and Thermodynamic Control of Flavylium Hydration in the Pelargonidin Cinnamic Acid Complexation - Origin of the Extraordinary Flower Color Diversity of Pharbitis-Nil. *J. Am. Chem. Soc.* **1993**, *115*, 3125−3132.
(196) Oliveira, H.; Basilio, N.; Pina, F.; Fernandes, I.; de Freitas, V.; Mateus, N. Purple-Fleshed Sweet Potato Acylated Anthocyanins: Equilibrium Network and Photophysical Properties. *Food Chem.* **2019**, *288*, 386−394.
(197) McClelland, R. A.; McGall, G. H. Hydration of the Flvylium Ion.2. The 4'-Hydroxyflavylium Ion. *J. Org. Chem.* **1982**, *47*, 3730−3736.
(198) Pina, F. Anthocyanins and Related Compounds. Detecting the Change of Regime between Rate Control by Hydration or by Tautomerization. *Dyes Pigm.* **2014**, *102*, 308−314.
(199) Mistry, T. V.; Cai, Y.; Lilley, T. H.; Haslam, E. Polyphenol Interactions 0.5. Anthocyanin Copigmentation. *J. Chem. Soc., Perkin Trans. 2* **1991**, 1287−1296.
(200) Houbiers, C.; Lima, J. C.; Macanita, A. L.; Santos, H. Color Stabilization of Malvidin 3-Glucoside: Self-Aggregation of the Flavylium Cation and Copigmentation with the Z-Chalcone Form. *J. Phys. Chem. B* **1998**, *102*, 3578−3585.
(201) Kallam, K.; Appelhagen, I.; Luo, J.; Albert, N.; Zhang, H.; Deroles, S.; Hill, L.; Findlay, K.; Andersen, Ø. M.; Davies, K.; et al.

https://doi.org/10.1021/acs.chemrev.1c00399
Chem. Rev. 2022, 122, 1416−1481

Aromatic Decoration Determines the Formation of Anthocyanic Vacuolar Inclusions. *Curr. Biol.* **2017**, *27*, 945−957.
(202) Francis, F. J.; Markakis, P. C. Food Colorants: Anthocyanins. *Crit. Rev. Food Sci. Nutr.* **1989**, *28*, 273.
(203) Jurd, L. Acid Fruit and Vegetable Food and Method of Coloring Emplying Benzopyrylium Compounds. US Patent 3,301,683, January 31, 1967.
(204) Roehri-Stoeckel, C.; Gonzalez, E.; Fougerousse, A.; Brouillard, R. Synthetic Dyes: Simple and Original Ways to 4-Substituted Flavylium Salts and Their Corresponding Vitisin Derivatives. *Can. J. Chem.* **2001**, *79*, 1173−1178.
(205) Duenas, M.; Salas, E.; Cheynier, V.; Dangles, O.; Fulcrand, H. Uv-Visible Spectroscopic Investigation of the 8,8-Methylmethine Catechin-Malvidin 3-Glucoside Pigments in Aqueous Solution: Structural Transformations and Molecular Complexation with Chlorogenic Acid. *J. Agric. Food Chem.* **2006**, *54*, 189−196.
(206) Melo, M. J.; Sousa, M.; Parola, A. J.; de Melo, J. S. S.; Catarino, F.; Marcalo, J.; Pina, F. Identification of 7,4 '-Dihydroxy-5-Methoxyflavylium in "Dragon's Blood": To Be or Not to Be an Anthocyanin. *Chem. - Eur. J.* **2007**, *13*, 1417−1422.
(207) Olaniyi, A. A.; Powell, J. W.; Whalley, W. B. Pigments of Dragons-Blood Resin.7. Synthesis of (±)-Draconol, (±)-O-Methyldraconol, (±)-O-Methylisodraconol and Derivatives - Structure of Dracorubin. *J. Chem. Soc., Perkin Trans. 1* **1973**, 179−184.
(208) Agbakwuru, E. O. P.; Whalley, W. B. Pigments of Drgoon's Blood Resin.8. Synthesis of (+or-)-Dracorubin and of (+or-)-Nordracorubin. *J. Chem. Soc., Perkin Trans. 1* **1976**, 1392−1394.
(209) CameiradosSantos, P. J.; Brillouet, J. M.; Cheynier, V.; Moutounet, M. Detection and Partial Characterisation of New Anthocyanin-Derived Pigments in Wine. *J. Sci. Food Agric.* **1996**, *70*, 204−208.
(210) Fulcrand, H.; dos Santos, P. J. C.; Sarni Manchado, P.; Cheynier, V.; Favre Bonvin, J. Structure of New Anthocyanin-Derived Wine Pigments. *J. Chem. Soc., Perkin Trans. 1* **1996**, 735−739.
(211) Bakker, J.; Timberlake, C. F. Isolation, Identification, and Characterization of New Color-Stable Anthocyanins Occurring in Some Red Wines. *J. Agric. Food Chem.* **1997**, *45*, 35−43.
(212) Chassaing, S.; Isorez, G.; Kueny-Stotz, M.; Brouillard, R. En Route to Color-Stable Pyranoflavylium Pigments - a Systematic Study of the Reaction between 5-Hydroxy-4-Methylflavylium Salts and Aldehydes. *Tetrahedron Lett.* **2008**, *49*, 6999−7004.
(213) Chassaing, S.; Isorez-Mahler, G.; Kueny-Stotz, M.; Brouillard, R. Aged Red Wine Pigments as a Source of Inspiration for Organic Synthesis the Cases of the Color-Stable Pyranoflavylium and Flavylium-(4 -> 8)-Flavan Chrornophores. *Tetrahedron* **2015**, *71*, 3066−3078.
(214) Oliveira, J.; Araújo, P.; Fernandes, A.; Brás, N. F.; Mateus, N.; Pina, F.; de Freitas, V. Influence of the Structural Features of Amino-Based Pyranoanthocyanins on Their Acid-Base Equilibria in Aqueous Solutions. *Dyes Pigm.* **2017**, *141*, 479−486.
(215) Silva, C. P.; Silva, G. T. M.; Costa, T. D.; Carneiro, V. M. T.; Siddique, F.; Aquino, A. J. A.; Freitas, A. A.; Clark, J. A.; Espinoza, E. M.; Vullev, V. I.; et al. Chromophores Inspired by the Colors of Fruit, Flowers and Wine. *Pure Appl. Chem.* **2020**, *92*, 255−263.
(216) Quijada-Morin, N.; Dangles, O.; Rivas-Gonzalo, J. C.; Escribano-Bailon, M. T. Physico-Chemical and Chromatic Characterization of Malvidin 3-Glucoside-Vinylcatechol and Malvidin 3-Glucoside-Vinylguaiacol Wine Pigments. *J. Agric. Food Chem.* **2010**, *58*, 9744−9752.
(217) Rentzsch, W.; Schwarz, M.; Winterhalter, P. Pyranoanthocyanins - an Overview on Structures, Occurrence, and Pathways of Formation. *Trends Food Sci. Technol.* **2007**, *18*, 526−534.
(218) De Freitas, V.; Mateus, N. Formation of Pyranoanthocyanins in Red Wines: A New and Diverse Class of Anthocyanin Derivatives. *Anal. Bioanal. Chem.* **2011**, *401*, 1463−1473.
(219) Cruz, L.; Petrov, V.; Teixeira, N.; Mateus, N.; Pina, F.; De Freitas, V. Establishment of the Chemical Equilibria of Different Types of Pyranoanthocyanins in Aqueous Solutions: Evidence for the Formation of Aggregation in Pyranomalvidin-3-O-Coumaroylglucoside-(+)-Catechin. *J. Phys. Chem. B* **2010**, *114*, 13232−13240.
(220) Oliveira, J.; Mateus, N.; De Freitas, V. Previous and Recent Advances in Pyranoanthocyanins Equilibria in Aqueous Solution. *Dyes Pigm.* **2014**, *100*, 190−200.
(221) Gomez-Alonso, S.; Blanco-Vega, D.; Gomez, M.; Hermosin-Gutierrez, I. Synthesis, Isolation, Structure Elucidation, and Color Properties of 10-Acetyl-Pyranoanthocyanins. *J. Agric. Food Chem.* **2012**, *60*, 12210−12223.
(222) Mazza, G.; Brouillard, R. Color Stability and Structural Transformations of Cyanidin 3,5-Diglucoside and Four 3-Deoxyanthocyanins in Aqueous Solutions. *J. Agric. Food Chem.* **1987**, *35*, 422−426.
(223) Oliveira, J.; Petrov, V.; Parola, A. J.; Pina, F.; Azevedo, J.; Teixeira, N.; Bras, N. F.; Fernandes, P. A.; Mateus, N.; Ramos, M. J.; et al. Chemical Behavior of Methylpyranomalvidin-3-O-Glucoside in Aqueous Solution Studied by Nmr and Uv-Visible Spectroscopy. *J. Phys. Chem. B* **2011**, *115*, 1538−1545.
(224) Vallverdu-Queralt, A.; Biler, M.; Meudec, E.; Le Guerneve, C.; Vernhet, A.; Mazauric, J. P.; Legras, J. L.; Loonis, M.; Trouillas, P.; Cheynier, V.; et al. p-Hydroxyphenyl-Pyranoanthocyanins: An Experimental and Theoretical Investigation of Their Acid-Base Properties and Molecular Interactions. *Int. J. Mol. Sci.* **2016**, *17*, 1842.
(225) Oliveira, J.; Mateus, N.; Silva, A. M. S.; De Freitas, V. Equilibrium Forms of Vitisin B Pigments in an Aqueous System Studied by Nmr and Visible Spectroscopy. *J. Phys. Chem. B* **2009**, *113*, 11352−11358.
(226) Oliveira, J.; Mateus, N.; de Freitas, V. Network of Carboxypyranomalvidin-3-O-Glucoside (Vitisin a) Equilibrium Forms in Aqueous Solution. *Tetrahedron Lett.* **2013**, *54*, 5106−5110.
(227) Chakravarty, G.; Seshadri, T. R. Study of 3,2-Furanoflavylium Chlorides. *Indian J. Chem.* **1964**, *2*, 319−323.
(228) Alejo-Armijo, A.; Basilio, N.; Freitas, A. A.; Macanita, A. L.; Lima, J. C.; Parola, A. J.; Pina, F. Ground and Excited State Properties of Furanoflavylium Derivatives. *Phys. Chem. Chem. Phys.* **2019**, *21*, 21651−21662.
(229) Berland, H.; Albert, N. W.; Stavland, A.; Jordheim, M.; McGhie, T. K.; Zhou, Y. F.; Zhang, H. B.; Deroles, S. C.; Schwinn, K. E.; Jordan, B. R.; et al. Auronidins Are a Previously Unreported Class of Flavonoid Pigments That Challenges When Anthocyanin Biosynthesis Evolved in Plants. *Proc. Natl. Acad. Sci. U. S. A.* **2019**, *116*, 20232−20239.
(230) Snell, K. R. S.; Kokubun, T.; Griffiths, H.; Convey, P.; Hodgson, D. A.; Newsham, K. K. Quantifying the Metabolic Cost to an Antarctic Liverwort of Responding to an Abrupt Increase in Uvb Radiation Exposure. *Glob. Chang. Biol.* **2009**, *15*, 2563−2573.
(231) Kunz, S.; Becker, H. Bibenzyl Derivatives from the Liverwort Ricciocarpos Natans. *Phytochemistry* **1994**, *36*, 675−677.
(232) Taniguchi, S.; Yazaki, K.; Yabu-uchi, R.; Kawakami, K.; Ito, H.; Hatano, T.; Yoshida, T. Galloylglucoses and Riccionidin a in Rhus Javanica Adventitious Root Cultures. *Phytochemistry* **2000**, *53*, 357−363.
(233) Dyker, G.; Bauer, M. Synthesis of 2,3,6,8-Tetrahydroxybenzofuro 3,2-B 1 Benzopyrylium Chloride (Riccionidin a). *J. Prakt. Chem./Chem.-Ztg.* **1998**, *340*, 271−273.
(234) Alejo-Armijo, A.; Parola, A. J.; Pina, F. Ph-Dependent Multistate System Generated by a Synthetic Furanoflavylium Compound: An Ancestor of the Anthocyanin Multistate of Chemical Species. *ACS Omega* **2019**, *4*, 4091−4100.
(235) Gomes, R.; Diniz, A. M.; Jesus, A.; Parola, A. J.; Pina, F. The Synthesis and Reaction Network of 2-Styryl-1-Benzopyrylium Salts: An Unexploited Cass of Potential Colorants. *Dyes Pigm.* **2009**, *81*, 69−79.
(236) Pina, F.; Melo, M. J.; Parola, A. J.; Maestri, M.; Balzani, V. Ph-Controlled Photochromism of Hydroxyflavylium Ions. *Chem. - Eur. J.* **1998**, *4*, 2001−2007.
(237) Felle, H. H. Ph Regulation in Anoxic Plants. *Ann. Bot.* **2005**, *96*, 519−532.
(238) Echeverria, E.; Burns, J.; Felle, H. Compartmentation and Cellular Conditions Controlling Sucrose Breakdown in Mature Acid Lime Fruits. *Phytochemistry* **1992**, *31*, 4091−4095.

https://doi.org/10.1021/acs.chemrev.1c00399
Chem. Rev. 2022, 122, 1416−1481

(239) Figueiredo, P.; George, F.; Tatsuzawa, F.; Toki, K.; Saito, N.; Brouillard, R. New Features of Intramolecular Copigmentation by Acylated Anthocyanins. *Phytochemistry* **1999**, *51*, 125−132.
(240) Moloney, M.; Robbins, R. J.; Collins, T. M.; Kondo, T.; Yoshida, K.; Dangles, O. Red Cabbage Anthocyanins: The Influence of D-Glucose Acylation by Hydroxycinnamic Acids on Their Structural Transformations in Acidic to Mildly Alkaline Conditions and on the Resulting Color. *Dyes Pigm.* **2018**, *158*, 342−352.
(241) Gerard, V.; Ay, E.; Morlet-Savary, F.; Graff, B.; Galopin, C.; Ogren, T.; Mutilangi, W.; Lalevee, J. Thermal and Photochemical Stability of Anthocyanins from Black Carrot, Grape Juice, and Purple Sweet Potato in Model Beverages in the Presence of Ascorbic Acid. *J. Agric. Food Chem.* **2019**, *67*, 5647−5660.
(242) Gras, C. C.; Nemetz, N.; Carle, R.; Schweiggert, R. M. Anthocyanins from Purple Sweet Potato (Ipomoea Batatas (L.) Lam.) and Their Color Modulation by the Addition of Phenolic Acids and Food-Grade Phenolic Plant Extracts. *Food Chem.* **2017**, *235*, 265−274.
(243) Li, J.; Li, X. D.; Zhang, Y.; Zheng, Z. D.; Qu, Z. Y.; Liu, M.; Zhu, S. H.; Liu, S.; Wang, M.; Qu, L. Identification and Thermal Stability of Purple-Fleshed Sweet Potato Anthocyanins in Aqueous Solutions with Various Ph Values and Fruit Juices. *Food Chem.* **2013**, *136*, 1429−1434.
(244) Sigurdson, G. T.; Robbins, R. J.; Collins, T. M.; Giusti, M. M. Molar Absorptivities (Epsilon) and Spectral and Colorimetric Characteristics of Purple Sweet Potato Anthocyanins. *Food Chem.* **2019**, *271*, 497−504.
(245) Eichhorn, S.; Winterhalter, P. Anthocyanins from Pigmented Potato (Solanum Tuberosum L.) Varieties. *Food Res. Int.* **2005**, *38*, 943−948.
(246) Li, A. R.; Xiao, R. S.; He, S. J.; An, X. Y.; He, Y.; Wang, C. T.; Yin, S.; Wang, B.; Shi, X. W.; He, J. R. Research Advances of Purple Sweet Potato Anthocyanins: Extraction, Identification, Stability, Bioactivity, Application, and Biotransformation. *Molecules* **2019**, *24*, 3816.
(247) Zhao, C. L.; Yu, Y. Q.; Chen, Z. J.; Wen, G. S.; Wei, F. G.; Zheng, Q.; Wang, C. D.; Xiao, X. L. Stability-Increasing Effects of Anthocyanin Glycosyl Acylation. *Food Chem.* **2017**, *214*, 119−128.
(248) Sharif, N.; Khoshnoudi-Nia, S.; Jafari, S. M. Nano/Micro-encapsulation of Anthocyanins; a Systematic Review and Meta-Analysis. *Food Res. Int.* **2020**, *132*, 109077.
(249) Yousuf, B.; Gul, K.; Wani, A. A.; Singh, P. Health Benefits of Anthocyanins and Their Encapsulation for Potential Use in Food Systems: A Review. *Crit. Rev. Food Sci. Nutr.* **2016**, *56*, 2223−2230.
(250) Celli, G. B.; Ghanem, A.; Brooks, M. S. L. Optimized Encapsulation of Anthocyanin-Rich Extract from Haskap Berries (*Lonicera Caerulea L.*) in Calcium-Alginate Microparticles. *J. Berry Res.* **2016**, *6*, 1−11.
(251) Guldiken, B.; Gibis, M.; Boyacioglu, D.; Capanoglu, E.; Weiss, J. Impact of Liposomal Encapsulation on Degradation of Anthocyanins of Black Carrot Extract by Adding Ascorbic Acid. *Food Funct.* **2017**, *8*, 1085−1093.
(252) Zhao, L.-y.; Chen, J.; Wang, Z.-q.; Shen, R.-m.; Cui, N.; Sun, A.-d. Direct Acylation of Cyanidin-3-Glucoside with Lauric Acid in Blueberry and Its Stability Analysis. *Int. J. Food Prop.* **2016**, *19*, 1−12.
(253) Cruz, L.; Fernandes, V. C.; Araújo, P.; Mateus, N.; de Freitas, V. Synthesis, Characterisation and Antioxidant Features of Procyanidin B4 and Malvidin-3-Glucoside Stearic Acid Derivatives. *Food Chem.* **2015**, *174*, 480−486.
(254) Grajeda-Iglesias, C.; Salas, E.; Barouh, N.; Baréa, B.; Figueroa-Espinoza, M. C. Lipophilization and Ms Characterization of the Main Anthocyanins Purified from Hibiscus Flowers. *Food Chem.* **2017**, *230*, 189−194.
(255) Cruz, L.; Guimaraes, M.; Araujo, P.; Evora, A.; de Freitas, V.; Mateus, N. Malvidin 3-Glucoside-Fatty Acid Conjugates: From Hydrophilic toward Novel Lipophilic Derivatives. *J. Agric. Food Chem.* **2017**, *65*, 6513−6518.
(256) De Castro, V. C.; Alves da Silva, P. H.; de Oliveira, E. B.; Desobry, S.; Humeau, C. Extraction, Identification and Enzymatic Synthesis of Acylated Derivatives of Anthocyanins from Jaboticaba (*Myrciaria Cauliflora*) Fruits. *Int. J. Food Sci. Technol.* **2014**, *49*, 196−204.
(257) Yang, W.; Kortesniemi, M.; Yang, B.; Zheng, J. Enzymatic Acylation of Anthocyanins Isolated from Alpine Bearberry (*Arctostaphylos Alpina*) and Lipophilic Properties, Thermostability, and Antioxidant Capacity of the Derivatives. *J. Agric. Food Chem.* **2018**, *66*, 2909−2916.
(258) Cruz, L.; Benohoud, M.; Rayner, C. M.; Mateus, N.; de Freitas, V.; Blackburn, R. S. Selective Enzymatic Lipophilization of Anthocyanin Glucosides from Blackcurrant (*Ribes Nigrum L.*) Skin Extract and Characterization of Esterified Anthocyanins. *Food Chem.* **2018**, *266*, 415−419.
(259) Cruz, L.; Fernandes, I.; Guimaraes, M.; de Freitas, V.; Mateus, N. Enzymatic Synthesis, Structural Characterization and Antioxidant Capacity Assessment of a New Lipophilic Malvidin-3-Glucoside-Oleic Acid Conjugate. *Food Funct.* **2016**, *7*, 2754−2762.
(260) Cruz, L.; Guimarães, M.; Araújo, P.; Évora, A.; de Freitas, V.; Mateus, N. Malvidin 3-Glucoside−Fatty Acid Conjugates: From Hydrophilic toward Novel Lipophilic Derivatives. *J. Agric. Food Chem.* **2017**, *65*, 6513−6518.
(261) Guimarães, M.; Mateus, N.; de Freitas, V.; Cruz, L. Improvement of the Color Stability of Cyanidin-3-Glucoside by Fatty Acid Enzymatic Acylation. *J. Agric. Food Chem.* **2018**, *66*, 10003−10010.
(262) Mendoza, J.; Pina, F.; Basílio, N.; Guimarães, M.; de Freitas, V.; Cruz, L. Extending the Stability of Red and Blue Colors of Malvidin-3-Glucoside-Lipophilic Derivatives in the Presence of Sds Micelles. *Dyes Pigm.* **2018**, *151*, 321−326.
(263) Cruz, L.; Basílio, N.; de Freitas, V. Color Stabilization of Cyanidin-3-Glucoside-Based Dyes by Encapsulation with Biocompatible Pegylated Phospholipid Micelles. *Dyes Pigm.* **2020**, *181*, 108592.
(264) Lima, J. C.; Vautier-Giongo, C.; Lopes, A.; Melo, E.; Quina, F. H.; Macanita, A. L. Color Stabilization of Anthocyanins: Effect of Sds Micelles on the Acid-Base and Hydration Kinetics of Malvidin 3-Glucoside (Oenin). *J. Phys. Chem. A* **2002**, *106*, 5851−5859.
(265) Bandara, H. M. D.; Burdette, S. C. Photoisomerization in Different Classes of Azobenzene. *Chem. Soc. Rev.* **2012**, *41*, 1809−1825.
(266) Irie, M.; Fukaminato, T.; Matsuda, K.; Kobatake, S. Photochromism of Diarylethene Molecules and Crystals: Memories, Switches, and Actuators. *Chem. Rev.* **2014**, *114*, 12174−12277.
(267) Klajn, R. Spiropyran-Based Dynamic Materials. *Chem. Soc. Rev.* **2014**, *43*, 148−184.
(268) Kortekaas, L.; Browne, W. R. The Evolution of Spiropyran: Fundamentals and Progress of an Extraordinarily Versatile Photochrome. *Chem. Soc. Rev.* **2019**, *48*, 3406−3424.
(269) Silva, V. O.; Freitas, A. A.; Maçanita, A. L.; Quina, F. H. Chemistry and Photochemistry of Natural Plant Pigments: The Anthocyanins. *J. Phys. Org. Chem.* **2016**, *29*, 594−599.
(270) Xiong, Y.; Zhang, P. Z.; Warner, R. D.; Fang, Z. X. 3-Deoxyanthocyanidin Colorant: Nature, Health, Synthesis, and Food Applications. *Compr. Rev. Food Sci. Food Saf.* **2019**, *18*, 1533−1549.
(271) Pina, F.; Melo, M. J.; Ballardini, R.; Flamigni, L.; Maestri, M. Flash Photolysis of 4',7-Dihydroxyflavylium Perchlorate. *New J. Chem.* **1997**, *21*, 969−976.
(272) Castet, F.; Champagne, B.; Pina, F.; Rodriguez, V. A Multistate Ph-Triggered Nonlinear Optical Switch. *ChemPhysChem* **2014**, *15*, 2221−2224.
(273) Gago, S.; Basílio, N.; Moro, A. J.; Pina, F. Flavylium Based Dual Photochromism: Addressing Cis−Trans Isomerization and Ring Opening-Closure by Different Light Inputs. *Chem. Commun.* **2015**, *51*, 7349−7351.
(274) Horiuchi, H.; Shirase, H.; Okutsu, T.; Matsushima, R.; Hiratsuka, H. Photochromism of 2-Hydroxy-4″-Methoxychalcone: A Novel Photon-Mode Erasable Optical Memory System with Nondestructive Readout Ability. *Chem. Lett.* **2000**, *29*, 96−97.
(275) Wünscher, H.; Haucke, G.; Czerney, P.; Kurzer, U. Photochromic Properties of Hydrolyzed Benzopyrylium Salts—the Influence of Substituents. *J. Photochem. Photobiol., A* **2002**, *151*, 75−82.
(276) Costa, D.; Galvão, A. M.; Di Paolo, R. E.; Freitas, A. A.; Lima, J. C.; Quina, F. H.; Maçanita, A. L. Photochemistry of the Hemiketal

https://doi.org/10.1021/acs.chemrev.1c00399
Chem. Rev. 2022, 122, 1416−1481

Form of Anthocyanins and Its Potential Role in Plant Protection from Uv-B Radiation. *Tetrahedron* **2015**, *71*, 3157−3162.
(277) Weller, A. Allgemeine Basenkatalyse Bei Der Elektrolytischen Dissoziation Angeregter Naphthole. *Zeitschrift für Elektrochemie, Berichte der Bunsengesellschaft für physikalische Chemie* **1954**, *58*, 849−853.
(278) Basilio, N.; Laia, C. A. T.; Pina, F. Excited-State Proton Transfer in Confined Medium. 4-Methy1−7-Hydroxyflavylium and Beta-Naphthol Incorporated in Cucurbit 7 Uril. *J. Phys. Chem. B* **2015**, *119*, 2749−2757.
(279) In reference Basílio, N.; Laia, C. A. T. Excited-State Proton Transfer in Confined Medium. 4-Methy1-7-hydroxyflavylium and beta-Naphthol Incorporated in Cucurbit[7]uril. *J. Phys. Chem. B* **2015**, *119*, 2749−2757 where is written k_{ap}^{*} shoul be k_{a}^{*} (rate constant that gives A* from AH^{+*}) in Scheme 6.1.
(280) Moreira, P. F.; Giestas, L.; Yihwa, C.; Vautier-Giongo, C.; Quina, F. H.; Macanita, A. L.; Lima, J. C. Ground- and Excited-State Proton Transfer in Anthocyanins: From Weak Acids to Super-photoacids. *J. Phys. Chem. A* **2003**, *107*, 4203−4210.
(281) Lima, J. C.; Abreu, I.; Brouillard, R.; Macanita, A. L. Kinetics of Ultra-Fast Excited State Proton Transfer from 7-Hydroxy-4-Methyl-flavylium Chloride to Water. *Chem. Phys. Lett.* **1998**, *298*, 189−195.
(282) Freitas, A. A.; Quina, F. H.; Macanita, A. A. L. Femtosecond and Temperature-Dependent Picosecond Dynamics of Ultrafast Excited-State Proton Transfer in Water-Dioxane Mixtures. *J. Phys. Chem. A* **2014**, *118*, 10448−10455.
(283) Pina, F.; Melo, M. J.; Santos, H.; Lima, J. C.; Abreu, I.; Ballardini, R.; Maestri, M. Excited State Proton Transfer in Synthetic Flavylium Salts: 4-Methyl-7-Hydroxyflavylium and 4 ',7-Dihydroxy-flavylium - Example of a Four-Level Molecular Device to Invert the Population of the Excited State. *New J. Chem.* **1998**, *22*, 1093−1098.
(284) Freitas, A. A.; Silva, C. P.; Silva, G. T. M.; Macanita, A. L.; Quina, F. H. Ground- and Excited-State Acidity of Analogs of Red Wine Pyranoanthocyanins. *Photochem. Photobiol.* **2018**, *94*, 1086−1091.
(285) Freitas, A. A.; Silva, C. P.; Silva, G. T. M.; Macanita, A. L.; Quina, F. H. From Vine to Wine: Photophysics of a Pyranoflavylium Analog of Red Wine Pyranoanthocyanins. *Pure Appl. Chem.* **2017**, *89*, 1761−1767.
(286) Silva, G. T. M.; Thomas, S. S.; Silva, C. P.; Schlothauer, J. C.; Baptista, M. S.; Freitas, A. A.; Bohne, C.; Quina, F. H. Triplet Excited States and Singlet Oxygen Production by Analogs of Red Wine Pyranoanthocyanins. *Photochem. Photobiol.* **2019**, *95*, 176−182.
(287) Lakowicz, J. R. *Principles of Fluorescence Spectroscopy*; Springer: New York, 2006; pp 623−673.
(288) Czerney, P.; Graness, G.; Birckner, E.; Vollmer, F.; Rettig, W. Molecular Engineering of Cyanin-Type Fluorescent and Lases-Dyes. *J. Photochem. Photobiol., A* **1995**, *89*, 31−36.
(289) Lindauer, H.; Czerney, P.; Mohr, G. J.; Grummt, U.-W. New near Infrared Absorbing Acidochromic Dyes and Their Application in Sensor Techniques. *Dyes Pigm.* **1994**, *26*, 229−235.
(290) Rettig, W.; Majenz, W.; Lapouyade, R.; Haucke, F. Multi-dimensional Photochemistry in Flexible Dye Systems. *J. Photochem. Photobiol., A* **1992**, *62*, 415−427.
(291) Chen, H.; Dong, B.; Tang, Y.; Lin, W. A Unique "Integration" Strategy for the Rational Design of Optically Tunable near-Infrared Fluorophores. *Acc. Chem. Res.* **2017**, *50*, 1410−1422.
(292) Zhou, L.; Wang, Q.; Tan, Y.; Lang, M. J.; Sun, H.; Liu, X. Rational Development of near-Infrared Fluorophores with Large Stokes Shifts, Bright One-Photon, and Two-Photon Emissions for Bioimaging and Biosensing Applications. *Chem. - Eur. J.* **2017**, *23*, 8736−8740.
(293) Chen, H.; Lin, W.; Jiang, W.; Dong, B.; Cui, H.; Tang, Y. Locked-Flavylium Fluorescent Dyes with Tunable Emission Wavelengths Based on Intramolecular Charge Transfer for Multi-Color Ratiometric Fluorescence Imaging. *Chem. Commun.* **2015**, *51*, 6968−6971.
(294) Pessêgo, M.; Gago, S.; Basílio, N.; Laia, C. A. T.; Jorge Parola, A.; Lima, J. C.; Pina, F. Hiding and Unveiling Trans-Chalcone in a Constrained Derivative of 4′,7-Dihydroxyflavylium in Water: A Versatile Photochromic System. *Org. Biomol. Chem.* **2017**, *15*, 338−347.
(295) Kopainsky, B.; Qiu, P.; Kaiser, W.; Sens, B.; Drexhage, K. H. Lifetime, Photostability, and Chemical-Structure of Ir Heptamethine Cyanine Dyes Absorbing Beyond 1 Mu-Mm. *Appl. Phys. B: Photophys. Laser Chem.* **1982**, *29*, 15−18.
(296) Cosco, E. D.; Caram, J. R.; Bruns, O. T.; Franke, D.; Day, R. A.; Farr, E. P.; Bawendi, M. G.; Sletten, E. M. Flavylium Polymethine Fluorophores for near- and Shortwave Infrared Imaging. *Angew. Chem., Int. Ed.* **2017**, *56*, 13126−13129.
(297) Cherepy, N. J.; Smestad, G. P.; Gratzel, M.; Zhang, J. Z. Ultrafast Electron Injection: Implications for a Photoelectrochemical Cell Utilizing an Anthocyanin Dye-Sensitized Tio2 Nanocrystalline Electrode. *J. Phys. Chem. B* **1997**, *101*, 9342−9351.
(298) Calogero, G.; Sinopoli, A.; Citro, I.; Di Marco, G.; Petrov, V.; Diniz, A. M.; Parola, A. J.; Pina, F. Synthetic Analogues of Anthocyanins as Sensitizers for Dye-Sensitized Solar Cells. *Photochem. Photobiol. Sci.* **2013**, *12*, 883−894.
(299) Pinto, A. L.; Cruz, L.; Gomes, V.; Cruz, H.; Calogero, G.; de Freitas, V.; Pina, F.; Parola, A. J.; Carlos Lima, J. Catechol Versus Carboxyl Linkage Impact on Dssc Performance of Synthetic Pyranoflavylium Salts. *Dyes Pigm.* **2019**, *170*, 107577.
(300) Phan, K.; De Meester, S.; Raes, K.; De Clerck, K.; Van Speybroeck, V. A Comparative Study on the Photophysical Properties of Anthocyanins and Pyranoanthocyanins. *Chem. - Eur. J.* **2021**, *27*, 5956−5971.
(301) Blanco-Gómez, A.; Cortón, P.; Barravecchia, L.; Neira, I.; Pazos, E.; Peinador, C.; García, M. D. Controlled Binding of Organic Guests by Stimuli-Responsive Macrocycles. *Chem. Soc. Rev.* **2020**, *49*, 3834−3862.
(302) Grzelczak, M.; Liz-Marzan, L. M.; Klajn, R. Stimuli-Responsive Self-Assembly of Nanoparticles. *Chem. Soc. Rev.* **2019**, *48*, 1342−1361.
(303) Qu, D. H.; Wang, Q. C.; Zhang, Q. W.; Ma, X.; Tian, H. Photoresponsive Host-Guest Functional Systems. *Chem. Rev.* **2015**, *115*, 7543−7588.
(304) Ceroni, P.; Credi, A.; Venturi, M. Light to Investigate (Read) and Operate (Write) Molecular Devices and Machines. *Chem. Soc. Rev.* **2014**, *43*, 4068−4083.
(305) Szymanski, W.; Beierle, J. M.; Kistemaker, H. A. V.; Velema, W. A.; Feringa, B. L. Reversible Photocontrol of Biological Systems by the Incorporation of Molecular Photoswitches. *Chem. Rev.* **2013**, *113*, 6114−6178.
(306) Steed, J. W.; Atwood, J. L. *Supramolecular Chemistry*; John Wiley & Sons, 2013.
(307) Szejtli, J. Introduction and General Overview of Cyclodextrin Chemistry. *Chem. Rev.* **1998**, *98*, 1743−1753.
(308) Connors, K. A. The Stability of Cyclodextrin Complexes in Solution. *Chem. Rev.* **1997**, *97*, 1325−1357.
(309) Crini, G. Review: A History of Cyclodextrins. *Chem. Rev.* **2014**, *114*, 10940−10975.
(310) Del Valle, E. M. M. Cyclodextrins and Their Uses: A Review. *Process Biochem.* **2004**, *39*, 1033−1046.
(311) Dangles, O.; Brouillard, R. A Spectroscopic Method Based on the Anthocyanin Copigmentation Interaction and Applied to the Quantitative Study of Molecular-Complexes. *J. Chem. Soc., Perkin Trans. 2* **1992**, *2*, 247−257.
(312) Yamada, T.; Komiya, T.; Akaki, M. Formation of an Inclusion Complex of Anthocyanin with Cyclodextrin. *Agric. Biol. Chem.* **1980**, *44*, 1411−1413.
(313) Dangles, O.; Wigand, M. C.; Brouillard, R. Anthocyanin Anti-Copigment Effect. *Phytochemistry* **1992**, *31*, 3811−3812.
(314) Fernandes, A.; Sousa, A.; Azevedo, J.; Mateus, N.; de Freitas, V. Effect of Cyclodextrins on the Thermodynamic and Kinetic Properties of Cyanidin-3-O-Glucoside. *Food Res. Int.* **2013**, *51*, 748−755.
(315) Fernandes, A.; Ivanova, G.; Bras, N. F.; Mateus, N.; Ramos, M. J.; Rangel, M.; de Freitas, V. Structural Characterization of Inclusion Complexes between Cyanidin-3−0-Glucoside and Beta-Cyclodextrin. *Carbohydr. Polym.* **2014**, *102*, 269−277.

https://doi.org/10.1021/acs.chemrev.1c00399
Chem. Rev. 2022, 122, 1416−1481

(316) Dangles, O.; Stoeckel, C.; Wigand, M. C.; Brouillard, R. Two Very Distinct Types of Anthocyanin Complexation: Copigmentation and Inclusion. *Tetrahedron Lett.* **1992**, *33*, 5227−5230.
(317) Nepogodiev, S. A.; Stoddart, J. F. Cyclodextrin-Based Catenanes and Rotaxanes. *Chem. Rev.* **1998**, *98*, 1959−1976.
(318) Kaifer, A. E. Interplay between Molecular Recognition and Redox Chemistry. *Acc. Chem. Res.* **1999**, *32*, 62−71.
(319) Harada, A.; Takashima, Y.; Yamaguchi, H. Cyclodextrin-Based Supramolecular Polymers. *Chem. Soc. Rev.* **2009**, *38*, 875−882.
(320) Harada, A.; Hashidzume, A.; Yamaguchi, H.; Takashima, Y. Polymeric Rotaxanes. *Chem. Rev.* **2009**, *109*, 5974−6023.
(321) Harada, A. Cyclodextrin-Based Molecular Machines. *Acc. Chem. Res.* **2001**, *34*, 456−464.
(322) Basilio, N.; Fernandes, A.; de Freitas, V.; Gago, S.; Pina, F. Effect of Beta-Cyclodextrin on the Chemistry of 3 ',4 ',7-Trihydroxyflavylium. *New J. Chem.* **2013**, *37*, 3166−3173.
(323) Petrov, V.; Stanimirov, S.; Petrov, I. K.; Fernandes, A.; de Freitas, V.; Pina, F. Emptying the Beta-Cyclodextrin Cavity by Light: Photochemical Removal of the Trans-Chalcone of 4 ',7-Dihydroxyflavylium. *J. Phys. Chem. A* **2013**, *117*, 10692−10701.
(324) Gago, S.; Basilio, N.; Fernandes, A.; Freitas, V.; Quintas, A.; Pina, F. Photochromism of the Complex between 4'-(2-Hydroxyethoxy)-7-Hydroxyflavylium and Beta-Cyclodextrin, Studied by H-1 Nmr, Uv-Vis, Continuous Irradiation and Circular Dichroism. *Dyes Pigm.* **2014**, *110*, 106−112.
(325) Lopes-Costa, T.; Basilio, N.; Pedrosa, J. M.; Pina, F. Photochromism of the Natural Dye 7,4 '-Dihydroxy-5-Methoxyflavylium (Dracoflavylium) in the Presence of (2-Hydroxypropyl)-Beta-Cyclodextrin. *Photochem. Photobiol. Sci.* **2014**, *13*, 1420−1426.
(326) Petrov, V.; Slavcheva, S.; Stanimirov, S.; Pina, F. Origin of the Metastable Stability in Flavylium Multistate Systems. *J. Phys. Chem. A* **2015**, *119*, 2908−2918.
(327) Gago, S.; Basilio, N.; Quintas, A.; Pina, F. Effect of Beta-Cyclodextrin on the Multistate Species Distribution of 3-Methoxy-4',7-Dihydroxyflavylium. Discrimination of the Two Hemiketal Enantiomers. *J. Agric. Food Chem.* **2017**, *65*, 6346−6358.
(328) Mendoza, J.; Basilio, N.; Dangles, O.; Mora, N.; Al Bittar, S.; Pina, F. Binding of the Five Multistate Species of the Anthocyanin Analog 7-Beta-D-Glucopyranosyloxy-4'-Hydroxyflavylium to the Beta-Cyclodextrin Derivative Captisol. *Dyes Pigm.* **2017**, *143*, 479−487.
(329) Basilio, N.; Pina, F. Flavylium Network of Chemical Reactions in Confined Media: Modulation of 3 ',4 ',7-Trihydroxyflavilium Reactions by Host-Guest Interactions with Cucurbit[7]Uril. *ChemPhysChem* **2014**, *15*, 2295−2302.
(330) Basilio, N.; Cabrita, L.; Pina, F. Mimicking Positive and Negative Copigmentation Effects in Anthocyanin Analogues by Host-Guest Interaction with Cucurbit[7]Uril and Beta-Cyclodextrins. *J. Agric. Food Chem.* **2015**, *63*, 7624−7629.
(331) Basilio, N.; Petrov, V.; Pina, F. Host-Guest Complexes of Flavylium Cations and Cucurbit[7]Uril: The Influence of Flavylium Substituents on the Structure and Stability of the Complex. *ChemPlusChem* **2015**, *80*, 1779−1785.
(332) Diniz, A. M.; Basilio, N.; Cruz, H.; Pina, F.; Parola, A. J. Spatiotemporal Control over the Co-Conformational Switching in Ph-Responsive Flavylium-Based Multistate Pseudorotaxanes. *Faraday Discuss.* **2015**, *185*, 361−379.
(333) Basilio, N.; Cruz, L.; de Freitas, V.; Pina, F. A Multistate Molecular Switch Based on the 6,8-Rearrangement in Bromo-Apigeninidin Operated with Ph and Host- Guest Inputs. *J. Phys. Chem. B* **2016**, *120*, 7053−7061.
(334) Basilio, N.; Pischel, U. Drug Delivery by Controlling a Supramolecular Host-Guest Assembly with a Reversible Photoswitch. *Chem. - Eur. J.* **2016**, *22*, 15208−15211.
(335) Seco, A.; Diniz, A. M.; Sarrato, J.; Mourao, H.; Cruz, H.; Parola, A. J.; Basilio, N. A Pseudorotaxane Formed from a Cucurbit[7] Uril Wheel and a Bioinspired Molecular Axle with Ph, Light and Redox-Responsive Properties. *Pure Appl. Chem.* **2020**, *92*, 301−313.
(336) Romero, M. A.; Fernandes, R. J.; Moro, A. J.; Basilio, N.; Pischel, U. Light-Induced Cargo Release from a Cucurbit[8]Uril Host by Means of a Sequential Logic Operation. *Chem. Commun.* **2018**, *54*, 13335.
(337) Held, B.; Tang, H.; Natarajan, P.; da Silva, C. P.; Silva, V. D.; Bohne, C.; Quina, F. H. Cucurbit[7]Uril Inclusion Complexation as a Supramolecular Strategy for Color Stabilization of Anthocyanin Model Compounds. *Photochem. Photobiol. Sci.* **2016**, *15*, 752−757.
(338) Zubillaga, A.; Ferreira, P.; Parola, A. J.; Gago, S.; Basilio, N. Ph-Gated Photoresponsive Shuttling in a Water-Soluble Pseudorotaxane. *Chem. Commun.* **2018**, *54*, 2743−2746.
(339) Basilio, N.; Laia, C. A. T.; Pina, F. Excited-State Proton Transfer in Confined Medium. 4-Methy1−7-Hydroxyflavylium and Beta-Naphthol Incorporated in Cucurbit[7]Uril. *J. Phys. Chem. B* **2015**, *119*, 2749−2757.
(340) Lagona, J.; Mukhopadhyay, P.; Chakrabarti, S.; Isaacs, L. The Cucurbit[N]Uril Family. *Angew. Chem., Int. Ed.* **2005**, *44*, 4844−4870.
(341) Kim, K.; Selvapalam, N.; Ko, Y. H.; Park, K. M.; Kim, D.; Kim, J. Functionalized Cucurbiturils and Their Applications. *Chem. Soc. Rev.* **2007**, *36*, 267−279.
(342) Barrow, S. J.; Kasera, S.; Rowland, M. J.; del Barrio, J.; Scherman, O. A. Cucurbituril-Based Molecular Recognition. *Chem. Rev.* **2015**, *115*, 12320−12406.
(343) Assaf, K. I.; Nau, W. M. Cucurbiturils: From Synthesis to High-Affinity Binding and Catalysis. *Chem. Soc. Rev.* **2015**, *44*, 394−418.
(344) Cao, L. P.; Sekutor, M.; Zavalij, P. Y.; Mlinaric-Majerski, K.; Glaser, R.; Isaacs, L. Cucurbit[7]Uril.Guest Pair with an Attomolar Dissociation Constant. *Angew. Chem., Int. Ed.* **2014**, *53*, 988−993.
(345) Ghosh, I.; Nau, W. M. The Strategic Use of Supramolecular Pk(a) Shifts to Enhance the Bioavailability of Drugs. *Adv. Drug Delivery Rev.* **2012**, *64*, 764−783.
(346) Biedermann, F.; Uzunova, V. D.; Scherman, O. A.; Nau, W. M.; De Simone, A. Release of High-Energy Water as an Essential Driving Force for the High-Affinity Binding of Cucurbit[N]Urils. *J. Am. Chem. Soc.* **2012**, *134*, 15318−15323.
(347) Basilio, N.; Mendoza, J.; Gago, S.; Parola, A. J. Ph-Driven Self-Sorting in a Four Component Host-Guest System. *Chem. Commun.* **2017**, *53*, 6472−6475.
(348) Basilio, N.; Gago, S.; Parola, A. J.; Pina, F. Contrasting Pk(a) Shifts in Cucurbit[7]Uril Host-Guest Complexes Governed by an Interplay of Hydrophobic Effects and Electrostatic Interactions. *ACS Omega* **2017**, *2*, 70−75.
(349) de Silva, A. P.; McClenaghan, N. D. Molecular-Scale Logic Gates. *Chem. - Eur. J.* **2004**, *10*, 574−586.
(350) Andreasson, J.; Pischel, U. Molecules with a Sense of Logic: A Progress Report. *Chem. Soc. Rev.* **2015**, *44*, 1053−1069.
(351) de Silva, P. A.; Gunaratne, N. H. Q.; McCoy, C. P. A Molecular Photoionic and Gate Based on Fluorescent Signalling. *Nature* **1993**, *364*, 42−44.
(352) Liu, Y. L.; Yu, Y.; Gao, J. A.; Wang, Z. Q.; Zhang, X. Water-Soluble Supramolecular Polymerization Driven by Multiple Host-Stabilized Charge-Transfer Interactions. *Angew. Chem., Int. Ed.* **2010**, *49*, 6576−6579.
(353) Appel, E. A.; del Barrio, J.; Loh, X. J.; Scherman, O. A. Supramolecular Polymeric Hydrogels. *Chem. Soc. Rev.* **2012**, *41*, 6195−6214.
(354) Yang, H.; Yuan, B.; Zhang, X.; Scherman, O. A. Supramolecular Chemistry at Interfaces: Host-Guest Interactions for Fabricating Multifunctional Biointerfaces. *Acc. Chem. Res.* **2014**, *47*, 2106−2115.
(355) Zhang, J.; Coulston, R. J.; Jones, S. T.; Geng, J.; Scherman, O. A.; Abell, C. One-Step Fabrication of Supramolecular Microcapsules from Microfluidic Droplets. *Science* **2012**, *335*, 690−694.
(356) Wiemann, M.; Jonkheijm, P. Stimuli-Responsive Cucurbit[N]-Uril-Mediated Host-Guest Complexes on Surfaces. *Isr. J. Chem.* **2018**, *58*, 314−325.
(357) van Dun, S.; Ottmann, C.; Milroy, L. G.; Brunsveld, L. Supramolecular Chemistry Targeting Proteins. *J. Am. Chem. Soc.* **2017**, *139*, 13960−13968.
(358) Nguyen, H. D.; Dang, D. T.; van Dongen, J. L. J.; Brunsveld, L. Protein Dimerization Induced by Supramolecular Interactions with Cucurbit[8]Uril. *Angew. Chem., Int. Ed.* **2010**, *49*, 895−898.

https://doi.org/10.1021/acs.chemrev.1c00399
Chem. Rev. 2022, 122, 1416−1481

(359) Heitmann, L. M.; Taylor, A. B.; Hart, P. J.; Urbach, A. R. Sequence-Specific Recognition and Cooperative Dimerization of N-Terminal Aromatic Peptides in Aqueous Solution by a Synthetic Host. *J. Am. Chem. Soc.* **2006**, *128*, 12574−12581.
(360) de Vink, P. J.; Briels, J. M.; Schrader, T.; Milroy, L. G.; Brunsveld, L.; Ottmann, C. A Binary Bivalent Supramolecular Assembly Platform Based on Cucurbit[8]Uril and Dimeric Adapter Protein 14−3-3. *Angew. Chem., Int. Ed.* **2017**, *56*, 8998−9002.
(361) Guo, D.-S.; Wang, K.; Liu, Y. Selective Binding Behaviors of P-Sulfonatocalixarenes in Aqueous Solution. *J. Inclusion Phenom. Mol. Recognit. Chem.* **2008**, *62*, 1−21.
(362) Guo, D.-S.; Liu, Y. Supramolecular Chemistry of P-Sulfonatocalix[N]Arenes and Its Biological Applications. *Acc. Chem. Res.* **2014**, *47*, 1925−1934.
(363) Ghale, G.; Nau, W. M. Dynamically Analyte-Responsive Macrocyclic Host−Fluorophore Systems. *Acc. Chem. Res.* **2014**, *47*, 2150−2159.
(364) Hof, F. Host−Guest Chemistry That Directly Targets Lysine Methylation: Synthetic Host Molecules as Alternatives to Bio-Reagents. *Chem. Commun.* **2016**, *52*, 10093−10108.
(365) Romero, M. A.; Mateus, P.; Matos, B.; Acuna, A.; Garcia-Rio, L.; Arteaga, J. F.; Pischel, U.; Basílio, N. Binding of Flavylium Ions to Sulfonatocalix[4]Arene and Implication in the Photorelease of Biologically Relevant Guests in Water. *J. Org. Chem.* **2019**, *84*, 10852−10859.
(366) Baroncini, M.; Silvi, S.; Credi, A. Photo- and Redox-Driven Artificial Molecular Motors. *Chem. Rev.* **2020**, *120*, 200−268.
(367) Erbas-Cakmak, S.; Leigh, D. A.; McTernan, C. T.; Nussbaumer, A. L. Artificial Molecular Machines. *Chem. Rev.* **2015**, *115*, 10081−10206.
(368) Pezzato, C.; Cheng, C. Y.; Stoddart, J. F.; Astumian, R. D. Mastering the Non-Equilibrium Assembly and Operation of Molecular Machines. *Chem. Soc. Rev.* **2017**, *46*, 5491−5507.
(369) Coskun, A.; Spruell, J. M.; Barin, G.; Dichtel, W. R.; Flood, A. H.; Botros, Y. Y.; Stoddart, J. F. High Hopes: Can Molecular Electronics Realise Its Potential? *Chem. Soc. Rev.* **2012**, *41*, 4827−4859.
(370) Bruns, C. J.; Stoddart, J. F. Rotaxane-Based Molecular Muscles. *Acc. Chem. Res.* **2014**, *47*, 2186−2199.
(371) Blanco, V.; Leigh, D. A.; Marcos, V. Artificial Switchable Catalysts. *Chem. Soc. Rev.* **2015**, *44*, 5341−5370.
(372) Chen, W.; Glackin, C. A.; Horwitz, M. A.; Zink, J. I. Nanomachines and Other Caps on Mesoporous Silica Nanoparticles for Drug Delivery. *Acc. Chem. Res.* **2019**, *52*, 1531−1542.
(373) Li, Z. X.; Barnes, J. C.; Bosoy, A.; Stoddart, J. F.; Zink, J. I. Mesoporous Silica Nanoparticles in Biomedical Applications. *Chem. Soc. Rev.* **2012**, *41*, 2590−2605.
(374) Ma, X.; Tian, H. Bright Functional Rotaxanes. *Chem. Soc. Rev.* **2010**, *39*, 70−80.
(375) Sharif, N.; Khoshnoudi-Nia, S.; Jafari, S. M. Nano/Micro-encapsulation of Anthocyanins; a Systematic Review and Meta-Analysis. *Food Res. Int.* **2020**, *132*, 109077.
(376) Cortez, R.; Luna-Vital, D. A.; Margulis, D.; de Mejia, E. G. Natural Pigments: Stabilization Methods of Anthocyanins for Food Applications. *Compr. Rev. Food Sci. Food Saf.* **2017**, *16*, 180−198.
(377) Silva, G. T. M.; Silva, K. M.; Silva, C. P.; Gonçalves, J. M.; Quina, F. H. Hybrid Pigments from Anthocyanin Analogues and Synthetic Clay Minerals. *ACS Omega* **2020**, *5*, 26592−26600.
(378) Kohno, Y.; Shibata, Y.; Oyaizu, N.; Yoda, K.; Shibata, M.; Matsushima, R. Stabilization of Flavylium Dye by Incorporation into the Pore of Protonated Zeolites. *Microporous Mesoporous Mater.* **2008**, *114*, 373−379.
(379) Gago, S.; Pessêgo, M.; Laia, C. A. T.; Parola, A. J. Ph-Tunable Fluorescence and Photochromism of a Flavylium-Based Mcm-41 Pigment. *ACS Omega* **2017**, *2*, 122−126.
(380) Brandão Lima, L. C.; Castro-Silva, F.; Silva-Filho, E. C.; Fonseca, M. G.; Jaber, M. Saponite-Anthocyanin Pigments: Slipping between the Sheets. *Microporous Mesoporous Mater.* **2020**, *300*, 110148.
(381) Silva, G. T. M.; Silva, C. P.; Gehlen, M. H.; Oake, J.; Bohne, C.; Quina, F. H. Organic/Inorganic Hybrid Pigments from Flavylium Cations and Palygorskite. *Appl. Clay Sci.* **2018**, *162*, 478−486.
(382) Silva, G. T. M.; da Silva, K. M.; Silva, C. P.; Rodrigues, A. C. B.; Oake, J.; Gehlen, M. H.; Bohne, C.; Quina, F. H. Highly Fluorescent Hybrid Pigments from Anthocyanin- and Red Wine Pyranoanthocyanin-Analogs Adsorbed on Sepiolite Clay. *Photochem. Photobiol. Sci.* **2019**, *18*, 1750−1760.
(383) Li, S.; Ding, J.; Mu, B.; Wang, X.; Kang, Y.; Wang, A. Acid/Base Reversible Allochroic Anthocyanin/Palygorskite Hybrid Pigments: Preparation, Stability and Potential Applications. *Dyes Pigm.* **2019**, *171*, 107738.
(384) Li, S.; Mu, B.; Wang, X.; Kang, Y.; Wang, A. A Comparative Study on Color Stability of Anthocyanin Hybrid Pigments Derived from 1d and 2d Clay Minerals. *Materials* **2019**, *12*, 3287.
(385) Lima, L. C. B.; Silva, F. C.; Silva-Filho, E. C.; Fonseca, M. G.; Zhuang, G.; Jaber, M. Saponite-Anthocyanin Derivatives: The Role of Organoclays in Pigment Photostability. *Appl. Clay Sci.* **2020**, *191*, 105604.
(386) Zhu, F. Interactions between Cell Wall Polysaccharides and Polyphenols. *Crit. Rev. Food Sci. Nutr.* **2018**, *58*, 1808−1831.
(387) Fernandes, A.; Bras, N. F.; Mateus, N.; de Freitas, V. Understanding the Molecular Mechanism of Anthocyanin Binding to Pectin. *Langmuir* **2014**, *30*, 8516−8527.
(388) Fernandes, A.; Oliveira, J.; Fonseca, F.; Ferreira-da-Silva, F.; Mateus, N.; Vincken, J. P.; de Freitas, V. Molecular Binding between Anthocyanins and Pectic Polysaccharides - Unveiling the Role of Pectic Polysaccharides Structure. *Food Hydrocolloids* **2020**, *102*, 105625.
(389) Fernandes, A.; Brandão, E.; Raposo, F.; Maricato, É.; Oliveira, J.; Mateus, N.; Coimbra, M. A.; de Freitas, V. Impact of Grape Pectic Polysaccharides on Anthocyanins Thermostability. *Carbohydr. Polym.* **2020**, *239*, 116240.
(390) Buchweitz, M.; Carle, R.; Kammerer, D. R. Bathochromic and Stabilising Effects of Sugar Beet Pectin and an Isolated Pectic Fraction on Anthocyanins Exhibiting Pyrogallol and Catechol Moieties. *Food Chem.* **2012**, *135*, 3010−3019.
(391) Jeong, D.; Na, K. Chondroitin Sulfate Based Nanocomplex for Enhancing the Stability and Activity of Anthocyanin. *Carbohydr. Polym.* **2012**, *90*, 507−515.
(392) Tan, C.; B. Celli, G.; Lee, M.; Licker, J.; Abbaspourrad, A. Polyelectrolyte Complex Inclusive Biohybrid Microgels for Tailoring Delivery of Copigmented Anthocyanins. *Biomacromolecules* **2018**, *19*, 1517−1527.
(393) Klimaviciute, R.; Navikaite, V.; Jakstas, V.; Ivanauskas, L. Complexes of Dextran Sulfate and Anthocyanins from *Vaccinium Myrtillus*: Formation and Stability. *Carbohydr. Polym.* **2015**, *129*, 70−78.
(394) Tan, C.; Celli, G. B.; Abbaspourrad, A. Copigment-Polyelectrolyte Complexes (Pecs) Composite Systems for Anthocyanin Stabilization. *Food Hydrocolloids* **2018**, *81*, 371−379.
(395) Tan, C.; Celli, G. B.; Selig, M. J.; Abbaspourrad, A. Catechin Modulates the Copigmentation and Encapsulation of Anthocyanins in Polyelectrolyte Complexes (Pecs) for Natural Colorant Stabilization. *Food Chem.* **2018**, *264*, 342−349.
(396) Araújo, P.; Basílio, N.; Fernandes, A.; Mateus, N.; de Freitas, V.; Pina, F.; Oliveira, J. Impact of Lignosulfonates on the Thermodynamic and Kinetic Parameters of Malvidin-3-O-Glucoside in Aqueous Solutions. *J. Agric. Food Chem.* **2018**, *66*, 6382−6387.
(397) Araújo, P.; Basílio, N.; Azevedo, J.; Fernandes, A.; Mateus, N.; Pina, F.; de Freitas, V.; Oliveira, J. Colour Modulation of Blue Anthocyanin-Derivatives. Lignosulfonates as a Tool to Improve the Water Solubility of Natural Blue Dyes. *Dyes Pigm.* **2018**, *153*, 150−159.
(398) Chung, C.; Rojanasasithara, T.; Mutilangi, W.; McClements, D. J. Stability Improvement of Natural Food Colors: Impact of Amino Acid and Peptide Addition on Anthocyanin Stability in Model Beverages. *Food Chem.* **2017**, *218*, 277−284.
(399) Dangles, O.; Brouillard, R. Polyphenol Interactions - the Copigmentation Case - Thermodynamic Data from Temperature-

https://doi.org/10.1021/acs.chemrev.1c00399
Chem. Rev. 2022, 122, 1416−1481

Variation and Relaxation Kinetics-Medium Effect. *Can. J. Chem.* **1992**, *70*, 2174−2189.
(400) Fasano, M.; Curry, S.; Terreno, E.; Galliano, M.; Fanali, G.; Narciso, P.; Notari, S.; Ascenzi, P. The Extraordinary Ligand Binding Properties of Human Serum Albumin. *IUBMB Life* **2005**, *57*, 787−796.
(401) Abou-Zied, O. K.; Al-Shihi, O. I. K. Characterization of Subdomain Iia Binding Site of Human Serum Albumin in Its Native, Unfolded, and Refolded States Using Small Molecular Probes. *J. Am. Chem. Soc.* **2008**, *130*, 10793−10801.
(402) Kanakis, C. D.; Tarantilis, P. A.; Polissiou, M. G.; Diamantoglou, S.; Tajmir-Riahi, H. A. Antioxidant Flavonoids Bind Human Serum Albumin. *J. Mol. Struct.* **2006**, *798*, 69−74.
(403) Cahyana, Y.; Gordon, M. H. Interaction of Anthocyanins with Human Serum Albumin: Influence of Ph and Chemical Structure on Binding. *Food Chem.* **2013**, *141*, 2278−2285.
(404) Matei, I.; Hillebrand, M. Interaction of Kaempferol with Human Serum Albumin: A Fluorescence and Circular Dichroism Study. *J. Pharm. Biomed. Anal.* **2010**, *51*, 768−773.
(405) Sengupta, B.; Sengupta, P. K. The Interaction of Quercetin with Human Serum Albumin: A Fluorescence Spectroscopic Study. *Biochem. Biophys. Res. Commun.* **2002**, *299*, 400−403.
(406) Tang, L.; Zuo, H.; Shu, L. Comparison of the Interaction between Three Anthocyanins and Human Serum Albumins by Spectroscopy. *J. Lumin.* **2014**, *153*, 54−63.
(407) Al Bittar, S.; Mora, N.; Loonis, M.; Dangles, O. Chemically Synthesized Glycosides of Hydroxylated Flavylium Ions as Suitable Models of Anthocyanins: Binding to Iron Ions and Human Serum Albumin, Antioxidant Activity in Model Gastric Conditions. *Molecules* **2014**, *19*, 20709−20730.
(408) Tang, L.; Li, S.; Bi, H.; Gao, X. Interaction of Cyanidin-3-O-Glucoside with Three Proteins. *Food Chem.* **2016**, *196*, 550−559.
(409) Cheng, J.; Liu, J.-H.; Prasanna, G.; Jing, P. Spectrofluorimetric and Molecular Docking Studies on the Interaction of Cyanidin-3-O-Glucoside with Whey Protein, B-Lactoglobulin. *Int. J. Biol. Macromol.* **2017**, *105*, 965−972.
(410) He, Z.; Zhu, H.; Xu, M.; Zeng, M.; Qin, F.; Chen, J. Complexation of Bovine B-Lactoglobulin with Malvidin-3-O-Glucoside and Its Effect on the Stability of Grape Skin Anthocyanin Extracts. *Food Chem.* **2016**, *209*, 234−240.
(411) Xu, J.; Hao, M.; Sun, Q.; Tang, L. Comparative Studies of Interaction of B-Lactoglobulin with Three Polyphenols. *Int. J. Biol. Macromol.* **2019**, *136*, 804−812.
(412) He, Z.; Xu, M.; Zeng, M.; Qin, F.; Chen, J. Interactions of Milk A- and B-Casein with Malvidin-3-O-Glucoside and Their Effects on the Stability of Grape Skin Anthocyanin Extracts. *Food Chem.* **2016**, *199*, 314−322.
(413) Casanova, F.; Chapeau, A.-L.; Hamon, P.; de Carvalho, A. F.; Croguennec, T.; Bouhallab, S. Ph- and Ionic Strength-Dependent Interaction between Cyanidin-3-O-Glucoside and Sodium Caseinate. *Food Chem.* **2018**, *267*, 52−59.
(414) Pitkowski, A.; Nicolai, T.; Durand, D. Scattering and Turbidity Study of the Dissociation of Casein by Calcium Chelation. *Biomacromolecules* **2008**, *9*, 369−375.
(415) Soares, S.; Kohl, S.; Thalmann, S.; Mateus, N.; Meyerhof, W.; De Freitas, V. Different Phenolic Compounds Activate Distinct Human Bitter Taste Receptors. *J. Agric. Food Chem.* **2013**, *61*, 1525−1533.
(416) Ferrer-Gallego, R.; Soares, S.; Mateus, N.; Rivas-Gonzalo, J.; Escribano-Bailón, M. T.; Freitas, V. d. New Anthocyanin−Human Salivary Protein Complexes. *Langmuir* **2015**, *31*, 8392−8401.
(417) Soares, S.; Santos Silva, M.; García-Estévez, I.; Brandão, E.; Fonseca, F.; Ferreira-da-Silva, F.; Teresa Escribano-Bailón, M.; Mateus, N.; de Freitas, V. Effect of Malvidin-3-Glucoside and Epicatechin Interaction on Their Ability to Interact with Salivary Proline-Rich Proteins. *Food Chem.* **2019**, *276*, 33−42.
(418) Paissoni, M. A.; Waffo-Teguo, P.; Ma, W.; Jourdes, M.; Rolle, L.; Teissedre, P. L. Chemical and Sensorial Investigation of in-Mouth Sensory Properties of Grape Anthocyanins. *Sci. Rep.* **2018**, *8*, 17098.
(419) García-Estévez, I.; Cruz, L.; Oliveira, J.; Mateus, N.; de Freitas, V.; Soares, S. First Evidences of Interaction between Pyranoanthocyanins and Salivary Proline-Rich Proteins. *Food Chem.* **2017**, *228*, 574−581.
(420) Astruc, D.; Boisselier, E.; Ornelas, C. Dendrimers Designed for Functions: From Physical, Photophysical, and Supramolecular Properties to Applications in Sensing, Catalysis, Molecular Electronics, Photonics, and Nanomedicine. *Chem. Rev.* **2010**, *110*, 1857−1959.
(421) Caminade, A.-M.; Turrin, C.-O.; Laurent, R.; Ouali, A.; Delavaux-Nicot, B. *Dendrimers: Towards Catalytic, Material and Biomedical Uses*; John Wiley & Sons, Ltd: Chichester, UK, 2011; pp 1−566.
(422) Yesil-Celiktas, O.; Pala, C.; Cetin-Uyanikgil, E. O.; Sevimli-Gur, C. Synthesis of Silica-Pamam Dendrimer Nanoparticles as Promising Carriers in Neuro Blastoma Cells. *Anal. Biochem.* **2017**, *519*, 1−7.
(423) Cruz, L.; Basílio, N.; Mendoza, J.; Mateus, N.; de Freitas, V.; Tawara, M. H.; Correa, J.; Fernandez-Megia, E. Impact of a Water-Soluble Gallic Acid-Based Dendrimer on the Color-Stabilizing Mechanisms of Anthocyanins. *Chem. - Eur. J.* **2019**, *25*, 11696−11706.
(424) Silva-Pereira, M. C.; Teixeira, J. A.; Pereira-Júnior, V. A.; Stefani, R. Chitosan/Corn Starch Blend Films with Extract from Brassica Oleraceae (Red Cabbage) as a Visual Indicator of Fish Deterioration. *LWT-Food Sci. Technol.* **2015**, *61*, 258−262.
(425) Choi, I.; Lee, J. Y.; Lacroix, M.; Han, J. Intelligent Ph Indicator Film Composed of Agar/Potato Starch and Anthocyanin Extracts from Purple Sweet Potato. *Food Chem.* **2017**, *218*, 122−128.
(426) Yoshida, C. M. P.; Maciel, V. B. V.; Mendonça, M. E. D.; Franco, T. T. Chitosan Biobased and Intelligent Films: Monitoring Ph Variations. *LWT-Food Sci. Technol.* **2014**, *55*, 83−89.
(427) Pourjavaher, S.; Almasi, H.; Meshkini, S.; Pirsa, S.; Parandi, E. Development of a Colorimetric Ph Indicator Based on Bacterial Cellulose Nanofibers and Red Cabbage (Brassica Oleraceae) Extract. *Carbohydr. Polym.* **2017**, *156*, 193−201.
(428) Pereira, V. A., Jr; de Arruda, I. N. Q.; Stefani, R. Active Chitosan/Pva Films with Anthocyanins from Brassica Oleraceae (Red Cabbage) as Time−Temperature Indicators for Application in Intelligent Food Packaging. *Food Hydrocolloids* **2015**, *43*, 180−188.
(429) Pacquit, A.; Frisby, J.; Diamond, D.; Lau, K. T.; Farrell, A.; Quilty, B.; Diamond, D. Development of a Smart Packaging for the Monitoring of Fish Spoilage. *Food Chem.* **2007**, *102*, 466−470.
(430) Maciel, V. B. V.; Yoshida, C. M. P.; Franco, T. T. Chitosan/Pectin Polyelectrolyte Complex as a Ph Indicator. *Carbohydr. Polym.* **2015**, *132*, 537−545.
(431) Maciel, V. B. V.; Yoshida, C. M. P.; Franco, T. T. Development of a Prototype of a Colourimetric Temperature Indicator for Monitoring Food Quality. *J. Food Eng.* **2012**, *111*, 21−27.
(432) Lakade, A. J.; Sundar, K.; Shetty, P. H. Nanomaterial-Based Sensor for the Detection of Milk Spoilage. *LWT-Food Sci. Technol.* **2017**, *75*, 702−709.
(433) Kuswandi, B.; Jayus; Restyana, A.; Abdullah, A.; Heng, L. Y.; Ahmad, M. A Novel Colorimetric Food Package Label for Fish Spoilage Based on Polyaniline Film. *Food Control* **2012**, *25*, 184−189.
(434) Dudnyk, I.; Janeček, E.-R.; Vaucher-Joset, J.; Stellacci, F. Edible Sensors for Meat and Seafood Freshness. *Sens. Actuators, B* **2018**, *259*, 1108−1112.
(435) Li, Y.; Wu, K.; Wang, B.; Li, X. Colorimetric Indicator Based on Purple Tomato Anthocyanins and Chitosan for Application in Intelligent Packaging. *Int. J. Biol. Macromol.* **2021**, *174*, 370−376.
(436) Fenger, J. A.; Moloney, M.; Robbins, R. J.; Collins, T. M.; Dangles, O. The Influence of Acylation, Metal Binding and Natural Antioxidants on the Thermal Stability of Red Cabbage Anthocyanins in Neutral Solution. *Food Funct.* **2019**, *10*, 6740−6751.
(437) Duenas, M.; Fulcrand, H.; Cheynier, V. Formation of Anthocyanin-Flavanol Adducts in Model Solutions. *Anal. Chim. Acta* **2006**, *563*, 15−25.
(438) El-Meligy, A. B.; Ishihara, T.; Oyama, K.; El-Nahas, A. M.; Yoshida, K. The First Synthesis of 3-O-Methylcyanidin and the Effect of 3-O-Substitution on the Stability under Acidic Conditions. *Heterocycles* **2018**, *97*, 946−959.
(439) Lopes, P.; Richard, T.; Saucier, C.; Teissedre, P.-L.; Monti, J.-P.; Glories, Y. Anthocyanone A: A Quinone Methide Derivative Resulting

https://doi.org/10.1021/acs.chemrev.1c00399
Chem. Rev. 2022, 122, 1416−1481

from Malvidin 3-O-Glucoside Degradation. *J. Agric. Food Chem.* **2007**, *55*, 2698−2704.
(440) de Oliveira, K. G.; Queiroz, V. A. V.; Carlos, L. D.; Cardoso, L. D.; Pinheiro-Sant'Ana, H. M.; Anunciacao, P. C.; de Menezes, C. B.; da Silva, E. C.; Barros, F. Effect of the Storage Time and Temperature on Phenolic Compounds of Sorghum Grain and Flour. *Food Chem.* **2017**, *216*, 390−398.
(441) Cabrita, L.; Petrov, V.; Pina, F. On the Thermal Degradation of Anthocyanidins: Cyanidin. *RSC Adv.* **2014**, *4*, 18939−18944.
(442) Furtado, P.; Figueiredo, P.; das Neves, H. C.; Pina, F. Photochemical and Thermal Degradation of Anthocyanins. *J. Photochem. Photobiol., A* **1993**, *75*, 113−118.
(443) Woodward, G.; Kroon, P.; Cassidy, A.; Kay, C. Anthocyanin Stability and Recovery: Implications for the Analysis of Clinical and Experimental Samples. *J. Agric. Food Chem.* **2009**, *57*, 5271−5278.
(444) Fenger, J. A.; Robbins, R. J.; Collins, T. M.; Dangles, O. The Fate of Acylated Anthocyanins in Mildly Heated Neutral Solution. *Dyes Pigm.* **2020**, *178*, 108326.
(445) Pina, F.; Melo, M. J.; Laia, C. A. T.; Parola, A. J.; Lima, J. C. Chemistry and Applications of Flavylium Compounds: A Handful of Colours. *Chem. Soc. Rev.* **2012**, *41*, 869−908.
(446) Giestas, L.; Folgosa, F.; Lima, J. C.; Parola, A. J.; Pina, F. Bio-Inspired Multistate Networks Responsive to Light, Ph and Thermal Inputs − an Example of a Multistate System Operating through Different Algorithms. *Eur. J. Org. Chem.* **2005**, *2005*, 4187−4200.
(447) Moncada, M. C.; Fernández, D.; Lima, J. C.; Parola, A. J.; Lodeiro, C.; Folgosa, F.; Melo, M. J.; Pina, F. Multistate Properties of 7-(N,N-Diethylamino)-4′-Hydroxyflavylium. An Example of an Unidirectional Reaction Cycle Driven by Ph. *Org. Biomol. Chem.* **2004**, *2*, 2802−2808.
(448) Adaku, C.; Skaar, I.; Berland, H.; Byamukama, R.; Jordheim, M.; Andersen, O. M. Anthocyanins from Mauve Flowers of Erlangea Tomentosa (Bothriocline Longipes) Based on Erlangidin - the First Reported Natural Anthocyanidin with C-Ring Methoxylation. *Phytochem. Lett.* **2019**, *29*, 225−230.
(449) Wang, D.; Ma, Y.; Zhang, C.; Zhao, X. Y. Thermal Characterization of the Anthocyanins from Black Soybean (Glycine Max L.) Exposed to Thermogravimetry. *LWT-Food Sci. Technol.* **2014**, *55*, 645−649.
(450) Das, A. B.; Goud, V. V.; Das, C. Degradation Kinetics of Anthocyanins from Purple Rice Bran and Effect of Hydrocolloids on Its Stability. *J. Food Process Eng.* **2020**, *43*, e13360.
(451) Sadilova, E.; Carle, R.; Stintzing, F. C. Thermal Degradation of Anthocyanins and Its Impact on Color and in Vitro Antioxidant Capacity. *Mol. Nutr. Food Res.* **2007**, *51*, 1461−1471.
(452) Sadilova, E.; Stintzing, F. C.; Carle, R. Thermal Degradation of Acylated and Nonacylated Anthocyanins. *J. Food Sci.* **2006**, *71*, C504−C512.
(453) Chen, C.-C.; Lin, C.; Chen, M.-H.; Chiang, P.-Y. Stability and Quality of Anthocyanin in Purple Sweet Potato Extracts. *Foods* **2019**, *8*, 393.
(454) Sheldon, R. *Metal-Catalyzed Oxidations of Organic Compounds*, 1st ed.; Academic Press, 1981.
(455) Vogel, F.; Harf, J.; Hug, A.; von Rohr, P. R. Promoted Oxidation of Phenol in Aqueous Solution Using Molecular Oxygen at Mild Conditions. *Environ. Prog.* **1999**, *18*, 7−13.
(456) Janeiro, P.; Brett, A. M. O. Redox Behavior of Anthocyanins Present in Vitis Vinifera L. *Electroanalysis* **2007**, *19*, 1779−1786.
(457) Satake, R.; Yanase, E. Mechanistic Studies of Hydrogen-Peroxide-Mediated Anthocyanin Oxidation. *Tetrahedron* **2018**, *74*, 6187−6191.
(458) Nkhili, E.; Loonis, M.; Mihai, S.; El Hajji, H.; Dangles, O. Reactivity of Food Phenols with Iron and Copper Ions: Binding, Dioxygen Activation and Oxidation Mechanisms. *Food Funct.* **2014**, *5*, 1186−1202.
(459) Ryan, P.; Hynes, M. J. The Kinetics and Mechanisms of the Complex Formation and Antioxidant Behaviour of the Polyphenols Egcg and Ecg with Iron(Iii). *J. Inorg. Biochem.* **2007**, *101*, 585−93.
(460) Elstner, E. F.; Osswald, W. Mechanisms of Oxygen Activation During Plant Stress. *Proc. R. Soc. Edinburgh, Sect. B: Biol. Sci.* **1994**, *102*, 131−154.
(461) Oren-Shamir, M. Does Anthocyanin Degradation Play a Significant Role in Determining Pigment Concentration in Plants? *Plant Sci.* **2009**, *177*, 310−316.
(462) Movahed, N.; Pastore, C.; Cellini, A.; Allegro, G.; Valentini, G.; Zenoni, S.; Cavallini, E.; D'Incà, E.; Tornielli, G. B.; Filippetti, I. The Grapevine Vviprx31 Peroxidase as a Candidate Gene Involved in Anthocyanin Degradation in Ripening Berries under High Temperature. *J. Plant Res.* **2016**, *129*, 513−526.
(463) Guo, J.; Wang, M.-H. Ultraviolet a-Specific Induction of Anthocyanin Biosynthesis and Pal Expression in Tomato (*Solanum Lycopersicum L.*). *Plant Growth Regul.* **2010**, *62*, 1−8.
(464) Jiang, M.; Ren, L.; Lian, H.; Liu, Y.; Chen, H. Novel Insight into the Mechanism Underlying Light-Controlled Anthocyanin Accumulation in Eggplant (Solanum Melongena L.). *Plant Sci.* **2016**, *249*, 46−58.
(465) Qiu, Z.; Wang, X.; Gao, J.; Guo, Y.; Huang, Z.; Du, Y. The Tomato Hoffman's Anthocyaninless Gene Encodes a Bhlh Transcription Factor Involved in Anthocyanin Biosynthesis That Is Developmentally Regulated and Induced by Low Temperatures. *PLoS One* **2016**, *11*, No. e0151067.
(466) Steyn, W. J.; Wand, S. J. E.; Holcroft, D. M.; Jacobs, G. Anthocyanins in Vegetative Tissues: A Proposed Unified Function in Photoprotection. *New Phytol.* **2002**, *155*, 349−361.
(467) Barbagallo, R. N.; Palmeri, R.; Fabiano, S.; Rapisarda, P.; Spagna, G. Characteristic of B-Glucosidase from Sicilian Blood Oranges in Relation to Anthocyanin Degradation. *Enzyme Microb. Technol.* **2007**, *41*, 570−575.
(468) Quattrocchio, F.; Verweij, W.; Kroon, A.; Spelt, C.; Mol, J.; Koes, R. Ph4 of Petunia Is an R2r3Myb Protein That Activates Vacuolar Acidification through Interactions with Basic-Helix-Loop-Helix Transcription Factors of the Anthocyanin Pathway. *Plant Cell* **2006**, *18*, 1274−1291.
(469) Vaknin, H.; Bar-Akiva, A.; Ovadia, R.; Nissim-Levi, A.; Forer, I.; Weiss, D.; Oren-Shamir, M. Active Anthocyanin Degradation in Brunfelsia Calycina (Yesterday−Today−Tomorrow) Flowers. *Planta* **2005**, *222*, 19−26.
(470) Borovsky, Y.; Oren-Shamir, M.; Ovadia, R.; De Jong, W.; Paran, I. The a Locus That Controls Anthocyanin Accumulation in Pepper Encodes a Myb Transcription Factor Homologous to Anthocyanin2 of Petunia. *Theor. Appl. Genet.* **2004**, *109*, 23−9.
(471) Povero, G.; Gonzali, S.; Bassolino, L.; Mazzucato, A.; Perata, P. Transcriptional Analysis in High-Anthocyanin Tomatoes Reveals Synergistic Effect of Aft and Atv Genes. *J. Plant Physiol.* **2011**, *168*, 270−279.
(472) Mennella, G.; Lo Scalzo, R.; Fibiani, M.; D'Alessandro, A.; Francese, G.; Toppino, L.; Acciarri, N.; de Almeida, A. E.; Rotino, G. L. Chemical and Bioactive Quality Traits During Fruit Ripening in Eggplant (S. Melongena L.) and Allied Species. *J. Agric. Food Chem.* **2012**, *60*, 11821−11831.
(473) Pandey, V.; Awasthi, M.; Singh, S.; Tiwari, S.; Dwivedi, U. A Comprehensive Review on Function and Application of Plant Peroxidases. *Biochem. Anal. Biochem.* **2017**, *6*, 1000308.
(474) Jolivet, S.; Arpin, N.; Wichers, H. J.; Pellon, G. Agaricus Bisporus Browning: A Review. *Mycol. Res.* **1998**, *102*, 1459−1483.
(475) Suttirak, W.; Manurakchinakorn, S. Potential Application of Ascorbic Acid, Citric Acid and Oxalic Acid for Browning Inhibition in Fresh-Cut Fruits and Vegetables. *Walailak J. Sci. Technol.* **2010**, *7*.514
(476) Blokhina, O.; Virolainen, E.; Fagerstedt, K.; Antioxidants, V. Oxidative Damage and Oxygen Deprivation Stress: A Review. *Ann. Bot.* **2003**, *91*, 179−94.
(477) Perron, N. R.; Brumaghim, J. L. A Review of the Antioxidant Mechanisms of Polyphenol Compounds Related to Iron Binding. *Cell Biochem. Biophys.* **2009**, *53*, 75−100.
(478) Fisher, G. R.; Gutierrez, P. L. Free Radical Formation and DNA Strand Breakage During Metabolism of Diaziquone by Nad(P)H

https://doi.org/10.1021/acs.chemrev.1c00399
Chem. Rev. 2022, 122, 1416−1481

Quinone-Acceptor Oxidoreductase (Dt-Diaphorase) and Nadph Cytochrome C Reductase. *Free Radical Biol. Med.* **1991**, *11*, 597−607.
(479) Cortez, R.; Luna-Vital, D. A.; Margulis, D.; Gonzalez de Mejia, E. Natural Pigments: Stabilization Methods of Anthocyanins for Food Applications. *Compr. Rev. Food Sci. Food Saf.* **2017**, *16*, 180−198.
(480) Coultate, T.; Blackburn, R. S. Food Colorants: Their Past, Present and Future. *Color. Technol.* **2018**, *134*, 165−186.
(481) Khoo, H. E.; Azlan, A.; Tang, S. T.; Lim, S. M. Anthocyanidins and Anthocyanins: Colored Pigments as Food, Pharmaceutical Ingredients, and the Potential Health Benefits. *Food Nutr. Res.* **2017**, *61*, 1361779−1361779.
(482) Shipp, J.; Abdel-Aal, E.-S. M. Food Applications and Physiological Effects of Anthocyanins as Functional Food Ingredients. *Open Food Sci. J.* **2010**, *4*, 7−22.
(483) Eder, R. *Pigments in Food Analysis by Hplc*; Nollet, L. M. L., Ed.; Marcel Dekker: New York, 2000.
(484) Rose, P. M.; Cantrill, V.; Benohoud, M.; Tidder, A.; Rayner, C. M.; Blackburn, R. S. Application of Anthocyanins from Blackcurrant (Ribes Nigrum L.) Fruit Waste as Renewable Hair Dyes. *J. Agric. Food Chem.* **2018**, *66*, 6790−6798.
(485) Chan, C. F.; Lien, C. Y. I.; Lai, Y. C.; Huang, C. L.; Liao, W. C. Influence of Purple Sweet Potato Extracts on the Uv Absorption Properties of a Cosmetic Cream. *J. Cosmet. Sci.* **2010**, *61*, 333−341.
(486) Gasparrini, M.; Forbes-Hernandez, T. Y.; Afrin, S.; Reboredo-Rodriguez, P.; Cianciosi, D.; Mezzetti, B.; Quiles, J. L.; Bompadre, S.; Battino, M.; Giampieri, F. Strawberry-Based Cosmetic Formulations Protect Human Dermal Fibroblasts against Uva-Induced Damage. *Nutrients* **2017**, *9*, 605.
(487) Soto, M. L.; Falqué, E.; Domínguez, H. Relevance of Natural Phenolics from Grape and Derivative Products in the Formulation of Cosmetics. *Cosmetics* **2015**, *2*, 259.
(488) McGhie, T. K.; Walton, M. C. The Bioavailability and Absorption of Anthocyanins: Towards a Better Understanding. *Mol. Nutr. Food Res.* **2007**, *51*, 702−713.
(489) Zhang, Y.; Seeram, N. P.; Lee, R.; Feng, L.; Heber, D. Isolation and Identification of Strawberry Phenolics with Antioxidant and Human Cancer Cell Antiproliferative Properties. *J. Agric. Food Chem.* **2008**, *56*, 670−675.
(490) Jing, P.; Bomser, J. A.; Schwartz, S. J.; He, J.; Magnuson, B. A.; Giusti, M. M. Structure−Function Relationships of Anthocyanins from Various Anthocyanin-Rich Extracts on the Inhibition of Colon Cancer Cell Growth. *J. Agric. Food Chem.* **2008**, *56*, 9391−9398.
(491) Wang, H.; Nair, M. G.; Strasburg, G. M.; Chang, Y.-C.; Booren, A. M.; Gray, J. I.; DeWitt, D. L. Antioxidant and Antiinflammatory Activities of Anthocyanins and Their Aglycon, Cyanidin, from Tart Cherries. *J. Nat. Prod.* **1999**, *62*, 294−296.
(492) Rose, P. M.; Cantrill, V.; Benohoud, M.; Tidder, A.; Rayner, C. M.; Blackburn, R. S. Application of Anthocyanins from Blackcurrant (Ribes Nigrum L.) Fruit Waste as Renewable Hair Dyes. *J. Agric. Food Chem.* **2018**, *66*, 6790−6798.
(493) Westfall, A.; Giusti, M. M. Color Profiles and Stability of Acylated and Nonacylated Anthocyanins as Novel Pigment Sources in a Lipstick Model: A Viable Alternative to Synthetic Colorants. *J. Cosmet. Sci.* **2017**, *68*, 233−244.
(494) Westfall, A.; Sigurdson, G. T.; Giusti, M. M. Antioxidant, UV Protection, and Antiphotoaging Properties of Anthocyanin-Pigmented Lipstick Formulations. *J. Cosmet. Sci.* **2019**, *70*, 63−76.

https://doi.org/10.1021/acs.chemrev.1c00399
Chem. Rev. 2022, 122, 1416−1481